Theses and Dissertations

2013

Reliability and Risk of Structural Systems under Progressive and Sudden Damage

Duygu Saydam
Lehigh University

Reliability and Risk of Structural Systems under

Progressive and Sudden Damage

by

Duygu Saydam

Presented to the Graduate and Research Committee

of Lehigh University

in Candidacy for the Degree of

Doctor of Philosophy

in

Structural Engineering

Lehigh University

September 2013

Approved and recommended for acceptance as a dissertation in partial

fulfillment of the requirements for the degree of Doctor of Philosophy.

_____
Date

_____
Dr. Dan M. Frangopol
Dissertation Advisor
Professor of Civil and
Environmental Engineering
Lehigh University

_____
Acceptance Date

Committee Members:

_____
Dr. John L. Wilson
Committee Chairperson
Professor of Civil and
Environmental Engineering
Lehigh University

_____
Dr. Richard Sause
Member
Professor of Civil and
Environmental Engineering
Lehigh University

_____
Dr. Clay J. Naito
Member
Professor of Civil and
Environmental Engineering
Lehigh University

_____
Dr. Joan R. Casas
Member
Professor of Construction
Engineering
Polytechnic University of Catalonia

ACKNOWLEDGEMENTS

This study was conducted at the Advanced Technology for Large Structural Systems (ATLSS) Engineering Research Center, Department of Civil and Environmental Engineering, Lehigh University, Bethlehem, Pennsylvania.

iv

I would like to thank former Research Associate Dr. Paolo Bocchini, former Ph.D. students Dr. Sunyong Kim and Dr. Nader Okasha, and current Ph.D. candidate You Dong for their cooperation, contributions and suggestions. Furthermore, I also thank to my colleagues Alberto Decò, Benjin Zhu, Mohamed Soliman, and Samantha Sabatino for their constructive discussions and warm friendship.

Finally and most importantly, I offer my sincere thanks and love to my parents Ruhan Saydam and Şevki Saydam, and my brother Kutlu Saydam. I couldn't have found the strength to pursue my Ph.D. degree without their support.

TABLE OF CONTENTS

xi

LIST OF TABLES

LIST OF FIGURES

xviii

xix

xx

xxi

xxii

ABSTRACT

Structural systems are usually subjected to progressive and/or sudden damage throughout their lifetime. Damage can cause a reduced level of safety and increase the life-cycle cost. In order to keep the safety and proper functionality of structures above prescribed thresholds, maintenance interventions should be well planned. Informed decision making for maintaining the required safety and serviceability levels of structural systems under uncertainty during their lifetime can only be achieved through integrated life-cycle management planning. Structural performance assessment and prediction, optimization of inspection and monitoring activities, updating the performance with information from inspection and monitoring, optimization of maintenance and repair activities and decision making are the main tasks of an integrated life-cycle management framework.

Accurate prediction and quantification of life-cycle performance is the most critical task in a life-cycle management framework. Uncertainty is inevitable in all aspects of this framework. Aggressive environmental conditions may cause the strength of a structure to deteriorate progressively in time. The deterioration process is complex and contains high uncertainty. Therefore, probabilistic methods are required for accurate assessment of structural performance. Reliability-based performance measures are the primary tool for structural management optimization frameworks. Extreme events such as floods, earthquakes, and blasts may cause sudden damage to structures. A structure must be able to withstand local damage without experiencing disproportionate consequences. Performance measures such as reliability, redundancy,

1

robustness, vulnerability and damage tolerance should be considered in the life-cycle management of structures. Risk-based approaches provide the means of combining the probability of structural failure with the consequences of this event. There is the need to effectively incorporate the risk-based performance measures into the life-cycle management frameworks by accounting for the probabilities of occurrence of failure events and the associated consequences using scenario-based approaches in a computationally efficient manner.

The main objective of this study is to develop means for integrating the reliability-based and risk-based performance indicators in a life-cycle management framework for structures undergoing progressive and sudden damage. An approach for quantifying time-variant reliability, redundancy, vulnerability, and robustness of structural systems in a life-cycle context is developed. A methodology for quantifying lifetime risk associated with the component failure and risk-based robustness of bridge superstructures is proposed. Furthermore, a risk-based maintenance optimization methodology for deteriorating bridges to establish optimum maintenance plans is proposed. A methodology to assess the time-dependent expected losses and risk-based robustness of highway bridge networks consisting of deteriorating bridges is established. In addition, a probabilistic approach for performance assessment of ship hulls under sudden damage accounting for different operational conditions is developed. Finally, the applicable range of simple expressions based on first-order second-moment method for bridge system reliability assessment is provided by investigating the amount of error associated with these simple expressions.

2

CHAPTER 1

INTRODUCTION:

OVERVIEW, OBJECTIVES, AND NOVELTIES

1.1 OVERVIEW

Civil infrastructure systems such as highways and bridges serve as the backbone of the economy of a country, carrying the bulk of the country's commercial goods movement as well as travel of people. A system of highways maintained in good condition will provide adequate safety, convenience and reduced vehicle operating costs. However, civil infrastructure systems are subjected to deterioration in strength and performance due to aggressive environmental stressors. This deterioration causes a reduced level of safety and increased life-cycle cost. According to FHWA (2012), approximately 25 percent of the highway bridges in the US are either structurally deficient or functionally obsolete. Life-cycle performance-based management of deteriorating structures such as bridges and ships is essential in order to allocate available funds in the most efficient way while ensuring the safety and integrity of these structures at a desirable level.

Effective decision making for maintaining the proper safety and functionality of structural systems under uncertainty during their lifetime can only be achieved through integrated life-cycle management planning. Figure 1.1 illustrates a comprehensive life-cycle management framework for structural systems under uncertainty. In this framework, structural performance assessment and prediction,

3

optimization of inspection and monitoring activities, updating the performance with information from inspection and monitoring, optimization of maintenance and repair activities and decision making are the main steps. Life-cycle performance assessment is the backbone of the process which requires current evaluation and future prediction. Uncertainty is inevitable in all aspects of a life-cycle management framework.

The most challenging task of a life-cycle framework is accurate prediction and quantification of life-cycle performance. Aggressive environmental conditions may cause the strength of a structure to deteriorate progressively in time. The deterioration process is complex and contains high uncertainty. Therefore, probabilistic methods are needed to be used for accurate assessment of performance. Consequently, reliability-based performance measures have been the primary tool for structural management optimization frameworks. Damage also may occur suddenly to structures due to abnormal events such as floods, earthquakes, intentional or accidental blasts and vehicle impact loads. A structure must be able to withstand an amount of local damage without experiencing disproportionate consequences. Modern structural design codes require that structures shall be robust so that they do not fail due to failure of one component. In spite of the importance of redundancy, robustness, damage tolerance and vulnerability concepts, neither such code requirements in further detail are available, nor engineering community has been able to agree on an implementation of these concepts which facilitates their quantification. A structure may experience more than one abnormal event during its lifetime. The effect of any abnormal event on the performance should be considered together with the effect of progressive damage. Performance measures regarding reliability, redundancy, robustness, vulnerability and

4

damage tolerance should be considered in the design and life-cycle management of structures under progressive and sudden damage.

Reliability-based performance assessment methods and performance indicators have been the primary tool in establishing life-cycle management frameworks. These indicators can account for both the aleatory and epistemic uncertainties. In most of the current structural design codes, strength requirements are based on single components. This approach does not provide the information about the interaction among the components and overall performance of the whole structure. However, accurate performance prediction of structures at *system level* is of interest in performance-based life-cycle assessment. Structural reliability theory offers a rational framework for quantification of system performance by including the uncertainties both in the resistance and the load effects, and correlations among different random variables. Reliability-based system performance indicators such as redundancy, vulnerability, and robustness should be integrated into the management frameworks for structures undergoing progressive and sudden damage. Despite the fact that reliability-based performance indicators associated with damage tolerance of structures are available in the literature, effective approaches integrating these indicators in life-cycle framework are yet to be developed.

When the economic aspects of failure become important such as those involved in highway bridge network analysis, the performance indicator used has to provide additional information (e.g., the consequence of failure event). However, the reliability-based indicators do not account for the outcome of a failure event in terms of economic losses. Recently, the interest in life-cycle management frameworks has

5

been shifting from *reliability-based approaches* towards *risk-based approaches*. Risk-based approaches provide the means of combining the probability of structural failure with the consequences of this event. Nevertheless, the integration of risk-based approaches in life-cycle management frameworks is in its early stages and is a challenging task. There is the need to effectively incorporate the risk-based performance measures into the life-cycle management frameworks by accounting for the probabilities of failure events and their consequences using scenario-based approaches in a computationally efficient manner.

Optimized life-cycle management frameworks will help allocating funds effectively on maintaining structures and infrastructure systems. The applications of such frameworks include bridges where the impact of structural aging is widely apparent and worsened by increase in traffic over time (Ellingwood 2005, Frangopol 2011). In addition, risks associated with networks of deteriorating bridges are enormous compared to single bridges; therefore, the need for effective risk-based life-cycle assessment methodologies is imminent. Deterioration due to environmental stressors is also a severe problem for marine infrastructure. Ships are subjected to corrosion throughout their lifetime in addition to sudden accidents such as grounding and collision. The decision making process regarding ships can be enhanced when the information regarding the reliability of damaged ship hulls after grounding and collision is available. Therefore, it is necessary to establish life-cycle performance assessment methodologies for ship undergoing progressive and sudden damage.

1.2 OBJECTIVES

6

The following are the main objectives of this study:

1. Investigate the reliability-based methodologies, indicators, and advanced tools for performance assessment of structural systems under uncertainty.

2. Develop approaches to integrate reliability-based methodologies and indicators in time-variant performance evaluation of structural systems undergoing progressive and sudden damage in a life-cycle framework.

3. Develop approaches to effectively combine reliability-based methods and consequence evaluation to establish a life-cycle framework for risk-based performance quantification of structures and infrastructures under uncertainty.

4. Develop approaches to incorporate the effects of maintenance in lifetime performance and establish risk-based life-cycle optimal management framework for deteriorating structural systems.

5. Develop approaches to apply the life-cycle framework to various types of infrastructure systems experiencing similar progressive and sudden damage mechanisms.

1.3 NOVELTIES

The topics covered in this study fall in several different tasks of the comprehensive life-cycle management framework shown in Figure 1.1. Most of the work presented herein is associated with the task "Structural Performance Assessment and Prediction". Some part of this study falls in line with the task "Optimization of Maintenance and Repair Activities". The tasks "Optimization of Inspection and Monitoring Activities" and "Updating Performance with Information from

7

Monitoring" are not the focus herein. The detailed frameworks associated with the methodologies developed are provided in the respective chapters of this study. The steps of developed methodologies have similarities as well as differences for various applications. The applications in this study include single highway bridges, highway bridge networks, and ships. Despite the varying details of the methodologies for these different applications, a general simplified scheme for a risk-based life-cycle management framework proposed is illustrated in Figure 1.2. This study is intended to contribute to the area of optimum management of structures under uncertainty in several aspects. These contributions are described in this section by mentioning the previous work that has been done in the respective topics. Each paragraph below refers to a contribution of this study.

In the field of damage tolerant structures, damage tolerance is referred with various related measures. These measures include collapse resistance (Ellingwood and Dusenberry 2005), vulnerability and damage tolerance (Frangopol et al. 1991, Lind 1995), robustness (Blockley et al. 2002, Maes, Fritzson, and Glowienka 2006, Baker, Schubert, and Faber 2008, Ghosn, Moses, and Frangopol 2010), and redundancy (Frangopol and Curley 1987, Fu and Frangopol 1990). The resistance to sudden local damage should be considered together with the effects of progressive deterioration in a life-cycle framework. Time-dependent redundancy of structures, in the context of availability of warning before structural failure under live load, was studied by Okasha and Frangopol (2009, 2010a and 2010b). Risk-based robustness of structures under deterioration was investigated by Baker, Schubert, and Faber (2008). However, time-dependent redundancy, as the availability of alternative load path under sudden local

8

damage, time-dependent vulnerability including combined effects of deterioration, and time-dependent robustness based on reliability have not been investigated in a life-cycle context yet. *The first contribution of this study is developing a methodology for quantifying time-variant reliability, redundancy, vulnerability, and robustness of structural systems and integrating these performance indicators within a comprehensive life-cycle management framework.* In a scenario-based approach, techniques such as finite element analysis, response surface approximation, and Latin Hypercube Sampling are integrated in order to investigate the time-dependent effects of corrosion on structural reliability, vulnerability, redundancy, and robustness.

Risk-based methodologies have been already applied to the management of the civil infrastructure. Stein et al. (1999) used the risk concept for prioritizing scour vulnerable bridges. Adey, Hajdin, and Brühwiler (2003) focused on the determination of optimal interventions for bridges affected by multiple hazards. Lounis (2004) presented a multi-criteria approach for maintenance optimization of bridge structures with emphasis on risk minimization. Ang (2011) focused on life-cycle considerations in risk-informed decisions for the design of civil infrastructure. Decò and Frangopol (2011) provided a framework for the quantitative risk assessment of single highway bridges under multiple hazards. However, there is still the need to establish a detailed framework for quantifying the risk specifically associated with deteriorating bridges which integrates the direct and indirect risks associated with each component. Markov-based models have been used extensively in estimating the time-variant performance of highway bridge structures. Golabi, Kulkarni, and Way (1982) developed a pavement management system based on a Markov decision model used in

9

the derivation of Pontis bridge management system. Jiang, Saito, and Sinha (1988) developed a bridge performance prediction model based on the Markov chain, which can be used to predict the percentages of bridges with different condition ratings. Gopal and Majidzadeh (1991) proposed a highway management method using the Markov decision process, which overcomes the shortage of methods based on level of service. Madanat (1993) presented a methodology for planning the maintenance and rehabilitation activities for transportation facilities based on the latent Markov decision process. Al-Wazeer (2007) proposed a methodology for defining bridge maintenance strategies based on risks associated with conditions of bridge elements and costs needed to improve these conditions. Markov chains are efficient tools to model time-dependent behavior of deteriorating bridge components, also due to the fact that condition rating systems which use discrete condition states to represent different deterioration levels of components already exist. However, Markov chains have not been integrated in a risk-based life-cycle assessment framework which is specifically designed for risk associated with deteriorating bridge components and accounts for different deterioration levels of components. *The second contribution of this study is developing a methodology for quantifying lifetime risk associated with the component failure and risk-based robustness of bridge superstructures.* It has been a common approach to assess the failure probabilities and risk-based on a certain time-dependent corrosion penetration level for components. In this study, the possibility of different corrosion levels at a time instant is considered by means of a set of mutually exclusive and collectively exhaustive condition states. The proposed methodology of

loss estimation takes into account the failure probability of different levels of component deterioration weighted by the occurrence probabilities of these levels.

Maintenance optimization problems under uncertainty are associated with various performance indicators. These include system reliability (Augusti, Ciampoli, and Frangopol 1998, Estes and Frangopol 1999), system reliability and redundancy (Okasha and Frangopol 2009), lifetime-based reliability (Yang et al. 2006), lifetime-based reliability and redundancy (Okasha and Frangopol 2010a), cost and spacing of corrosion rate sensors (Marsh and Frangopol 2007), and probabilistic condition and safety indices (Liu and Frangopol 2005a and 2005b, Neves, Frangopol, Cruz 2006 and Neves, Frangopol, and Petcherdchoo 2006, Frangopol and Liu 2007a and 2007b). Lounis (2006) presented a risk-based approach for maintenance optimization of a network of aging highway bridge decks integrating a stochastic deterioration model with an effective multi-objective optimization approach. Robelin and Madanat (2007) developed a bridge component maintenance and replacement optimization approach that uses a Markovian deterioration model, while accounting for aspects of the history of deterioration and maintenance. Zhu and Frangopol (2013) proposed an approach for assessing the time-dependent risks due to traffic and earthquake loads and establishing the optimum preventive and essential bridge maintenance strategies. *The third contribution of this study is developing a novel risk-based maintenance optimization methodology for deteriorating bridges to find the optimum maintenance options and their timing of applications. A significant contribution is finding the optimum maintenance actions and schedule for different components of bridges formulated as a multi-criteria optimization problem in which the lifetime maximum value of expected*

11

losses associated with failure and the lifetime total expected maintenance cost are considered as conflicting objectives.

The research interest on spatially distributed systems, especially highway bridge networks, has been increasing recently. Akgül and Frangopol (2003), and Liu and Frangopol (2006) have developed an integrated framework for reliability analysis, life-cycle cost assessment and maintenance optimization of bridge networks. Scott et al. (2005) proposed a robustness index for transportation networks for the evaluation of the critical importance of a given highway segment with respect to the overall system. Shinozuka et al. (2006) investigated the effectiveness of seismic bridge retrofit by applying a total social cost analysis that accounts for traffic flow redistribution. Dueñas-Osario and Vemuru (2009) focused on utility lifelines and their reliability under extreme events considering flow redistribution and cascading failures. Bocchini and Frangopol (2011a) proposed an approach to assess the life-cycle performance of highway bridge networks and their time-variant reliability combining three important features: reliability of the individual bridges, possible traffic flows, and correlation among states of bridges. Frangopol and Bocchini (2012) presented a critical review of the state-of-the-art in the field of bridge network performance analysis, reliability assessment, maintenance management and optimization. Due to their time efficiency, Markov chains are helpful tools to represent time-variant performance of deteriorating bridge networks. Smilowitz and Madanat (2000) presented a methodology for planning the maintenance and rehabilitation activities for transportation facilities based on the latent Markov decision process for network-level problems. Marcous et al. (2003) proposed an approach for effective decision making in redefining the

12

environmental conditions of bridge elements using Markov models. Kuhn and Madanat (2005) investigated the effect of model uncertainty on network-level infrastructure management on the basis of the Markov decision problem. Several researchers integrated the risk concept with seismic assessment of transportation networks. Kiremidjian et al. (2007) postulated a method for seismic risk assessment of transportation systems, which considers the direct cost of damage and costs due to time delays in the damaged system. Padgett, Desroches, and Nilsson (2010) conducted the seismic risk assessment of a region for a range of hazard levels. Ghosh et al. (2012) focused on the probabilistic seismic analysis of aging transportation networks. Elhag and Wang (2007) presented a bridge risk assessment method using neural networks based on qualitative bridge risk score and risk categories. Sathananthan et al. (2010) presented a qualitative risk ranking strategy for characterizing a network of bridges into groups with similar risk levels. They introduced a qualitative scoring system that uses the attributes to rank bridges in terms of their relative risk. Gómez et al. (2013) presented a hierarchical infrastructure network representation method for risk-based decision-making, which combines a systems approach with strategies for detecting the internal structure of networks, and providing flexibility and different levels of accuracy in estimating the extent of damage. However, the time-dependent risk and risk-based robustness of highway bridge network induced by deterioration of individual bridges under live loads were not investigated before. Recently, an efficient, acccurate, and simple Markov Chain model for the life-cycle analysis of bridge groups has been proposed by Bocchini, Saydam and Frangopol (2013). *Based on this Markov chain model, the fourth contribution of this study is developing a*

13

methodology to assess the time-dependent expected losses and risk-based robustness of highway bridge networks consisting of deteriorating bridges.

Research on performance assessment of damaged ships has attracted significant interest in the last two decades. Vertical bending moment capacity at critical sections has been the major performance indicator investigated. Paik et al. (1998) studied the residual strength of hull structures based on section modulus and ultimate bending strength and proposed a method for investigating the hull girder failure following collision and grounding. Wang et al. (2002) provided a review of the state-of-the-art research on ship collision and grounding focusing on the definition of accident scenarios, evaluation approaches and acceptance criteria. Zhu et al. (2002) studied the statistics of ship grounding incidents and presented damage extent distributions for certain types of ships. Wang, Spencer, and Chen (2002) proposed an analytical expression for assessing the residual strength of hull girders with damage and provided simple equations correlating residual strength with damage extent. Fang and Das (2005) applied structural reliability concepts to ship structures. They used Monte Carlo Simulation to assess the failure probability of damaged ships for different grounding and collision damage scenarios and external load conditions. Hussein and Guedes Soares (2009) studied the residual strength and reliability of double hull tankers for different damage scenarios. Decò, Frangopol, and Okasha (2011) investigated the time-variant reliability and redundancy of ship structures. Lee at al. (2012) compared the wave-induced loads on intact ship and damaged ship by means of experimental tests and computational analyses. Decò, Frangopol, and Zhu (2012) proposed a framework for the assessment of structural safety of ships under different

14

operational conditions by evaluating performance indicators such as reliability and redundancy. The availability of information on the residual strength of a damaged hull structure can be very helpful for making decisions on how to proceed with the damaged ships after accidents such as grounding and collision. However, there is the need for well establish probabilistic methods for performance assessment of damaged ships for different operational conditions. *The fifth contribution of this study is developing a probabilistic framework for performance assessment of ship hulls under sudden damage accounting for different operational conditions. The combined effects of sudden damage including grounding and collision, and progressive deterioration due to corrosion are investigated.* The reliability index and a probabilistic robustness index are investigated under varying operational conditions and in time.

Generally, it is impractical or impossible to compute the probability of failure or the reliability index analytically for a complex engineering structure in a system-based approach. Therefore, numerical methods such as Monte Carlo Simulation, first and second order reliability methods (FORM and SORM) are used (Fiessler, Neumann, and Rackwitz 1979, Hohenbichler and Rackwitz 1981, Hohenbichler et al. 1987). However, the procedures of applying these methods for system analysis may require a knowledge level beyond the skills of common engineer, efficient computational tools and time. It is possible to represent the performance of a structural system by a single limit state function based on a probabilistic finite element analysis. Der Kiureghian and Taylor (1983) introduced the use of first order second moment method (FOSM) with finite element method (FEM). Ghosn and Moses (1998) and Ghosn, Moses, and Frangopol (2010) used FOSM with FEM to investigate the system

15

reliability and redundancy of bridge structures assuming both load and resistance follow lognormal distribution. Although, the expressions by FOSM may provide good approximation when both load and system resistance follow lognormal distribution, the amount of error introduced can be significant when the random variables follow distribution other than lognormal, considering that it is reasonable to represent the maximum intensity of the live loads on bridge structures using extreme value distribution especially when supported by truck load survey data. *The sixth contribution in this study is providing the applicable range of simple expressions based on FOSM for bridge system reliability assessment by investigating the amount of error associated with these simple expressions in order to provide guidance to practitioners on using simple reliability expressions for bridge system reliability analysis.*

In summary, the novelties of this study are:

- Developing a methodology for quantifying time-variant reliability, redundancy, vulnerability, and robustness of structural systems and integrating these performance indicators into a comprehensive life-cycle management framework;

- Developing an approach for quantifying lifetime risk associated with the component failure and risk based robustness of bridge superstructures, accounting for the possibility of different corrosion levels;

- Developing a novel risk-based maintenance optimization methodology for deteriorating bridges based on most common condition rating system and Markov chains to minimize risk and minimize maintenance costs;

16

- Developing a methodology to assess the lifetime risk and risk-based robustness of highway bridge networks based on a Markov Chain model;

- Developing a probabilistic framework for performance assessment of ship hulls under sudden damage accounting for different operational conditions; and

- Providing the applicable range of simple expressions based on FOSM for bridge system reliability assessment by investigating the amount of error associated with these simple expressions.

1.4 OUTLINE

This study is divided into nine chapters. The following is a brief description of these chapters.

Chapter 1   serves as introduction.

Chapter 2   provides the relevant background information. Uncertainties in life-cycle structural performance evaluation are described. The levels of performance assessment for infrastructure systems are discussed. The system reliability assessment methodologies are summarized with emphasis on bridges. Structural performance indicators which are useful to quantify the performance of structures undergoing progressive and sudden damage are reviewed.

Chapter 3   presents an approach for assessing the life-cycle performance of structures regarding vulnerability, redundancy and robustness using advanced tools such as nonlinear incremental finite element analysis, response surface approximation, and Latin Hypercube Sampling. The time-dependent effects of corrosion on structural reliability, vulnerability, redundancy and robustness are investigated.

17

Chapter 4 provides the applicable range of simple expressions for bridge system reliability assessment. The amount of error associated with the simple expressions based on first order second moment method to compute the system reliability index of bridges is investigated. The results obtained provide guidance to engineers on using simple reliability expressions for bridge system reliability evaluation based on probabilistic finite element analysis.

Chapter 5 presents a methodology for quantifying lifetime risk associated with the component failure and risk based robustness of bridge superstructures. The risk is quantified in terms of the expected losses. The possibility of different corrosion levels at a time instant is considered by means of a set of mutually exclusive and collectively exhaustive condition states. The failure probabilities of different levels of component deterioration weighted by the occurrence probabilities of these levels are taken into account by the proposed methodology of loss estimation.

Chapter 6 presents a novel risk-based maintenance optimization methodology for deteriorating bridges to find the optimum maintenance options and timing based on the risk assessment methodology described in Chapter 5. A multi-criteria optimization problem in which the lifetime maximum value of expected losses associated with failure and the lifetime total expected maintenance cost are considered as the conflicting objectives is formulated. In addition, an approach for comparison of different maintenance strategies for bridge components without optimization is presented.

Chapter 7 presents a methodology to assess the time-dependent risk and risk-based robustness of highway bridge networks consisting of deteriorating bridges,

18

based on a Markov Chain model, which can combine the effects of time-dependent deterioration rates and the impacts of rehabilitations/reconstructions to predict the time-dependent performance of individual bridges. The time-dependent direct, indirect and total risk is formulated based on the transition probabilities among the states of the Markov Chain model.

Chapter 8 presents a probabilistic methodology for performance assessment of ship hulls under sudden damage accounting for different operational conditions. The combined effects of sudden damage and progressive deterioration due to corrosion are investigated. Under different operational conditions, the reliability index of intact and damaged ship hulls and the robustness index associated with various damage scenarios are evaluated in time.

Chapter 9 provides a summary of the study, the conclusions drawn from it and suggestions for future work.

Appendix A provides information about the computational platform used in the methodologies proposed in this study.

Appendix B presents brief summaries of some of other accomplished work by the author during his Ph.D. study.

Appendix C provides the list of symbols used in this study.
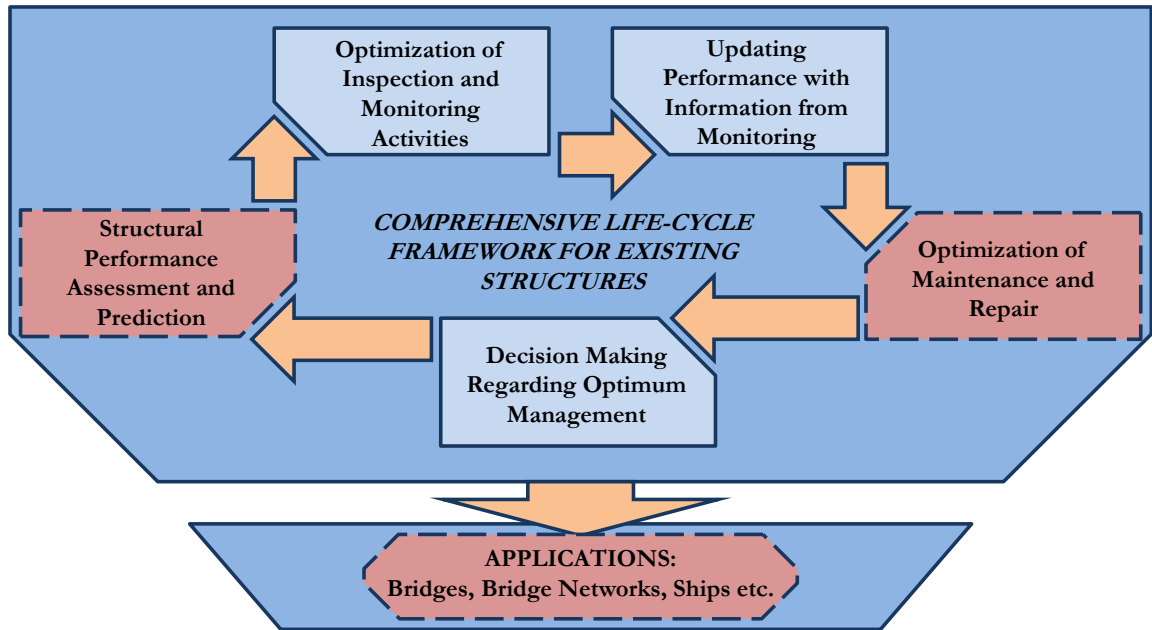
Figure 1.1   Comprehensive life-cycle management framework for existing structures
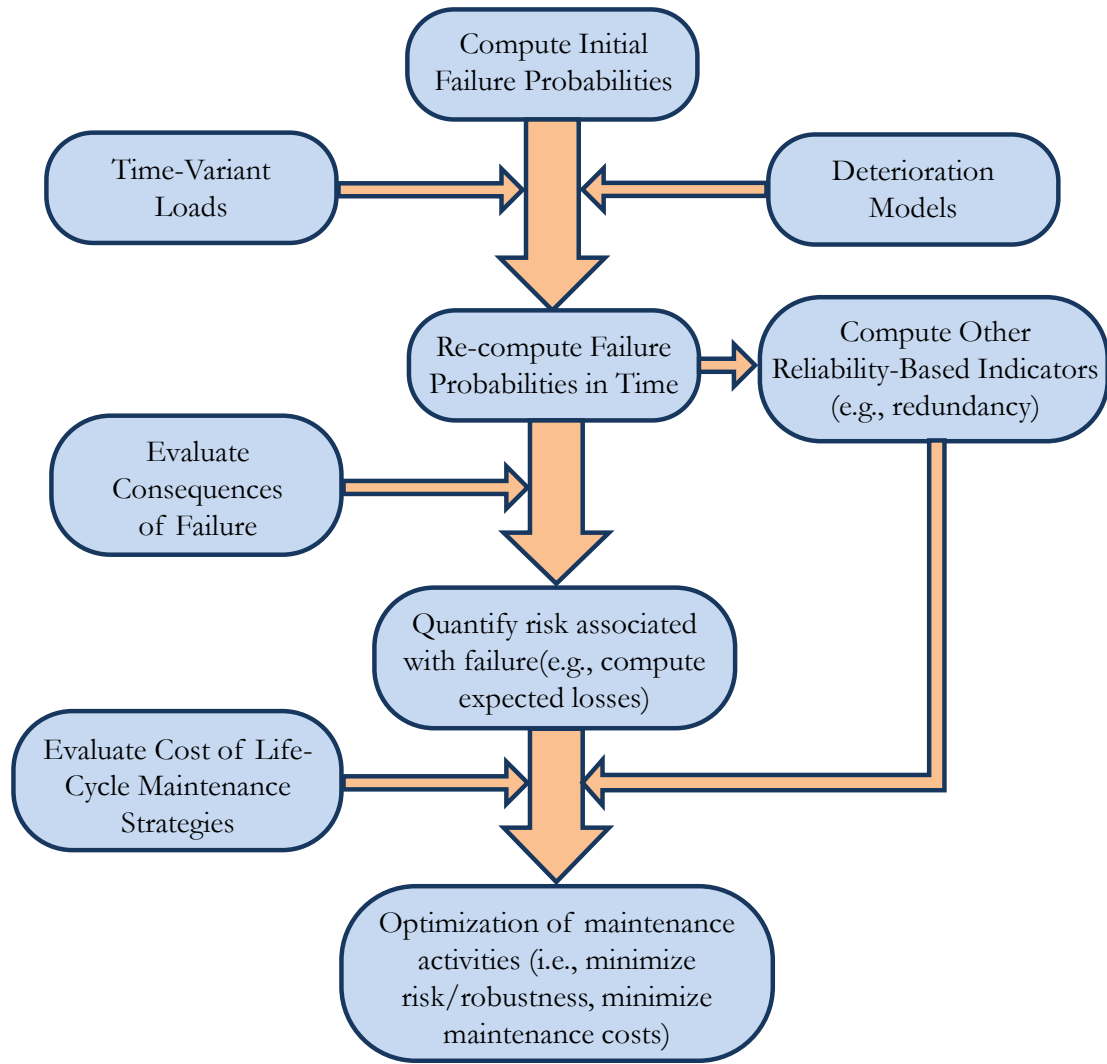
Figure 1.2   Simplified scheme for a risk-based life-cycle management framework

CHAPTER 2

BACKGROUND

2.1 INTRODUCTION

Performance of bridge structures is highly affected, in time, by the deterioration processes due to the aggressive environmental conditions (e.g., corrosion) and aging of the materials they are composed of. In order to avoid the consequences of structural failures, maintenance programs are carried out by the responsible authorities. It is necessary to predict the life-cycle performance of bridge structures accurately to establish a rational maintenance program. However, the prediction of life-cycle performance involves difficulties because of the complexity and uncertainties in loading and deterioration processes. Consequently, it is important to use proper indicators to evaluate the structural performance of bridges in a quantitative manner effectively.

Significant research has been done on quantifying structural performance with deterministic and probabilistic indicators such as safety factor and reliability index, respectively. Most recent bridge design codes consider uncertainty by including specific factors in the computation of structural resistance and load. However, the prediction of time-dependent bridge performance under uncertainty may require the use of several performance indicators. For example, system reliability measures (i.e., system probability of failure, system reliability index) may be adequate measures for quantifying the safety of a structure with respect to ultimate limit states, but system redundancy index is required to evaluate the availability of warning before final

22

failure. Moreover, performance indicators related to damage tolerance of structures, such as vulnerability and robustness are essential to consider for structures under deterioration and local damage together with the indicators related to ultimate limit states. In order to provide acceptable safety levels of bridges, the values of performance indicators under consideration shouldn't violate required threshold levels. On the other hand, life-cycle cost of bridge structures is another measure which decision makers have to balance with the performance indicators. Nevertheless, it is evident that evaluating bridge performance requires considering multiple indicators simultaneously.

2.2 UNCERTAINTIES IN BRIDGE LIFE-CYCLE PERFORMANCE EVALUATION

The major sources of uncertainty in engineering problems are classified into two groups: aleatory uncertainties and epistemic uncertainties (Ang and Tang 2007).

2.2.1 Aleatory Uncertainties

Aleatory uncertainty is associated with the randomness in the nature. For instance, in bridge engineering, the variability in material properties (e.g., steel yield strength, concrete compressive strength) exhibit aleatory type uncertainty. In addition, the variability of loads that a bridge structure is subjected through its lifetime is also considered as aleatory. Aleatory uncertainty can be observed by investigating the observational data associated with the structural resistance and loads. Aleatory uncertainty cannot be reduced as it is inherited from the randomness in the nature,

23

however, the availability of additional observational data may provide more accurate modeling of this uncertainty in our engineering problems (Ang 2011).

2.2.2 Epistemic Uncertainties

Epistemic uncertainty is associated with the imperfections in our engineering models and knowledge. For instance, the lack of adequate observational data and the error introduced by the assumptions in our engineering models are the major source of epistemic uncertainty. The failure probability of a structural system is quantified based on aleatory uncertainty. However, by taking into account the epistemic uncertainty, a probability distribution for the failure probability can be provided (Ang 2011). Unlike the aleatory uncertainty, the epistemic uncertainty can be reduced by improving the accuracy of our models that idealize the reality (Ang 2011).

2.3 LEVELS OF PERFORMANCE EVALUATION OF BRIDGE STRUCTURES

Performance of bridge structures can be quantified at cross-section level, member (component) level, overall structure (system) level, group of structures (network) level, and networks of network level (Figure 2.1). The strength of a bridge component under different loading conditions can be expressed in terms of the capacity of its most critical section when stability problems are not considered. Under consideration of stability problems, the performance is quantified at member level. In most of the current bridge design codes, strength requirements are based on component strength. Although such an approach may ensure an adequate level of safety of components, it

24

does not provide the information about the interaction between the components and overall performance of the whole structure. However, performance at system level is of concern in performance-based design. Structural reliability theory offers a rational framework for quantification of system performance by including the uncertainties both in the resistance and the load effects and correlations. In this section, the very basics of probabilistic performance analysis (e.g., reliability analysis) of bridge structures at component level and system level are presented.

2.3.1 Component-Based Approach

Performance evaluation of bridge cross-sections, bridge members and overall bridge structures is based on limit states defining the failure domain under specific loading conditions. The limit states defining the failure modes of components are included in design codes. The factors multiplying the load effects and nominal strength exist to ensure a predefined safety level of the component. However, if the purpose is to evaluate the performance of an existing bridge structure or design with respect to different target performance levels, the equation defining limit states must be in the pure form. A general representation of a limit state which is used in reliability analysis in terms of a performance function $g(\mathbf{X})$ can be expressed as

$$g(\mathbf{X}) = g(X_1, X_2, ..., X_n) = 0 \tag{2.1}$$

where $\mathbf{X} = (X_1, X_2, \ldots, X_n)$ is a vector of random variables of the system, and the performance function $g(\mathbf{X})$ determines the state of the system as $[g(\mathbf{X}) > 0] = $ "Safe state", and $[g(\mathbf{X}) < 0] = $ "Failure state". For instance, the limit state for the mid-span (positive) flexural failure of a composite bridge girder can be expressed as

25

$$g_{flexure+} = R - L = M_u - (M_{DLNC} + M_{DLC} + M_{LL+I}) = 0 \tag{2.2}$$

where R and L are the resistance and load effect respectively, and M_u, M_{DLNC}, M_{DLC}, and M_{LL+I} are the ultimate moment capacity, moment due to non-composite dead loads, moment due to composite dead loads, and moment due to live load including impact, respectively.

2.3.2 System-Based Approach

Overall bridge performance for a failure mode can be evaluated by modeling the bridge system failure as series or parallel or series-parallel combination of bridge component limit states (Hendawi and Frangopol, 1994). The failure domain (*FD*), representing the violation of bridge system limit state can be expressed in terms of bridge component limit states as (Ang and Tang, 1984):

(a) for series system $FD \equiv \bigcup\limits_{k=1}^{n} \{g_k(X) < 0\}$

(b) for parallel system $FD \equiv \bigcap\limits_{k=1}^{n} \{g_k(X) < 0\}$

(c) for series-parallel system $FD \equiv \bigcup\limits_{k=1}^{n} \bigcap\limits_{j=1}^{c_n} \{g_{k,j}(X) < 0\}$

where c_n is the number of components in the *n*-th cut set.

The performance of a system which consists of a number of subsystems depends not only on the performance of the subsystems but also on the interaction of these subsystems. An example of a system of systems is a highway bridge network, where each bridge is a system itself and interacts with the other bridges for the performance of whole network by means of traffic flow.

26

2.4 THE METHODOLOGIES IN SYSTEM ANALYSIS OF BRIDGE STRUCTURES

The reliability of bridge components with respect to different specific limit states can be estimated by using numerical methods (e.g., FORM, SORM and simulations). However, the reliability of the individual structural components does not provide the adequate information to assess the reliability of the whole bridge structural system. It is necessary to implement a methodology for system reliability assessment that accounts for the interaction between the components. In this section, two of the methodologies are summarized.

2.4.1 Series-Parallel System Approach

It is possible to evaluate the entire bridge structural system reliability by making appropriate assumptions (e.g., series, parallel and combined system assumptions) (Ditlevsen & Bjerager 1986, Hendawi & Frangopol 1994) regarding the interaction of individual components. In this method, the reliability of a bridge structural system is evaluated by considering the system failure as series-parallel combination of the component failures. The first step of such an approach is determining the random variables and their statistical parameters for component reliability analysis. All the limit states for all possible failure modes of the components should be included in the system model by considering proper assumptions. For instance the system reliability model of a girder bridge superstructure shown in Figure 2.2 (a), considering only the flexural and shear failure modes of the components (i.e., the girders and the slab), is

27

illustrated in Figure 2.2 (b). The derivation of a limit state equation for a bridge girder varies considerably depending on whether the girder is simply supported or continuous (Akgül and Frangopol 2004). Flexural or shear capacity for girders and the slab can be calculated using the formulas given in AASHTO LRFD Bridge Design Specification (AASHTO, 2010). One major assumption in this model is that the system failure is considered to occur when either slab fails or any two adjacent girders fail. The limitation of this approach is that it is not easy to account for the complex process of interaction between the components and load redistribution, especially when nonlinear behavior is concerned.

2.4.2 Finite Element Approach

Another approach for reliability assessment of bridges makes use of FE analysis, if the non-linear overall system behavior is of interest. A proper statistical distribution for the desired output of FE analysis (e.g., stress, displacement, bending moment) can be obtained by repeating the analysis for a large number of samples of the random variables associated with the structure. However, for complex structures, the time required to repeat FE analysis many times may be impractical. In such cases, Response Surface Method can be used to approximate the relation between the desired output of FE analysis and random variables by performing analyses for only a significantly less number of samples.

Load carrying capacity of a bridge superstructure can be expressed in terms of a load factor, *LF*, when the structure reaches its ultimate capacity or very large vertical displacements causing low levels of safety. Load factor, *LF*, indicates the ratio of the

28

maximum load carried by the bridge to the total weight of AASHTO HS-20 vehicle, when the applied load has the pattern of HS-20 vehicle loading. The failure of the bridge superstructure can be defined by the inequality

$$g = LF - LL < 0 \tag{2.3}$$

where *LL* is the live load effect in terms of the multiples of the AASHTO HS-20 vehicle weight and *g* is the performance function. The material and geometric nonlinearities should be included in the FE model for better accuracy in idealizing the reality. The material nonlinearity may induced by the steel girders, concrete girders and deck, and reinforcing steel. The details of such a procedure can be found in Ghosn, Moses, and Frangopol (2010), Saydam and Frangopol (2011).

2.5 METHODS OF ESTABLISHING SAFETY LEVELS

In the 1930s, when American Association of State Highway Officials (AASHO) started publishing the Standard Specifications for Highway Bridges, only one factor of safety was used to ensure adequate safety level of structural members. The design philosophy was called working stress design (WSD) or allowable stress design (ASD). Until early 1970s, WSD was embedded in the Standard Specifications. AASHTO adjusted WSD to reflect the variable predictability of certain load types by varying the factor of safety in 1970s. The design philosophy is called load factor design (LFD). WSD and LFD are embedded in the current edition of Standard Specification. Today, bridge engineering profession has moved towards a more rational methodology, called load and resistance factor design (LRFD), which accounts for the uncertainties in the structural resistance as well as the uncertainties in loads and their effects.

29

2.5.1 Working Stress Design

WSD establishes allowable stresses as a fraction or percentage of a given material's load-carrying capacity, and requires that calculated design stresses not exceed those allowable stresses. The limiting stress, which can be yield stress or stress at instability or fracture, is divided by a factor of safety to provide the allowable stress. The factor of safety is used to provide a design margin over the theoretical design capacity to allow for consideration of uncertainty due to any components of the design process including calculations, material strengths, and manufacture quality. The condition of safety with respect to the occurrence of a specific failure mode including the factor of safety can be written as

$$\frac{R_n}{FS} = \Sigma Q_i \tag{2.4}$$

where R_n is the member nominal resistance, FS is the factor of safety, and Q_i load effect. The advantage of WSD is its simplicity. However, it lacks the adequate account of uncertainty. Factor of safety does not depend on reliability theory and is chosen subjectively by the code writers. Furthermore, the stresses may not be a good measure of resistance.

2.5.2 Load Factor Design

In LFD, different types of loads have different load factors accounting for the uncertainties in these loads. The condition of safety with respect to the occurrence of specific failure mode including the load factors can be written as

30

$$R_n \geq \Sigma \gamma_i Q_i \qquad\qquad\qquad (2.5)$$

where γ_i is the load factor. Even though LFD is more complex than WSD, it does not involve safety assessment based on reliability theory.

2.5.3 Load and Resistance Factor Design

While considered to a limited extent in LFD, the design philosophy of LRFD takes uncertainty in the behavior of structural elements into account in an explicit manner. Load and resistance factors are used for design at section and component levels. LRFD suggests the use of resistance factor and partial load factors to account for the uncertainties in the resistance and the load effect. The partial load factor approach was originally developed during 1960s for reinforced concrete structures. It gives the opportunity for live and wind loads to have greater partial load factors than the dead load due to the fact that live loads and wind loads have greater uncertainty. The condition of safety with respect to the occurrence of specific failure mode including the reduced resistance and factored loads using resistance and partial load factors can be expressed as

$$\phi R_n \geq \eta_i \Sigma \gamma_i Q_i \qquad\qquad\qquad (2.6)$$

ϕ is the resistance factor and η_i is the load modifier (AASHTO, 2010).

Load and resistance factor design is based on the ultimate strength of critical member sections or the load carrying capacity of members (Ellingwood et al. 1980). In LRFD, the resistances R and the load effects Q are usually considered as statistically independent random variables. If the resistance R is greater than the load effect Q, a margin of safety exists. On the other hand, since resistance and load effect are random

variables, there is a probability that resistance is smaller than load effect. This probability is related to the overlap area of the frequency distributions of the resistance and load effect and their dispersions.

2.6 STRUCTURAL PERFORMANCE INDICATORS FOR BRIDGES

2.6.1 Performance Indicators Regarding Condition

The conditions of bridges in the United States are rated using two different methods based on visual inspection. The first method is using National Bridge Inventory (NBI) condition rating system (FHWA, 1995). According to NBI condition rating system, the evaluation is for the physical condition of the deck, superstructure, and substructure components of a bridge. The second method, Pontis (Cambridge Systematics, Inc., 2009), uses the element-level condition rating method to describe the conditions of bridges.

2.6.1.1 NBI Condition Ratings

Condition codes are properly used when they provide an overall characterization of the general condition of the entire component being rated. Conversely, they are improperly used if they attempt to describe localized or nominally occurring instances of deterioration. Correct assignment of a condition code should consider both the severity of the deterioration and the extent to which it is widespread throughout the component being rated. The load-carrying capacity of the structure has no influence on the condition ratings. NBI condition rating describes the conditions of bridge deck, superstructure and substructure using a scale of 0 to 9 (FHWA, 1995). These condition

states are described in Table 2.1. A highway bridge is classified as structurally deficient if the deck or superstructure or substructure has a condition rating of 4 or less in the NBI rating scale.

2.6.1.2 Pontis Condition Ratings

Pontis (Cambridge Systematics, Inc., 2009) is a bridge management system that assists transportation agencies in managing bridge inventories and making decisions about preservation and functional improvements for their structures. Based on visual inspection, Pontis assigns condition states for various bridge components among deck, superstructure and substructure (CDOT, 1998). The condition states vary between 1 and 5 (or 4), with increasing condition state indicating higher damage level. To illustrate, the condition states for an open, painted steel girder are provided in Table 2.2. Applications of Pontis condition rating to bridges can be found in Estes and Frangopol (2003) and Al-Wazeer (2007).

2.6.2 Performance Indicators Regarding Safety

The failure models in time-dependent system reliability analysis are based on four common indicators. These are the probability density function of time to failure, cumulative distribution function of time to failure, survivor function, and failure (hazard) rate function. These measures are mostly used when studying the structural performance until the structural system fails for the first time (e.g., no repair, no reconstruction). In this section, first probability of failure is defined, then the

33

indicators mentioned above are presented and finally the most common performance indicator for bridge structures, reliability index, is discussed.

2.6.2.1 Probability of Failure

The stochastic nature of the structural resistance and the load effects can be described by their probability density functions. The probability of failure of any section, component or system is defined as the probability of occurrence of the event that resistance is smaller than the load effects and can be evaluated by solving the following convolution integral:

$$P_f = P(g \leq 0) = \int_0^\infty F_R(s) f_Q(s) ds \tag{2.7}$$

where g is the performance function, R is the resistance in a certain failure mode, Q is the load effect in the same failure mode, F_R is the cumulative distribution function of R, and f_Q is the probability density function of the load effect Q.

Probability of failure is the basis for most probabilistic performance indicators. It is used at all levels (section, component, system, system of systems). In many cases, it is impossible or very demanding to evaluate P_f by analytical methods. Therefore, numerical methods such as Monte Carlo Simulations are used.

2.6.2.2 Probability Density Function of Time to Failure

The time elapsed from when the bridge structure is put into service until it fails is referred as the time to failure, T. Since the time to failure exhibit uncertainty it is considered as a random variable. The appropriate unit of the time to failure for bridge

structures is the calendar time units such as years and months. To illustrate probability density function (PDF) of time to failure, suppose a set of N_0 identical structures are put into service at time $t=0$. As time progresses, some of the structures may fail. Let $N_S(t)$ be the number of survivors at time t. The PDF of time to failure can be expressed as (Ramakumar, 1993)

$$f(t) = \lim_{\Delta t \to 0} \left[\frac{1}{N_0} \frac{N_s(t) - N_s(t + \Delta t)}{\Delta t} \right] = -\frac{1}{N_0} \frac{d}{dt} N_s(t) \tag{2.8}$$

2.6.2.3 Cumulative Distribution Function of Time to Failure

Cumulative distribution function (CDF) of time to failure is also known as cumulative probability of failure. The probability of failure until a certain time represents the CDF of time to failure. It can be expressed as (Rausand and Høyland, 2004)

$$F(t) = P(T \le t) = \int_0^t f(u) du \qquad for \ t > 0 \tag{2.9}$$

where $P(T \le t)$ is the probability of failure within time interval $(0, t]$, $f(t)$ is the PDF of the time to failure and u is the integration variable. $f(t)$ can be expressed in terms $F(t)$ as

$$f(t) = \frac{d}{dt} F(t) = \lim_{\Delta t \to 0} \left[\frac{F(t + \Delta t) - F(t)}{\Delta t} \right] = \lim_{\Delta t \to 0} \left[\frac{P(t \le T \le t + \Delta t)}{\Delta t} \right] \tag{2.10}$$

For small Δt, this implies (Rausand and Høyland, 2004)

$$P(t \le T \le t + \Delta t) \approx f(t) \cdot \Delta t \tag{2.11}$$

2.6.2.4 Survivor Function

35

Survivor function is the probability that a component or system survived until time *t* and still functioning at time *t*. It is also known as the reliability function. Survivor function is the complement of the cumulative time probability of failure and can be expressed as

$$S(t) = 1 - F(t) = P(T > t) = \int_{t_f}^{\infty} f(u)du \qquad for \ t > 0 \tag{2.12}$$

2.6.2.5 Failure (Hazard) Rate Function

Failure rate function is a measure of risk associated with an item at time *t*. It is also known as hazard rate or hazard function. Failure rate also can be defined as the conditional probability of failure in the time interval (*t*, *t*+Δt], given that a component was functioning at time *t* (Ramakumar, 1993). It can be expressed as (Rausand and Høyland, 2004)

$$h(t) = \lim_{\Delta t \to 0} \left[\frac{P(t \leq T \leq t + \Delta t \mid T > t)}{\Delta t} \right] = \lim_{\Delta t \to 0} \left[\frac{F(t + \Delta t) - F(t)}{\Delta t} \frac{1}{S(t)} \right] = \frac{f(t)}{S(t)} \tag{2.13}$$

where $P(\text{t} \leq T \leq t+\Delta t \mid T > t)$ indicates the probability that the structure will fail in the time interval (*t*, *t*+Δt], given that the structure had survived at time *t*. Similarly for PDF of time to failure, this implies for small Δt

$$P(t \leq T \leq t + \Delta t \mid T > t) \approx h(t) \cdot \Delta t \tag{2.14}$$

Failure rate function is a time-dependent performance indicator like the other reliability functions. Application of lifetime functions (e.g., PDF of time to failure, CDF of time to failure, survivor function, and failure rate function) to bridge

components and systems can be found in van Noortwijk and Klatter (2004), Yang et al. (2004), Okasha and Frangopol (2010a), Orcesi and Frangopol (2011).

2.6.2.6 Reliability Index

The reliability of a bridge structure can be expressed in terms of either probability of failure or its corresponding reliability index. As a measure of reliability, reliability index can be defined as the shortest distance from the origin to the limit state surface in the standard normal space. For normally distributed independent variables, the reliability index β can be calculated as

$$\beta = \frac{E(R) - E(Q)}{\sqrt{\sigma^2(R) + \sigma^2(Q)}} \tag{2.15}$$

where $E(R)$ and $E(Q)$ are the mean values of the resistance and load effect, and $\sigma(R)$ and $\sigma(Q)$ are the standard deviations of the resistance and load effect, respectively. First and second order reliability methods (FORM and SORM) which approximately provide the reliability index by searching the most probable point on the failure surface ($g_j = 0$), are the most common methods to compute reliability index. The probability of failure and reliability index are approximately related to each other as follows

$$P_f = 1 - \Phi(\beta) \tag{2.16}$$

where $\Phi(.)$ indicates the standard normal distribution function. Reliability index is one of the most common performance indicators for performance quantification of bridge structures. For instance, a reliability index level of 3.5 was targeted for establishing the safety levels in calibration of AASHTO LRFD Bridge Design Specification

37

(AASHTO, 2010). Application of reliability to bridge structures can be found in Enright and Frangopol (1999a, b), Estes and Frangopol (1999, 2001), and Akgül and Frangopol (2004a, b).

2.6.3 Performance Indicators Regarding Tolerance to Damage

2.6.3.1 Redundancy

There are several definitions and indicators for structural redundancy. A measure of redundancy, in the context of availability of warning before system failure, was proposed by Frangopol and Curley (1987) as

$$RI_1 = \frac{P_{f(dmg)} - P_{f(sys)}}{P_{f(sys)}} \tag{2.17}$$

where $P_{f(dmg)}$ is the probability of damage occurrence to the system, and $P_{f(sys)}$ is the probability of system failure.

A measure of redundancy, as the availability of alternative load path after sudden local damage, was proposed by Frangopol and Curley (1987) as

$$RI_2 = \frac{\beta_{intact}}{\beta_{intact} - \beta_{damaged}} \tag{2.18}$$

where β_{intact} is the reliability index of the intact system and $\beta_{damaged}$ is the reliability index of the damaged system.

Redundancy is a system performance measure. However, it is also applicable at the section and component levels as a measure of warning with respect to failure. AASHTO LRFD Bridge Design Specifications (2010) considers redundancy in bridge structures. The load modifier η_i in Equation 2.6, which accounts for redundancy level,

38

is based on the redundancy definition in Frangopol and Nakib (1991). Application of redundancy concept to deteriorating bridge structures can be found in Okasha and Frangopol (2009, 2010b), Ghosn, Moses, and Frangopol. (2010), and Saydam and Frangopol (2011).

2.6.3.2 Vulnerability and Damage Tolerance

Vulnerability is a performance measure used to capture the essential feature of damage tolerant structures. A probabilistic measure of vulnerability was proposed by Lind (1995), defined as the ratio of the failure probability of the damaged system to the failure probability of the undamaged system

$$V = \frac{P(r_d, Q)}{P(r_0, Q)} \tag{2.19}$$

where r_d indicates a particular damaged state, r_0 indicates a pristine system state, Q is the prospective loading, $P(r_d, Q)$ represents the probability of failure of the system in the damaged state, $P(r_0, Q)$ represents the probability of failure of the system in the pristine state, and V refers to vulnerability of the system in state r_d for prospective loading Q. The vulnerability V is 1.0 if the probabilities of failure of the damaged and intact systems are the same. Lind (1995) also defined the damage tolerance of a structure as the reciprocal of vulnerability. Vulnerability and damage tolerance are system level performance indicators. Application of time-dependent vulnerability concept to bridge structures can be found in Saydam and Frangopol (2011).

2.6.3.3 Robustness

39

Robustness is one of the key measures in the field of progressive collapse and damage tolerant structures. Although robustness is recognized as a desirable property in structures and systems, there is not a widely accepted theory on robust structures. Maes, Fritzson, and Glowienka (2006) defined robustness of a system as

$$ROI_1 = \min_i \frac{P_{f_0}}{P_{f_i}} \qquad (2.20)$$

where P_{f0} is the system failure probability of the undamaged system, and P_{fi} is the system failure probability assuming one impaired member i.

Baker *et al*. (2008) stated a robust system to be one where indirect risks do not contribute significantly to the total system risk, and proposed a robustness index defined as follows:

$$ROI_2 = \frac{R_{Dir}}{R_{Dir} + R_{Ind}} \qquad (2.21)$$

where R_{Dir} and R_{Ind} are the direct and indirect risks, respectively. This index varies between 0 and 1.0 with larger values representing a larger robustness. Robustness is a system performance indicator. Additional robustness indicators and applications to bridge structures are indicated in Ghosn and Frangopol (2007), Biondini, Frangopol, and Restelli (2008), Ghosn, Moses, and Frangopol (2010), Biondini and Frangopol (2010), and Saydam and Frangopol (2011).

2.6.4 Performance Indicators Regarding Cost

2.6.4.1 Life-Cycle Cost

40

One of the most important measures in evaluation of structural performance is life-cycle cost. The proper allocation of resources can be achieved by minimizing the total cost while keeping structural safety at a desired level. The expected total cost during the lifetime of a bridge structure can be expressed as (Frangopol et al. 1997)

$$C_{ET} = C_T + C_{PM} + C_{INS} + C_{REP} + C_F \qquad (2.23)$$

where C_T is the initial cost, C_{PM} is the expected cost of routine maintenance cost, C_{INS} is the expected cost of inspections, C_{REP} is the expected cost of repair, and C_F is expected failure cost.

Life-cycle cost and performance level of a bridge structure are two conflicting criteria. A lot of research has been done in the area of balancing cost and performance and optimum planning for life-cycle management of civil structures and infrastructures (Chang and Shinozuka 1996, Ang and De Leon 1997, Frangopol, Lin, and Estes 1997, Frangopol, Kong, and Gharaibeh 2001, Ang, Lee, and Pires 1998, Estes and Frangopol 1999, Okasha and Frangopol 2010c).

2.6.4.2 Risk

The most common formulation of risk in engineering is multiplication of probability of occurrence by the consequences of an event. Direct risk is the one associated with the damage occurrence itself while indirect risk is associated with the system failure as a result of the damage. Direct and indirect risks are formulated as (Baker, Schubert, and Faber 2008)

$$R_{Dir} = \iint_{x \, y} C_{Dir} f_{D|E}(y \mid x) f_E(x) dy dx \qquad (2.24)$$

41

$$R_{Indir} = \int_x \int_y C_{Indir} P(F \mid D = y) f_{D|E}(y \mid x) f_E(x) dy dx \qquad (2.25)$$

where C_{Dir} and C_{Indir} are the direct and indirect consequences, x and y are the random variables in the event tree, $f_X(x)$ and $f_Y(y)$ are used to denote the probability density functions of random variables x and y. E, D and F represent the hazard occurrence, damage occurrence, and system failure, respectively. These integrals can be computed with numerical integration or Monte Carlo Simulation. Risk is applicable at component and system levels as well as system of systems level.

Table 2.1   NBI condition ratings for deck, superstructure and substructure

(adopted from FHWA, 1995)

CODE	DESCRIPTION
N	NOT APPLICABLE
9	EXCELLENT CONDITION
8	VERY GOOD CONDITION - no problems noted.
7	GOOD CONDITION - some minor problems.
6	SATISFACTORY CONDITION - structural elements show some minor deterioration.
5	FAIR CONDITION - all primary structural elements are sound but may have minor section loss, cracking, spalling or scour.
4	POOR CONDITION - advanced section loss, deterioration, spalling or scour.
3	SERIOUS CONDITION - loss of section, deterioration, spalling or scour have seriously affected primary structural components.
2	CRITICAL CONDITION - advanced deterioration of primary structural elements. Unless closely monitored it may be necessary to close the bridge until corrective action is taken.
1	"IMMINENT" FAILURE CONDITION - major deterioration or section loss present in critical structural components or obvious vertical or horizontal movement affecting structure stability.
0	FAILED CONDITION - out of service - beyond corrective action.

Table 2.2   Pontis condition ratings for open, painted steel girder element (adopted

from CDOT, 1998)

CONDITION STATE	DESCRIPTION
1	There is no evidence of active corrosion and the paint system is sound and functioning as intended to protect the metal surface.
2	There is little or no active corrosion. Surface or freckled rust has formed or is forming. The paint system may be chalking, peeling, curling or showing other early evidence of paint system distress but there is no exposure of metal.
3	Surface or freckled rust is prevalent. The paint system is no longer effective. There may be exposed metal but there is no active corrosion which is causing loss of section.
4	The paint system has failed. Surface pitting may be present but any section loss due to active corrosion does not yet warrant structural analysis of either the element or the bridge.
5	Corrosion has caused section loss and is sufficient to warrant structural analysis to ascertain the impact on the ultimate strength and/or serviceability of either the element or the bridge.
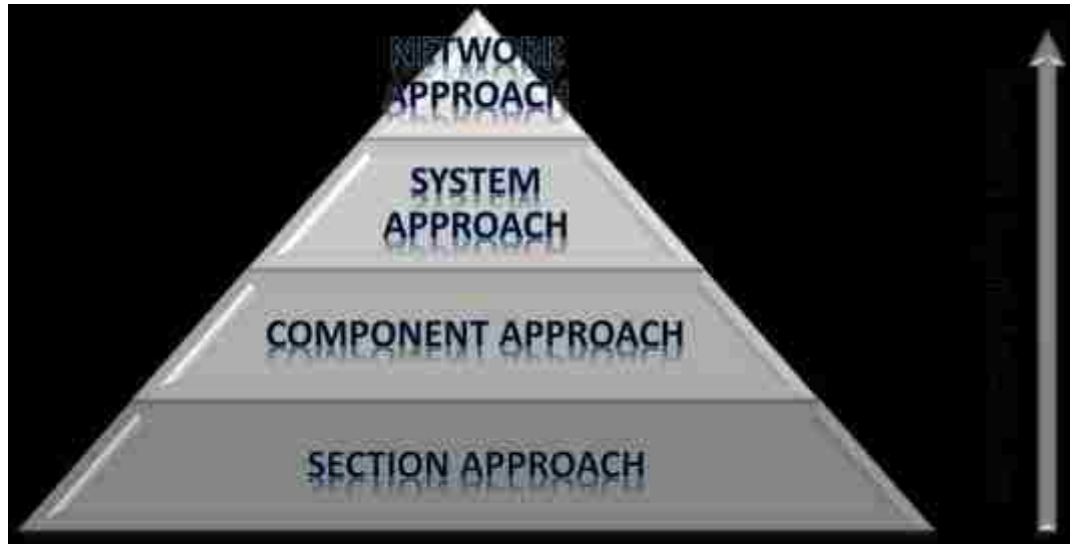
Figure 2.1   Levels of performance assessment for structures and infrastructures

45

SFS   : Shear failure of slab   FFS   : Flexural failure of slab
SFG1 : Shear failure of girder 1   FFG1 : Flexural failure of girder 1
SFG2 : Shear failure of girder 2   FFG2 : Flexural failure of girder 2
SFG3 : Shear failure of girder 3   FFG3 : Flexural failure of girder 3
SFG4 : Shear failure of girder 4   FFG4 : Flexural failure of girder 4
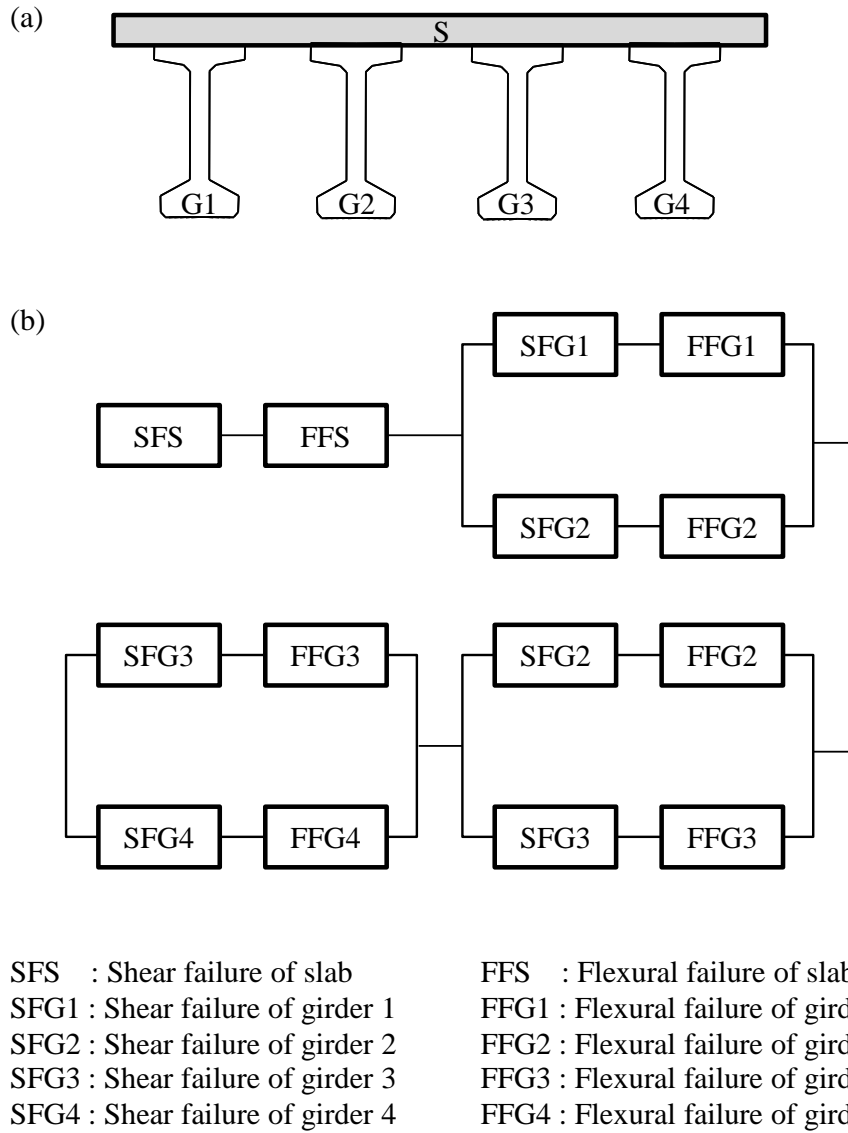
Figure 2.2   System reliability model for bridge superstructures

CHAPTER 3

TIME-DEPENDENT PERFORMANCE INDICATORS OF DAMAGED

BRIDGE SUPERSTRUCTURES

3.1 INTRODUCTION

Structural systems are required to maintain adequate levels of serviceability and safety throughout their lifetime. However, deterioration processes due to harsh environmental conditions and sudden localized damage caused by extreme events may lead to unacceptable levels of functionality and safety. Traditionally, structural design codes focus on the safety of individual components and connections among these components in order to ensure the overall safety of a structure. Nevertheless, the catastrophic failures in the past (e.g., terrorist attack on World Trade Center and collapse of I-35W Mississippi River Bridge in Minneapolis) showed that including system-based performance measures in the design is required in order to assure the global safety of structures.

A common terminology on damage tolerance is not available yet, even though it is a desired structural property. Several researchers focused on the field of damage tolerant structures and they referred damage tolerance with various related measures. These measures include collapse resistance (Ellingwood and Dusenberry 2005), vulnerability and damage tolerance (Lind, 1995), robustness (Blockley et al. 2002, Maes, Fritzson, and Glowienka 2006, Baker et al. 2008, Ghosn, Moses, and Frangopol 2010), and redundancy (Frangopol and Curley 1987, Fu and Frangopol 1990).

47

Civil structural and infrastructural systems are subjected to deterioration in strength and performance due to the aggressive environmental conditions (e.g., corrosion, fatigue). The serviceability and safety of these systems are highly influenced by their deteriorations. Furthermore, the ability of a structure to survive an extreme event without system collapse reduces in time due to the deterioration process. Therefore, in the lifetime management of structures and infrastructures, the resistance to sudden local damage has to be considered together with the effect of progressive deterioration. Time-dependent redundancy of structures, in the context of availability of warning before structural failure under live loading, was studied by Okasha and Frangopol (2009, 2010a and 2010b). Saydam and Frangopol (2010) studied time-dependent vulnerability of structural systems under progressive and sudden damage separately. Risk-based robustness of structures under deterioration was investigated by Baker, Schubert, and Faber (2008). However, to the best knowledge of the authors, time-dependent redundancy, as the availability of alternative load path under sudden local damage, time-dependent vulnerability including combined effects of deterioration, and time-dependent robustness based on reliability have not been investigated yet.

The aim of this chapter is to present a methodology for estimation of time-dependent performance indicators of civil structures and infrastructures including vulnerability, redundancy and robustness (Saydam and Frangopol 2011). A brief theoretical background and selected structural performance indicators regarding vulnerability, redundancy and robustness are presented. The framework is applied to an existing bridge, the I-39 Northbound Bridge over Wisconsin River. The approach is

48

based on probabilistic performance assessment supported by finite element analysis. A detailed finite element (FE) model of the bridge is built using FE software ABAQUS (ABAQUS 2009). Nonlinear incremental static analysis is performed to find the load carrying capacity of the bridge superstructure. Several local damage scenarios are applied by removal of structural members. Bridge load carrying capacity throughout the lifetime for each damage scenario is approximated by using Response Surface Method (RSM), (Box and Wilson 1953). Lifetime vulnerability, redundancy and robustness profiles for local damage scenarios are computed considering uncertainties. The software CalRel (Liu, Lin, and Kiureghian 1989) is used to compute the point-in-time reliability. The time-dependent effects of corrosion on structural reliability, vulnerability, redundancy and robustness are investigated.

3.2 METHODOLOGY TO ASSESS TIME-DEPENDENT PERFORMANCE

Time-dependent assessment of vulnerability, redundancy and robustness requires several methods from various disciplines. A step-by-step procedure is described herein. Since these performance indicators are event-based, the damage scenarios (e.g., sudden failure of a structural member) to be considered must be selected first. In addition, the time-dependent deterioration rate must be identified. The capacity of the structure in concern should be determined by means of structural analysis. Therefore, FE method is essential for complex structures. However, application of FE method in the whole random variable space is impractical in terms of the computational time. Further methods for approximating the structural response based on FE analysis results are required. RSM is one such method which provides a relation between the

49

structural response and the random variables associated with the resistance (Ghosn, Moses, and Frangopol 2010).

Once response functions corresponding to each damage scenario and each point in time are obtained, the next step is the computation of time-dependent system failure probabilities and reliability indices considering time-dependent load effects. Vulnerability, redundancy and robustness are functions of either system failure probability or reliability index and can be easily calculated after this step. A schematic representation of the computational procedure is shown in Figure 3.1. The results of such an analysis can be useful for design and maintenance optimization of bridge structures.

3.3 PROBABILISTIC ANALYSIS OF BRIDGE SUPERSTRUCTURE SYSTEM

There are basically three levels of probabilistic analysis of bridge structures (Barker and Puckett 2007). In the first level, the design equations contain only partial coefficients (i.e., load and resistance factors). Second level probabilistic methods include the second-moment method, which uses simpler statistical characteristics of the load and resistance variables. The third level probabilistic method is the most complex and requires the information on the probability distributions of each random variable and correlation among the variables. Failure probability is determined by performing a large number of computations using many combinations of possible values of the variables. In this study, third level probabilistic analysis is adopted.

Conventional design strategy of bridge structures is based on component safety checks often using elastic methods of structural analysis. However, this approach does

50

not account for the reserve capacity of the system. Since vulnerability, redundancy and robustness are indicators of system performance, a system-based reliability analysis method is applied in this study. System based reliability approach has been successfully integrated in the lifecycle performance assessment and management of bridge structures (Frangopol et al. 2001, Frangopol 2011).

Reliability analysis of bridge superstructures can be performed using FE method in a probabilistic manner. A proper statistical distribution for the desired output of FE analysis can be obtained by repeating the analysis for whole sample space of random variables associated with the FE model. However, the time required to repeat FE analysis for thousands of samples may be impractical, especially for complex structures. The desired output of FE analysis can be approximated with a significantly less number of samples by using RSM. The remaining part of this section describes the details of this approach.

3.3.1 Modeling Bridge Superstructural System Resistance

Load carrying capacity of a bridge superstructure can be expressed in terms of a load factor, *LF*, when the structure reaches its ultimate capacity or very large vertical displacements causing low levels of safety. Load factor, *LF*, indicates the ratio of the maximum load carried by the bridge to the total weight of AASHTO HS-20 vehicle (AASHTO 2007), when the applied load has the pattern of HS-20 vehicle loading. The vertical deformation limit at which the load carried will be considered as the capacity of the bridge was selected as 0.01 and 0.0075 of the loaded span in several previous

51

studies (Ghosn, Moses, and Frangopol 2010, Okasha and Frangopol 2010c). In this study, a vertical deformation limit of $0.0075L_{span}$ is selected.

The failure of the bridge superstructure can be defined by the inequality;

$$g(t) = LF(t) - LL(t) < 0 \tag{3.1}$$

where $LF(t)$ is the time-dependent load factor and $LL(t)$ is the time-dependent live load effect in terms of the multiples of the AASHTO HS-20 vehicle weight.

In order to compute the capacity of the bridge superstructure accurately, the material and geometric nonlinearities should be included in the FE model. The material nonlinearity is mainly caused by the steel girders, concrete girders and deck, and reinforcing steel. Once the FE model is completed, the most critical location of the bridge to be loaded incrementally should be determined by applying the considered load pattern on several candidate critical locations until the vertical displacement limit is reached in the vicinity of loading area. The loading location which results in the lowest load factor, LF, is assumed to be the correct location to evaluate the capacity of the structure.

3.3.2 Accounting Uncertainties Associated with Resistance

The nonlinear incremental FE analysis, described above, is one of the most accurate methods to find load carrying capacity of a structure. The time required to perform one FE analysis with the current high performance computers for even a complex structure is generally reasonable. The bridge FE model used herein, which consists of 20516 elements, can be analyzed to the failure in 8 minutes of wall clock time (2800 sec of CPU time) in average by using the DELL Precision T7400 workstation. However,

52

including uncertainties in the analysis by means of Monte Carlo Simulation requires repeating the procedure in very large numbers. Therefore, an expression for the capacity of the structure is needed in order to perform reliability analysis. Unfortunately, a closed form expression of the load factor, *LF*, cannot be obtained directly. In several studies, RSM was used to obtain the expression of structural capacity in terms of the random variables of the system (Liu, Ghosn, and Moses 2000, Ghosn and Moses 1998, Ghosn, Moses, and Frangopol 2010).

RSM originated from experimental design and was later introduced into reliability assessment of structural systems. In structural engineering, the basic purpose of RSM is to obtain approximate expressions for the structural resistance based on the FE results. In order to find a mathematical relationship between the response and the random variables, usually a low-order polynomial in some region of random variables is employed. A first order response surface function is in the form of

$$R = a_0 + \sum_{i=1}^{k} a_i x_i + e \tag{3.2}$$

where R is the approximated response, a_0 is a constant, a_i is the coefficient associated with the random variable x_i and e is approximation error (Vanderplaats 2010a). The method of least squares is often used to estimate the parameters in the approximating polynomials. The approximated response surface function can be used for further analysis (i.e., reliability analysis) instead of the exact response of the structure.

3.3.3 Time-dependent Resistance of Bridges

ال**منارة** للاستشارات

www.manaraa.com

Time-dependent resistance of a structure can be computed if the necessary information about the deterioration process is known. Corrosion and fatigue are the most common deterioration processes of bridge structures. In this study, corrosion of structural steel girders, steel bracing members and reinforcement steel bars is assumed to be the cause of deterioration.

The high rate corrosion penetration model described in Park and Nowak (1997) is applied to all girders. It is also assumed that corrosion penetrates to whole web surface and top surface of bottom flange only (Figure 3.2). The effect of corrosion can be modeled as reduction in the cross-sectional area of the steel members in the FE model. Then, the time-dependent mean resistance profile of a structure can be obtained by repeating the procedure including FE analysis and RSM for all points in time.

3.3.4 Bridge Superstructure Loading Model

The load carrying capacity estimation of a bridge structure requires two-step FE analysis. In the first step, the dead load of the structure is applied in a load controlled manner. In the second step, in addition to the loads in the first step, the live load on the structure is incremented until the critical section reached the predefined displacement threshold in a displacement controlled manner. In this chapter, the live load has the configuration of an AASHTO HS-20 design truck. The load from each wheel is represented by a concentrated force on the bridge deck. The position of the truck should be such that lowest load factor, *LF*, is obtained when the critical section reaches the predefined displacement limit.

54

The variation of the bridge live load over time is required in order to perform time-dependent reliability analysis. A time-dependent live load model is adopted herein. This model is based on the variation of the number of trucks passing the bridge over time and interpretation of this data by using extreme value statistics. The details of application of the live load model to bridge structures can be found in Estes (1997).

3.3.5 Bridge Reliability Analysis

Given the time-dependent resistance and load, the time-dependent failure probability of a bridge structure can be expressed as

$$P_f(t) = P[LF(t) - LL(t) < 0] \tag{3.3}$$

where $LF(t)$ and $LL(t)$ are the time-dependent load factor and time-dependent live load effect, respectively. The corresponding reliability index can be computed as

$$\beta(t) = \Phi^{-1}(1 - P_f(t)) \tag{3.4}$$

where $\Phi(.)$ is the cumulative distribution function of standard normal distribution.

3.4 STRUCTURAL VULNERABILITY, REDUNDANCY AND ROBUSTNESS

The design and assessment of structures that suffer from local damage due to abnormal events requires the use of the progressive collapse concept. Progressive collapse can be defined as structural failure that is initiated by localized structural damage and subsequently develops into a failure that involves a major portion of the structural system as a chain reaction (Ellingwood and Dusenberry 2005). Considering

55

multiple hazards and damage states, the probability of structural collapse can be expressed as

$$P(F) = \sum_i \sum_j P(F \mid D_j H_i) \cdot P(D_j \mid H_i) \cdot P(H_i) \tag{3.5}$$

where $P(H_i)$ = the probability of hazard H_i, $P(D_j/H_i)$ = the probability of local damage, D_j, given that H_i occurred, and $P(F/D_jH_i)$ = the probability of collapse, given that hazard and local damage occurred (Ellingwood 2006). The summations are taken over different hazards i and damage states j.

Prevention strategies against progressive collapse can be classified in two main categories: (a) providing the members of the structure adequate local resistance against the effects of the hazard, and (b) providing the structure the ability of surviving its functionality even if a local damage occurred. The latter option can use two different approaches. First approach is based on providing alternative load paths in the case of a critical member has failed. The second approach is based on limitation of local failure to only certain parts of the structure. Figure 3 illustrates the physical meaning of each multiplier in Equation 3.5, the expression for the collapse probability. The multiplier on the right side is related to hazard control which is not usually considered by the designer. The multiplier in the middle is related to the resistance of members against local damage occurrence. The design of structural members strong enough to resist specific hazards may not be efficient economically and also the reliable quantitative information on hazards may not be available. The multiplier on the left side is related to the ability of the structure to continue its functionality at acceptable level given that the local damage occurred. Several performance measures to quantify the tolerance of a structure to localized damage were proposed (Frangopol and Curley 1987, Lind

56

1995, Blockley et al. 2002, Maes, Fritzson, and Glowienka 2006, and Baker et al. 2008, Saydam and Frangopol 2011).

In the collapse analysis of structures there are two types of loadings: the load that causes the structural component to fail (primary load) and the loads that are generated due to the structural motions caused by sudden collapse of the element (secondary loads) (Marjanishvili 2004). The primary loads may result from external abnormal events such as blasts or earthquakes. On the other hand, the internal static and dynamic loads due to the sudden changes in the load path cause the secondary loads. This study focuses on the local damage of members regardless of the loads causing this damage.

The collapse resistance of a structure can be evaluated with several approaches. Indirect method is such an approach where the general design upgrades are implemented to enhance the overall robustness of the structure (Corley 2002). Alternate load path method and direct design method are direct methods. In direct design method, the actual loads that cause the failure of a critical structural member are used to estimate the likelihood of collapse. In the alternate load path method, a primary structural member is removed and the ability of the structure to continue its functionality is evaluated. The residual capacity and the optimum damage tolerant design of structures by removing the critical members were studied in Frangopol and Klisinski (1989) and Frangopol, Klisinski, and Iizuka (1991). In this chapter, the alternate load path approach is applied to evaluate structural vulnerability, redundancy and robustness.

The alternate load path method deals with conditional probability of failure given that the local damage already occurred. Regardless of the likelihood and the cause of the damage, failure probabilities are evaluated. In the remaining part of this section, several indicators of structural vulnerability, redundancy and robustness are presented. These indicators are later computed by using the alternate load path method.

3.4.1 Vulnerability

In structural engineering, vulnerability is one of the key measures used to capture the essential feature of damage tolerant structures. Based on Lind (1995), time-variant vulnerability can be defined as the ratio of the failure probability of the damaged system to the failure probability of the intact system

$$V(t) = \frac{P(r_d(t), Q(t))}{P(r_0, Q(t))} \tag{3.6}$$

where $r_d(t)$ is a particular damaged state, r_0 is a pristine system state, $Q(t)$ is the prospective loading, $P(r_d(t), Q(t))$ is the probability of failure of the system in the damaged state, $P(r_0, Q(t))$ is the probability of failure of the system in the pristine state (i.e., no sudden damage, no deterioration), and $V(t)$ is the vulnerability of the system in state r_d under the prospective loading $Q(t)$. The value of vulnerability is 1.0 if the probabilities of failure of the damaged and intact systems are the same. Lind (1995) also defined damage tolerance as the reciprocal of the vulnerability.

58

3.4.2 Redundancy

Redundancy, which is a measure of reserve capacity, can be defined as the availability of the alternative load paths within a structure. The failure of a single member will not cause the failure of a redundant structure. There are several measures for redundancy in the literature and one of them is presented here and used in this study. Based on Frangopol and Curley (1987), the time-variant redundancy index $RI(t)$ can be expressed as;

$$RI(t) = \frac{\beta_{\text{intact}}}{\beta_{\text{intact}} - \beta_{\text{damaged}}(t)} \tag{3.7}$$

where β_{intact} is the reliability index of the intact system (i.e., no sudden damage, no deterioration) and $\beta_{\text{damaged}}(t)$ is the reliability index of the damaged system.

3.4.3 Robustness

Robustness is generally referred to the ability of a structure to resist progressive collapse under sudden local damage. In other words, tolerance to damage from the extreme or accidental loads; however, it is also applicable to the systems under damage occurring progressively. Robustness is one of the key measures in the field of progressive collapse and damage tolerant structures. Although robustness is recognized as a desirable property in structures and systems, there is not a widely accepted measure of structural robustness. There are several measures for robustness in the literature (Maes, Fritzson, and Glowienka 2006, Baker, Schubert, and Faber 2008, Ghosn, Moses, and Frangopol 2010) and one of them is presented here and used in this study.

59

Maes, Fritzson, and Glowienka (2006) defined robustness for specified performance objectives of a given system, with specified perturbations being applied to the system. A probabilistic measure of robustness, R was proposed as (Maes, Fritzson, and Glowienka 2006)

$$R(t) = \min_i \frac{P_{s0}}{P_{si}(t)} \tag{3.8}$$

where P_{s0} is the system failure probability of the undamaged system, $P_{si}(t)$ is the system failure probability assuming one impaired member i. This chapter focuses on the robustness associated with each damage scenario rather than only the minimum ratio $P_{s0}/P_{si}(t)$. It is worthy to notify that robustness index for each considered damage scenario is identical to the damage tolerance index defined by Lind (1995).

3.5 CASE STUDY: I-39 NORTHBOUND BRIDGE OVER WISCONSIN RIVER

The procedure described to compute the time-dependent vulnerability, redundancy and robustness is applied to the I-39 Bridge which is located near Wausau, WI. It carries US 51 and I-39 Northbound over the Wisconsin River. A structural health monitoring program was conducted on the bridge between July and November 2004 by the personnel from ATLSS Engineering Research Center. According to the report on this program (Mahmoud, Connor, and Bowman 2005), the I-39 Bridge is a five span continuous steel girder bridge, which has slightly curved span lengths of 33.41 m, 42.64 m, 42.67 m, 42.64 m and 33.41 m. The built-up steel plate girders consist of the top and bottom flange plates and a web plate of 132.1 cm height. The steel used in the

60

girders has nominal yield strength of 345 MPa. The bridge was opened to traffic in 1961.

3.5.1 Finite Element Model of the Bridge

In order to find the load carrying capacity of the bridge, a FE model was built including material and geometric nonlinearities. The FE software ABAQUS (ABAQUS 2009) was used for this purpose. The Description of the FE model and the meshing is shown in Figure 3.4. Eight-node doubly curved thick shell elements with reduced integration are used to model the bridge deck and the plates of steel girders. Truss elements are used to model the bracing members between the girders in transverse direction. Uniformly distributed layers of steel rebars embedded into concrete in both longitudinal and transverse directions are used to represent reinforcement of concrete deck. The connections between the reinforced concrete deck and steel girders are modeled as tie connections where all degrees of freedom are identical. The truss members of bracing system are connected to the beams with simple connections.

The FE model was first loaded with the dead load of the bridge superstructure. To find the longitudinal position of the truck loading (HS20 truck), several critical locations on the first, second and third spans were loaded with the truck load pattern incrementally until the displacement threshold was reached. It was concluded that the worst loading position, which yields the lowest load factor, *LF*, is the position when the resultant force of the truck load is on the mid-length of the third span. Therefore, the bridge load carrying capacity is evaluated based on the displacement of this point.

61

The longitudinal position of HS-20 truck on the bridge is shown in Figure 3.5. The transverse position of the truck loading is also important. In reality, the position of a vehicle in transverse direction is a random variable. However, Ghosn, Moses, and Frangopol (2010) positioned two side-by-side trucks such that the outermost wheels of the exterior truck are over the exterior girder. In this study, right wheels of the truck are assumed to be over the exterior girder in a more conservative manner compared to assuming the position as a random variable. The position of the truck loading in transverse direction is presented in Figure 3.6.

3.5.2 Damage Scenarios

Vulnerability, redundancy and robustness, as described previously, are specific to damage scenarios. Several sudden damage scenarios are considered. These are the failure of Girder 2 or the failure of Girder 3 or the failure of Girder 4 or the failure of bracing members in the vicinity of critical section. It was noticed that Girder 1 (the girder most far from the truck load) does not have significant effect on the load carrying capacity. Therefore, failure of Girder 1 is not considered as a damage scenario. Also, considering failure of Girder 2 as a damage scenario may be questioned, since the structure has symmetry in both geometry and loading. However, symmetry in loading diminishes if one of the lanes is closed for traffic due to any reason. The girder numbering is defined in Figure 3.6. The sudden failure of the selected members is introduced to the finite element model by removing these elements from the model.

62

3.5.3 Structural Response of the Bridge

In Figure 3.7, the deformed shape of the original (no member removed) structure under truck loading when the displacement threshold reached is presented. It is obvious that most of the load is carried by Girder 4 and Girder 1 is not affected significantly because of its distance from the applied live load.

A diagram for the vertical displacement of midsection of third span vs. load factor is presented in Figure 3.8. The diagram belongs to the original structure. Because of the effect of the dead load, the initial displacement at zero load level is greater than zero, at Point A. The load factor, which is an indicator of load carrying capacity of the structure, is 7.4 when displacement threshold of 32 cm is reached (Point D). If the structure is further loaded vertically, the load factor increases. Although the ultimate capacity of the bridge model is not reached at the predefined displacement threshold, there may be problems, in reality, which are not accounted in FE model such as connection failure and local stability problems.

The nonlinearity observed in Figure 3.8 is basically due to the yielding of steel material. The progress of steel material yielding in the critical region of Girder 4 at various displacement levels is illustrated in Figures 3.9(a), (b) and (c). The yielding is not initiated at a vertical displacement 8 cm (Point B in Fig. 3.8). At 16 cm of vertical displacement (Point C in Fig. 3.8), yielding is spreading in the bottom flange; however web material is still in the elastic range. When the vertical displacement reaches the threshold level (i.e., 32 cm, Point D in Fig. 3.8), the yielding is already spreading through almost the entire mid-depth of the web. The increase in the curvature between

63

displacement levels of 16 cm and 32 cm, in Figure 3.8, can be explained by the spread of the yielding described above.

FE analyses are repeated at 20-year increments to account for the effect of corrosion. The effect of corrosion is introduced into the model by reducing the thickness of web and bottom flange of each girder (Figure 3.2) according to the high rate corrosion penetration model.

3.5.4 Probabilistic Model of Bridge Resistance and Loading

The material yield stress of each steel girder and the compressive strength of the concrete deck are considered as the random variables associated with system resistance. The steel yield stress of each girder is assumed to be log-normally distributed with mean value of 345 MPa and coefficient of variation of 0.11. The coefficient of correlation between the yield stress of girders is taken as 0.8 (Okasha and Frangopol, 2010c). The compressive strength of concrete slab is assumed to be log-normally distributed with mean value of 28 MPa and coefficient of variation of 0.18.

In order to obtain closed-form expression of bridge capacity, response of the bridge is approximated based on FE analysis results by using RSM. Optimization software VisualDOC (Vanderplaats, 2010b) is used for this purpose. Ghosn, Moses, and Frangopol (2010) used a first order Taylor series expansion to obtain the approximate closed-form of the bridge response. In this study, the load factors, *LF*s, were approximated for all damage cases and all points in time with a linear function of random variables. This is done to avoid the computational expense of full simulations

64

with FE analyses. The response function for the load factor which belongs to the case without damage is

$$LF = 3.789 + 10^{-6} \cdot F_{y1} + 9.24 \cdot 10^{-5} \cdot F_{y2} + 0.01057 \cdot F_{y3}$$
$$+ 0.03674 \cdot F_{y4} + 0.05823 \cdot f_c^{'} \qquad (3.9)$$

where F_{yi} is the yield stress of the steel material of ith girder and $f_c{'}$ is the compression strength of the concrete of the deck. It is observed that the coefficient multiplying yield strength of Girder 1 is very small compared to the others.

The time-dependent live load on the bridge is calculated by combining the traffic data provided in Mahmoud, Connor, and Bowman (2005) and extreme value statistics. The average daily truck traffic is assumed to be 12% of the average daily traffic (Mahmoud, Connor, and Bowman 2005). The parameters for the extreme value distribution of live load factor LL are computed at 20 years increments.

The limit state equation defining the failure of the whole bridge superstructural system can be written in terms of the random variables associated with resistance and the random variable associated with live load. For instance, limit state equation for the failure of the structure without sudden damage is

$$g = 3.789 + 10^{-6} \cdot F_{y1} + 9.24 \cdot 10^{-5} \cdot F_{y2} + 0.01057 \cdot F_{y3}$$
$$+ 0.03674 \cdot F_{y4} + 0.05823 \cdot f_c^{'} - LL = 0 \qquad (3.10)$$

The reliability analyses are performed for all damage cases at 20-year increments with reliability software CalRel (Liu, Lin, and Kiureghian 1989). Annual failure probabilities and corresponding reliability indices in time are obtained for the original (no member removed) structure and four damaged (a member removed) structures.

3.5.5 Time-Dependent Reliability of the Bridge

Time-variation of reliability indices for the original structure and four damage cases under the effects of both corrosion and the live load increase is presented in Figure 3.10(a). In this figure, the reliability curve for failure of a specific component indicates the reliability of structure without that component. In other words, if the failure of Girder 3 occurs when bridge is 40 years old, the reliability index of the structure will suddenly drop from Point A to Point B. For instance, the lifetime reliability profile in the case that girder 3 fails at year 40 and the lifetime reliability profile in the case that girder 3 fails at year 20 are illustrated in Figure 3.10(b). The failure of lateral bracing causes very small decrease in reliability index and is the least critical sudden damage scenario among the considered cases. Failure of Girder 2 and failure of Girder 3 follows, respectively. Failure of Girder 4 causes very large reduction in reliability index and is the most critical damage case due to the fact that truck load is mostly carried by it.

In order to observe the effects of only corrosion and the live load increase on time-dependent performance of the bridge, the reliability curves were split. This is performed by first keeping the live load constant at the initial value and computing the reliability indices under time-dependent corrosion only. Secondly, the steel sections were kept intact by corrosion and reliability indices were calculated considering live load increase in time. The reliability curves for the original structure, the failure of Girder 3 and the failure of Girder 4 with only corrosion, only the live load increase and both corrosion and live load increase are presented in Figure 3.10(c). It can be observed that the reduction in reliability indices due to live load increase is higher than

66

the reduction due to corrosion through the first 50 years of the lifespan. However, for the original structure and the failure of Girder 3, the effect of corrosion becomes more dominant after points A and B, respectively. The time-variation of corrosion penetration has significant effect on this. When Girder 4, which carries largest portion of the live load, fails, the load carrying contribution of the deck becomes much more significant and the effect of corrosion on steel girders gets smaller. Therefore, the curve for only corrosion and the curve for only live load increase for the failure of Girder 4 do not intersect throughout the lifetime. Another observation is that the reliability reduction for the case with both corrosion and the live load increase is not equal to the sum of the reductions for each separately, as expected. This is mostly due to several reasons such as nonlinearity in the structure and the nature of probabilistic analysis. The time-variation of failure probabilities corresponding to the reliability indices in Figure 3.10(a) are shown in logarithmic scale in Figure 3.11.

3.5.6 Time-Dependent Vulnerability of the Bridge

The vulnerability due to each damage case is computed as the ratio of the failure probability of the damaged structure (member removed and considering time-dependent load and resistance) to the failure probability of the intact structure (no member removed and considering initial load and resistance properties) as defined in Equation 3.6. The time-variation of the bridge vulnerability for the four damage cases under the effects of both corrosion and live load increase is presented in logarithmic scale in Figure 3.12(a). The vulnerability of the structure increases in time since the failure probability of the damaged structure is increasing due to the corrosion and the

67

live load increase while the failure probability of the intact structure is constant. To illustrate the computation of vulnerability, the value at Point A in Figure 3.12(a) (vulnerability for the failure of Girder 4 when the bridge is 40 years old) is obtained by dividing the value at Point A in Figure 3.11 (the bridge failure probability for failure of Girder 4 when the bridge is 40 years old) by the value at Point B in Figure 3.11 (the bridge failure probability for the failure of original structure initially). The failure of Girder 4 yields the highest vulnerability values among other damage cases. The failure of Girder 3, the failure of Girder 2 and the failure of the lateral bracing follows, respectively. It is observed from Figures 3.12(a) and (b) (in linear scale), that the time-dependent vulnerability of a deteriorating structure increases with low rates in the early stages of the lifespan. However, the variation rate increases dramatically through the end of lifespan as the effect of deterioration mechanisms become more significant. The rate of variation in vulnerability is highest for the most critical damage case and lowest for the least critical damage case.

Figures 3.12(b) and (c) compare the effects of only the corrosion, only the live load increase and both the corrosion and the live load increase on the vulnerability for the failure of Girder 3 and the failure Girder 4, respectively. The vulnerability for the failure of Girder 3 (Fig. 3.12(b)) increases in time with a much higher rate under combined effects of the corrosion and the live load increase than the effects of only the corrosion and only the live load increase, separately. The vulnerability under only corrosion is less than that under only the live load increase through almost first 50 years of the lifespan. However, the effect of the corrosion becomes more significant after Point A in Figure 3.12(a), similar to case for the reliability index.

68

3.5.7 Time-Dependent Redundancy of the Bridge

The redundancy index for each damage case is computed by dividing the reliability index of the intact structure (no member removed and considering initial load and resistance properties) by the difference between the reliability indices of the intact structure and the damaged structure (member removed and considering time-dependent load and resistance), as defined in Equation 3.7. The time-variation of the redundancy index for the four damage cases under the effects of both the corrosion and the live load increase is presented in Figure 3.13(a). The redundancy index decreases in time since the reliability index of the damaged structure decreases while the reliability index of the intact structure is constant, yielding the denominator increase. As an example for computation of the redundancy index, the value at Point A in Figure 3.13(a) (the redundancy index for the failure of Girder 3 when the bridge is 40 years old) is obtained by dividing the value at Point C in Figure 3.10(a) (the reliability index for the intact structure) by the difference between the value at Point C and Point B in Figure 3.10(a) (the reliability index for the failure of Girder 3 when the bridge is 40 years old). The structure is most redundant for the failure of the bracing and least redundant for the failure of Girder 4. It is observed that the redundancy index decreases with higher rates in the early stages (between Points B and C in Figure 3.13(a)) compared to the rest of the lifespan, as the denominator (β_{intact} - $\beta_{damaged}$) increases causing very low levels of the redundancy index. The rate of variation in the redundancy index is highest for the least critical damage scenario and lowest for the most critical damage scenario.

69

Figures 3.13(b) and (c) compare the effects of only the corrosion, only the live load increase and both the corrosion and the live load increase on the redundancy for the failure of Girder 3 and the failure Girder 4, respectively. It is observed from Figure 3.13(b) that the redundancy for the failure of Girder 3 under only the live load increase reduces with significantly higher rates than the redundancy under only the corrosion in the early stages (between Points A and B). The effect of the corrosion starts becoming more significant after Point B and causes more reduction in the redundancy index that the increase in live load after Point C. However, this behavior is not observed for the failure of Girder 4 (Fig. 3.13(c)) since the effect of the corrosion of steel girders on the load carrying capacity is much less than that in the other damage cases.

3.5.8 Time-Dependent Robustness of the Bridge

The robustness for each damage case is calculated as the ratio of the failure probability of the intact structure to the failure probability of the damaged structure (Equation 3.8). The time-variation of the robustness for the four damage cases under the effects of both the corrosion and the live load increase is presented in logarithmic scale in Figure 3.14(a). The robustness decreases in time since the failure probability of the damaged structure increases while the failure probability of the intact structure is constant. For instance, the robustness value at Point A in Figure 3.14(a) (the robustness for the failure of Girder 4 when the bridge is 40 years old) is obtained by dividing the value at Point B in Figure 3.11 (the failure probability for the intact structure) by the Point A in Figure 3.11 (the bridge failure probability for the failure of Girder 4 when the bridge is 40 years old). The structure is most robust for the failure

70

of the bracing and least redundant for failure of Girder 4. It is observed that robustness decreases with much higher rates in the early stages (between Points A and B in Figure 3.14(b)) compared to the rest of the lifespan, as the denominator ($P_{f,damaged}$) increases causing very low levels of the robustness. The rate of variation in the robustness is highest for the failure of bracing and lowest for the failure of Girder 4.

Figures 3.14(b) and (c) compare the effects of only the corrosion, only the live load increase and both the corrosion and the live load increase on the robustness for the failure of Girders 3 and 4, respectively. It is observed from Figure 3.14(b) that the robustness for the failure of Girder 3 under only the live load increase reduces with significantly higher rates than redundancy under only the corrosion in the early stages (between Points A and B). The effect of the corrosion starts becoming more significant after Point B and causes more reduction in the redundancy index than the increase in live load after Point C. However, this behavior is not observed for the failure of Girder 4 (Fig. 3.14(c)) due to the reason explained previously for the reliability index and the redundancy index.

It is worthy to notify that the redundancy and the robustness indicators used in this study are the measures of similar features of a structure. However, they are defined in different mathematical form. The redundancy is the availability of alternate load path in the case of a critical member is not functioning. Although robustness has a wider definition, the robustness index used herein refers to the ability of the structure to continue its function in the absence of a critical member. The vulnerability indicator is the reciprocal of the robustness used in this study. This can be easily observed by examining the Figures 3.12(a) and 3.14(a) since they are plotted in logarithmic scale.

71

The variation of the vulnerability and the redundancy index with respect to time-dependent reliability index is illustrated in Figure 3.15. The horizontal axis depicts the reliability index values through the lifetime of the structure for the failure of Girder 3 scenario. The vulnerability and the reliability have an inverse relationship, as the vulnerability is low for higher values of the reliability index and high for lower values of the reliability index. However, it is observed that there is a positive correlation between the redundancy index and the reliability index. As the reliability index decreases in time, the redundancy also decreases.

3.6 CONCLUSIONS

The interest on structural vulnerability, redundancy and robustness has been increasing in recent years. Even though the concepts regarding damage tolerance are not strictly enforced in practice by the current structural codes, there is tendency to design more redundant and robust structures. Nevertheless, design and maintenance of damage tolerant bridge structures requires life-cycle assessment, since performance regarding vulnerability, redundancy and robustness reduces in time due to the environmental sources of deterioration.

In this chapter, a framework for predicting the lifetime vulnerability, redundancy and robustness of bridge superstructures is presented. The framework is based on probabilistic performance assessment supported by FE analysis. Selected indicators of vulnerability, redundancy and robustness, available in the literature, are described and a brief theoretical background is presented. A five-span, steel girder bridge is investigated as a case study. The computation of the vulnerability,

redundancy and robustness indicators requires advanced modeling techniques of estimating the life-cycle performance. An FE model of the bridge superstructure is built using the software ABAQUS in order to perform nonlinear incremental static analyses. RSM is used to establish closed form relation between the structural capacity and the random variables using the software VisualDOC. The point-in-time reliability is computed using the reliability software CalRel. The performance of a structural system is represented by a single limit state function based on probabilistic FEA. The lifetime vulnerability, redundancy and robustness indicators are computed at 20-year increments.

The following conclusions can be drawn:

1. Structural performance indicators of bridges associated with reliability, vulnerability, redundancy and robustness deteriorate in time due to various causes such as corrosion and live load increase. The dominant cause of performance reduction may change throughout the lifespan. In general, at the early stages of lifetime, the live load increase is dominant; however, the effect of corrosion becomes more dominant as section loss due to the corrosion gets significant at later stages.

2. The vulnerability for a predefined damage scenario may increase significantly in time due to the corrosion and the live load increase. This increase starts with relatively low rates in the early stages of lifespan and continues with high rate through the end of lifespan. The rate of variation in the vulnerability is highest for the most critical damage case and lowest for the least critical damage case.

73

3. The redundancy of a structure for a predefined damage scenario may decrease rapidly in time. This reduction is largest for the damage case with the lowest redundancy. The redundancy decreases with higher rates at early stages compared to the rest of the lifespan.

4. The robustness follows similar trends like the redundancy. It decreases very rapidly at early stages of the lifespan. The robustness related to only the live load increase reduces with significantly higher rates than the robustness related to only the corrosion in the early stages and the effect of the corrosion becomes more significant later on.

5. The bridge superstructure analyzed in this chapter has relatively few strong girders. Therefore the failure of one girder yields high level of vulnerability, depending on the position of the load. However, a bridge with more girders which are weaker can be more robust and redundant because of the availability of alternate load paths.

6. Reliability, vulnerability, redundancy and robustness are very sensitive to the location of the loading within the presented framework. Various transverse locations of different loadings should be considered in performance assessment and prediction of bridge structures.

The purpose of obtaining lifetime profiles of vulnerability, redundancy and robustness is to use them in design and maintenance optimization of structures. One objective of such optimization problems can be minimization of vulnerability, maximization of redundancy or robustness; while other objectives will be minimization of total life-cycle cost and maximization of reliability. It is worthy to

74

notice that conditional probability of failure, given the damage occurred, is used to compute the vulnerability, redundancy and robustness indicators. Another methodology can be based on the unconditional probability of failure including the probability of hazard and probability of damage occurrence when the hazard has affected the structure. It is possible to combine structural performance for different damage scenarios in a rational way with this approach. Nevertheless, obtaining adequate and reliable data on the hazard probabilities and estimating the probability of damage occurrence given the hazard is a very difficult task.

75

Select sudden damage
scenarios and corrosion
rate to be considered

Build finite element
model of bridge
superstructure

Determine random
variables associated
with resistance

Obtain response surface
function based on
random variables

Input time-dependent
load

Obtain probability of
system failure and
system reliability index

Compute time-dependent
vulnerability, redundancy
and robustness indices

Obtain lifetime profiles

Use the data in
lifetime management
of the structure

REPEAT FOR ALL SUDDEN DAMAGE SCENARIOS

REPEAT FOR DESIRED POINTS IN TIME

Figure 3.1   Flowchart for obtaining lifetime vulnerability, redundancy and
robustness

76
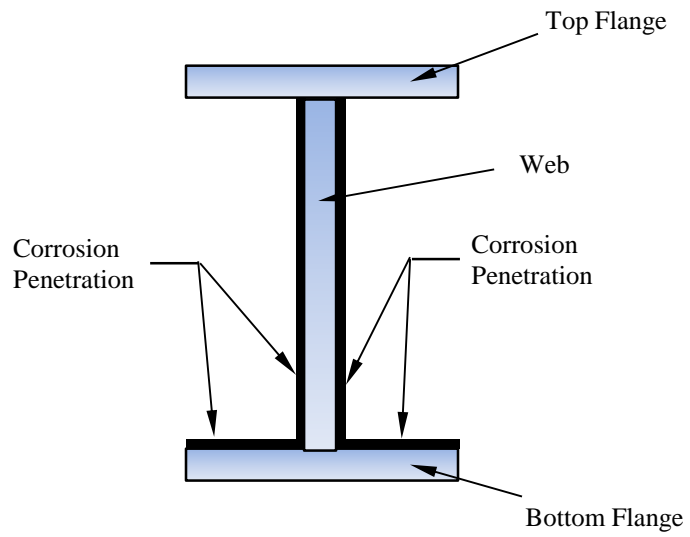
Figure 3.2   Corrosion penetration pattern on steel girders

77

$$P(F) = \underbrace{P(F\,|\,DH)}_{\substack{\text{-VULNERABILITY} \\ \text{-ROBUSTNESS}}} \cdot \overbrace{P(D\,|\,H)}^{\substack{\text{MEMBER} \\ \text{RESISTANCE} \\ \text{TO DAMAGE}}} \cdot \overbrace{P(H)}^{\substack{\text{HAZARD} \\ \text{CONTROL}}}$$

ALTERNATIVE
LOAD PATH

LIMITATION OF LOCAL
DAMAGE TO CERTAIN
PARTS OF THE STRUCTURE

REDUNDANCY

Figure 3.3   Components of collapse resistance
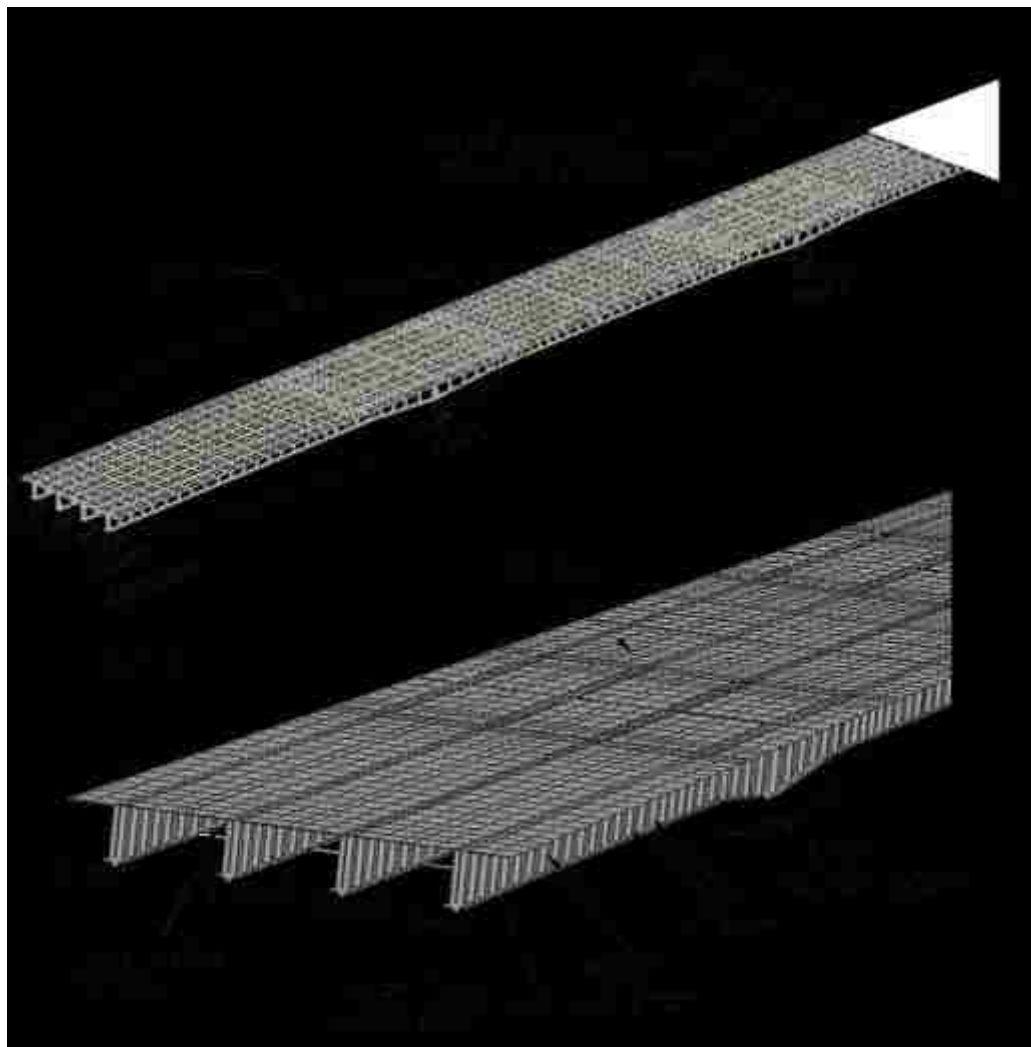
Figure 3.4   Finite element model view (South end)

Detail A

Axis of symmetry of bridge in longitudinal direction and center of gravity of HS20 truck
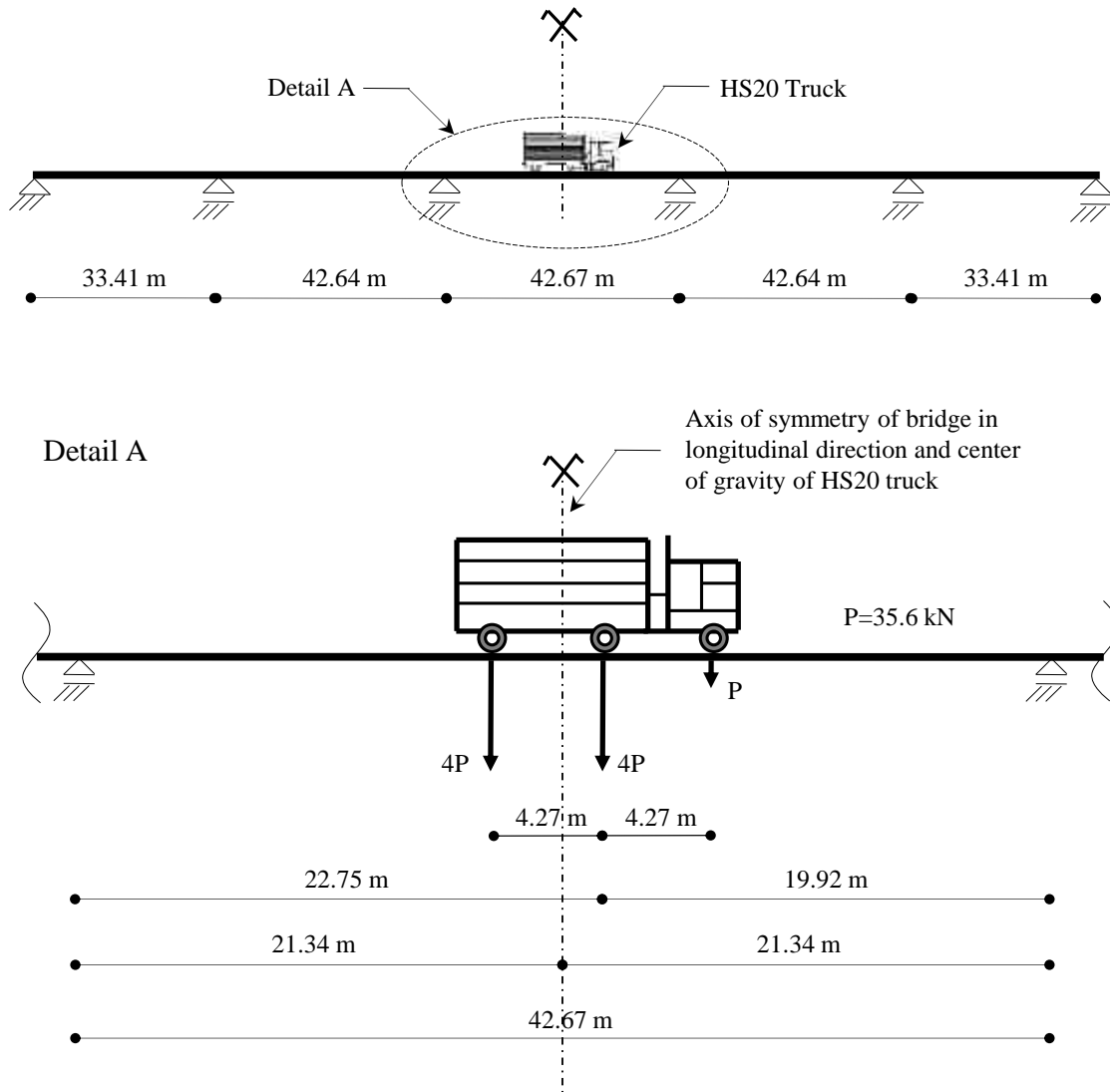
Figure 3.5   Longitudinal position of the truck loading pattern
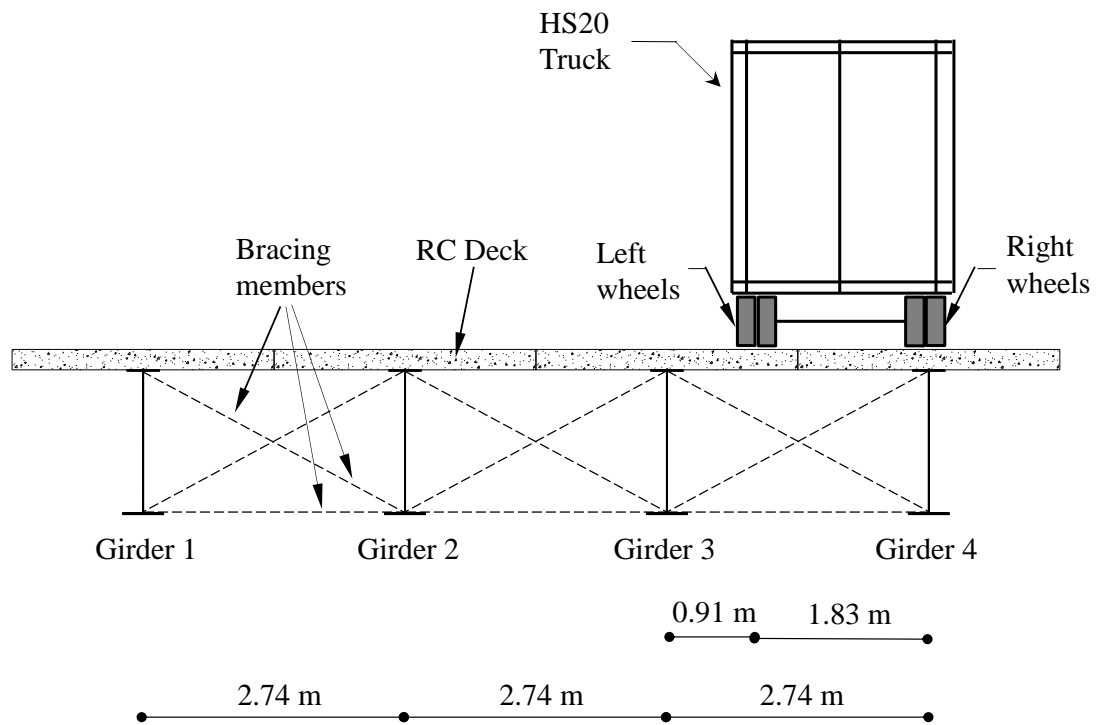
Figure 3.6   Lateral position of truck loading
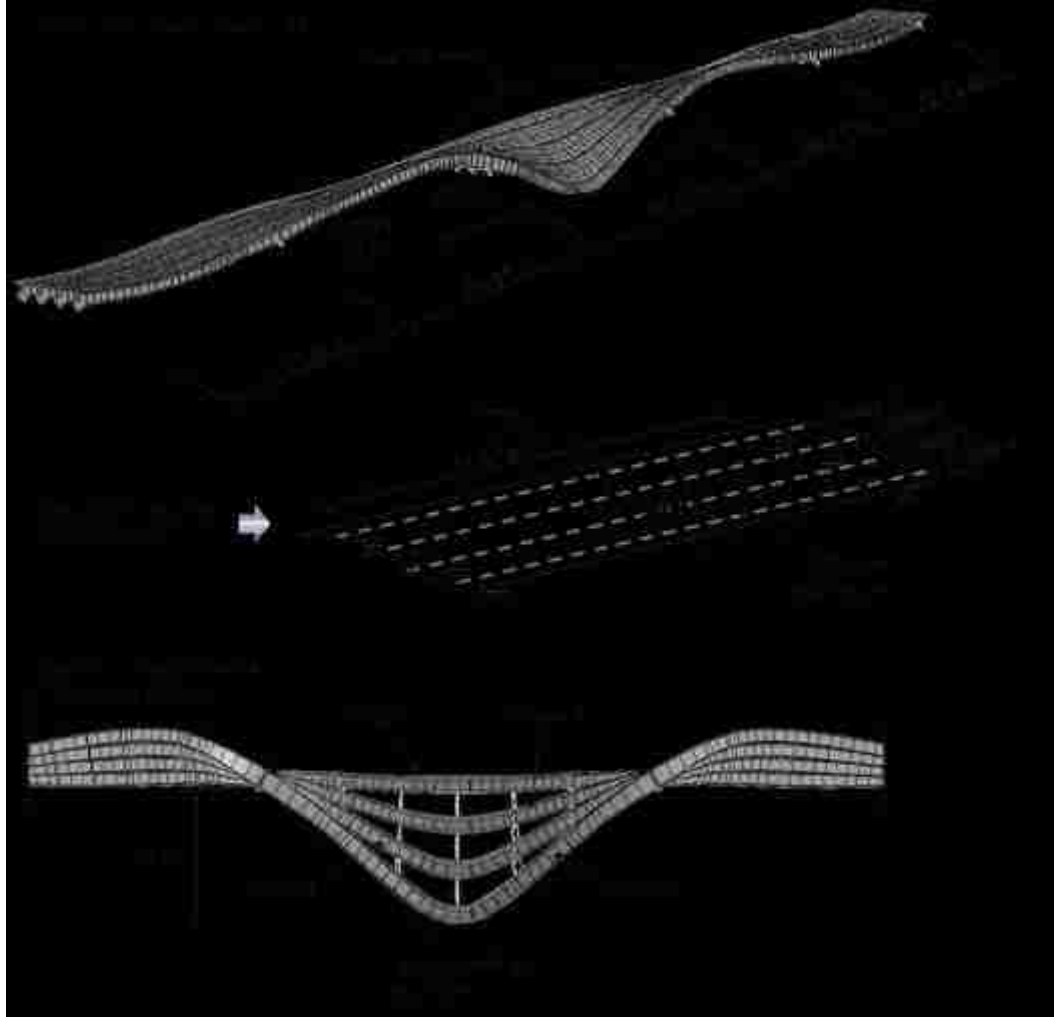
Figure 3.7   Deformed shape of bridge (original structure)
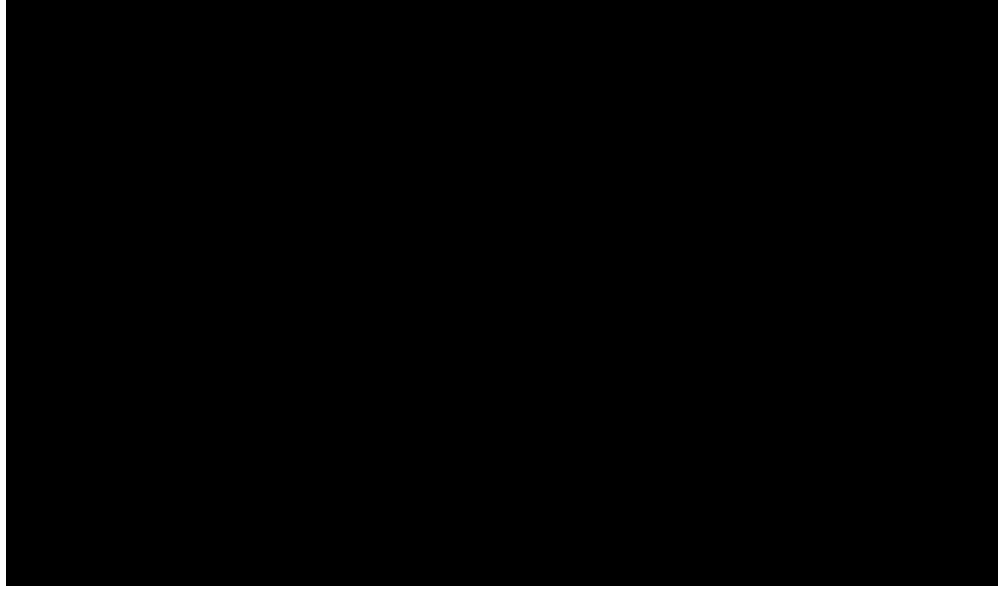
Figure 3.8   Diagram for live load factor vs. vertical displacement of midsection of

third span (belongs to original structure)
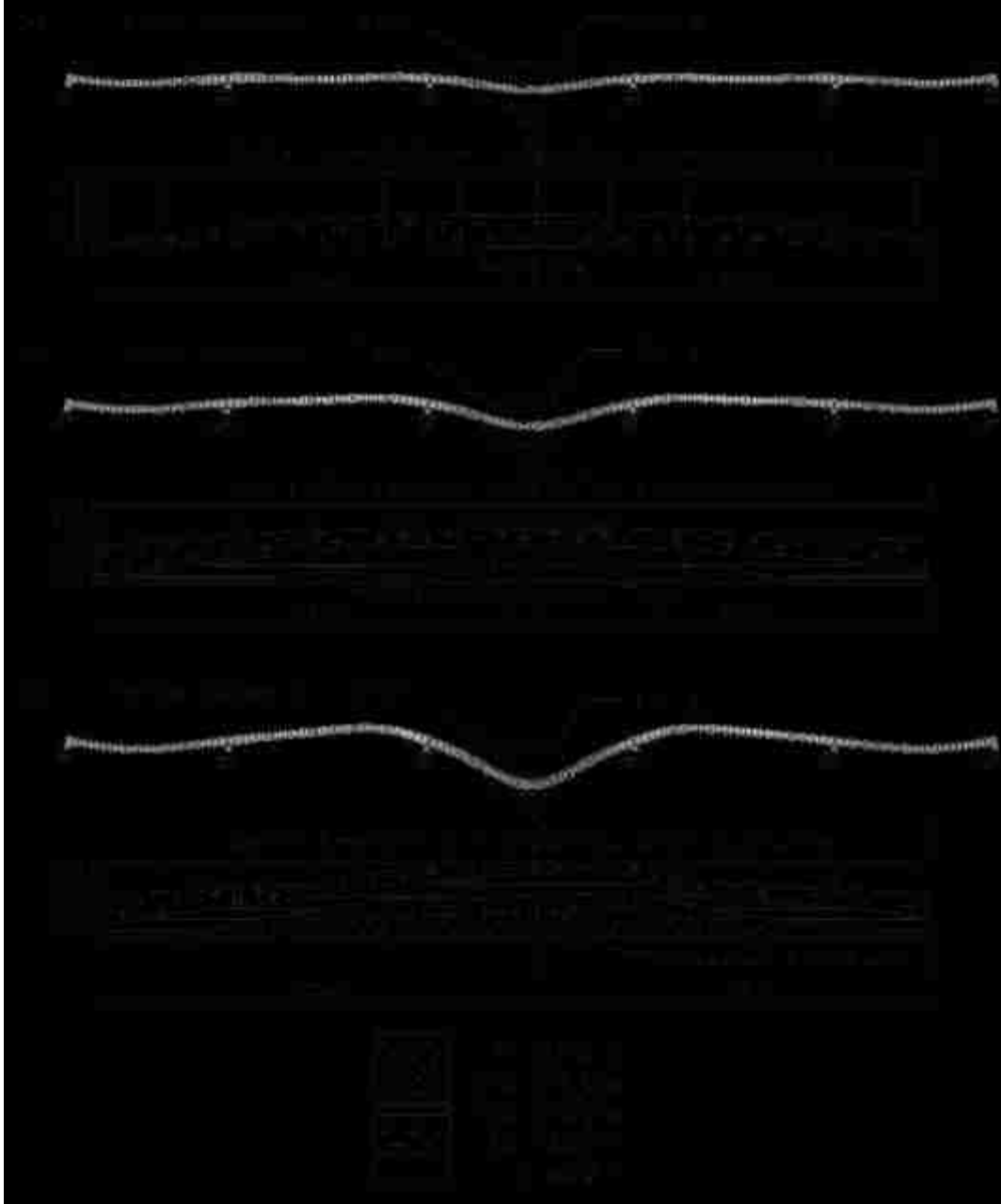
Figure 3.9   Spread of yielding in loading area (belongs to intact structure) at (a) vertical displacement = 8 cm, (b) vertical displacement = 16 cm and (c) vertical displacement = 32 cm.
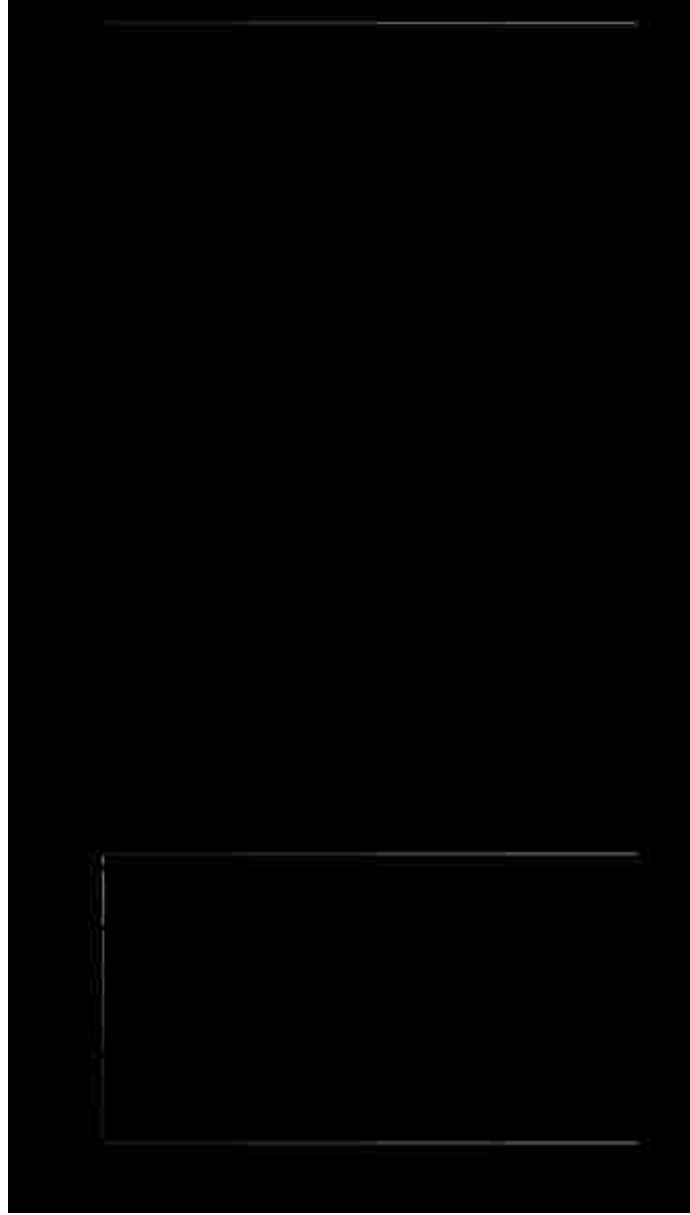
Figure 3.10   (a) Time-variation of reliability index under effects of both corrosion
and increase in live load; (b) illustrative reliability profiles under
sudden damage; (c) comparison of the effects of only corrosion, only
live load increase and both corrosion and live load increase on
reliability for original structure, failure of girder 3 and failure of girder
4
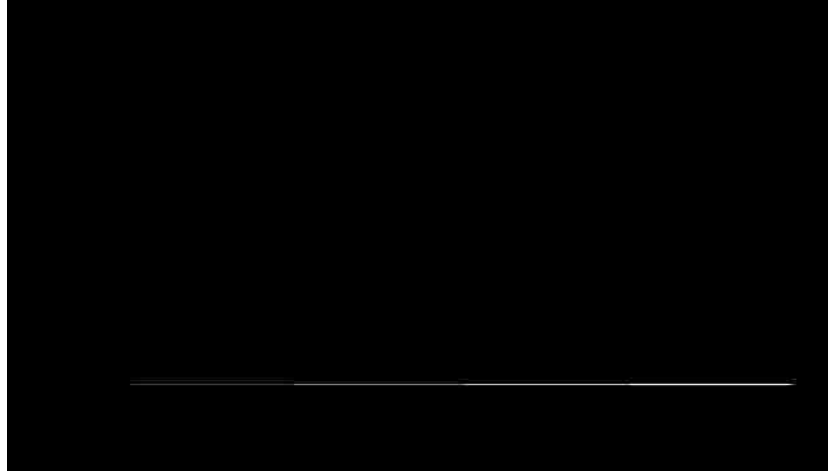
Figure 3.11   Time-variation of system failure probability (in logarithmic scale) under effects of both corrosion and increase in live load
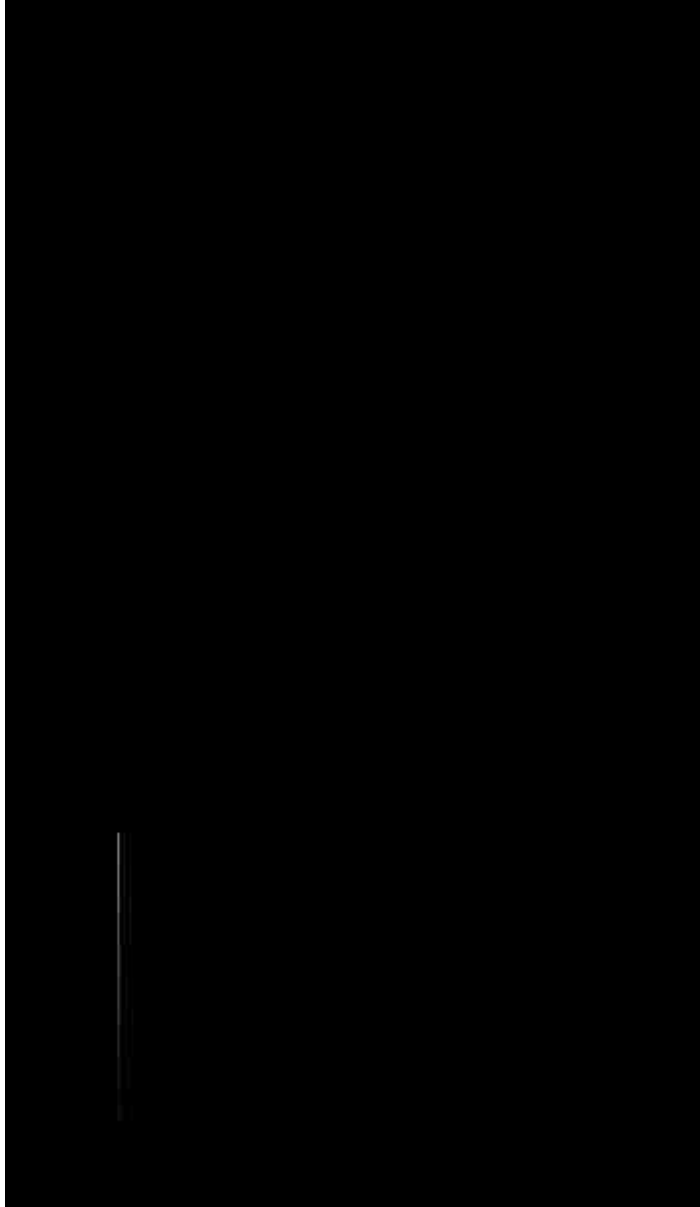
Figure 3.12   (a) Time-variation of vulnerability (in logarithmic scale) under effects

of both corrosion and increase in live load; comparison of the effects of

only corrosion, only live load increase and both corrosion and live load

increase on vulnerability for (b) failure of Girder 3; (c) failure of

Girder4
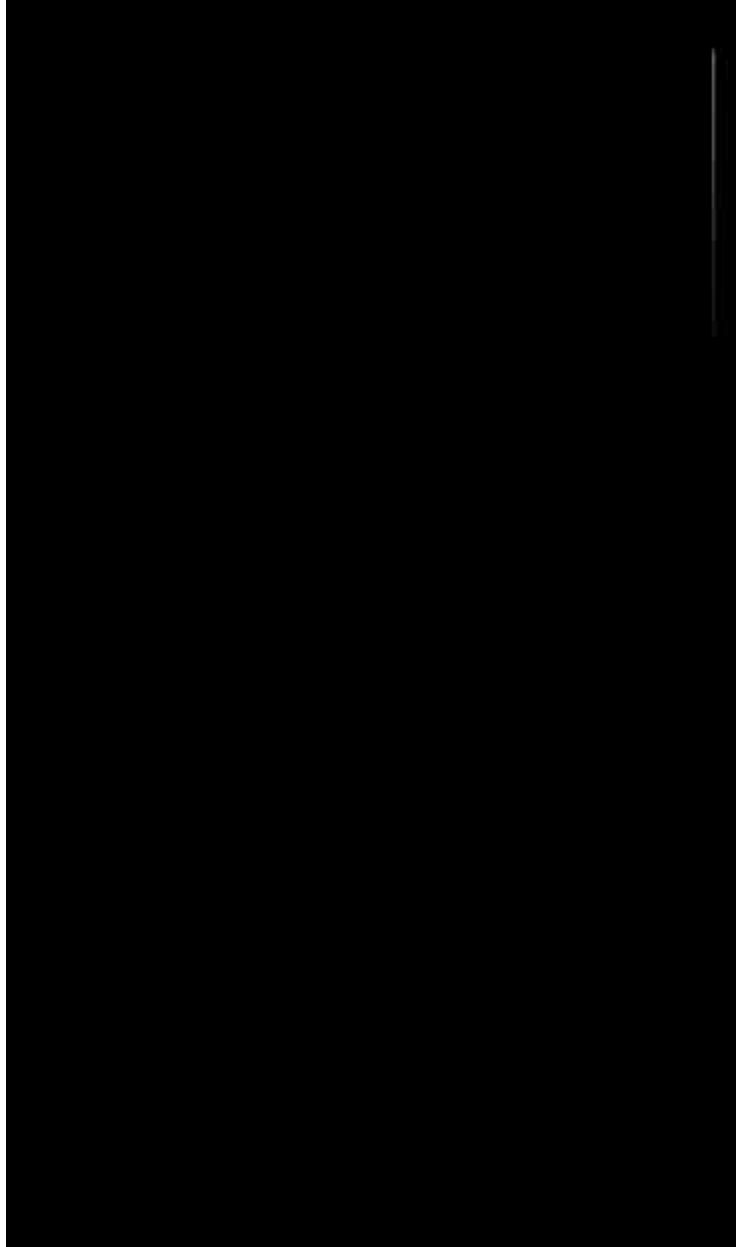
Figure 3.13   (a) Time-variation of redundancy under effects of both corrosion and increase in live load; comparison of the effects of only corrosion, only live load increase and both corrosion and live load increase on redundancy for (b) failure of Girder 3; (c) failure of Girder4

88
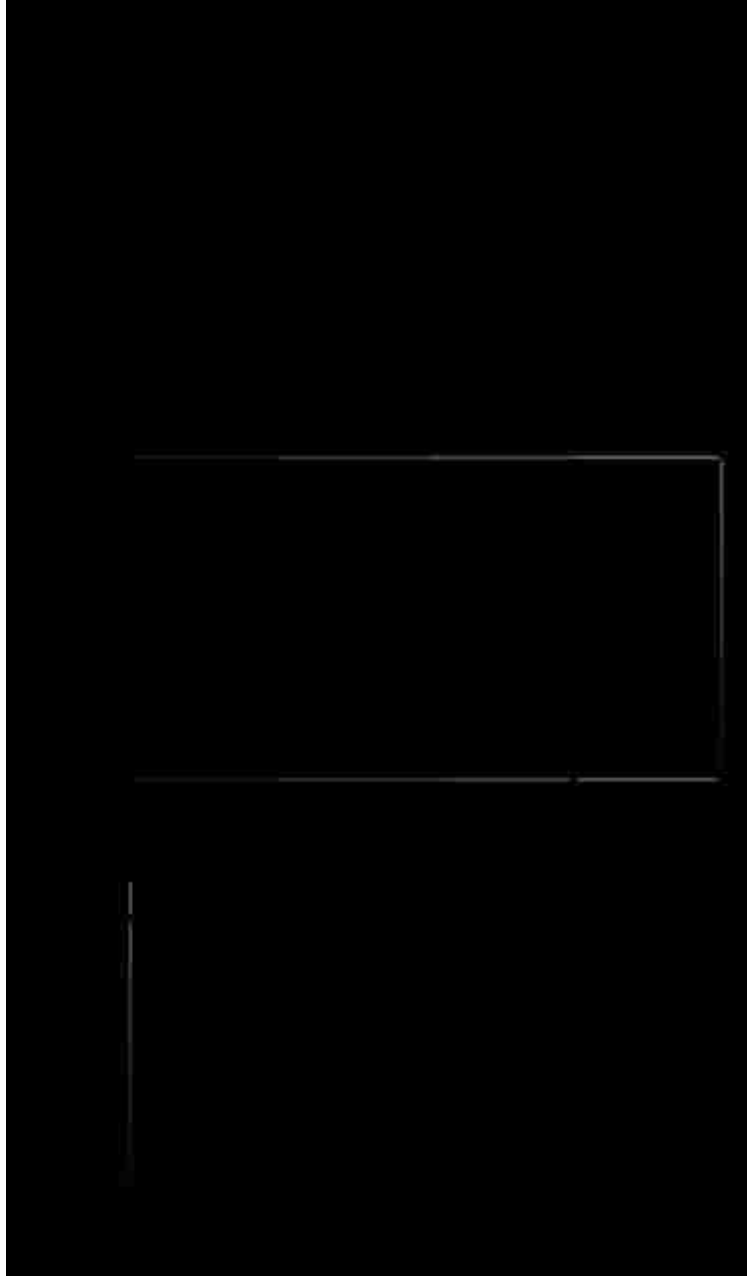
Figure 3.14   (a) Time-variation of robustness under effects of both corrosion and increase in live load; comparison of the effects of only corrosion, only live load increase and both corrosion and live load increase on robustness for (b) failure of Girder 3; (c) failure of Girder 4

89
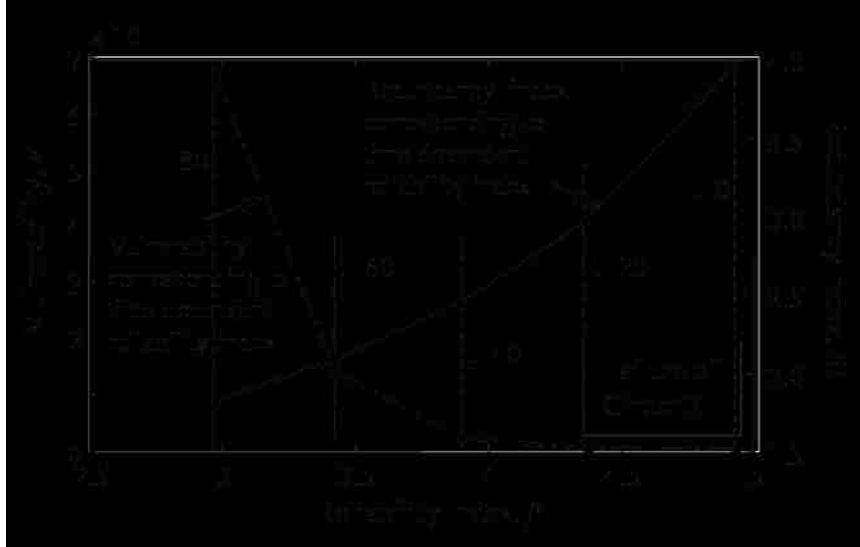
Figure 3.15   Variation of vulnerability and redundancy with respect to time-variant

reliability for the failure of Girder 3

CHAPTER 4

APPLICABILITY OF SIMPLE EXPRESSIONS FOR

BRIDGE SYSTEM RELIABILITY ASSESSMENT

4.1 INTRODUCTION

Performance evaluation of structural systems includes uncertainties associated with the material properties, the interaction between components, and the deterioration processes, among others. In addition, there are uncertainties in predicting the loads and their effects on structures. Therefore, the current evaluation philosophy of structural safety relies on probabilistic concepts and methods. The most common performance indicators used to take into account the uncertainties are probability of failure and reliability index. These two performance indicators are not only the most common indicators of structural safety, but also they are the basis for other performance indicators associated with structural damage tolerance such as redundancy, robustness, vulnerability and risk.

Usually, it is impractical to compute the probability of failure or the reliability index analytically for a complex engineering structure in a system-based approach. Therefore, numerical methods such as Monte Carlo Simulation, first and second order reliability methods (FORM and SORM) are used (Fiessler, Neumann, and Rackwitz 1979, Hohenbichler and Rackwitz 1981, Hohenbichler et al. 1987). However, the procedures of applying these methods for system analysis may require a knowledge level beyond the skills of common engineer, efficient computational tools and time. It is possible to represent the performance of a structural system by a single limit state

91

function based on a probabilistic finite element analysis (FEA). In this case, the interaction among the components of the system is accounted through FEA, rather than assumptions on series-parallel combination of components. The associated system reliability index can be computed using simple expressions based on first-order second-moment method (FOSM). These expressions provide exact results if both the load effects and the resistance follow normal or lognormal distributions. Cornell (1969) defined the reliability index as the ratio of the expected value of a performance function over its standard deviation on the basic assumption that the resulting probability of this function is a normal distribution, which is the basis for mean value first-order second-moment method (MVFOSM). Hasofer and Lind (1974) developed a new method, called advanced first-order second-moment method (AFOSM) to tackle the invariant reliability problem in MVFOSM, and they defined the reliability index as the shortest distance from the origin of reduced variables to the limit state surface. Due to its simplicity, FOSM has been used widely in estimating the component reliability. In fact, FOSM can be also used for system reliability when supported with finite element method (FEM). Der Kiureghian and Taylor (1983) introduced the use of FOSM with FEM. Ghosn and Moses (1998) and Ghosn, Moses, and Frangopol (2010) used FOSM with FEM to investigate the system reliability and redundancy of bridge structures assuming both load and resistance follow lognormal distribution. Although, the expressions by FOSM may provide good approximation when both load and system resistance follow lognormal distribution, the amount of error introduced can be significant when the random variables follow distribution other than lognormal, considering that it is reasonable to represent the maximum intensity of the live loads

92

on bridge structures using extreme value distribution especially when supported by truck load survey data.

The scope of this chapter is to provide the applicable range of the simple expressions based on FOSM to compute the system reliability index of bridges by investigating the amount of error (Saydam and Frangopol 2013a). The results obtained provide guidance to engineers on using simple reliability expressions for bridge system reliability analysis. It is assumed that the performance of a structural system is represented by a single limit state function based on probabilistic FEA. The term *reliability* refers to the *system reliability* throughout the chapter. First, brief information on reliability index and bridge capacity evaluation is provided. In order to investigate the amount of error for the case when both load and system resistance follow lognormal distribution, a selected bridge superstructure is studied. The system reliability indices are computed for varying coefficients of variation and mean values of load and resistance using the expressions that provide exact and approximate results for the special case with lognormal resistance and load effects. The system reliability indices and the amount of error introduced by using the expression that provides approximate results instead of the expression that provides exact results are presented in function of central safety factors for various coefficients of variation of resistance and load effect. Furthermore, by using the same structure, the case when system resistance follows lognormal distribution and loads follow extreme value type I largest distribution is investigated. In this case the system reliability indices are computed for varying coefficients of variation and mean values of load and system resistance using the FORM and the expressions that provide exact and approximate results for the

93

special case with lognormal resistance and load effects. The amount of error introduced by using these expressions instead of FORM is presented in function of central safety factor for various coefficients of variation of system resistance and load effect. The reliability software RELSYS (Estes and Frangopol 1998) is used for this purpose. A numerical example is provided.

4.2 RELIABILITY INDEX

As a measure of reliability, reliability index can be defined as the shortest distance from the origin to the limit state surface in the standard normal space. FORM and SORM, which approximately provide the reliability index by searching the most probable point on the failure surface ($g = 0$), are the most common methods to compute reliability index. However, for specific cases there exist simple expressions based on FOSM for the reliability index in terms of the parameters of the random variables within the limit state equation. For a component or system with lognormally distributed and statistically independent resistance and load effect, the reliability index β_1 can be calculated as

$$\beta_1 = \frac{\ln\left[\dfrac{E(R)}{E(L)}\sqrt{\dfrac{1+\delta^2(L)}{1+\delta^2(R)}}\right]}{\sqrt{\ln[(1+\delta^2(R))(1+\delta^2(L))]}} \tag{4.1}$$

where $E(R)$ and $E(L)$ are the mean values of the resistance and load effect; and $\delta(R)$ and $\delta(L)$ are the coefficients of variation of the resistance and load effect, respectively. For lognormally distributed and independent R and L, this expression provides the exact solutions to reliability index. However, it is also common in the literature that a

94

simplified version of this expression is used to compute reliability index β_2 for the case with lognormally distributed and statistically independent random variables as

$$\beta_2 = \frac{\ln\left[\dfrac{E(R)}{E(L)}\right]}{\sqrt{\delta^2(R) + \delta^2(L)}} \tag{4.2}$$

Detailed information on reliability index and structural reliability analysis can be found in Melchers (1999). Other probabilistic performance indicators associated with redundancy, robustness, vulnerability (Saydam and Frangopol 2011) and risk (Zhu and Frangopol 2012) may be formulated based on reliability index and probability of failure.

4.3 RELIABILITY ANALYSIS OF BRIDGE SUPERSTRUCTURES

Reliability index is one of the most common indicators for performance quantification of bridge structures. For instance, a reliability index level of 4.5 was targeted for establishing the safety levels of bridge components in calibration of AASHTO LRFD Bridge Design Specification (AASHTO 2010). However, the system effects were considered only approximately in some subsequent correction factors. System reliability analysis of bridge superstructures can be performed using FEM in a probabilistic manner. A proper statistical distribution for the desired output of FEA can be obtained by repeating the analysis for a large number of samples of the random variables associated with the finite element model. However, the time required to repeat FEA for thousands of samples may be impractical, especially for complex structures. The desired output of FEA can be approximated with a significantly less

number of samples by using Response Surface Method (RSM). The details of such a procedure will not be discussed in this chapter and can be found in Ghosn, Moses, and Frangopol (2010), Saydam and Frangopol (2011), Okasha and Frangopol (2010), Moses (1982), Bucher and Bourgund (1990), Liu and Moses (1994), Ellingwood (1996), and Wang, Ellingwood, and Zureick (2011). However, basic concepts will be introduced herein since the random variables that are used in the illustration of the approach are based on these concepts.

Load carrying capacity of a bridge superstructure can be expressed in terms of a load factor, *LF*, when the structure reaches its ultimate capacity or very large vertical displacements causing low levels of safety, serviceability, or both. Load factor, *LF*, indicates the ratio of the maximum load carried by the bridge system to the total weight of AASHTO HS-20 vehicle, when the applied load has the pattern of HS-20 vehicle loading. The failure of the bridge superstructure can be defined by the inequality in Equation 2.47.

If the parameters of random variables, resistance (*LF*) and live load effect (*LL*) are known, the failure probability of a bridge structure can be expressed as

$$P_f = P[LF - LL < 0] \tag{4.3}$$

The corresponding reliability index can be computed as

$$\beta = \Phi^{-1}(1 - P_f) \tag{4.4}$$

where $\Phi^{-1}(.)$ is the inverse of cumulative distribution function of standard normal variate.

It is also possible to obtain the reliability index directly. Ghosn, Moses, and Frangopol (2010) proposed to use the expression in Equation (4.2) for the relationship

96

between the system reliability index, the load factor, LF, and the live load effect, LL, for a bridge superstructure subjected to HS-20 truck loading as

$$\beta_2 = \frac{\ln\left[\dfrac{E(R)}{E(L)}\right]}{\sqrt{\delta^2(R) + \delta^2(L)}} = \frac{\ln\left[\dfrac{E(LF) \cdot P_{HS-20}}{E(LL) \cdot P_{HS-20}}\right]}{\sqrt{\delta^2(LF) + \delta^2(LL)}} = \frac{\ln\left[\dfrac{E(LF)}{E(LL)}\right]}{\sqrt{\delta^2(LF) + \delta^2(LL)}} \tag{4.5}$$

where $E(LF)$ and $E(LL)$ are the mean values of LF and LL; $\delta(LF)$ and $\delta(LL)$ are the coefficients of variation of LF and LL; P_{HS-20} is the weight of AASHTO HS-20 vehicle. Although, this expression may provide good approximation when both load effect and resistance follow lognormal distribution, the amount of error introduced can be significant when the random variables follow distribution other than lognormal, considering that it is reasonable to represent the maximum intensity of the live loads on bridge structures using extreme value distribution especially when supported by truck load survey data. The distribution type of the live load effects depends not only on the maximum intensity but also on the structural analysis process through the impact factor.

4.4 COMPARISON OF RELIABILITY INDEX VALUES COMPUTED WITH DIFFERENT EXPRESSIONS

Error quantification, herein, is based on the assumption that system resistance, LF, is already obtained through FEA, and probability distribution parameters for LF and LL are known. In this section, the system reliability index for a selected bridge superstructure is computed for different coefficients of variation and mean values of the load effect and the resistance using the first order reliability method (FORM) and

97

the expressions that provide exact (Equation 4.1) and approximate (Equation 4.2) results for the special case with lognormal resistance and live load effects. Firstly, considering the lognormal distributions for both LF and LL, the error introduced by the expression in Equation 4.2 is investigated in comparison to the expression in Equation 4.1. Then, the amount of error introduced by using Equation 4.1 and Equation 4.2 is presented and compared with the results obtained by using FORM, if LF has lognormal distribution and LL has extreme value type I largest distribution. For numerical illustration, the prestressed concrete I-girder bridge superstructure [5], shown in Figure 4.1, is used. Ghosn, Moses, and Frangopol (2010) performed nonlinear FEA of the bridge superstructure by incrementing the live load pattern in Figure 4.1, consisting of two side by side HS-20 trucks. They obtained the ultimate load capacity of the superstructure (load factor) as LF_u=5.28, which means that the total load that the structure can carry is equivalent to 5.28 times the weight of the couple of HS-20 trucks. The ultimate capacity was considered as the load when the external girder was crushed as the plastic rotation of the beam reached a value of 0.0247 rad. In order to perform simplified reliability analysis, Ghosn, Moses, and Frangopol (2010) used E(LF)=5.28 and E(LL)=1.89 as the mean values of the load factor and the load effect, respectively, and δ(LF)=0.14 and δ(LL)=0.19 as the coefficients of variation of the load factor and the load effect, respectively. These values are also used in this study. For instance, when investigating the effect of variation in mean values of the system resistance and the load effect, the coefficients of variation are kept constant at δ(LF)=0.14 and δ(LL)=0.19. The results obtained in

98

this chapter are valid for the case when system resistance and load effect are statistically independent.

4.4.1 Case I - Lognormal System Resistance and Lognormal Load

In the first case investigated, both system resistance (i.e., load factor *LF*) and live load effect (i.e., load multiplier *LL*) are assumed lognormally distributed. The PDF (Probability Density Function) of lognormally distributed random variable *X* is expressed as (Ang and Tang 2007)

$$f_X = \frac{1}{\sqrt{2\pi}\,(\zeta x)} \exp\left[-\frac{1}{2}\left(\frac{\ln x - \lambda}{\zeta}\right)^2\right] \qquad x \geq 0 \tag{4.6}$$

where λ and ζ are the central value and dispersion parameters of the lognormal distribution, respectively, computed as

$$\lambda = E(\ln x) \tag{4.7}$$

$$\zeta = \sqrt{Var(\ln x)} \tag{4.8}$$

where Var(z) is the variance of random variable Z.

The definitions of the reliability indices and the types of errors associated with the investigated cases are illustrated in Figure 4.2. The reliability indices associated with Case I are β_1 and β_2, which are the reliability indices computed using the expressions that provide exact (Equation 4.1) and approximate (Equation 4.2) results for the special case with lognormal resistance and load effects, respectively. The error associated with Case I is the error in reliability index computed using the approximate expression (Equation 4.2) with respect to the reliability index computed using the

99

exact expression (Equation 4.1) and is called herein error type *A*, e_A. In other words, the error type *A*, e_A, is the error in β_2 with respect to β_1.

The reliability index in function of the coefficient of variation of the load multiplier $\delta(LL)$ up to 0.50 at constant mean values E(*LF*)=5.28 and E(*LL*)=1.89 for four different values of the coefficient of variation of the load factor ($\delta(LF)$=0.1, $\delta(LF)$=0.2, $\delta(LF)$=0.3, and $\delta(LF)$=0.4) using exact (Equation 4.1) and approximate (Equation 4.2) expressions is presented in Figure 4.3 (a). A more detailed view of the intersection zone for the system reliability curves for $\delta(LF)$=0.2, computed with exact and approximate expressions is provided in Figure 4.3 (b) to illustrate the region where the approximate expression is not conservative. The region where β_2 is greater than β_1, represents the non-conservative region. The other region represents the conservative side (i.e., $\beta_2 < \beta_1$). As the point of interest gets away from the intersection point, the error introduced by using the approximate expression becomes higher on both the conservative and non-conservative sides. The error e_A introduced by using the approximate expression for the four different reliability curve sets is presented in Fig. 3(c) and computed as

$$e_A = \left| \frac{\beta_2 - \beta_1}{\beta_1} \right| \tag{4.9}$$

where |*z*| represents the absolute value of the number *z*. At low levels of $\delta(LL)$, the error is on the non-conservative side for all four different levels of $\delta(LF)$, resulting in higher error for the cases with higher $\delta(LF)$ (e.g., the error is highest for $\delta(LF)$=0.4). As $\delta(LL)$ increases, the error on non-conservative side decreases and becomes zero at the intersection point of the system reliability index curves with exact and

www.manaraa.com

approximate expressions. Further increase of δ(*LL*) results in higher error on conservative side. The conservative error goes up to about 14% for the case with δ(*LF*)=0.1.

The case with varying mean values of the system resistance and load effect at constant coefficient of variation is also investigated. The variation of the reliability index with respect to the mean value of the load multiplier E(*LL*) varying between 1.5 and 4 at constant coefficients of variation δ(*LF*)=0.14 and δ(*LL*)=0.19 for three different values of mean values of the load factor (E(*LF*)=4, E(*LF*)=6, and E(*LF*)=8) using exact (Equation 4.1) and approximate (Equation 4.2) expressions is presented in Figure 4.4 (a). A more detailed view of the reliability curves computed with exact and approximate expressions for E(*LF*)=4 is provided in Figure 4.4 (b) to illustrate that the approximate expression (Equation 4.2) is conservative within the whole investigated range of E(*LL*). The type I error, e_A, introduced by using the approximate expression for the three different reliability curve sets is presented in Figure 4.4 (c).

4.4.2 Case II - Lognormal System Resistance and Extreme Value Type I Largest Load

Another case investigated is the case when the system resistance (i.e., load factor *LF*) is lognormally distributed and load effect (i.e., load multiplier *LL*) has extreme value type I largest distribution, which is a common situation in the reliability analysis of the bridge structures under the live loads especially when supported by truck load survey data. The PDF of random variable Y_n from type I largest extreme value distribution is expressed as (Ang and Tang 2007)

101

$$f_{Y_n}(y) = \alpha_n e^{-\alpha_n(y-u_n)} \exp[-e^{-\alpha_n(y-u_n)}] \tag{4.10}$$

where u_n is the most probable value of Y_n and α_n is an inverse measure of the dispersion of values of Y_n. The mean and the variance of Y_n are related to these parameters as

$$\mu_{Y_n} = u_n + \frac{\gamma}{\alpha_n} \tag{4.11}$$

$$\sigma_{Y_n}^2 = \frac{\pi^2}{6\alpha_n^2} \tag{4.12}$$

where γ is the Euler number ($\gamma = 0.577216$).

The definitions of the reliability indices and the types of errors associated with this case are illustrated in Figure 4.2. The reliability indices associated with Case II are β_1, β_2, and β_3 which are the reliability indices computed using Equation 4.1, Equation 4.2, and FORM. In this case, β_1 and β_2 are the results of Equation 4.1 and Equation 4.2, which assumes both lognormal system resistance and load effect, while β_3 is based on FORM, which accounts for lognormal system resistance and extreme value type I largest load effect. The errors associated with Case II are the error type B, e_B, and error type C, e_C. These are the errors in reliability index computed using the expression which provides exact (Equation 4.1) results for lognormal resistance and load effect condition with respect to the reliability index computed using FORM and the errors in reliability index computed using the expression which provides approximate (Equation 4.2) results for lognormal resistance and load effect condition with respect to the reliability index computed using FORM, respectively. In other

102

words, the error type B, e_B, is the error in β_1 with respect to β_3, and the error type C, e_C, is the error in β_2 with respect to β_3.

In this case, both Equation 4.1 and Equation 4.2 do not provide correct results. Therefore, the results obtained by these expressions are compared with those obtained by using FORM. Reliability software RELSYS (Estes and Frangopol 1998) is used for this purpose. The system reliability index as a function of $\delta(LL)$ at constant $E(LF)$=5.28 and $E(LL)$=1.89 for several values of $\delta(LF)$ ($\delta(LF)$=0.10, $\delta(LF)$=0.15, $\delta(LF)$=0.20, $\delta(LF)$=0.25, and $\delta(LF)$=0.40) using FORM, Equation 4.1 and Equation 4.2 is presented in Figure 4.5 (a). A more detailed view of the intersection zones for the reliability curves for $\delta(LF)$=0.2, is provided in Figure 4.5 (b) to illustrate the regions where Equation 4.1 and Equation 4.2 are non-conservative. The region where the system reliability index computed using Equation 4.2 is higher than the system reliability index computed using the FORM (i.e., $\beta_2 < \beta_3$) represents the non-conservative region for Equation 4.2, and similarly, the region where the reliability index computed using Equation 4.1 is higher than the reliability index computed using the FORM (i.e., $\beta_1 < \beta_3$) represents the non-conservative region for Equation 4.1. The errors introduced by using Equation 4.1 (error type B, e_B) and Equation 4.2 (error type C, e_C) for the five different reliability curve sets are presented in Figure 4.6 (a) and (b). These errors are computed as

$$e_B = \left| \frac{\beta_1 - \beta_3}{\beta_3} \right| \tag{4.13}$$

$$e_C = \left| \frac{\beta_2 - \beta_3}{\beta_3} \right| \tag{4.14}$$

103

Unlike the case with lognormally distributed system resistance and load effect, the error in the non-conservative side reaches almost 30% for smaller $\delta(LF)$ with Equation 4.1 and Equation 4.2 (i.e., error for $\delta(LF)$=0.10 in Figure 4.6 (a) and (b)). The error curves for Equation 4.1 and Equation 4.2 exhibit very similar pattern, except that the one for Equation 4.2 reaches high error levels and then the zero error point slightly earlier than the one for Equation 4.1. For this reason, the error in conservative side for Equation 4.2 reaches higher levels (as high as 0.19 for $\delta(LF)$=0.25 in Figure 4.6 (b)) than the one for Equation 4.1. It is obvious that when the resistance and the load effect are not both lognormally distributed, the error in both conservative and non-conservative sides can be very high for some values of $\delta(LF)$ and $\delta(LL)$.

The case with varying mean values of the resistance and the load effect at constant coefficient of variation is also investigated. The variation of the reliability index with respect to the mean value of the load multiplier E(LL) varying between 1.5 and 4.0 at constant coefficients of variation $\delta(LF)$=0.19 and $\delta(LL)$=0.14 for three different values of the mean values of the load factor (E(LF)=4, E(LF)=6, and E(LF)=8) using the FORM, Equation 4.1 and Equation 4.2 is presented in Figure 7 (a). A more detailed view of the intersection zones for the reliability curves for E(LF)=4, computed with the FORM, Equation 4.1 and Equation 4.2 is provided in Figure 4.7 (b) to illustrate the regions where Equation 4.1 and Equation 4.2 are not conservative. The error introduced by using Equation 4.1 and Equation 4.2 for the three different reliability curve sets are presented in Figure 4.8 (a) and (b), respectively. The errors are computed using Equation 4.13 and Equation 4.14. The error introduced by Equation 4.1 for E(LF)=6 and E(LF)=8 is in the non-conservative side within the

104

whole investigated range of E(*LL*). However, for E(*LF*)=4, the error increases in the conservative side as the mean values of the resistance and load effect gets closer. Similar conclusion is reached for the error introduced by the Equation 4.2.

4.4 PRESENTATION OF ERROR IN A MORE COMPACT WAY

It is obvious, from Equation 4.1 and Equation 4.2, that the reliability index does not only depend on the mean values of the resistance and load effect, but also on the ratio of the mean values. This is valid also for the reliability index β_3 obtained using FORM. For instance, the reliability indices at E(*LL*)=2 on the curve for E(*LF*)=4, E(*LL*)=3 on the curve for E(*LF*)=6, and E(*LL*)=4 on the curve for E(*LF*)=8 are all equal to 2.78. In the light of this information, the results can be presented in a more compact way using central safety factor. Central safety factor is defined as the ratio of the mean values of the resistance and load effect and is expressed as

$$\theta_0 = \frac{E(LF)}{E(LL)} \tag{4.15}$$

The reliability index in function of the central safety factor, θ_0, varying between 1.05 and 5.0 at constant mean value of the load effect E(*LL*)=1.0 for nine different sets of the coefficients of variation of the resistance and load effect (δ(*LF*)=0.1, δ(*LL*)=0.1; δ(*LF*)=0.1, δ(*LL*)=0.3; δ(*LF*)=0.1, δ(*LL*)=0.5; δ(*LF*)=0.2, δ(*LL*)=0.1; δ(*LF*)=0.2, δ(*LL*)=0.3; δ(*LF*)=0.2, δ(*LL*)=0.5; δ(*LF*)=0.3, δ(*LL*)=0.1; δ(*LF*)=0.3, δ(*LL*)=0.3; δ(*LF*)=0.3, δ(*LL*)=0.5) using Eq. (1) and Eq. (2) is presented in Figure 4.9 (a), (b), and (c) for case I (lognormal resistance and lognormal load effect).

The type A error, e_A, with respect to the central safety factor, θ_0, for these nine sets is shown in Figure 4.10 (a), (b), and (c).

The system reliability index in function of the central safety factor, θ_0, varying between 1.05 and 5.0 at constant mean value of the load effect E(LL)=1.0 for the nine different sets of the coefficients of variation of the resistance and load effect using Equation 4.1, Equation 4.2 and FORM is presented in Figure 4.11 (a), (b), and (c) for case II (lognormal system resistance and type I largest load effect). The type B error, e_B, with respect to the central safety factor, θ_0, for these nine sets is shown in Figure 12 (a), (b), and (c). Focusing on the most practical case where θ_0 is between 2 and 4, the type B error is mostly on the conservative side except for the sets with $\delta(LF)$=0.1, $\delta(LL)$=0.1 and $\delta(LF)$=0.1, $\delta(LL)$=0.3. For instance, focusing on error type B in Figure 4.12 (a), the error ranges between 20% and 34% from θ_0=2 to θ_0=4 for δ(LF)=0.1 and δ(LL)=0.1 on the non-conservative side. These error values may seem to be high; however, $\delta(LF)$=0.1 and $\delta(LL)$=0.1 values do not represent the most common cases for bridge systems. In general, coefficient of variation of load is much higher than that of the resistance. In the same figure (Figure 4.12 (a)), if more practical cases are considered where $\delta(LL)$ is larger than $\delta(LF)$, for instance $\delta(LF)$=0.1 and $\delta(LL)$=0.3, the error ranges between 3% and 5% from θ_0=2 to θ_0=4 on still the non-conservative side (much smaller than the above value). If the case $\delta(LF)$=0.1 and $\delta(LL)$=0.5 is considered, the error ranges between 1% and 7% from θ_0=2 to θ_0=4 on the conservative side. As the coefficient of variation of the resistance increases, the error tends to increase on the conservative side. For example, in Figure 4.12 (b), type B error ranges between 21% and 15% from θ_0=2 to θ_0=4 for $\delta(LF)$=0.2 and $\delta(LL)$=0.1 on

106

the conservative side. If a more practical case is considered where $\delta(LL)$ is larger than $\delta(LF)$, for instance $\delta(LF)=0.2$ and $\delta(LL)=0.3$, the error ranges between 10% and 8% from $\theta_0=2$ to $\theta_0=4$ on still the conservative side, yielding smaller error. The type C error, e_C, with respect to the central safety factor, θ_0, for these nine sets is shown in Figure 4.13 (a), (b), and (c). Similarly, focusing on the most practical case where θ_0 is between 2 and 4, the type C error shows a similar trend with a little higher values than the type B error.

4.5 ILLUSTRATIVE EXAMPLE

The example is on the reliability of highway bridge substructures. In this example, the reliability indices and errors are first obtained based on Figures 4.9 to 4.13 and then they are computed exactly for comparison. Ghosn, Moses, and Frangopol (2010) investigated the redundancy of bridge substructures based on the reliability index regarding the failure of the first member failure and the system failure. The mean value of the ultimate lateral load carrying capacity of a bridge substructure was computed to be 5922 kN. The coefficient of variation associated with this resistance was determined as $\delta(LF)=0.13$. The coefficient of variation associated with the load effect was assumed as $\delta(LL)=0.5$. For four different values of the mean value of the lateral load applied on the substructure, 1500 kN, 2000 kN, 3000 kN, and 4000 kN, the central safety factor, θ_0, becomes 3.948, 2.961, 1.974, and 1.481, respectively. If both the system resistance and the load effect are assumed to be distributed lognormally, the corresponding system reliability indices by Equation 4.1 and Equation 4.2 can be approximated using Figure 4.9 (a). The values of the reliability

107

indices β_1 and β_2 obtained from Figure 4.9 (a) for $\delta(LF)$=0.10 and $\delta(LL)$=0.50 are presented in Table 4.1. The type A error, e_A, introduced by using Equation 4.2 instead of Equation 4.1 can also be approximated using Figure 4.10 (a). The values of the type A error e_A obtained from Figure 4.10(a) are presented in Table 4.1. If the resistance is lognormally distributed and the load effect follows extreme value type I largest distribution, the correct reliability indices by FORM, β_3, can be easily approximated using Figure 4.11 (a). The values of the reliability indices β_3 obtained from Figure 4.11 (a) for $\delta(LF)$=0.10 and $\delta(LL)$=0.50 are presented in Table 4.1. The type B error, e_B, introduced by using Equation 4.1 instead of FORM can be approximated using Figure 4.12 (a). Similarly, the type C error, e_C, introduced by using Equation 4.2 instead of FORM can be approximated using Figure 4.13 (a). The values of the type B error e_B and the type C error e_C obtained from Figure 4.12 (a) and Figure 4.13 (a) are presented in Table 4.1. The values of β_1, β_2, β_3, e_A, e_B, and e_C are also computed for the exact values of θ_0=3.948, θ_0=2.961, θ_0=1.974, and θ_0=1.481 with $\delta(LF)$=0.13, $\delta(LL)$=0.5. The results are tabulated in Table 4.2. It can be concluded that the values obtained from Figures 4.9 to 4.13 provide close approximations to the exact values. It is also possible that the exact reliability index can be approximated with a backward computation of the error formula given θ_0, $\delta(LF)$, $\delta(LL)$, the associated errors obtained from the figures provided. In other words, the exact reliability index can be obtained without performing FORM from Equation 4.13 and Equation 4.14 using the error charts provided. For instance, in Table 4.1, $\beta_2 = 2.72$ for θ_0=3.95 is computed using Equation 4.2 and the associated error with respect to β_3 (FORM) is provided as $e_C = $

108

0.186. The correct reliability index $\beta_3 = 3.34$ can be calculated substituting these two values in Equation 4.14 and solving for β_3 without performing FORM.

4.6 CONCLUSIONS

In this chapter, assuming that the system performance of a bridge structure is represented by a single limit state function based on probabilistic FEA, the amount of error introduced by using FOSM to compute bridge system reliability index is investigated. A selected bridge superstructure is studied by comparing expressions which provide exact and approximate results for the case with lognormal system resistance and lognormal load effect, in order to investigate the amount of error for the case when both the load effect and the system resistance follow the lognormal distribution. The system reliability indices are computed for varying coefficients of variation and mean values of the load and the system resistance using the expressions which provide exact and approximate results for the case with lognormal resistance and lognormal load effect. The amount of error introduced by using the expression which provides approximate results instead of the expression which provides exact results is presented in function of central safety factor for various coefficients of variation of system resistance and load effect. In addition, the case with lognormal resistance and extreme value type I largest load effect is investigated. In this case, the reliability indices are computed for varying coefficients of variation and mean values of load and resistance using FORM and the simple expressions. The amount of error introduced by using expressions which provide exact (Equation 4.1) and approximate (Equation 4.2) results instead of FORM is presented in function of central safety factor

109

for various coefficients of variation of system resistance and load effect. The reliability software RELSYS (Estes and Frangopol 1999) is used for this purpose.

This study is intended to provide guidance to engineers on using simple reliability expressions based on FOSM for system reliability analysis of bridge structures. As the results indicate, it is not always recommended to use simple expressions in the reliability analysis of bridge structures. On the other hand, the expression which gives approximate results for the case with lognormal system resistance and lognormal load effect can provide acceptable approximations even for the case with lognormal system resistance and extreme value type I largest load effect especially on the conservative side. Depending on the coefficients of variation and the ratio between the mean values of system resistance and load effect, the acceptable levels of error can be identified.

Depending on the cases investigated, the following conclusions can be drawn. The amount of error introduced by using simple expressions in system reliability analysis depends not only on the coefficient of variation of the resistance and load effect but also the ratio between the mean values of resistance and load effect. When both the system resistance and the load effect are lognormally distributed, the expression which provides approximate results introduces error in both the conservative and the non-conservative sides. The error in the non-conservative side seems to be lower than the error in the conservative side within the investigated range of coefficients of variation of the load effect and the system resistance at constant mean values. The error introduced by the expression which provides approximate results dramatically increases in the conservative side as the mean values of the system

110

resistance and load effect get closer to each other. Both the conservative and non-conservative errors tend to decrease with increasing central safety factor. In addition, the error remains constant with varying central safety factor if the coefficients of variation of system resistance and load effect are equal. When the system resistance is lognormally distributed and the load effect has extreme value type I largest distribution, the simple expressions of system reliability index may introduce significant error in both the conservative and the non-conservative sides. The error mainly remains in the non-conservative side. However, it increases in the conservative side as the mean values of resistance and load effect get closer to each other. Furthermore, the non-conservative error due to the expressions which provide exact and approximate results with respect to FORM may be as high as 30-40% within the practical range of central safety factor (2.0-4.0). In such case, using the simple expressions should be avoided. The conservative error due to the expressions which provide exact and approximate results with respect to FORM may be as high as 50% within the practical range of central safety factor. Although the error is high, in this case, it is conservative. Depending on the judgment of the analyst, the simple expressions can be used or avoided.

Table 4.1 – Illustrative example data obtained from the reliability and error figures

Central Safety Factor, θ_0	Data from Figure 9 to 13 for $\delta(LF)=0.1$ and $\delta(LL)=0.5$					
	β_1	β_2	β_3	e_A	e_B	e_C
3.95	3.09	2.72	3.34	0.121	0.075	0.186
2.96	2.50	2.15	2.62	0.137	0.047	0.178
1.97	1.66	1.36	1.67	0.179	0.007	0.185
1.48	1.06	0.80	1.02	0.250	0.035*	0.224

*Non-conservative error

Table 4.2 – Illustrative example exact data

Central Safety Factor, θ_0	Exact values for $\delta(LF)=0.13$ and $\delta(LL)=0.5$					
	β_1	β_2	β_3	e_A	e_B	e_C
3.95	3.01	2.66	3.23	0.118	0.066	0.176
2.96	2.43	2.10	2.53	0.134	0.410	0.177
1.97	1.60	1.32	1.60	0.177	0.002	0.179
1.48	1.01	0.76	0.97	0.246	0.040*	0.219

*Non-conservative error
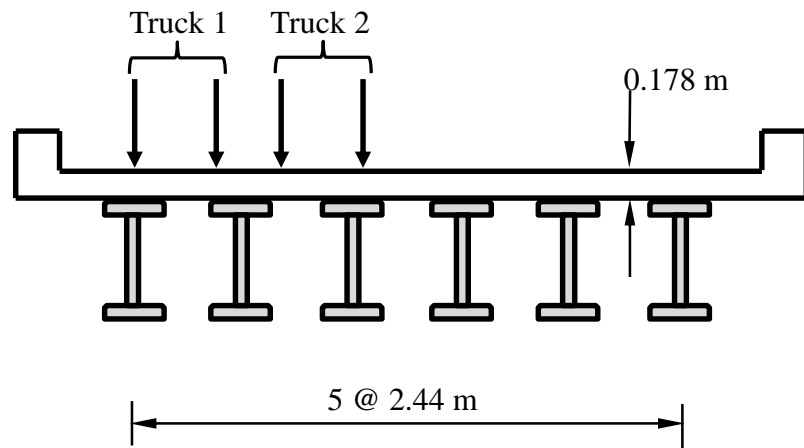
Figure 4.1   Prestressed concrete bridge superstructure (adapted from Hasofer and
Lind 1974)

114

System performance represented by a single limit state function based on FEM

Investigated Cases with Respect to Distribution Types

Case I

System Resistance (*LF*): lognormal
Load (*LL*): lognormal

System Reliability Indices Associated with Case I:

β_1: computed using the formula which provides exact results for the case with lognormal resistance and lognormal load

β_2: computed using the formula which provides approximate results for the case with lognormal resistance and lognormal load

e_A

Error Associated with Case I:

Error type *A* (e_A):
error in β_2 with respect to β_1

$$e_A = \left| \frac{\beta_2 - \beta_1}{\beta_1} \right|$$

Case II

System Resistance (*LF*): lognormal
Load (*LL*): type I largest

System Reliability Indices Associated with Case II:

β_1: computed using the formula which provides exact results for the case with lognormal resistance and lognormal load, identical to β_1 in Case I, assumes both resistance and load as lognormal

β_2: computed using the formula which provides approximate results for the case with lognormal resistance and lognormal load, identical to β_2 in Case I, assumes both resistance and load as lognormal

β_3: computed using FORM for lognormal resistance and extreme value type I largest load

e_B

e_C

Error(s) Associated with Case II:

Error type *B* (e_B):
error in β_1 with respect to β_3

$$e_B = \left| \frac{\beta_1 - \beta_3}{\beta_3} \right|$$

Error type *C* (e_C):
error in β_2 with respect to β_3

$$e_C = \left| \frac{\beta_2 - \beta_3}{\beta_3} \right|$$

Figure 4.2   Investigated cases, definitions of the system reliability indices, and the

error types associated with these cases

115
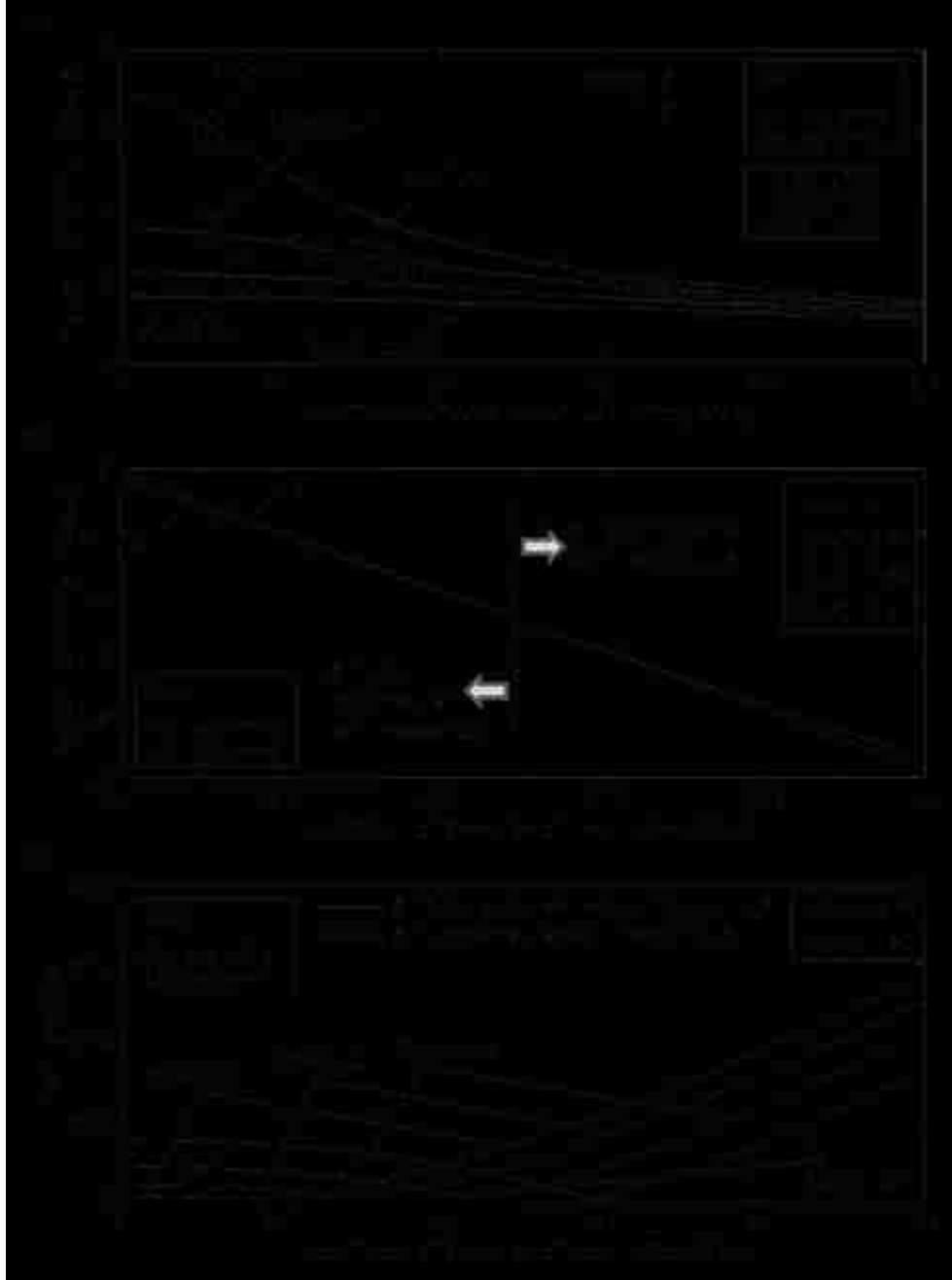
Figure 4.3   Comparison for the case with lognormal system resistance and lognormal load effect, varying coefficient of variation and constant mean value of the load effect and the system resistance; (a) and (b) the reliability indices, β_1 and β_2, (c) the type A error, e_A.
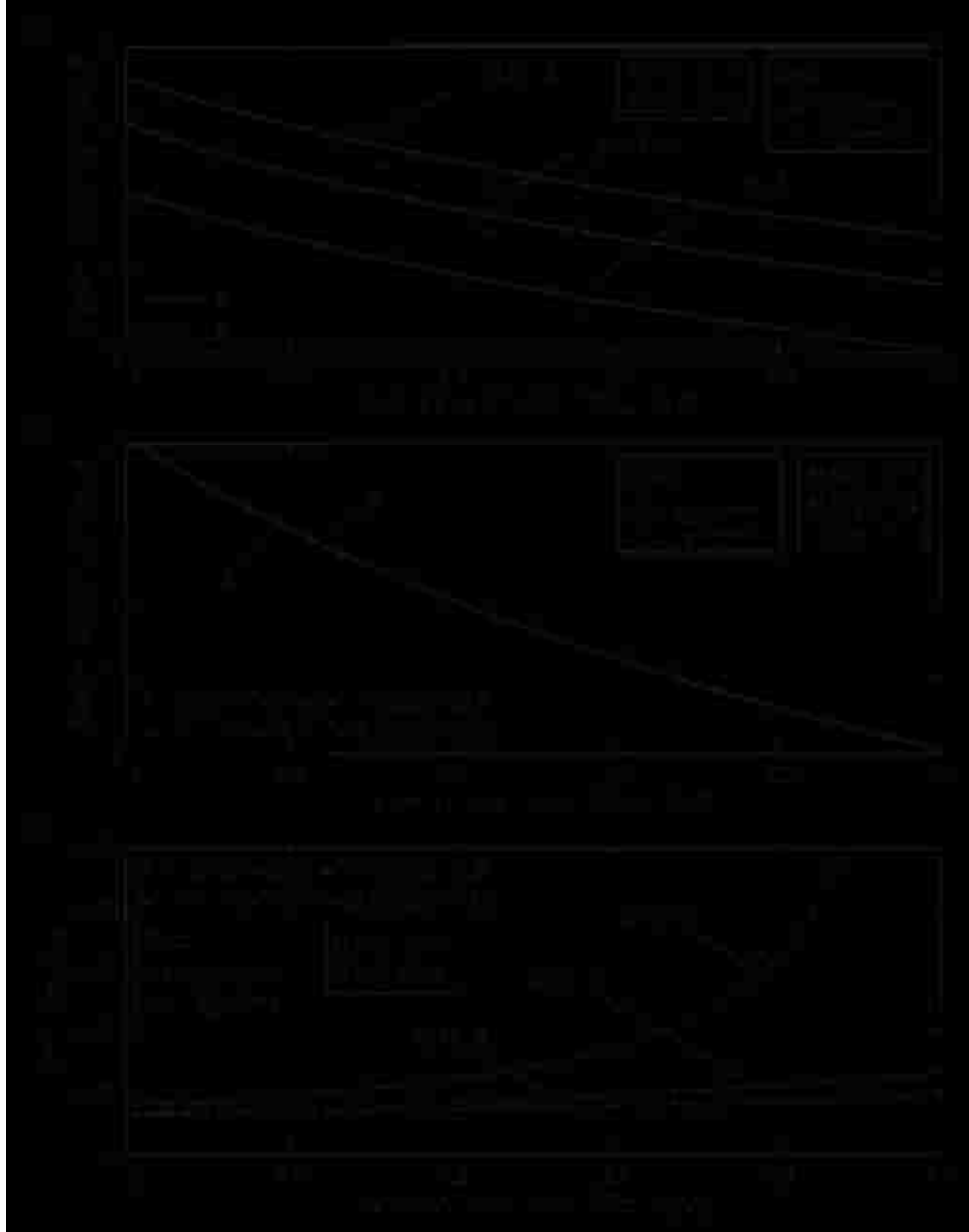
Figure 4.4 Comparison for the case with lognormal system resistance and lognormal load effect, varying mean value and constant coefficient of variation of the load effect and system resistance; (a) and (b) the reliability indices, β_1 and β_2, (c) the type A error, e_A.

117
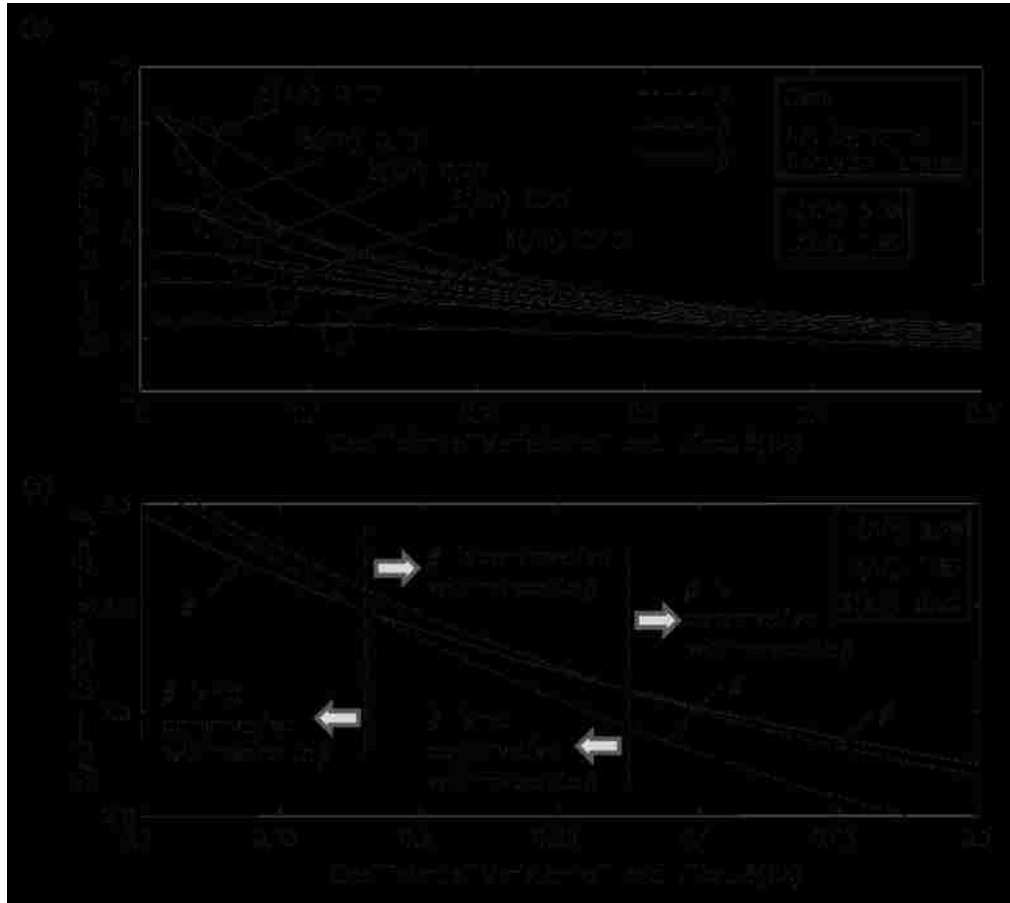
Figure 4.5   Comparison for the case with lognormal system resistance and extreme value type I largest load effect, varying coefficient of variation and constant mean value of the load effect and system resistance; (a) and (b) the reliability indices, β_1, β_2, and β_3.
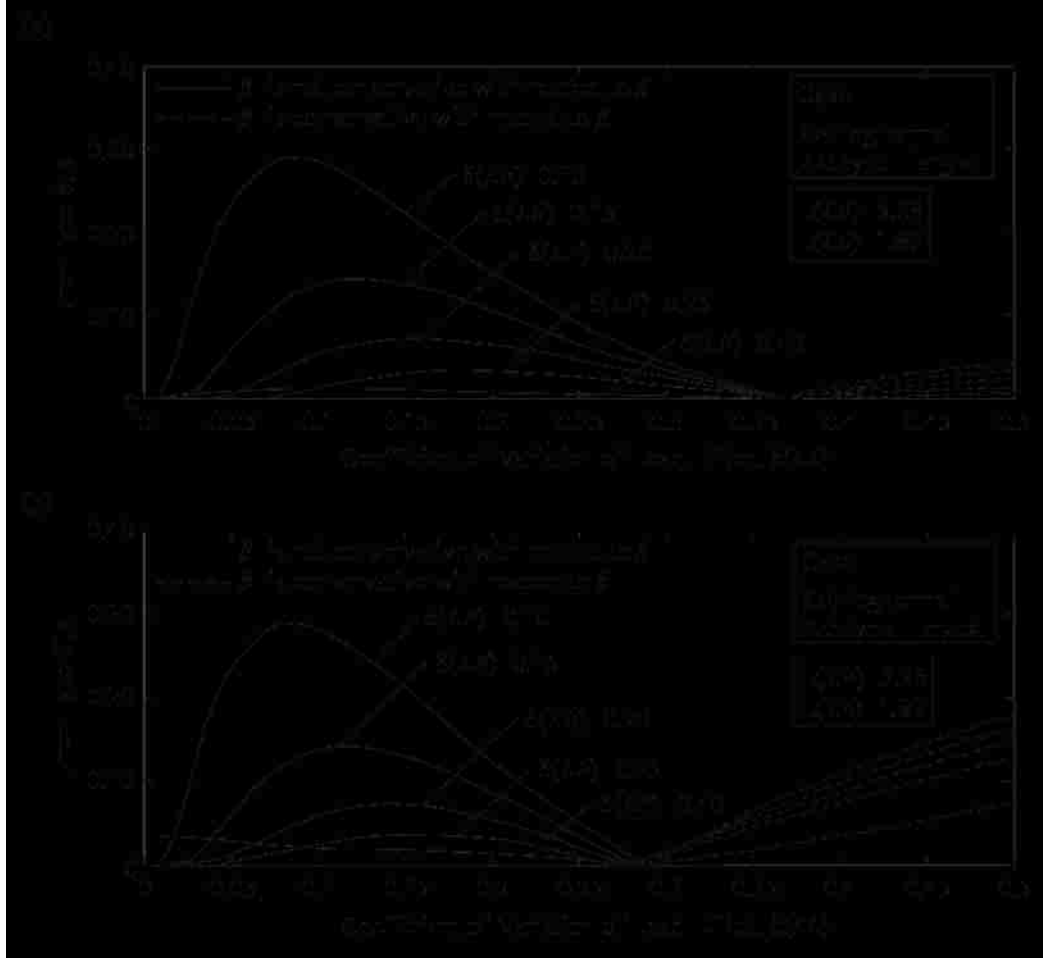
Figure 4.6   Comparison for the case with lognormal system resistance and extreme value type I largest load effect, varying coefficient of variation and constant mean value of the load effect and system resistance; (a) the type B error, e_B, and (b) the type C error, e_C.
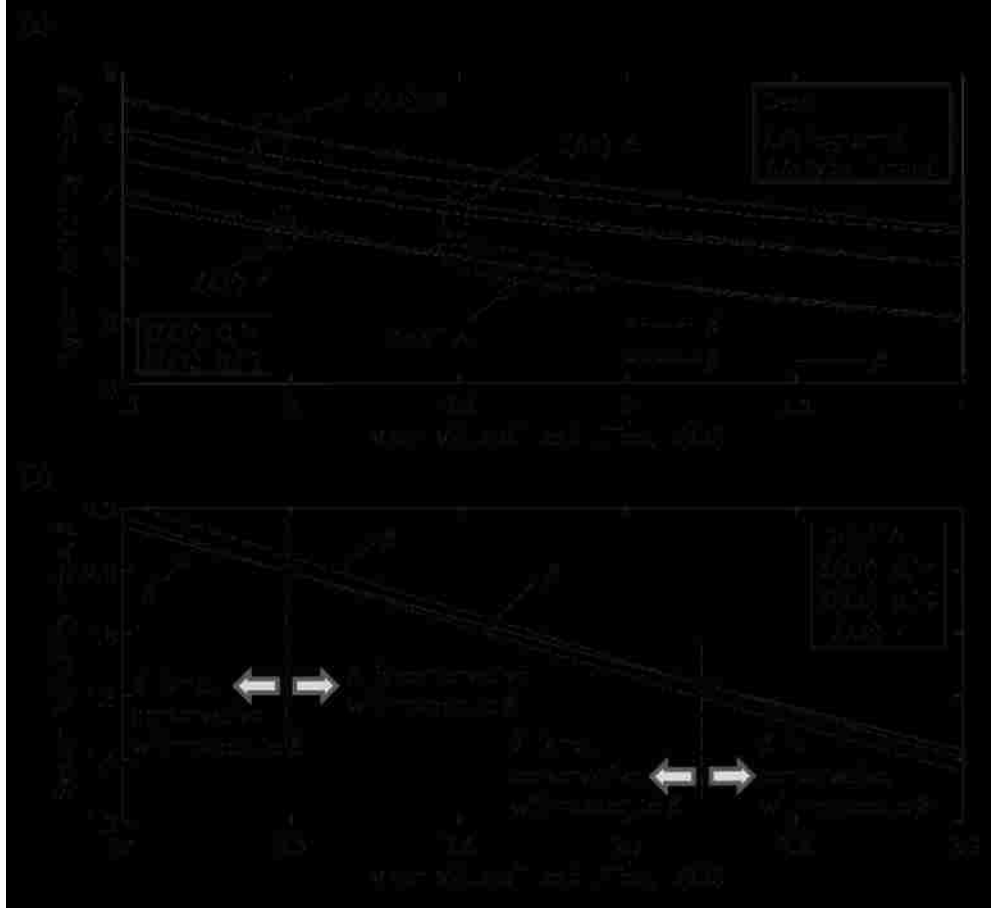
Figure 4.7   Comparison for the case with lognormal system resistance and extreme value type I largest load effect, varying mean value and constant coefficient of variation of the load effect and system resistance; (a) and (b) the reliability indices, β_1, β_2, and β_3.
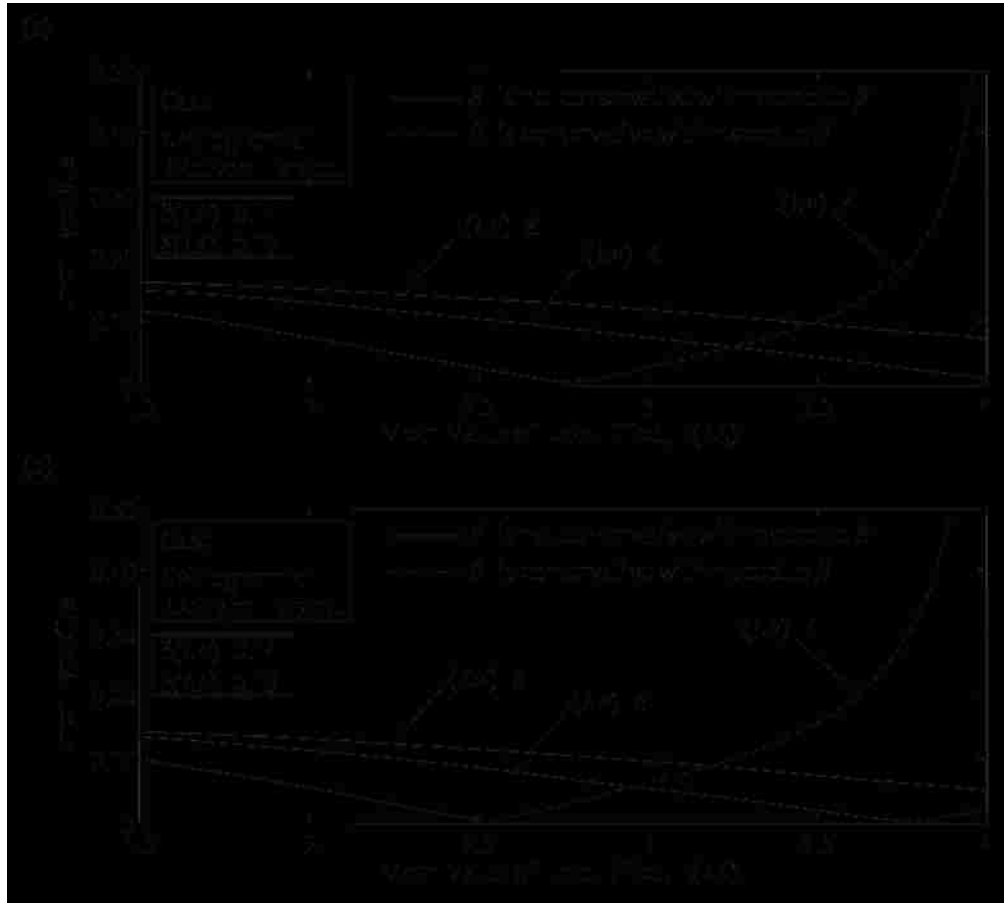
Figure 4.8   Comparison for the case with lognormal system resistance and extreme
value type I largest load effect, varying mean value and constant
coefficient of variation of the load effect and system resistance; (a) the
type B error, e_B, and (b) the type C error, e_C.

Figure 4.9   Comparison for the case with lognormal system resistance and load effect, varying central safety factor and constant mean value of load effect; (a), (b) and (c) the reliability indices, β_1 and β_2.
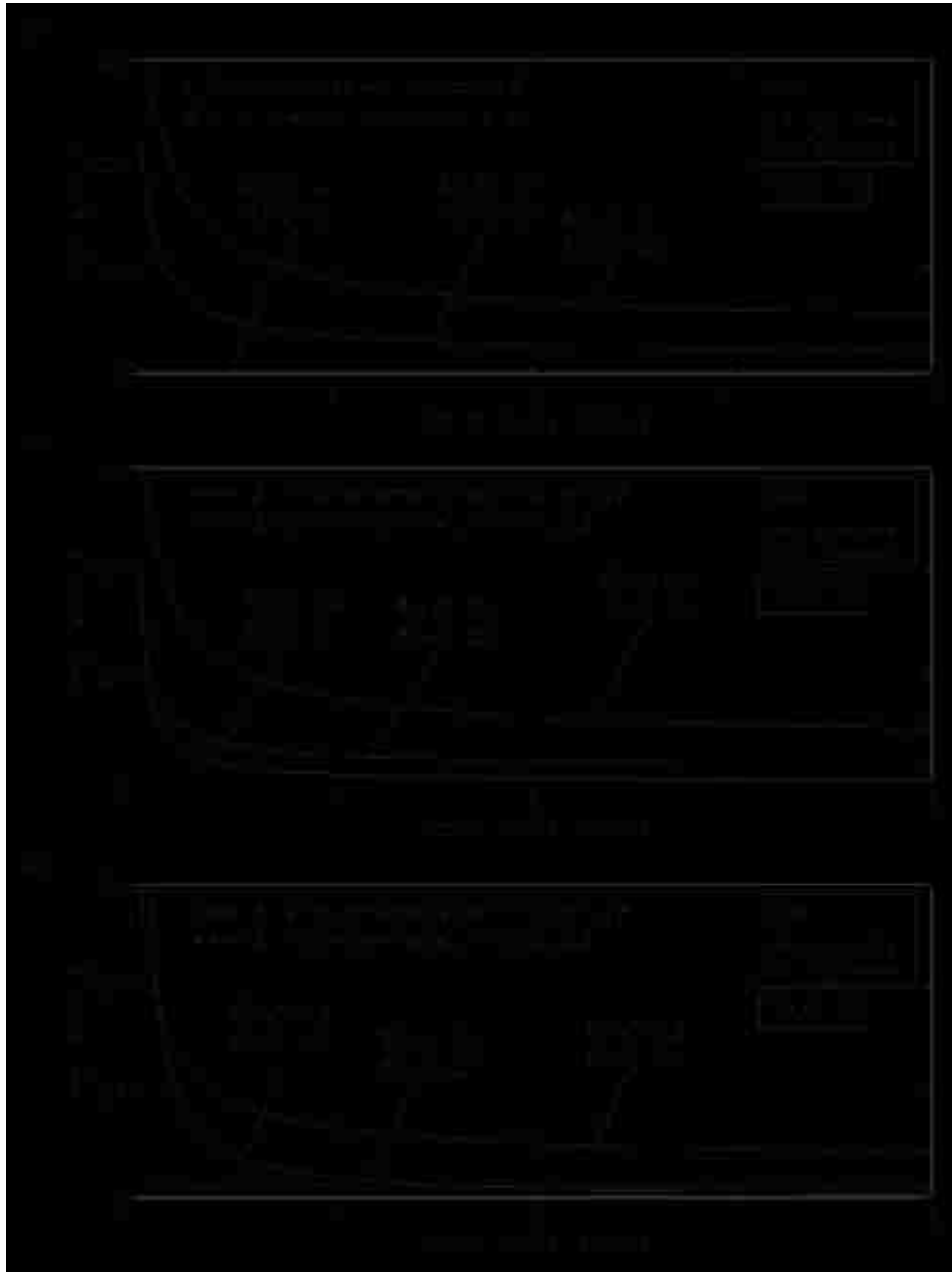
Figure 4.10 Comparison for the case with lognormal system resistance and load effect, varying central safety factor and constant mean value of load effect; (a), (b) and (c) the type *A* error, e_A.

123

Figure 4.11   Comparison for the case with lognormal system resistance and extreme

value type I largest load effect, varying central safety factor and

constant mean value of load effect; (a), (b) and (c) the reliability

indices, β_1, β_2, and β_3.

Figure 4.12   Comparison for the case with lognormal system resistance and extreme value type I largest load effect, varying central safety factor and constant mean value of load effect; (a), (b) and (c) the type *B* error, *e_B*.
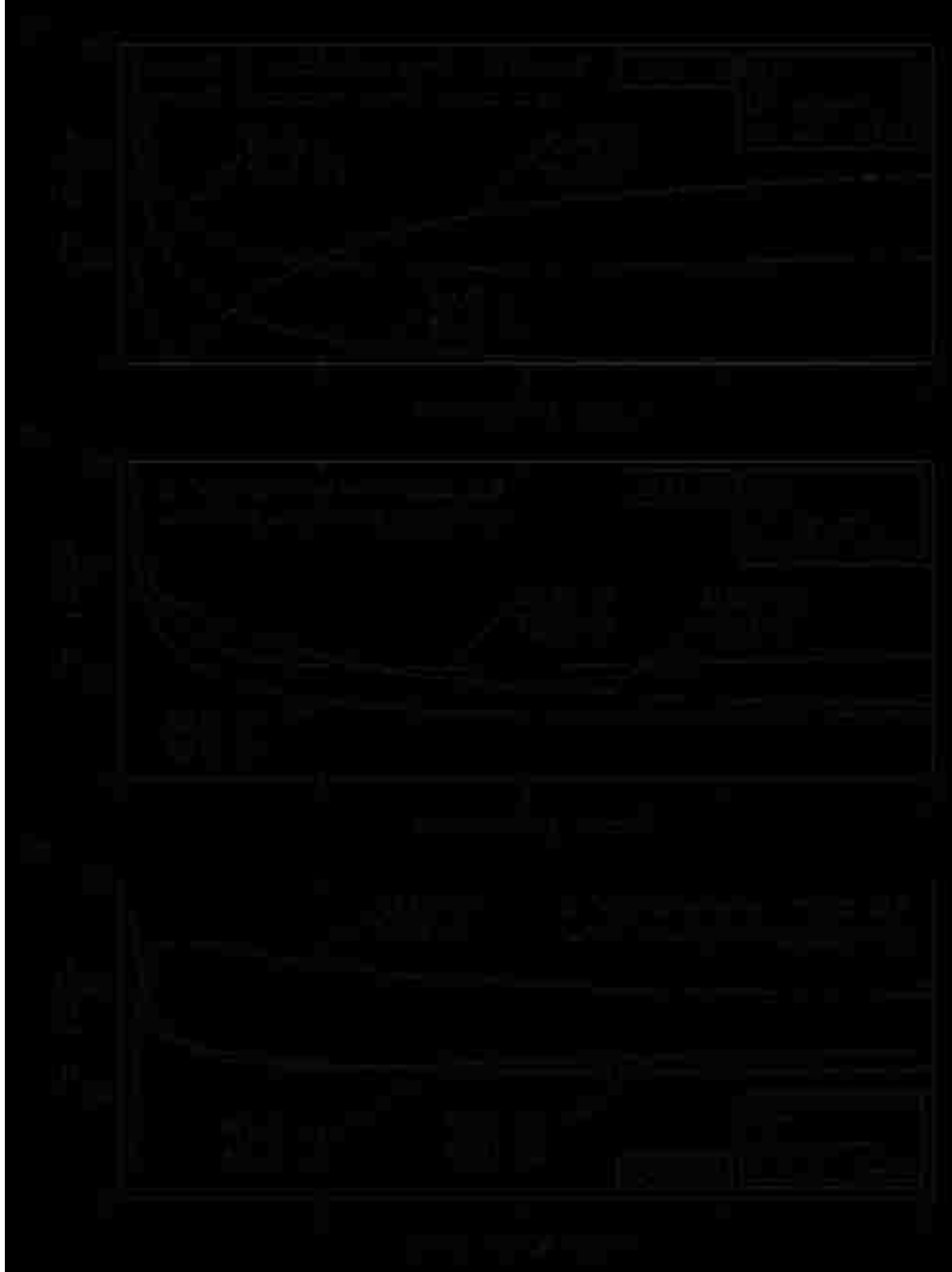
Figure 4.13   Comparison for the case with lognormal system resistance and extreme
value type I largest load effect, varying central safety factor and
constant mean value of load effect; (a), (b) and (c) the type C error, e_C.

CHAPTER 5

ASSESSMENT OF RISK USING BRIDGE ELEMENT CONDITION RATINGS

5.1 INTRODUCTION

In performance evaluation of structures under uncertainty, reliability-based structural performance indicators have become the major tool. They reflect the uncertainty in the load and resistance. However, they do not account for the outcome of a failure event in terms of economic losses. Risk-based performance measures provide the means of combining the probability of component or system failure with the consequences of this event. It is important to make use of risk-based performance indicators in the management of bridge structures, which have significant economic impact on the society, and allocating resources efficiently. Risk-based performance indicators can be used to determine optimal maintenance strategies. Priority ranking of bridges for maintenance can be based on risk and benefit-cost analysis. However, quantifying risk is a challenging task. In quantification of risk-based measures, the major aspects are the probability of failure and consequences of failure. Bridge element condition ratings can be used in quantifying the risk from failure at component and system levels. The probability of a bridge component to be in a specific condition state is time-variant. The risk associated with the failure of a component is the sum of the risks associated with the failure of this component in various condition states. Therefore, the total risk associated with component failure increases their deterioration. The events that a bridge component is in a specific condition state are mutually exclusive and collectively exhaustive under the assumption that the level of

127

deterioration is uniform along the length of the component. A bridge component can be discretized into sub-components where the variation of the deterioration level along the length of each sub-component is negligible. In this way, the assumption that a bridge component can only belong to one condition at any specific time is extended to the bridge sub-components. This offers a rational way of combining the consequences of different component failures within a system.

Risk-based methodologies have been already applied to the management of the civil infrastructure. Stein et al. (1999) used the risk concept for prioritizing scour vulnerable bridges. Adey et al. (2003) focused on the determination of optimal interventions for bridges affected by multiple hazards. Lounis (2004) presented a multi-criteria approach for maintenance optimization of bridge structures with emphasis on risk minimization. Ang (2011) focused on life-cycle considerations in risk-informed decisions for the design of civil infrastructure. Decò and Frangopol (2011) provided a framework for the quantitative risk assessment of individual highway bridges under multiple hazards.

Markov-based models have been used extensively in estimating the time-variant performance of highway bridge structures. Golabi, Kulkarni, and Way (1982) developed a pavement management system based on a Markov decision model used in the derivation of Pontis bridge management system. Jiang, Saito, and Sinha (1988) developed a bridge performance prediction model based on the Markov chain, which can be used to predict the percentages of bridges with different condition ratings. Gopal and Majidzadeh (1991) proposed a highway management method using the Markov decision process, which overcomes the shortage of methods based on level of

128

service. Madanat (1993) presented a methodology for planning the maintenance and rehabilitation activities for transportation facilities based on the latent Markov decision process. Al-Wazeer (2007) proposed a methodology for defining bridge maintenance strategies based on risks associated with conditions of bridge elements and costs needed to improve these conditions.

In this chapter, a methodology for quantifying lifetime risk associated with the component failure and risk based robustness of bridge superstructures is presented. The risk is quantified in terms of the expected losses (Saydam, Frangopol, and Dong 2012). The expected losses are categorized in direct and indirect losses. It has been a common approach to assess the failure probabilities and risk based on a certain time-dependent corrosion penetration curve for components. In this chapter, the possibility of different corrosion levels at a time instant is considered by means of a set of mutually exclusive and collectively exhaustive condition states. The proposed methodology of loss estimation takes into account the failure probability of different levels of component deterioration weighted by the occurrence probabilities of these levels. A scenario-based approach, which uses the Pontis element condition rating system, is used for identifying expected losses. The deterioration process of bridge components regarding the transition between the condition states are modeled as a Markov process. In addition, a reliability-based approach is applied to compute the component and system failure probabilities given the condition states. The methodology is illustrated on an existing bridge, the I-39 Bridge which is located near Wausau, WI. The expected losses associated with the flexural failure of girders are quantified in time. Furthermore, the time-variant risk-based robustness index, which is

129

the ratio of expected value of direct loss to the expected value of total loss, is investigated.

5.2 PONTIS BRIDGE ELEMENT CONDITION RATING SYSTEM

Pontis is a bridge management system developed to assist the transportation agencies in decision making about activities involving preservation or improvement of bridge structures (Cambridge Systematics, Inc. 2009). Pontis stores complete bridge inventory and inspection data, including detailed element conditions; formulates network-wide preservation and improvement policies for use in evaluating the needs of each bridge in a network; makes project recommendations to derive maximum benefit from limited funds; reports network and project-level results; and estimates individual bridge life-cycle deterioration and costs (Cambridge Systematics, Inc. 2009).

Based on visual inspection results, Pontis assigns condition states for bridge components to indicate their level of deterioration. The condition states vary between 1 and 5 (or 4), with increasing condition state indicating higher damage level. In this paper, the methodology is illustrated on a steel girder bridge superstructure with a reinforced concrete (RC) deck. Pontis defines five condition states for painted open steel girder (Cambridge Systematics, Inc. 2009; Thompson et al. 1998). In the first condition state, there is no evidence of active corrosion and the paint system is sound and functioning as intended to protect the metal surface. In the second condition state, there is little or no active corrosion, surface or freckled rust has formed or is forming

130

and the paint system distress but there is no exposure of metal. In the third condition state, surface or freckled rust is prevalent, the paint system is no longer effective, and there may be exposed metal but there is no active corrosion. In the fourth condition state, the paint system has failed, the surface pitting may be present but any section loss due to active corrosion does not yet warrant structural analysis of either the element or the bridge. In the fifth condition state, corrosion has caused section loss and is sufficient to warrant structural analysis to ascertain the impact on the ultimate strength or serviceability of either the element or the bridge.

A component can only be in one specific condition state at a time instant assuming the deterioration level is constant over the length and the probabilities that a component is in different condition states add up to 1.0. Therefore, these condition states form a set of mutually exclusive and collectively exhaustive events. In Figure 5.1, the possible condition states of a bridge component (i.e., painted steel girder) are illustrated in a Venn diagram with five mutually exclusive and collectively exhaustive events.

5.3 MODELING COMPONENT DETERIORATION USING MARKOV CHAIN

Markov chain is a common methodology to predict the deterioration of bridge components and systems. Deterioration model used in Pontis bridge management system is based on Markov chain. There are two fundamental rules of the Markov chain theory. In a Markov process, the probability of transition to a future state, given the current state, is independent of the past states. The rate of transition from one state

131

to another is constant over time. A change of state occurs only at the end of the time period and nothing happens during the time period chosen. The probability of moving from any given state i to state j on the next time interval is called the transition probability p_{ij}. In Pontis bridge management system, transition probabilities are also assumed to be stationary over the time. Considering a bridge component with a condition state space $\{1, 2, \ldots, m, m+1\}$, under the assumption that the component is not repaired as it deteriorates and the transition happens only between the subsequent states, the transition probability matrix used in the prediction of the component performance is

$$\mathbf{TP} = \begin{bmatrix} p_{11} & 1-p_{11} & \cdots & 0 & 0 \\ 0 & p_{22} & \cdots & 0 & 0 \\ \vdots & \vdots & \ddots & \vdots & \vdots \\ 0 & 0 & \cdots & p_{mm} & 1-p_{mm} \\ 0 & 0 & \cdots & 0 & 1 \end{bmatrix} \tag{5.1}$$

where p_{ii} are the probabilities that the component will remain in the same condition state in the transition. It is important to note that the worst state $m+1$ is considered as an absorbing state. Assuming that the initial state probability vector of a steel girder element with five possible condition states is $\mathbf{S}(0)=[1\ 0\ 0\ 0\ 0]$, the state probability vector after t transitions is

$$\mathbf{S}(t) = \mathbf{S}(0) \cdot \mathbf{TP}^t \tag{5.2}$$

where $\mathbf{TP}^t$ is the tth power of the transition probability matrix.

The transition probability matrix is the core of Markov chain. A homogeneous Markov chain model is used in this paper as Pontis bridge management system does; however, time-variant transition probability matrices can be easily adopted. The

132

estimation of the transition probabilities depends on the inspection data acquired from many bridges over time. In the case of available adequate inspection data, different transition probability matrices can be used to represent the deterioration of different class of bridges under various environmental conditions (e.g., high corrosion zone, low corrosion zone).

5.4 THE METHODOLOGY OF ASSESSING RISK

The procedure of risk assessment starts with identifying the vulnerable components of a system to be included in the analysis. The risk assessment methodology in this paper makes use of Markov chain to model the deterioration of the components based on condition ratings. The transition probability matrices are identified for each component. Using these transition probability matrices, the time-variant Markov chain state probabilities for bridge components (i.e., the probability that a bridge component is in a certain condition state) are computed. After identifying the random variables associated with the component resistance and load effects, the time-variant component failure probabilities for the possible condition states are obtained. For instance, the corrosion level is different for different condition states. Therefore, the failure probabilities of a girder are different for different condition states. The effect of time-variant corrosion level can be accounted by updating the cross-section dimensions at each point in time depending on the corrosion penetration. The direct risk is the one associated with the component failure only (i.e., the subsequent system failure initiated by the component failure is not accounted in direct risk). The direct

133

consequences of component failure are identified. The expected direct loss for a single component is computed by combining the condition state probabilities, the component failure probabilities in different condition states and the direct consequences of the component failure. The total expected direct loss is the sum of the expected direct losses for all components. On the other hand, the indirect risk is the one associated with the system failure initiated by the component failure. The indirect consequences of component failure are identified. A scenario-based approach regarding the condition states of the components is applied for the computation of the expected indirect losses. For instance, it is possible that a bridge component fails in condition state 3 while two other components are in condition states 4 and 5, respectively. Similarly, it is possible that the same component fails in condition state 5 while two other components are in condition states 2 and 3, respectively. Therefore, a set of scenarios are considered. The expected indirect loss for each scenario is computed by combining the condition state probabilities of components, the component failure probabilities in different condition states, the system failure probabilities given the component has already failed, and the indirect consequences of the component failure. The total expected indirect loss is the summation of the expected indirect losses for all scenarios. Finally, the time-variant risk-based robustness index is computed as the ratio of the expected direct loss to the sum of the expected direct and indirect losses. The methodology for assessing the expected losses and the risk-based robustness index is illustrated in Figure 5.2.

134

5.5 RELIABILITY ASSESSMENT AT COMPONENT AND SYSTEM LEVELS

It is possible to evaluate the bridge system reliability by making appropriate assumptions (e.g., series, parallel and combined system assumptions) regarding the interaction of individual components (Ditlevsen and Bjerager 1986, Hendawi and Frangopol 1994). In this method, the reliability of a bridge structural system is evaluated by considering the system failure as series-parallel combination of the component limit states. The first step of such an approach is determining the random variables and their statistical parameters for component reliability analysis. All the limit states for all possible failure modes of the components should be included in the system model by considering proper assumptions. For instance the system reliability model of the girder bridge superstructure shown in Figure 5.3(a), considering only the flexural and shear failure modes of the components (i.e., the four girders G1 to G4 and the slab S), is illustrated in Figure 5.3(b). The derivation of a limit state equation for a bridge girder varies considerably depending on whether the girder is simply supported or continuous (Akgül and Frangopol 2004). Flexural and shear capacity of girders and slab can be calculated according to AASHTO LRFD Bridge Design Specification (AASHTO, 2010).

In order to account for the time effects and sudden damage, it is possible to compute the component and system failure probabilities by updating the resistance of the component or system in the limit state functions based on the time-variant deterioration or damage level of the structure. So, the component failure probabilities for different condition states can be determined if the deterioration level at each condition state is known. These component failure probabilities for different condition

135

states can be combined with the time-variant Markov chain state probabilities (i.e., probabilities of a component being in certain condition states at a point-in-time). The time-variant component failure probability weighted with Markov chain state probability for a certain condition state, $P_{(CFij)}(t)$, can be expressed as

$$P_{(CF_{ij})}(t) = P_{(CS_i = S_j)}(t) \cdot P_{(CF_i|CS_i = S_j)}(t) \tag{5.3}$$

where $P_{(CSi=Sj)}(t)$ is the probability of component i being in condition state j at time t, and $P_{(CFi|CSi = Si)}(t)$ is the conditional failure probability of component i given the component is in condition state j at time t. In other words, probability $P_{(CFi|CSi = Si)}(t)$ is the conditional probability of component failure given a certain level of deterioration (e.g., corrosion penetration). Index i varies over the number of the components within the structure and index j varies over the number of condition states for a component. Equation 5.3 does not account for the system failure and is involved in the formulation of expected direct loss.

Since the indirect losses are associated with system failure, one more step in Equation 5.3 is required for the assessment of indirect loss, which is including the system failure probability. Depending on the redundancy of a structure, the system failure probability increases following the failure of a component. Therefore, system failure following the failure of different components has to be accounted. On the other hand, the failure of a component can occur in different condition states as it is accounted in Equation 5.3. In addition, while the failing component is in a certain condition state, the other components can be in any other condition states as the system fails, which results in a set of scenarios to consider in the risk assessment. The scenario-based approach will be described in details in the following sections. The

136

time-variant system failure probability weighted with Markov chain state probability following the failure of a certain component (i) at a certain condition state (j) at a time instant, $P_{(SFij)}(t)$, can be expressed as

$$P_{(SF_{ij})}(t) = P_{(CS_i=S_j)}(t) \cdot P_{(CF_i|CS_i=S_j)}(t) \cdot P_{(SF_i|CF_{ij})}(t) \tag{5.4}$$

where $P_{(SFi|CFi)}(t)$ is the conditional probability of system failure given that component i has already failed.

5.6 CONSEQUENCES OF COMPONENT AND SYSTEM FAILURE

The consequences of component and system failure depend on the structure type, size, and its importance. This paper focuses on the consequences of failure in highway bridge structures. Although the consequences are random variables in reality, in this study the expected values of consequences are used for the clarity of the approach. The consequences of bridge component failure are categorized in direct and indirect consequences. Both types of consequences are quantified in monetary value. In this way, the relationship between the amount of a future expenditure and its equivalent present value is calculated using the discount rate. The value of consequences for each specific year t is determined as follows:

$$FV(t) = PV(1+r)^t \tag{5.5}$$

where PV is the present value of the expenditure; $FV(t)$ is the value of an expenditure made after t years; r is the annual discount rate.

In this paper, the direct consequence of component failure is considered as the replacement cost of the component. However, any other costs, such as the repair cost,

137

can be included within the framework. The replacement cost of a component can be approximately estimated if the unit price of the component is known. For instance, the direct consequence of a bridge girder failure can be expressed as

$$C_{Direct}(t) = c_g G_g L_g (1 + r)^t \tag{5.6}$$

where c_g is the price of the girder for unit weight in unit length, G_g is the weight of the girder in unit length, and L_g is the length of the girder.

The indirect consequences are divided in two groups. The first group includes the indirect consequences of component failure if a subsequent system failure occurs. These consequences are considered as the rebuilding cost of the structure, the running cost of the detouring vehicles, and time loss due to the unavailability of the highway segment. The second group consists of the consequences of component failure if a subsequent system failure does not occur. These consequences depend on the assumptions used in the risk analysis. For example, in case of lane closure on the bridge, although the system failure did not occur, among the indirect consequences, there will be the additional running cost of the detouring vehicles and time loss. The cost of rebuilding a bridge structure can be expressed as (Stein et al. 1999)

$$C_{Reb}(t) = c_{Reb} WL(1 + r)^t \tag{5.7}$$

where c_{Reb} is the rebuilding cost per unit area of the bridge; W is the width of the structure; and L is the length of structure. The running cost of the detouring vehicles and time loss due to the unavailability of the highway segment can be computed as (Decò and Frangopol 2011)

$$C_{Run}(t) = \left(c_{Run,car}(1 - \frac{T}{100}) + c_{Run,truck} \frac{T}{100} \right) D_l A(t) d(1 + r)^t \tag{5.8}$$

138

$$C_{Tl}(t) = \left(c_{AW} O_{car} (1 - \frac{T}{100}) + (c_{ATC} O_{truck} + c_{good}) \frac{T}{100} \right) \frac{D_l A(t) d}{S} (1+r)^t \qquad (5.9)$$

where $c_{Run,car}$ and $c_{Run,truck}$ is the cost of running for cars and trucks (USD/km), respectively; D_l is the detour length (km); $A(t)$ is the average daily traffic (ADT) at year t (number of vehicles per day); d is the duration of detour (days); T is the average daily truck traffic (ADTT, %); c_{AW} and c_{ATC} is the average wage per hour (USD/h); O_{car} and O_{truck} are the occupancy rate for cars and trucks, respectively; c_{good} is the time value of the goods transported in a cargo (USD/h); and S is average detour speed (km/h). The duration of the detour is referred as a function of ADT. For a bridge with higher ADT, it requires quicker repair than those with lower ADTs. Accordingly, the repair time can be considered 36 months for ADT≤100; 24 months for 100<ADT≤500; 18 months for 500<ADT≤1000; 12 months for 1000<ADT≤5000; and 6 months for ADT>5000 (Stein et al. 1999).

The total indirect consequences are the sum of the rebuilding cost, the running cost of the detouring vehicles and time loss due to the unavailability of the highway segment. These consequences can be expressed as

$$C_{Indirect}(t) = C_{Reb}(t) + C_{Run}(t) + C_{Tl}(t) \qquad (5.10)$$

5.7 QUANTIFYING RISK AT COMPONENT AND SYSTEM LEVELS

In this paper, risk assessment is based on the quantification of the expected value of losses. In its general form, expected value of loss can be formulated as (based on CIB 2001)

139

$$L = \int\limits_{-\infty}^{\infty}\int\limits_{-\infty}^{\infty}\cdots\int\limits_{-\infty}^{\infty} C(x_1, x_2, \cdots, x_m) \cdot f_{\mathbf{X}}(x_1, x_2, \cdots, x_m) \cdot dx_1 \cdot dx_2 \cdots dx_m \qquad (5.11)$$

where C represents the consequences, $\mathbf{x}=\{x_1, x_2,\ldots, x_m\}$ is the set of random variables associated with the consequences, and $f_{\mathbf{X}}(\mathbf{x})$ is the joint probability density function of the random variables. The probabilities of components being in each condition state can be computed using the Markov model presented previously. In addition, the consequences associated with component failure and system failure can be identified as explained in the previous section. In this section, the procedure to combine the probabilities and consequences to estimate the time-variant expected loss is presented. Risk assessment of structures requires considering all possible damage and failure scenarios in the analysis. Scenarios should be based on the state (e.g., functioning or not functioning; moderate damage or severe damage) of each component within a system. The assessment of expected direct losses is based on component failure in different states. For instance, a component of the structure may fail at a point in time with the possibility of being in various condition states (e.g., a certain level of deterioration). In this paper, the total loss is computed based-on discrete scenarios regarding condition states of components weighted with the Markov state probabilities. The expected direct loss associated with the failure of a component is the sum of the expected direct losses of the component failure in all possible condition states for this component. The total expected direct loss is the sum of the expected direct losses associated with all the vulnerable components within the structure expressed as

140

$$L_{Direct}(t) = \sum_{j=1}^{n} \sum_{i=1}^{m} P_{(CS_i=S_j)}(t) \cdot P_{(CF_i|CS_i=S_j)}(t) \cdot C_{Direct,i}(t) \qquad (5.12)$$

where m is the number of condition states for a component, and n is the number of components included in the risk analysis, and $C_{Direct,j}$ is the direct consequence of the failure of component i.

A scenario based approach regarding the condition states of the components is adopted for the assessment of the indirect losses. These scenarios are based on the component failure events in different condition states while other components within the structure are in different condition states. For instance in a structure with five components, a component may fail in condition state 3 while the other components were in condition states 4, 3, 2 and 5. The same component may fail in condition state 2 while the other four components were in condition states 3, 2, 4, and 4. Considering these combinations for all components yields to large set of scenarios in the risk analysis.

The total expected indirect loss expressed as

$$
\begin{aligned}
L_{Indirect}(t) = \sum_{i=1}^{n} \sum_{p=1}^{m} \sum_{j=1}^{n-1} \sum_{q=1}^{m} \cdots \sum_{k=1}^{n-1} \sum_{r=1}^{m} &\left(\begin{array}{l} P_{(CS_j=S_q)}(t) \cdot \left(1 - P_{(CF_j|CS_j=S_q)}(t)\right) \cdot \ldots \cdot P_{(CS_k=S_r)}(t) \cdot \\ \left(1 - P_{(CF_k|CS_k=S_r)}(t)\right) \end{array} \right). \\
&\cdot P_{(CS_i=S_p)}(t) \cdot P_{(CF_i|CS_i=S_p)}(t) \cdot P_{(SF_i|CF_i)}(t) \cdot C_{Indirect}(t)
\end{aligned} \qquad (5.13)
$$

is the sum of indirect losses associated with each scenario, where products of probabilities and consequences are summed over the number of components that are failing and surviving and over all possible condition states of these components.

141

5.8 RISK-BASED ROBUSTNESS INDEX

A system can be considered as robust if the indirect risks do not contribute significantly to the total system risk (Baker, Schubert, and Faber 2008). An index of robustness was proposed as the ratio of the direct risk to the total risk (Baker, Schubert, and Faber 2008). In this paper, the robustness index is formulated as

$$I_{Rob} = \frac{L_{Direct}}{L_{Direct} + L_{Indirect}} \tag{5.14}$$

where L_{Direct} and $L_{Indirect}$ are the expected values of direct and indirect losses, respectively. This index varies between 0 and 1 with larger values representing a higher robustness. Applications of risk-based robustness concept to structures and infrastructures can be found in Faber et al. (2006), Schubert (2006), Baker, Schubert, and Faber (2008), and Saydam, Frangopol, and Dong (2012).

5.9 CASE STUDY: I-39 NORTHBOUND BRIDGE OVER WISCONSIN RIVER

The procedure described to compute the time-variant expected losses and risk-based robustness is applied to the I-39 Bridge which is located near Wausau, WI. It carries US 51 and I-39 Northbound over the Wisconsin River. A structural health monitoring program was conducted on the bridge between July and November 2004 by the personnel from ATLSS Engineering Research Center at Lehigh University. According to the report on this program (Mahmoud, Connor, and Bowman 2005), the I-39 Bridge is a five span continuous steel girder bridge, which has slightly curved span lengths of 33.41 m, 42.64 m, 42.67 m, 42.64 m and 33.41 m. The built-up steel plate girders

142

consist of the top and bottom flange plates and a web plate of 132.1 cm height. The steel used in the girders has nominal yield strength of 345 MPa. A hypothetical scheme for the bridge superstructure system consisting of four steel girders and reinforced concrete (RC) deck is provided in Figure 5.3(a). The risk associated with the flexural girder failure in the mid-section of the third span is quantified in terms of the expected losses, for the sake of clarity, although the system failure is not defined by only one location and single failure mode.

5.9.1 Time-variant Condition State Probabilities for the Components of the Bridge

In this paper, the time effects associated with the resistance of the bridge components are modeled by time-variant Markov chain state probabilities of component condition states. The condition state of a component at a time instant is random and this randomness is represented by the Markov chain probabilities. Pontis bridge management system defines five condition states for open, painted steel girders and RC deck. In this case study, the parameters defining the deterioration of the two exterior girders 1 and 4, and the two interior girders 2 and 3 are considered identical, respectively. The initial state probability vector for the exterior and interior girders and the RC deck is S(0)=[1 0 0 0 0]. Estimation of the transition probabilities for bridge components requires adequate available inspection data history for large number structures and the probabilistic methodologies to process the available data. Methods for estimating transition probability matrix include arithmetic method, Pontis method, and the method proposed by Fu and Devaraj (2008). Arithmetic method uses the data

143

regarding observed condition change over a time period and creates the transition probability matrix that can produce exactly the observed condition changes. Pontis method depends on expert elicitation and historical inspection data. In this approach, the difference between the predicted probabilistic conditions and the inspection based conditions are minimized to estimate the homogenous transition probability matrix. Fu and Devaraj (2008) used a similar approach to estimate the non-homogenous transition probability matrix. Estimation of transition probabilities is out of the scope of this paper. In this case study, the transition probabilities for bridge components are assumed based on those used in Al-Wazeer (2007) as

$$TP_{G1} = TP_{G4} = \begin{bmatrix} 0.96 & 0.04 & 0 & 0 & 0 \\ 0 & 0.92 & 0.08 & 0 & 0 \\ 0 & 0 & 0.88 & 0.12 & 0 \\ 0 & 0 & 0 & 0.84 & 0.16 \\ 0 & 0 & 0 & 0 & 1 \end{bmatrix} \qquad (5.15)$$

$$TP_{G2} = TP_{G3} = \begin{bmatrix} 0.97 & 0.03 & 0 & 0 & 0 \\ 0 & 0.94 & 0.06 & 0 & 0 \\ 0 & 0 & 0.91 & 0.09 & 0 \\ 0 & 0 & 0 & 0.88 & 0.12 \\ 0 & 0 & 0 & 0 & 1 \end{bmatrix} \qquad (5.16)$$

$$TP_{Deck} = \begin{bmatrix} 0.95 & 0.05 & 0 & 0 & 0 \\ 0 & 0.90 & 0.10 & 0 & 0 \\ 0 & 0 & 0.85 & 0.15 & 0 \\ 0 & 0 & 0 & 0.80 & 0.20 \\ 0 & 0 & 0 & 0 & 1 \end{bmatrix} \qquad (5.17)$$

where TP_{G1}, TP_{G1}, TP_{G1}, and TP_{G1} are the annual transition probability matrices of the girders and TP_{Deck} is the annual transition probability matrices of the deck. The time-variant condition state probabilities of the five components are computed using

144

Equation 5.2 and presented in Figure 5.4(a), (b) and (c). The condition state probabilities of higher condition states for the deck (in Figure 5.4(c)) increase faster than those for the girders as expected from the transition probabilities.

5.9.2 Reliability Analysis of the Components and the System

The yield stress of each steel girder, the compressive strength of the concrete deck, and the yield stress of steel reinforcement in the deck are considered as the random variables associated with component and system resistance. All random variables are considered lognormally distributed. The mean values of the girder steel yield stress, the compressive strength of the concrete slab, and yield stress of the deck steel reinforcement are 345 MPa, 28 MPa, and 414 MPa, and their coefficients of variation are 0.11, 0.18, and 0.11, respectively.

The limit states defined in AASHTO (2010) for the flexural failure of girders and the deck are adopted for the component reliability analyses. In order to compute the moment capacity of the components in a probabilistic manner, a sample space with 2000 samples is created using Latin Hypercube Sampling Method (McKay, Beckman, and Conover 1979). Then, the best distribution type for the moment capacity of the girders and the deck is found to be lognormal. The live load effect on the bridge is computed by combining the traffic data provided in Mahmoud, Connor, and Bowman (2005) and extreme value statistics. The average daily truck traffic is assumed to be 12% of the average daily traffic (Mahmoud, Connor, and Bowman 2005). The details

145

of application of the live load model to bridge structures can be found in Estes (1997) and Akgül (2002).

In the proposed risk assessment methodology, although the time effects for resistance are represented by Markov model, time-variant reliability analysis is required since the live loads on the bridge increase over time. The time-variant reliability of the components in different condition states has to be identified. In other words, the time-variant failure probability of a girder is computed for five different deterioration levels (condition states). The corrosion penetration pattern is illustrated in Figure 5.5. In this study, the section loss due to corrosion penetration in different condition states of steel girders is assumed to have a triangular probability density function (PDF) (a, b, c where a=min, b=mode, c=max) and the PDFs of girder section loss percentages in five condition states are presented in Figure 5.6. The relation between the section loss percentage (Δ) in different condition states of girders, the dimensions of the steel section, and the corrosion penetration on the surface can be expressed as

$$\Delta = \delta \cdot \frac{2d_w + 2d_{bf} + t_{tf} - t_w}{d_w t_w + t_{tf} d_{tf} + t_{bf} d_{bf}} \tag{5.18}$$

where Δ is percentage of section loss; δ is the corrosion penetration on the surface; d_w is the height of the web; t_w is the thickness of the web; d_{tf} is the width of the top flange; t_{tf} is the thickness of the top flange; d_{bf} is the width of the bottom flange; t_{bf} is the thickness of the bottom flange.

The corrosion in the steel reinforcement of the deck cannot be directly observed using visual inspection. One option is to estimate the randomness of section

146

loss of the reinforcement from the observed areas, observing number and width of cracks, degree of efflorescence, and percentage of surface spalls (Estes and Frangopol 2003). Thoft-Christensen (2001) has developed a relationship between the crack width on the surface of a concrete slab or beam and the section loss of the corroding reinforcing member. The relationship between the increase in crack width Δw over a period of time and the reduction in reinforcement diameter ΔD can be expressed as (Thoft-Christensen 2001)

$$\frac{1}{2} \cdot \left(\frac{\frac{D}{2}}{\frac{D}{2}+c} + 1 \right) \cdot c \cdot \Delta w = (\alpha_d - 1) \cdot \pi \cdot D \cdot \frac{\Delta D}{2} \tag{5.19}$$

where D is the original bar diameter, c is distance from the concrete surface to the steel reinforcement, and α_d is ratio of density of the corrosion rust product to the density of the reinforcing steel. The triangular distribution parameters for the observable crack width in RC deck in different condition states are presented in Table 5.1.

The reliability analyses of components are performed according to the described procedure for each condition state of these components. The time-variant probabilities of failure in five condition states are presented in Figure 7(a), (b), and (c) for exterior girders, interior girders, and the deck, respectively. It is worthy to note that the increase in the component failure probability over time is due to the increase in the live loads as the resistance is kept constant according to the deterioration level defined by the each condition state.

147

The system reliability analysis is based on the series-parallel combination of components. It is assumed that the system failure occurs if the deck fails or any two adjacent girders fail. The system failure model for the intact structure is illustrated in Figure 8(a). On the other hand, the risk of girder failure is assessed based on scenario associated with single girder failure in this paper. Therefore, the failure probability of the remaining system given one of the girders has already failed is also required. The remaining structure after the failure of an external girder and an internal girder is illustrated in Figures 9(a) and (b), respectively. The series-parallel system failure models for these two cases are presented in Figures 8(b) and (c). In this paper, it is assumed that when a girder fails, the lane on the girder side is closed and all the traffic is flowing through the other lane. An important aspect to consider is the fact that after the failure of a component, the load distributed to the girders does not remain the same. The new load shares of each girder are updated based on the live load distribution factors provided in AASHTO (2010).

5.9.3 Consequences of Girder Failure and System Failure

The direct consequence of girder failure is computed according to Equation 5.6. In this study, it is assumed that when a girder fails, the lane above it is closed. Therefore, even the system failure does not occur, it is necessary to consider the indirect consequence due to the lane closure. The consequence of the lane closure is computed as the sum of running cost of detouring vehicles and the cost of time loss, expressed in Equation 5.8 and Equation 5.9, respectively. The bridge is carrying two traffic lanes in

148

the northbound direction. The half of the ADT is assumed to be diverted from the bridge in order to reflect the effect of lane closure. In addition, the expected loss profiles for different values of the ratio of ADT diverted (θ) is obtained, which will be discussed in the next section. The replacement time of a failed girder is considered as four months. An annual discount ratio (r) of 2% is used in the calculations. The indirect consequences of girder failure followed by the system failure are computed according to Equation 5.7, Equation 5.8, Equation 5.9, and Equation 5.10. The values of the parameters used in the computation of consequences are provided in Table 5.2.

5.9.4 Expected Value of Losses

In this paper, risk of component failure is quantified in terms of the expected value of losses. The expected direct loss associated with the failure of one girder in a certain condition state can be quantified as the product the probability of the girder being in the certain condition state (Markov chain state probability), the failure probability of the girder given the girder is in that certain condition state and the direct consequence of failure of the girder. In Figure 5.10(a), the time-variant expected direct losses associated with the failure of girder 1 in condition state 3, the failure of girder 1 in condition state 4, the failure of girder 1 in condition state 5, the failure of girder 2 in condition state 4, the failure of girder 2 in condition state 5 are presented. The expected direct losses are negligible for most of the curves in this figure; however, they may reach significant values at the end of the considered time span, especially in the case of the failure of girder 1 in condition state 5. The expected direct losses associated with the girder 1 is higher than those of girder 3, since the deterioration of

149

the external girders are faster than the interior girders and the moment carrying capacity of the exterior girders are slightly smaller.

The expected indirect losses are quantified according to a scenario based approach. The scenarios are considered as failure events under different conditions. For instance, one scenario is the failure of the system given that girder 2 has failed in condition state 4 while girder 1, girder 3, girder 4 and the deck were in condition states 5, 4, 5, and 4 respectively. Another scenario is the failure of the system given that girder 2 has failed in condition state 3 while girder 1, girder 3, girder 4 and the deck were in condition states 4, 3, 4, and 5 respectively. Considering the possible conditions in this way, the total number of scenarios to consider is $4 \times 5 \times 5 \times 5 \times 5 \times 5 = 12,500$. Herein, it is assumed that girder 1 and girder 4 (exterior girders) are in the same condition state while girder 2 and girder 3 (interior girders) are in the same condition state. Therefore, the total number of scenarios accounted for is $4 \times 5 \times 5 \times 5 = 500$. The expected indirect loss associated with a scenario can be quantified as the product of a set of probabilities. This set of probabilities includes the probability of the girder being in the certain condition state (Markov chain state probability), the failure probability of the girder given the girder is in that certain condition state, the system failure probability given the girder has failed already, the product of the Markov chain state probabilities and the girder survival probabilities for all the other components surviving. In Figure 5.10(b), the time-variant expected indirect losses associated with 15 scenarios resulting in highest contribution to loss at the end of investigated time horizon. The most significant among these 15 scenarios include the failure of girder 1 in condition state 5 while girder 2, girder 3, girder 4 and the deck were in condition

150

states 5, 5, 5, and 5 respectively; the failure of girder 1 in condition state 5 while girder 2, girder 3, girder 4 and the deck were in condition states 4, 4, 5, and 5 respectively; the failure of girder 1 in condition state 5 while girder 2, girder 3, girder 4 and the deck were in condition states 3, 3, 5, and 5 respectively; the failure of girder 2 in condition state 5 while girder 1, girder 3, girder 4 and the deck were in condition states 5, 5, 5, and 5 respectively.

The total value of the expected direct and indirect losses is computed according to Equations 5.15 and 5.16, respectively. The variation of the expected direct, indirect and total losses in time is presented in Figure 5.11(a) in logarithmic scale. The results indicate that the expected indirect loss is significantly higher than the expected direct loss through the investigated time span. The difference between the expected direct and indirect losses increases with time. Both the total expected direct and indirect losses manifest their maximum value at the end of the investigated time span since no rehabilitation and reconstruction actions are considered. The risk-based robustness index is computed as the ratio of the expected direct loss to the expected total loss. The variation of the robustness index in time is presented in Figure 5.11(b). The robustness index starts with a value of 0.13 and increases to a peak value of 0.29 in 10 years and decreases to 0.02 at the end of the investigated time horizon. It is important to note that the increase in the value robustness index at early stages is not due to actually any improvement in the system behavior. It is rather related to the expression defining the index. Local peaks may occur depending not only on the values the expected direct and indirect losses, but also on their rate of increase in time. It is concluded that the risk-based robustness index is a more reliable performance

151

indicator for relatively longer time spans. In Figure 5.11(c), the time-variation of the contribution ratio of the 15 most significant scenarios mentioned previously (Figure 5.10(b)) is presented. The contribution ratio is basically the ratio of the summation of expected indirect loss associated with these 15 scenarios to summation of expected indirect loss associated with all scenarios. The contribution ratio of these 15 scenarios is very small within the first ten years. It starts to increase rapidly after this point and reaches almost 80% of the total value of the expected indirect loss. This is due to the fact that these 15 scenarios are low probability – high consequence events at the early stages. However, as the probability of components being in condition state 5 increases in time, these scenarios become high probability – high consequence events, resulting in high values of expected indirect loss. Therefore, their contribution to the total expected indirect loss is getting higher in time. It is also worthy to note that, there does not exist a set of few scenarios which results in a greater portion of the indirect loss at the early stages. There is a balance between high probability – low consequence scenarios and low probability – high consequence scenarios at the early stages. The results shown in Figure 5.10(a) and (b), and Figure 5.11(a) are in terms of expected losses which are computed based on the mean value of consequences. In order to illustrate the variation in the loss, methodology is repeated using the parameters of random variables associated with the consequences. Figure 5.12(a), (b), and (c) shows the variation of the indirect, direct, and total losses at the end of investigated horizon (*bridge age* = 70 years). The variation of the total loss at *bridge age* = 40 years is presented in Figure 5.12(c). It is the purpose of this example to demonstrate that the

152

methodology can be applied to existing bridges easily and the results obtained are in line with what could be expected.

In order to investigate the effect of the detour duration (d) due to the reconstruction of the bridge, the risk analysis described is performed for different values of d. The variation of expected indirect loss for three values of d=6 months, d=12 months, and d=18 months is presented in Figure 5.13(a). d=18 months yields the highest expected indirect loss among three values as expected. The difference between the curves gets more significant with time. The expected direct loss is not affected by this parameter. The variation of robustness index for three values of d=6 months, d=12 months, and d=18 months is presented in Figure 5.13(b). d=6 months yields the highest robustness index although the difference is not so significant.

To illustrate the effect of the ADT diverted from the bridge (θ) due to closing a lane, the risk analysis described is performed for different values of θ. The variation of expected indirect loss for three values of θ=25%, θ=50%, and θ=75% is presented in Figure 5.14(a). θ=75% yields the highest expected indirect loss among three values. The expected direct loss is not affected by this parameter. The variation of robustness index for three values of θ=25%, θ=50%, and θ=75% is presented in Figure 5.14(b). θ=25% months yields the highest robustness index. Although the difference is seems to be relatively high in the peak region, which should be ignored, it is not significant in overall through the investigated time span.

The methodology can be used as an intuitive tool for obtaining optimal policies for bridge maintenance. Knowing the contributions of different components to the total expected loss may provide support in priority ranking for maintenance actions

153

intuitively. It is possible that the priority ranks of components can vary over time as components deteriorate with different rates and as any bridge repair actions are done. In addition, the methodology may provide guidance for the timing of maintenance activities. Authorities may set thresholds for the risk they may not want to have, and perform the required maintenance activities when these thresholds are reached. With the availability of more powerful analysis tools, the methodology can be integrated in a maintenance optimization framework with conflicting criteria and multiple constraints in a life-cycle context.

5.10 CONCLUSIONS

This paper presents a methodology for quantifying lifetime risk of bridge superstructures. The risk is quantified in terms of the expected direct and indirect losses. Assessing failure probabilities and risk based on a single time-variant corrosion penetration curve for components has been a common approach in the previous studies. In this paper, the possibility of different corrosion levels at a time instant is considered by means of a set of mutually exclusive and collectively exhaustive condition states. A scenario-based approach integrating the Pontis element condition rating system into risk assessment procedure is used to identify expected losses. A Markov process is used to model the deterioration of bridge components regarding the transition between the condition states. In addition, a reliability-based approach is applied to compute the component and system failure probabilities given the condition states. An existing bridge is used to illustrate the methodology. The expected losses

154

associated with the flexural failure of girders are quantified in time. The time-variant risk-based robustness index, which is the ratio of expected value of direct loss to the expected value of total loss, is also computed.

The following conclusions are drawn:

1. The expected indirect loss is significantly higher than the expected direct loss through the investigated time span. The difference between the expected direct and indirect losses increases with time.

2. The contribution of damage scenarios to the total expected loss is far from being similar. In fact, a relatively small number of scenarios yield a significant contribution to the total expected loss.

3. The risk-based robustness index is a useful performance indicator. However, its variation with time could exhibit local peaks regardless of an improvement in the structural performance.

4. The detour duration due to the reconstruction of a bridge has an impact on the expected losses. The impact of this parameter on the overall trend of expected loss and risk-based robustness index is increasing in time significantly.

5. The ADT diverted from the bridge due to lane closure also has an impact on the expected loss. This impact fades over time.

The proposed methodology relies on the availability of reliable data regarding the transition probabilities between condition states of each component within a system. The purpose of investigating time-variant expected loss and risk-based robustness indicators is to use them in design and maintenance optimization of deteriorating

155

components and structural systems. Minimizing the expected losses, maximizing robustness index and minimizing total life-cycle cost are among the objectives of such optimization problems.

Table 5.1   Observable crack width in RC deck as random variable with respect to

the condition states

	Triangular Distribution Parameters for the Crack width in RC deck		
Condition State	a (mm)	b (mm)	c (mm)
1	0.00	0.80	0.04
2	0.00	2.00	1.00
3	0.00	2.50	1.25
4	0.00	3.00	1.50
5	2.50	4.50	3.50

157

Table 5.2 – Parameters used in the computation of consequences in the case study

Parameters Used in the Computation of Consequences	Mean Value	Coefficient of Variation	Reference
ADT	4514-33,458	-	Mahmoud, Connor, and Bowman (2005)
ADTT/ADT ratio	0.12	0.20	Mahmoud, Connor, and Bowman (2005)
Average compensation(truck drivers)	26.97 USD/h	0.15	Decò and Frangopol (2011)
Average detour speed	50 km/h	0.15	Decò and Frangopol (2011)
Average vehicle occupancies for cars	1.5	0.15	Decò and Frangopol (2011)
Average vehicle occupancies for trucks	1.05	0.15	Decò and Frangopol (2011)
Average wage (car drivers)	22.82 USD/h	0.15	Decò and Frangopol (2011)
Discount rate	2%	0.15	Assumed
Length of detour	2.9 km	0.15	Decò and Frangopol (2011)
Rebuilding costs	894 USD/m2	0.20	Stein et al. (1999)
Running costs for cars	0.08 USD/km	0.20	Decò and Frangopol (2011)
Running costs for trucks	0.375 USD/km	0.20	Decò and Frangopol (2011)
Time value of a cargo	4 USD/h	0.20	Decò and Frangopol (2011)
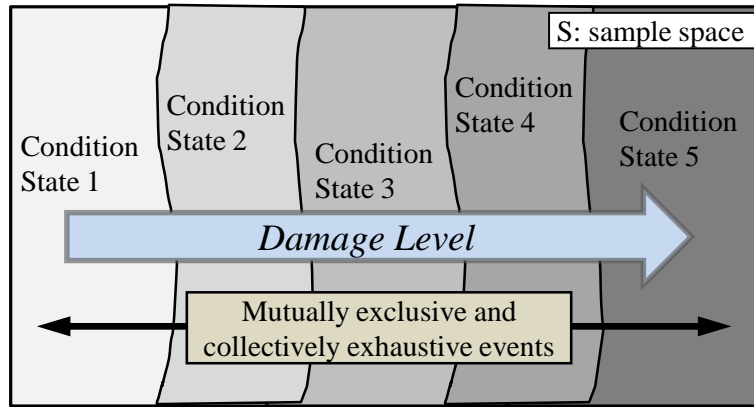
Figure 5.1   Pontis condition states for bridge components: mutually exclusive and

collectively exhaustive sets
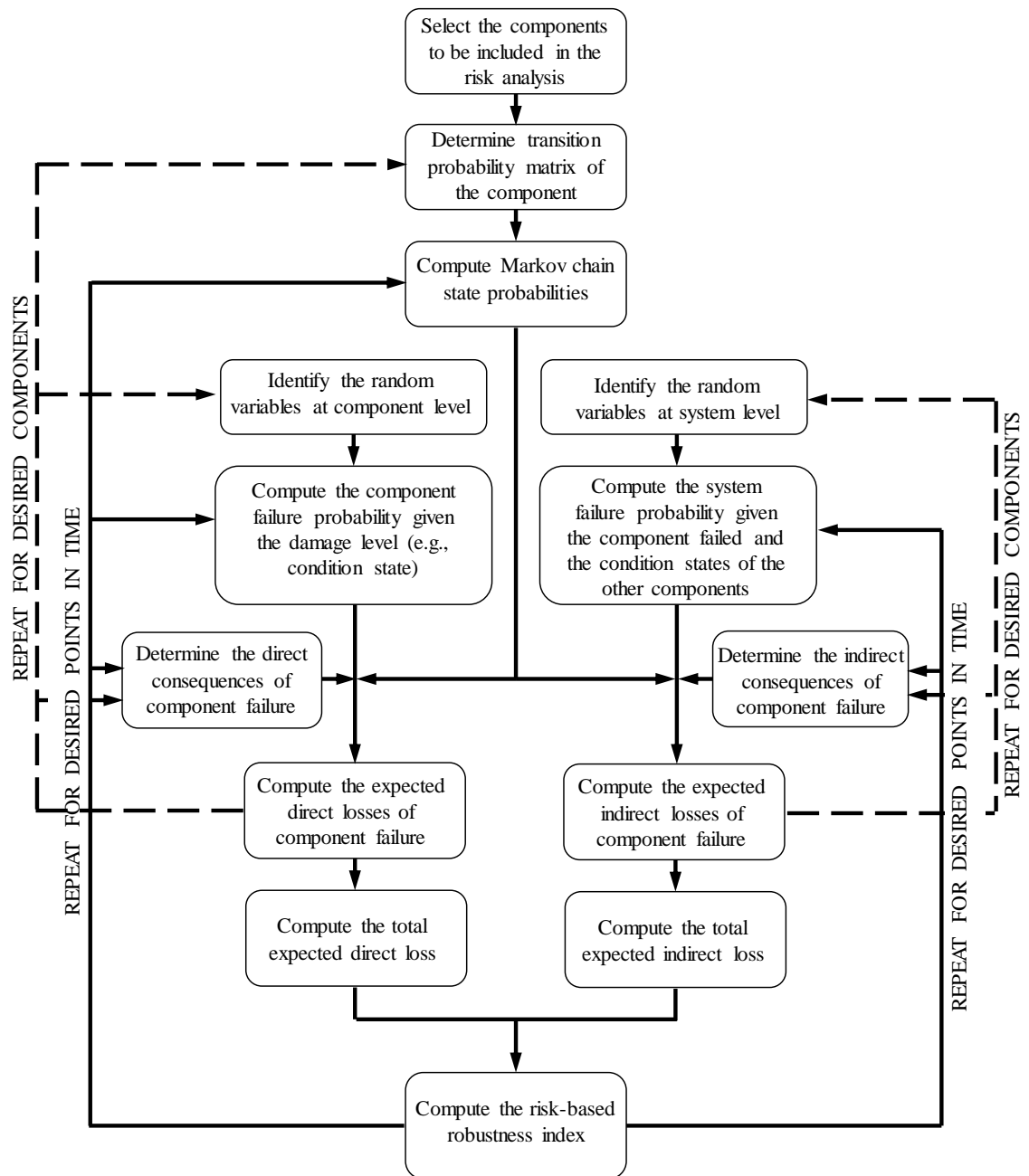
Figure 5.2   The framework of the methodology

160

(a)

S

G1   G2   G3   G4

(b)

S_S S_F $G1_S$ $G1_F$ $G2_S$ $G2_F$ $G3_S$ $G3_F$

$G2_S$ $G2_F$ $G3_S$ $G3_F$ $G4_S$ $G4_F$

S_S : Shear failure of slab S_F : Flexural failure of slab
$G1_S$: Shear failure of girder 1 $G1_F$: Flexural failure of girder 1
$G2_S$: Shear failure of girder 2 $G2_F$: Flexural failure of girder 2
$G3_S$: Shear failure of girder 3 $G3_F$: Flexural failure of girder 3
$G4_S$: Shear failure of girder 4 $G4_F$: Flexural failure of girder 4
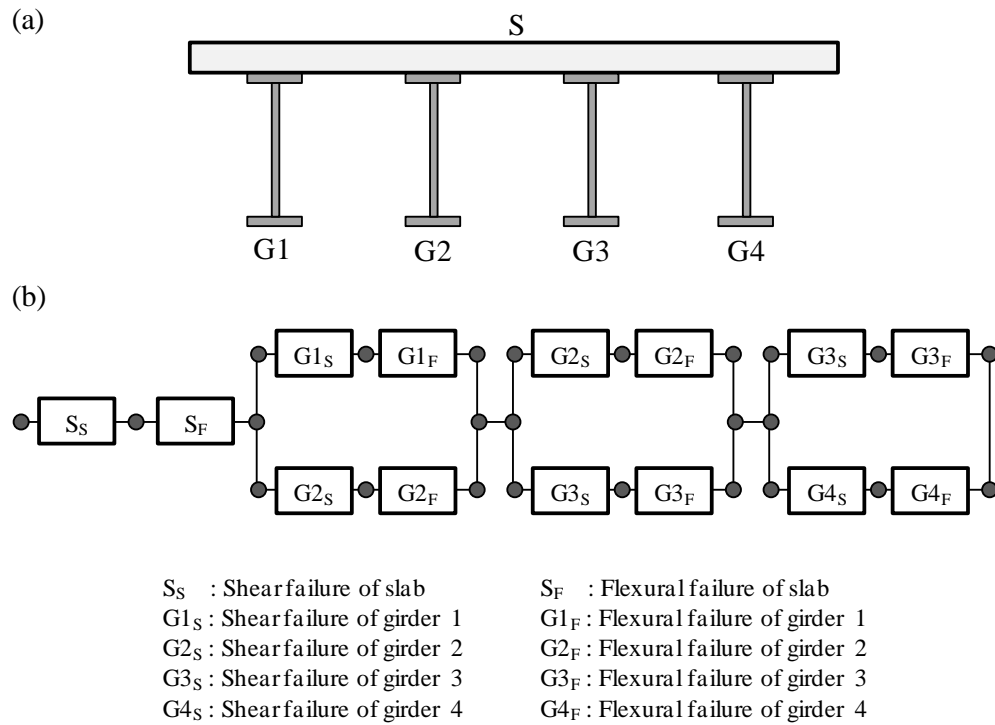
Figure 5.3   (a) Bridge superstructure system, and (b) bridge system failure model

161
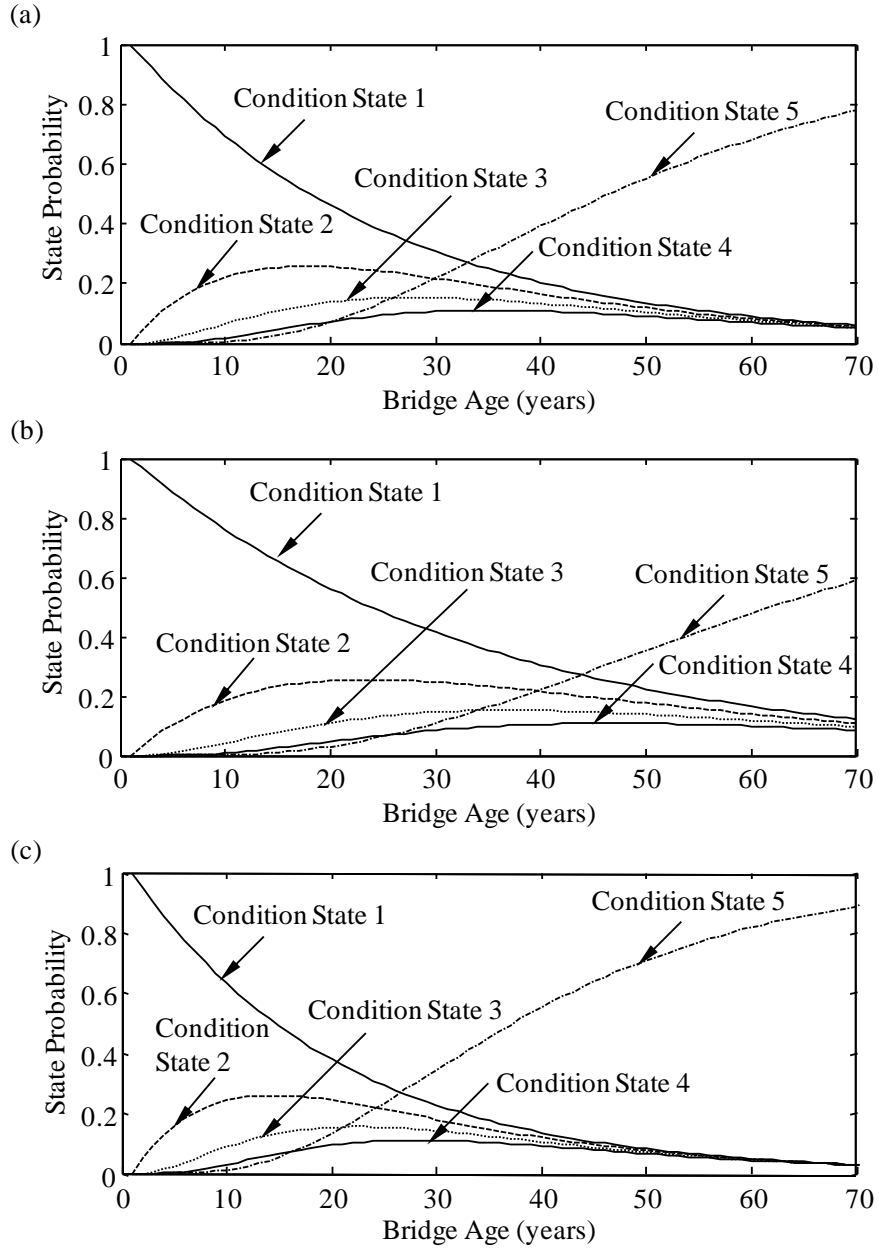
Figure 5.4   Time-variant Markov chain state probabilities for (a) girder 1 and

girder 4, (b) girder 2 and girder 3, and (c) deck

162
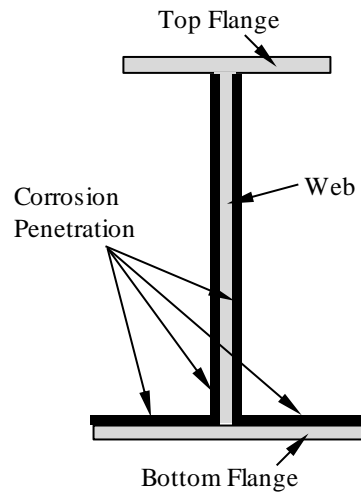
Figure 5.5   Corrosion penetration pattern in steel girders

163
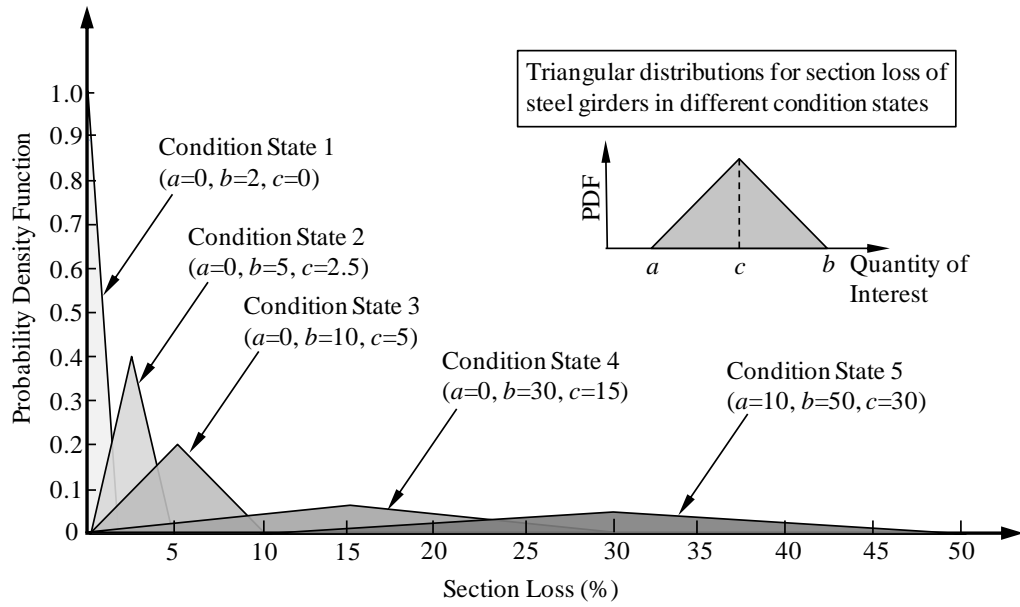
Figure 5.6   Amount of section loss considered for the condition states of steel girders
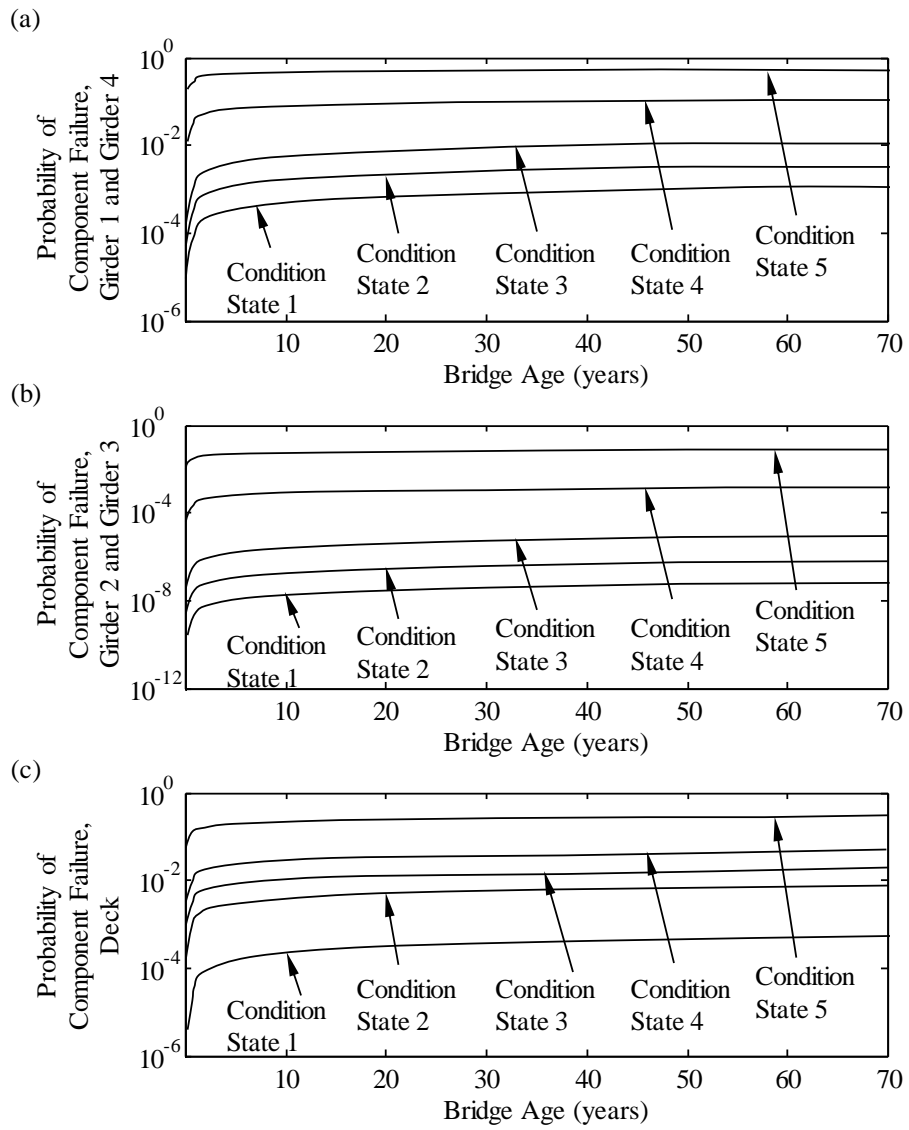
Figure 5.7   Time-variant conditional failure probabilities given the components is

in a specific condition state for (a) girder 1 and girder 4, (b) girder 2

and girder 3, and (c) the deck

165

(a)

(b)

(c)

S_F : Flexural failure of slab $G3_F$: Flexural failure of girder 3
$G1_F$: Flexural failure of girder 1 $G4_F$: Flexural failure of girder 4
$G2_F$: Flexural failure of girder 2
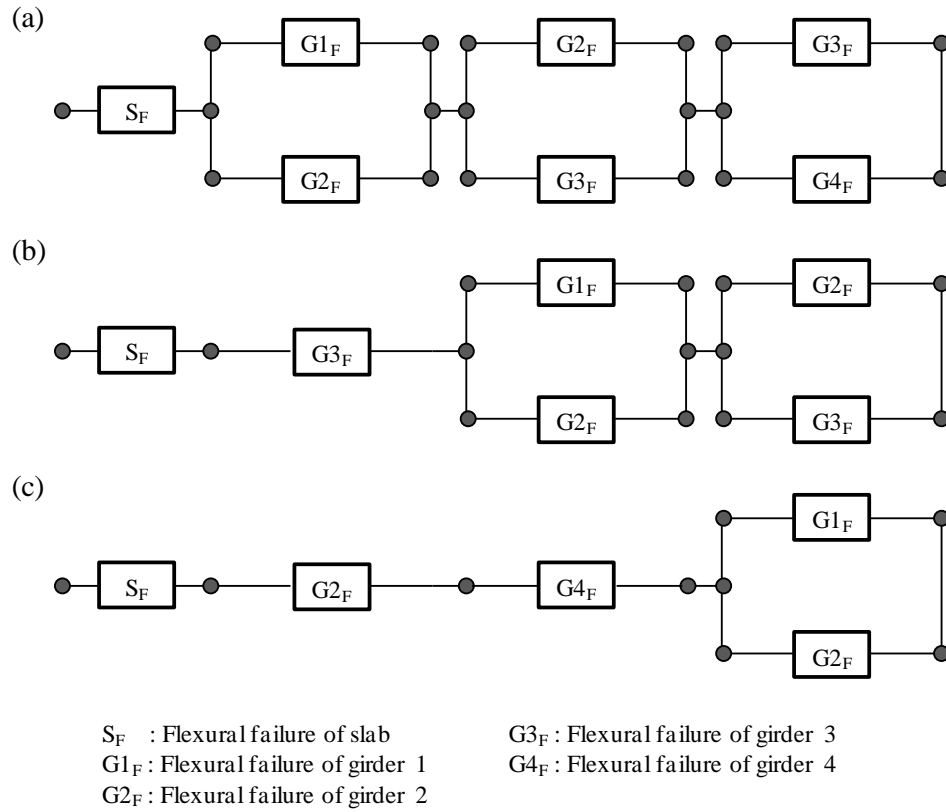
Figure 5.8   System failure models for (a) intact structure, (b) risk scenario associated with exterior girder failure, and (c) risk scenario associated with interior girder failure
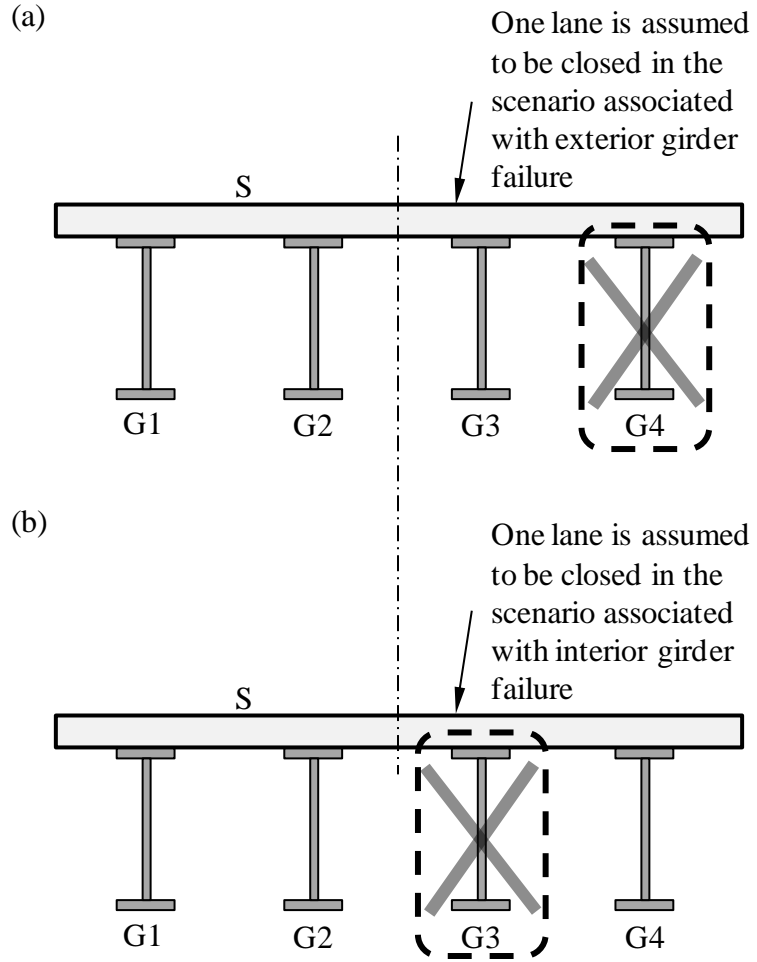
Figure 5.9   Remaining system in the risk scenario associated with (a) exterior

girder failure, and (b) interior girder failure

167
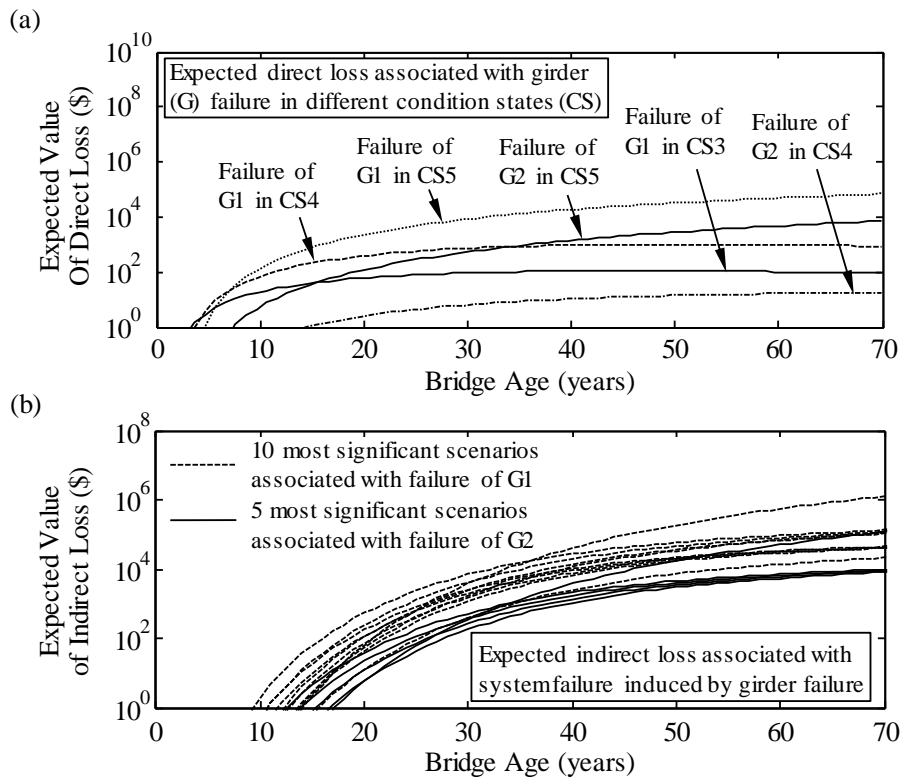
Figure 5.10   Variation of expected value of loss in time for selected individual

scenarios (a) expected direct loss and (b) expected indirect loss of 15

scenarios with highest lifetime maximum loss

168
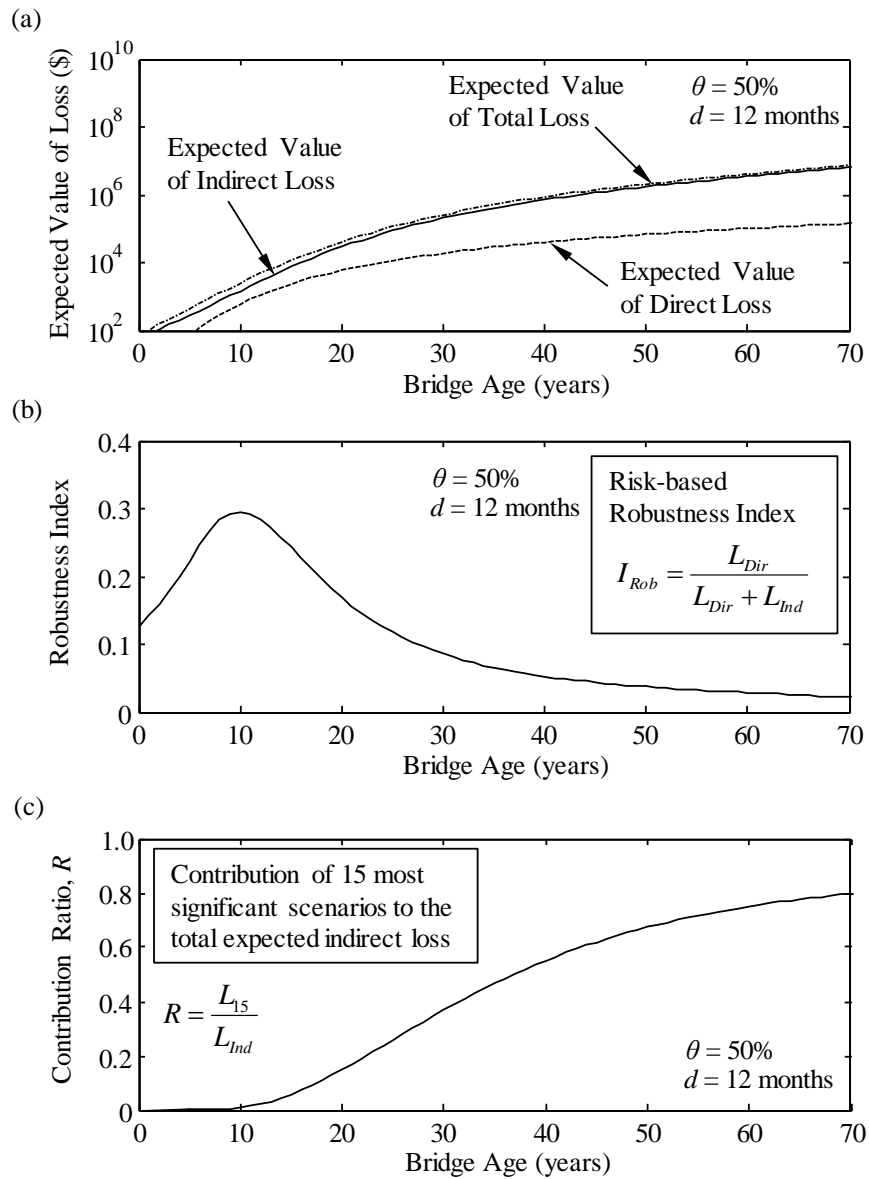
Figure 5.11 Time variation of (a) expected direct, indirect and total losses in logarithmic scale, (b) risk-based robustness index, and (c) contribution ratio of the 15 most significant scenarios to the total expected indirect loss

169
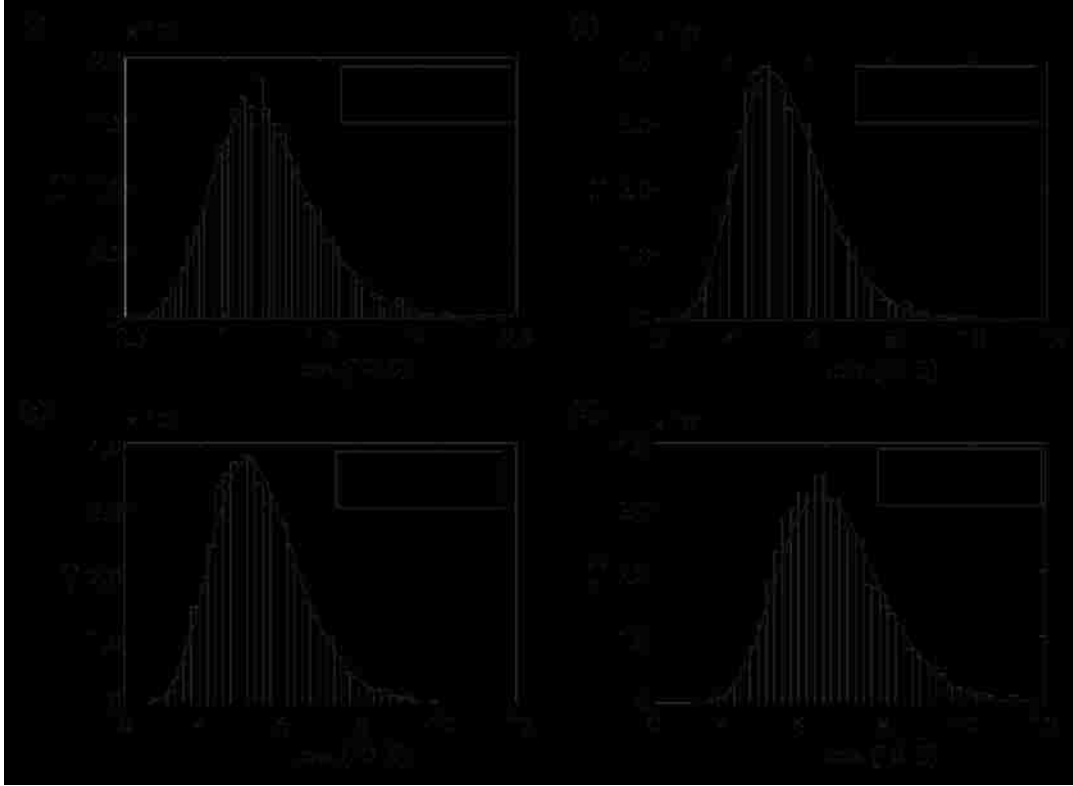
Figure 5.12   PDF of (a) direct loss at *bridge age* = 70 years, (b) indirect loss at *bridge age* = 70 years, (c) total loss at *bridge age* = 70 years, and (d) total loss at *bridge age* = 40 years.
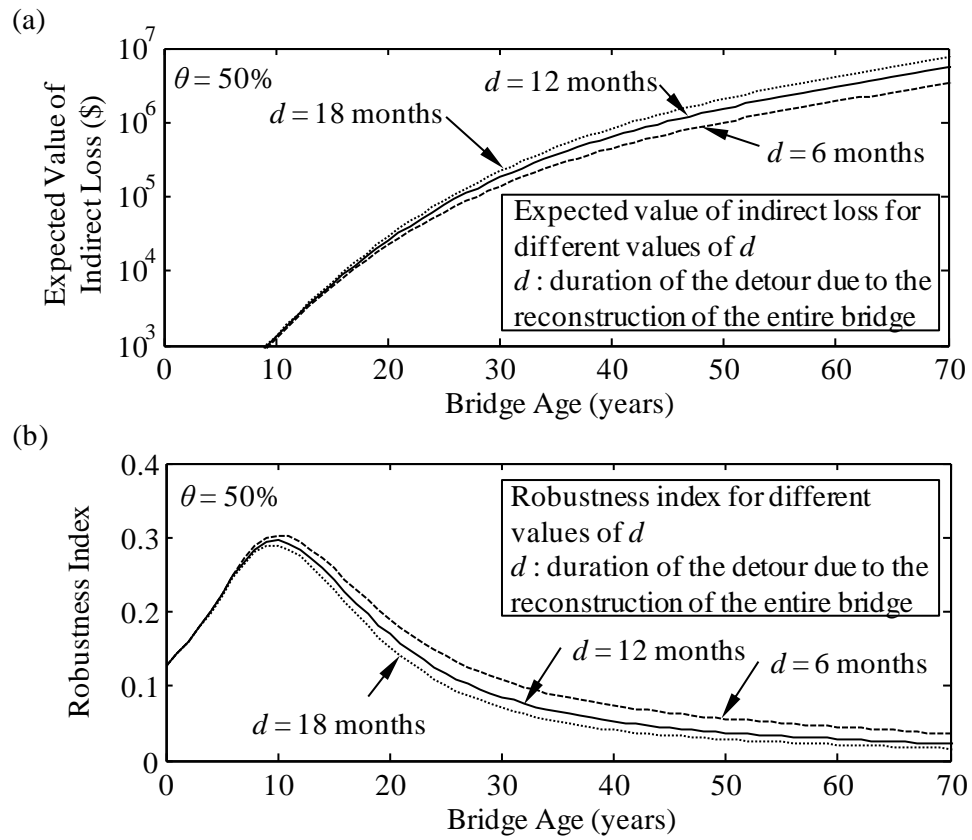
Figure 5.13   Effect of the detour duration on (a) expected indirect loss and (b) risk-

based robustness index

(a)

Expected Value of Indirect Loss ($)

$d = 12$ months

$\theta = 50\%$

$\theta = 75\%$

$\theta = 25\%$

Expected value of indirect loss for
different values of θ
θ : the percentage of the ADT that is
diverted when a lane is closed

Bridge Age (years)

(b)

Robustness Index

$\theta = 25\%$

$\theta = 50\%$

$\theta = 75\%$

Robustness index for different
values of θ
θ : the percentage of the ADT that is
diverted when a lane is closed

$d = 12$ months

Bridge Age (years)
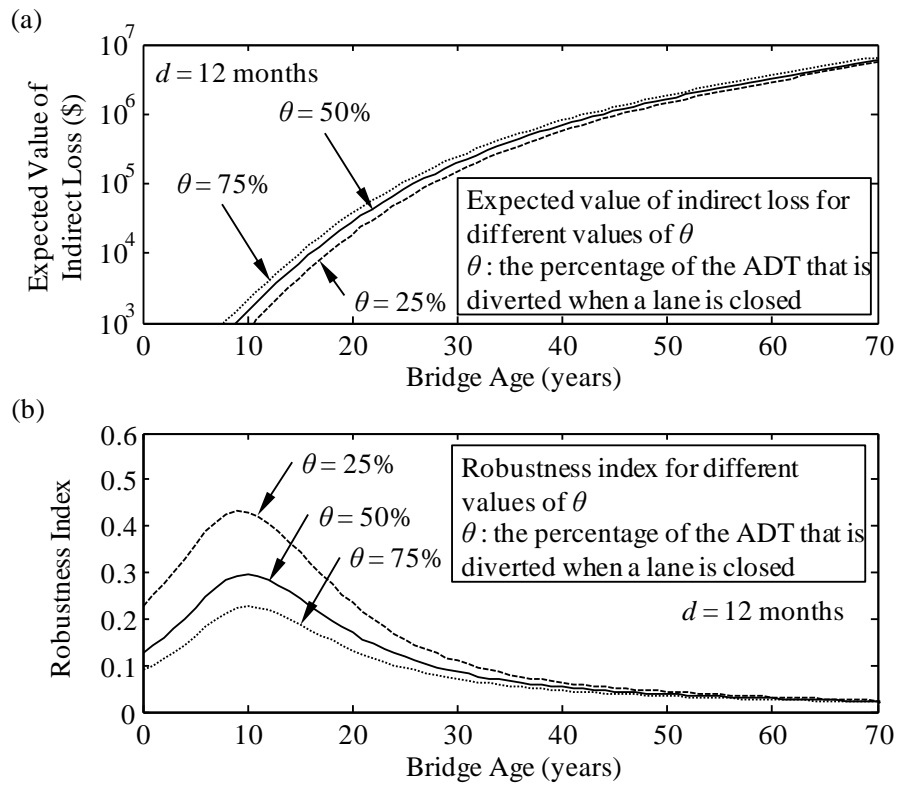
Figure 5.14   Effect of ADT percentage diverted due to one lane closure on (a)

expected indirect loss and (b) risk-based robustness index

172

CHAPTER 6

RISK-BASED MAINTENANCE OPTIMIZATION OF DETERIORATING

BRIDGES

6.1 INTRODUCTION

The trend in life-cycle structural maintenance optimization has been shifting from reliability-based to risk-based approaches, recently. Risk-based performance measures integrate probability of component or system failure with the consequences of this event. Quantifying risk in a life-cycle context is a challenging task including the prediction of different damage level probabilities, assessment of reliability of a structure in these different damage levels, and identification of the consequences associated with component and system failure. Saydam, Frangopol, and Dong (2012) proposed a methodology for quantifying lifetime risk associated with the component failure of bridge superstructures. The risk was quantified in terms of the expected losses. Using Pontis bridge element condition ratings and Markov chains, they took into account the failure probability of different levels of component deterioration weighted by the occurrence probabilities of these deterioration levels. The aim of this chapter is to extend the risk assessment approach described in Chapter 5 (Saydam, Frangopol, and Dong 2012) into a risk-based maintenance optimization methodology for bridges.

Maintenance optimization problems under uncertainty are associated with various performance indicators. These include system reliability (Augusti et al. 1998, Estes and Frangopol 1999), system reliability and redundancy (Okasha and Frangopol

173

2009), lifetime-based reliability (Yang et al. 2006b), lifetime-based reliability and redundancy (Okasha and Frangopol 2010c), cost and spacing of corrosion rate sensors (Marsh and Frangopol 2007), and probabilistic condition and safety indices (Liu and Frangopol 2005a and b, Neves et al. 2006a and b, Frangopol and Liu 2007a and b). Lounis (2006) presented a risk-based approach for maintenance optimization of a network of aging highway bridge decks integrating a stochastic deterioration model with an effective multi-objective optimization approach. Robelin and Madanat (2007) developed a bridge component maintenance and replacement optimization approach that uses a Markovian deterioration model, while accounting for aspects of the history of deterioration and maintenance. Zhu and Frangopol (2013) proposed an approach for assessing the time-dependent risks due to traffic and earthquake loads and establishing the optimum preventive and essential bridge maintenance strategies.

In this chapter, a risk-based maintenance optimization methodology for deteriorating bridges to find the optimum maintenance options and timing is proposed. Finding the optimum maintenance actions and schedule for different components of bridges is formulated as a multi-criteria optimization problem in which the lifetime maximum value of expected losses associated with failure and the lifetime total expected maintenance cost are considered as the conflicting objectives. The risk assessment approach consists of assessing time-variant probabilities of different condition states regarding the deterioration level of bridge components, time-variant component and system failure probabilities for various scenarios associated with these different condition states of components, and the consequences of the failure events. The effects of maintenance actions are reflected by modifying the time-variant

174

condition state probabilities that are evaluated using Markov chains. The expected maintenance costs are evaluated using the condition state probabilities and the cost of upgrading current condition state to an improved one. The methodology is illustrated on a bridge superstructure. The Pareto optimal solutions regarding the maintenance options and their timing for components are obtained using genetic algorithms. The effects of assumed lifespan and availability of maintenance options on optimum solutions are also investigated.

6.2 APPLICATION OF MAINTENANCE WITHIN THE RISK ASSESSMENT METHODOLOGY WITHOUT OPTIMIZATION

In the risk assessment methodology described in Chapter 5 (Saydam, Frangopol, and Dong 2012), the effects of maintenance were not considered. This section presents an approach to include the effects of maintenance on the time-dependent risk of bridge structures. The maintenance strategy can be expressed as "when the component hits condition state i, recover it back to condition state j".

Based on visual inspection results, Pontis (Cambridge Systematics, Inc. 2009) assigns condition states for bridge components to indicate their level of deterioration. The condition states vary between 1 and 5 (or 4), with increasing condition state indicating higher damage level. Considering a bridge component with a condition state space {1, 2, 3, 4, 5}, under the assumption that the component is not repaired as it deteriorates and the transition happens only between the subsequent states, the transition probability matrix used in the prediction of the component performance is

175

$$\mathbf{TP} = \begin{bmatrix} p_{11} & 1-p_{11} & 0 & 0 & 0 \\ 0 & p_{22} & 1-p_{22} & 0 & 0 \\ 0 & 0 & p_{33} & 1-p_{33} & 0 \\ 0 & 0 & 0 & p_{44} & 1-p_{44} \\ 0 & 0 & 0 & 0 & 1 \end{bmatrix} \tag{6.1}$$

where p_{ii} are the probabilities that the component will remain in the same condition state in the transition and i takes values from 1 to the number of condition states. Assuming that the initial state probability vector of a steel girder element with five possible condition states is $\mathbf{S}(0)=[1\ 0\ 0\ 0\ 0]$, the state probability vector after t transitions is

$$\mathbf{S}(t) = \mathbf{S}(0) \cdot \mathbf{TP}^{t} \tag{6.2}$$

where $\mathbf{TP}^{t}$ is the tth power of the transition probability matrix.

The maintenance action can be represented in matrix form (Zhang et al. 2005, Augenbroe and Park 2002). For instance, several maintenance strategies are illustrated in Figure 6.1, including "No Maintenance (Do Nothing)" approach. These maintenance strategies can be represented in the matrix form as

$$\mathbf{M}_{0} = \begin{bmatrix} 1 & 0 & 0 & 0 & 0 \\ 0 & 1 & 0 & 0 & 0 \\ 0 & 0 & 1 & 0 & 0 \\ 0 & 0 & 0 & 1 & 0 \\ 0 & 0 & 0 & 0 & 1 \end{bmatrix} \tag{6.3}$$

$$\mathbf{M}_{1} = \begin{bmatrix} 1 & 0 & 0 & 0 & 0 \\ 0 & 1 & 0 & 0 & 0 \\ 0 & 0 & 1 & 0 & 0 \\ 0 & 0 & 0 & 1 & 0 \\ 0 & 0 & 0 & 1 & 0 \end{bmatrix} \tag{6.4}$$

176

$$\mathbf{M}_2 = \begin{bmatrix} 1 & 0 & 0 & 0 & 0 \\ 0 & 1 & 0 & 0 & 0 \\ 0 & 0 & 1 & 0 & 0 \\ 0 & 0 & 1 & 0 & 0 \\ 0 & 0 & 1 & 0 & 0 \end{bmatrix} \tag{6.5}$$

$$\mathbf{M}_3 = \begin{bmatrix} 1 & 0 & 0 & 0 & 0 \\ 0 & 1 & 0 & 0 & 0 \\ 0 & 1 & 0 & 0 & 0 \\ 0 & 0 & 1 & 0 & 0 \\ 0 & 0 & 1 & 0 & 0 \end{bmatrix} \tag{6.6}$$

$$\mathbf{M}_4 = \begin{bmatrix} 1 & 0 & 0 & 0 & 0 \\ 1 & 0 & 0 & 0 & 0 \\ 0 & 1 & 0 & 0 & 0 \\ 0 & 0 & 1 & 0 & 0 \\ 0 & 0 & 1 & 0 & 0 \end{bmatrix} \tag{6.7}$$

where $\mathbf{M}_0$, $\mathbf{M}_1$, $\mathbf{M}_2$, $\mathbf{M}_3$, and $\mathbf{M}_4$ are the matrix form representation for no maintenance and maintenance strategies form 1 to 4, respectively.

In Figure 6.1(c), maintenance strategy 2 indicates that when the component hits condition state 4 or higher, it is returned to condition state 3. Similarly, maintenance strategy 4 illustrated in Figure 6.1(e), indicates that when the component hits condition states 2, 3, 4, and 5, it is returned to the condition states 1, 2, 3, and 3, respectively.

The time-dependent state vector for component condition states with a maintenance strategy matrix $\mathbf{M}$ can be computed as

$$\mathbf{S}(t) = \mathbf{S}(0) \cdot \left[\mathbf{M} \cdot \mathbf{TP} \right]^t \tag{6.8}$$

The total expected cost of maintenance actions can be computed based on maintenance cost matrices for each individual component. The maintenance cost

177

matrix for a component can be expressed in terms of its rebuilding cost. An example

maintenance cost matrix for a component is

$$\mathbf{MC} = \begin{bmatrix} 0 & 0 & 0 & 0 & 0 \\ 0.15 & 0 & 0 & 0 & 0 \\ 0.30 & 0.15 & 0 & 0 & 0 \\ 0.45 & 0.30 & 0.15 & 0 & 0 \\ 0.60 & 0.45 & 0.30 & 0.15 & 0 \end{bmatrix} \cdot C_{reb} \qquad (6.9)$$

where C_{reb} is the rebuilding cost of the component. The cost matrix of the applied

maintenance action for a component at a time instant t can be obtained as

$$AMC_{ij}(t) = M_{ij} \cdot MC_{ij}(t) \qquad (6.10)$$

where $AMC_{ij}(t)$ is the component of applied maintenance cost matrix $\mathbf{AMC}$ in the ith

row and jth column, M_{ij} is the component of maintenance strategy matrix $\mathbf{M}$ in the ith

row and jth column, and MC_{ij} is the component of maintenance cost matrix $\mathbf{MC}(t)$ in

the ith row and jth column. The expected maintenance cost for a single component can

be computed based on the probabilities of condition states (Markov chain state

probabilities) and the applied maintenance cost matrix as

$$EMC(t) = \sum_i^5 S_i(t) \cdot \left(\sum_{j=1}^5 AMC_{ij}(t) \right) \qquad (6.11)$$

where $S_i(t)$ is the probability of the component being in state i. Then, the total

expected maintenance cost for the entire bridge is the sum of EMC over the

components. The assumption in this approach is that there is no delay in performing

the maintenance action after the threshold condition state is reached.

The procedure is applied to the superstructure of E-16-FK Bridge in Colorado.

E-16-FK is composed of five steel girders and reinforced concrete deck. The bridge is

178

a four span continuous steel girder bridge. The superstructure is illustrated in Figure 6.2 conceptually. The details of this bridge can be found in Akgül (2002).

Pontis bridge management system defines five condition states for open, painted steel girders and reinforced concrete deck. In this example, the parameters defining the deterioration of the two exterior girders 1 and 5, the three interior girders 2, 3, and 4 are considered identical, respectively. The transition probabilities for bridge components are assumed as

$$\mathbf{TP}_{G1} = \mathbf{TP}_{G5} = \begin{bmatrix} 0.96 & 0.04 & 0 & 0 & 0 \\ 0 & 0.92 & 0.08 & 0 & 0 \\ 0 & 0 & 0.88 & 0.12 & 0 \\ 0 & 0 & 0 & 0.84 & 0.16 \\ 0 & 0 & 0 & 0 & 1 \end{bmatrix} \tag{6.12}$$

$$\mathbf{TP}_{G2} = \mathbf{TP}_{G3} = \mathbf{TP}_{G4} = \begin{bmatrix} 0.97 & 0.03 & 0 & 0 & 0 \\ 0 & 0.94 & 0.06 & 0 & 0 \\ 0 & 0 & 0.91 & 0.09 & 0 \\ 0 & 0 & 0 & 0.88 & 0.12 \\ 0 & 0 & 0 & 0 & 1 \end{bmatrix} \tag{6.13}$$

$$\mathbf{TP}_{Deck} = \begin{bmatrix} 0.95 & 0.05 & 0 & 0 & 0 \\ 0 & 0.90 & 0.10 & 0 & 0 \\ 0 & 0 & 0.85 & 0.15 & 0 \\ 0 & 0 & 0 & 0.80 & 0.20 \\ 0 & 0 & 0 & 0 & 1 \end{bmatrix} \tag{6.14}$$

where $\mathbf{TP}_{G1}$, $\mathbf{TP}_{G2}$, $\mathbf{TP}_{G3}$, $\mathbf{TP}_{G4}$, $\mathbf{TP}_{G5}$, and $\mathbf{TP}_{Deck}$ are the annual transition probability matrices of the girders and the deck. The initial state vector for all components is $\mathbf{S}(0)=[1\ 0\ 0\ 0\ 0]$. The time-variant state probabilities for girder 1 with respect to various maintenance strategies are computed using Equations 6.2 and 6.8 and presented in Figures 6.3(a) to (e). The maintenance strategies applied are illustrated in

179

Figure 6.1 and the corresponding maintenance strategy matrices are given in Equations 6.3 to 6.7.

According to the risk assessment procedure described in Chapter 5, the time-dependent reliability analyses of individual components in different condition states and the system are required. The yield stress of each steel girder, the compressive strength of the concrete deck, and the yield stress of steel reinforcement in the deck are considered as the random variables associated with component and system resistance. All random variables are considered lognormally distributed. The mean values of the girder steel yield stress, the compressive strength of the concrete slab, and yield stress of the deck steel reinforcement are 345 MPa, 28 MPa, and 414 MPa, and their coefficients of variation are 0.11, 0.18, and 0.11, respectively. The limit state considered in the reliability analyses is the longitudinal bending moment failure of the girders and the deck at around the mid-section of the first span (Akgül 2002). The reliability of a component is varying with the condition state the section loss is different in each condition state. The time-dependent probabilities of failure in different condition states for girder 1 are presented in Figure 6.4. In this figure, the variation in time is due to the increase in live load and each curve corresponds to a condition state. In addition to component analyses, system reliability analyses in the absence of a component with respect to different combinations of component condition states are required. The system reliability models for the superstructure system including the intact system and the cases with the failure one of exterior girder, one interior girder and the middle girder are illustrated in Figure 6.5. These are used to find the conditional probabilities of system failure given failure of a component. The

system failure is assumed to happen if any two adjacent girders fail or the slab fails. Reliability software RELSYS (Estes and Frangopol, 1998) is used for the component and the system reliability analyses.

The risk is quantified in terms of the expected losses. The direct and indirect expected losses are computed using Equations 5.15 and 5.16. Information evaluating consequences and more detail explanation on computation of expected losses is provided in Chapter 5. In this example, the emphasis is on the effect of maintenance strategies on the lifetime risk associated with component failure. In Figure 6.6(a), the annual expected value of loss with respect to different maintenance strategies is presented. The same maintenance strategies are applied to all components in this figure. As expected, the maintenance strategies 1 and 4 provide the lowest and the highest reduction in annual expected loss, respectively. The annual expected cost associated with these maintenance strategies are presented in Figure 6.6(b). These costs are computed according to Equations 6.9 to 6.11. The annual expected cost for maintenance strategy 1 is the lowest during the first half of the service life. However, it becomes the most costly maintenance strategy after the mid-life, although it results in the highest expected loss. On the other hand, the annual expected cost of maintenance strategy 4 is the highest among others at early stages of the service life. After about 30 years, it becomes the least costly maintenance strategy in addition to the fact that it results in the least annual expected loss.

6.3 LIFE-CYCLE PERFORMANCE CONSIDERING THE EFFECTS OF MAINTENANCE ACTIONS IN AN OPTIMIZATION APPROACH

A bridge component can experience several major maintenance actions throughout its lifetime. The life-cycle performance profile of a component depends not only on the initial performance level and the rate of deterioration but also on the types and timing of the maintenance actions. When maintenance is applied to a component at a point in time, there will be a sudden improvement in its performance. In conventional approaches where the value of the performance indicator (e.g., reliability index, survivor function, condition state) is known at different points in time, the value of the performance indicator after the maintenance action can be easily estimated based on the performance level before the maintenance and the effect of the maintenance on the performance. The maintenance actions can be described as the activities that change the condition back to a better state than the current one. However, when Markov chains are used to evaluate the future condition state of a component, the condition state at a time instant is not certain and, therefore, is expressed in terms of probability. The maintenance actions are assumed to be associated with restoring the condition state of a component to an improved condition state. For instance, if the maintenance action is described as bringing the condition of the component to condition state 2, the probabilities of being in condition states 3, 4, and 5 will be 0 after the maintenance action is applied. However, the component could be in condition state 1 with a certain probability at the time of the maintenance action. Therefore, the probability of being in condition state 1 remains unaffected since it already satisfies the requirements of state 2. This can be expressed in a general form as

182

$$\mathbf{S}^+(t) = \begin{cases} [1 & 0 & 0 & 0 & 0] & m=1 \\ [p_1^-(t) & 1-p_2^-(t) & 0 & 0 & 0] & m=2 \\ [p_1^-(t) & p_2^-(t) & 1-p_1^-(t)-p_2^-(t) & 0 & 0] & m=3 \\ [p_1^-(t) & p_2^-(t) & p_3^-(t) & 1-p_1^-(t)-p_2^-(t)-p_3^-(t) & 0] & m=4 \\ [p_1^-(t) & p_2^-(t) & p_3^-(t) & p_4^-(t) & p_5^-(t)] & m=5 \end{cases}$$

(6.15)

where $\mathbf{S}^+(t)$ is the state vector including the effects of maintenance at time instant t (approaching t from right side), $p_i^-(t)$ is the probability of the component being in condition state i at time t (approaching t from left side) before the maintenance action, and m is the maintenance option. In Equation 6.15, $m = 5$ corresponds to "do nothing". In Figure 6.7, the lifetime condition state probability profiles for a component are presented qualitatively. Figure 6.7(a) illustrates the case without maintenance. Figure 6.7(b) illustrates the case where maintenance option $m = 1$ is applied at $t = t_1$ and maintenance option $m = 2$ is applied at $t = t_2$. In this figure, $p_i^-(t)$ and $p_i^+(t)$ are the probabilities of the component being in condition state i before and after a maintenance action, respectively. It should be noted that these probabilities satisfy $\sum_{i=1}^{5} p_i^-(t) = 1$ and $\sum_{i=1}^{5} p_i^+(t) = 1$.

The risk assessment methodology used requires reliability analyses of (a) the components in different condition states and (b) the system for different scenario failure events regarding the possible combinations of condition states of different components. A major advantage of using this assessment methodology in risk-based maintenance optimization is that the reliability analyses are not necessarily repeated for each iteration of an optimization algorithm. They are rather performed once for

183

each failure scenario, and then the probability of failure for each of these scenarios is weighted by the condition state probabilities of components. In other words, the deterioration of components is modeled using condition state probabilities (Markov chain state probabilities) and the effects of maintenance actions are reflected through only condition state probabilities. This provides significant time efficiency in maintenance optimization computations where many iterations are required to find an optimum solution.

The maintenance optimization problem is formulated based on the consequence and expected maintenance cost which are transformed to the values at a reference point in time using discount rate of money in order to make fair comparisons among the solution candidates. The direct expected loss including the effects of maintenance can be computed as

$$L^+_{Direct}(t) = \sum_{i=1}^{a} \sum_{j=1}^{b} P^+_{(CS_i=j)}(t) \cdot P_{(CF_i|CS_i=j)}(t) \cdot \frac{C'_{Direct,i}}{(1+r)^t} \tag{6.16}$$

where $P^+_{(CS_i=j)}(t)$ is the time-variant probability of component i being in condition state j considering the effects of maintenance actions, $C'_{Direct,i}$ is the direct consequence of component failure in terms of monetary value, and r is the discount rate of money. Similarly, the indirect expected loss including the effects of maintenance can be computed as

$$L^+_{Indirect}(t) = \sum_{i=1}^{a} \sum_{p=1}^{b} \sum_{j=1}^{a-1} \sum_{q=1}^{b} \cdots \sum_{k=1}^{a-1} \sum_{r=1}^{b} \left(\begin{matrix} P^+_{(CS_j=q)}(t) \cdot \left(1 - P_{(CF_j|CS_j=q)}(t)\right) \cdot \ldots \cdot P^+_{(CS_k=r)}(t) \\ \cdot \left(1 - P_{(CF_k|CS_k=r)}(t)\right) \end{matrix} \right) \cdot \\ \cdot P^+_{(CS_i=p)}(t) \cdot P_{(CF_i|CS_i=p)}(t) \cdot P_{(SF_i|CF_i)}(t) \cdot \frac{C'_{Indirect}}{(1+r)^t} \tag{6.17}$$

184

where the condition state probabilities (obtained through Markov chain) of components include the effects of maintenance actions, and $C'_{Indirect}$ is the indirect consequence of component failure in terms of monetary value. The total expected loss is

$$L^+_{Total}(t) = L^+_{Direct}(t) + L^+_{Indirect}(t) \tag{6.18}$$

which is the sum of the expected direct and indirect losses.

6.4 EXPECTED COST OF MAINTENANCE ACTIONS

For the maintenance strategy $m = 4$ in Equation 6.15, there is only one maintenance action available, which is restoring condition state 4 if the component was in condition state 5. If the component was in condition state 1, 2, 3, or 4, no action is required to satisfy $m = 4$. For the maintenance option $m = 3$, the available maintenance actions are: (a) restoring condition state 3 if the component was in condition state 4 and (b) restoring condition state 3 if the component was in condition state 5. Similarly, for the maintenance strategy $m = 2$, the available maintenance actions are: (a) restoring condition state 2 if the component was in condition state 3, (b) restoring condition state 2 if the component was in condition state 4, and (c) restoring condition state 2 if the component was in condition state 5. For the maintenance strategy $m = 1$, the available maintenance actions are: (a) restoring condition state 1 if the component was in condition state 2, (b) restoring condition state 1 if the component was in condition state 3, (c) restoring condition state 1 if the component was in condition state 4, and

185

(d) restoring condition state 1 if the component was in condition state 5. The costs of these maintenance actions are different and they can be expressed in matrix form as

$$\mathbf{MC} = \begin{bmatrix} 0 & 0 & 0 & 0 & 0 \\ mc_{21} & 0 & 0 & 0 & 0 \\ mc_{31} & mc_{32} & 0 & 0 & 0 \\ mc_{41} & mc_{42} & mc_{43} & 0 & 0 \\ mc_{51} & mc_{52} & mc_{53} & mc_{54} & 0 \end{bmatrix} \tag{6.19}$$

where mc_{ij} is the cost of the maintenance action which refers to restoring condition state i if the structure was in condition state j, where $j > i$. The time-variant expected cost of a maintenance action can be expressed in terms of the condition state probabilities and the maintenance costs defined in Equation 6.19 as

$$EMC(t) = \begin{cases} \dfrac{p_2(t_m) \cdot mc_{21} + p_3(t_m) \cdot mc_{31} + p_4(t_m) \cdot mc_{41} + p_5(t_m) \cdot mc_{51}}{(1+r)^t} & if \quad m = 1 \\[2ex] \dfrac{p_3(t_m) \cdot mc_{32} + p_4(t_m) \cdot mc_{42} + p_5(t_m) \cdot mc_{52}}{(1+r)^t} & if \quad m = 2 \\[2ex] \dfrac{p_4(t_m) \cdot mc_{43} + p_5(t_m) \cdot mc_{53}}{(1+r)^t} & if \quad m = 3 \\[2ex] \dfrac{p_5(t_m) \cdot mc_{54}}{(1+r)^t} & if \quad m = 4 \\[2ex] 0 & if \quad m = 5 \end{cases}$$

(6.20)

where $p_i(t_m)$ is the probability of the component being in state i at the time of maintenance activity t_m. The expected cost of maintenance actions for a component within its entire lifespan can be computed as

$$EMC_{Lifetime} = \sum_{i=1}^{z} EMC_i(t) \tag{6.21}$$

where $EMC_i(t)$ is the expected cost of i-th maintenance action and z is the number of the maintenance actions within the lifetime. Equations 6.19 to 6.21 are for a single

186

component. The total expected maintenance cost for the entire structure can be computed as

$$EMC_{Total} = \sum_{i=1}^{b} EMC^{i}_{Lifetime}$$ (6.22)

where $EMC^{i}_{Lifetime}$ is the lifetime expected maintenance cost of component i and b is the total number of components.

6.5 FORMULATION OF THE RISK-BASED MAINTENANCE OPTIMIZATION

The design variables considered are the times and types of the maintenance actions for each component. The objectives of the optimization are minimizing both the lifetime maximum value of the expected loss and the total expected cost of maintenance actions. It is a multi-objective optimization problem with conflicting objectives. Therefore, there will not be only one optimum solution but there will be a set of optimum solutions. This set is called Pareto set (or Pareto front). A solution is Pareto optimal only if no other solution yields an improvement in one of the objectives without worsening another. Genetic algorithms (Holland 1972) are practical and general-purpose stochastic search-based optimization techniques that provide sufficient level of accuracy while being more efficient than conventional optimization techniques. Genetic algorithms were developed in the 1970s based on the principles of natural selection, genetics, and evolution theory, and are highly recognized for their computational efficiency. This is due to the fact that other techniques select a single solution and randomly change it until it reaches the best solution, which requires

187

several iterations. However, genetic algorithms store multiple solutions to the problem (i.e. population) and use probabilistic rules to generate new and better populations, providing more efficiency and likelihood of finding optimal solutions in a timely fashion (Goldberg 1989).

The optimization for the risk-based maintenance optimization approach is formulated in its most general form as

Find:

- The time span between successive maintenance actions Δt_m
- The type of maintenance actions m for each component

Given that:

- Initial condition state probabilities for components
- Condition state transition probabilities for components
- Time-variant probabilities of component failure in different condition states
- Time-variant probabilities of system failure for different scenarios
- Direct and indirect consequences
- Lifespan of the structure
- Discount rate of money

So that:

- Lifetime maximum value of expected loss $\max(L^M_{Total}(t))$ is minimum
- Lifetime expected cost of maintenance actions EMC_{Total} is minimum

Subject to:

- Lower time limit between successive maintenance actions $\leq \Delta t_m$

188

The interaction among the modules of the proposed maintenance optimization methodology is illustrated in Figure 6.8. The performance module handles the Markov chain (condition state probability) computations, the reliability analyses for failure scenarios, the evaluation of consequences, and the calculation of the expected loss. The optimization module sends the candidates for the design variables which are the timings and types of maintenance action for each component to the performance module. First, the Markov chain computations are affected by the maintenance actions. As explained previously, the reliability analyses for the scenarios and evaluation of consequences are not affected by the maintenance strategies. The performance module delivers the value of the first objective function, which is the lifetime maximum value of expected loss to the optimization module. The maintenance cost module also requires the Markov chain probabilities. The cost of maintenance actions are affected by the timing of the maintenance actions due to the discount rate of money. The maintenance cost module returns the lifetime expected cost of maintenance actions to the optimization module. After an adequate number of generations, the optimization module provides the Pareto optimum solutions for the timing and the type of the maintenance actions.

6.6 ILLUSTRATIVE EXAMPLE

The risk-based maintenance optimization framework described is illustrated on the superstructure of E-16-FK Bridge in Colorado, which has four continuous spans with lengths of 17.4 m, 21.8 m, 19.6 m, and 19.5 m, a total length of 69.2 m between the

189

centerlines of the abutment bearings, and concrete deck on five rolled I-beams. The details of this bridge can be found in Akgül (2002). First, the risk associated with the flexural girder failure in the mid-section of the third span is quantified in terms of the expected losses. Then genetic algorithms are used to find the optimum maintenance options and timing for girders.

6.6.1 Evaluation of Time-variant Expected Losses Associated with Girder Failure

The condition state of a component at a time instant is random and this randomness is represented by the Markov chain probabilities. Pontis bridge management system defines five condition states for open, painted steel girders and RC deck. In this example, the parameters defining the deterioration of the two exterior girders 1 and 5, and the three interior girders 2, 3, and 4 are considered identical, respectively. The initial state probability vector for the exterior and interior girders and the RC deck is $S(0)=[1 \; 0 \; 0 \; 0 \; 0]$. The transition probabilities for bridge components should be estimated based on adequate available bridge inspection data history and the probabilistic methodologies to process the available data. Information on estimation of transition probabilities can be found in Al-Wazeer (2007) and Fu and Devaraj (2008). In this example, the transition probabilities for bridge components are assumed as

$$\mathbf{P}_{G1} = \mathbf{P}_{G5} = \begin{bmatrix} 0.96 & 0.04 & 0 & 0 & 0 \\ 0 & 0.92 & 0.08 & 0 & 0 \\ 0 & 0 & 0.88 & 0.12 & 0 \\ 0 & 0 & 0 & 0.84 & 0.16 \\ 0 & 0 & 0 & 0 & 1 \end{bmatrix} \tag{6.23}$$

$$\mathbf{P}_{G2} = \mathbf{P}_{G3} = \mathbf{P}_{G4} = \begin{bmatrix} 0.97 & 0.03 & 0 & 0 & 0 \\ 0 & 0.94 & 0.06 & 0 & 0 \\ 0 & 0 & 0.91 & 0.09 & 0 \\ 0 & 0 & 0 & 0.88 & 0.12 \\ 0 & 0 & 0 & 0 & 1 \end{bmatrix} \quad (6.24)$$

$$\mathbf{P}_{Deck} = \begin{bmatrix} 0.95 & 0.05 & 0 & 0 & 0 \\ 0 & 0.90 & 0.10 & 0 & 0 \\ 0 & 0 & 0.85 & 0.15 & 0 \\ 0 & 0 & 0 & 0.80 & 0.20 \\ 0 & 0 & 0 & 0 & 1 \end{bmatrix} \quad (6.25)$$

where $\mathbf{P}_{G1}$, $\mathbf{P}_{G2}$, $\mathbf{P}_{G3}$, $\mathbf{P}_{G4}$, and $\mathbf{P}_{G5}$ are the annual transition probability matrices of the girders and $\mathbf{P}_{Deck}$ is the annual transition probability matrix of the deck. The time-variant condition state probabilities of the components are computed using Equation 6.15. The condition state probabilities for interior and exterior girders with no maintenance actions taken during the lifetime are presented in Figure 6.9(a) and (b), respectively.

The time-dependent reliability analyses of individual components in different condition states and the system are required. The yield stress of each steel girder, the compressive strength of the concrete deck, and the yield stress of steel reinforcement in the deck are considered as the random variables associated with component and system resistance. All random variables are considered lognormally distributed. The mean values of the girder steel yield stress, the compressive strength of the concrete slab, and yield stress of the deck steel reinforcement are 253 MPa, 20 MPa, and 309 MPa, and their coefficients of variation are 0.11, 0.18, and 0.11, respectively (Akgül, 2002). The limit state considered in the reliability analyses is the longitudinal bending

191

moment failure of the girders and the deck at around the mid-section of the first span (Akgül, 2002). The reliability of a component varies with the condition state since the section loss is different in each condition state. The section loss percentages of steel sections in different condition states are considered to follow triangular distribution. More information on the reliability analyses for components in different condition states and the relation among section loss percentages and condition states is provided in Chapter 5. The time-variant probabilities of failure in different condition states for the exterior girders (girders 1 and 5) are presented in Figure 6.10. In this figure, the variation in time is due to the increase in live load and each curve corresponds to a condition state. In Figure 6.9(c), the total expected loss with no maintenance actions taken during the lifetime are presented.

6.6.2 Pareto Optimum Solutions

The problem to find the optimum maintenance options and timing for the components is formulated as

Find:

Δt_{mi}, m_i^E, and m_i^I $i = 1, 2,\ldots, 5$

Given that:

$\mathbf{S}_{G1}(0)$, $\mathbf{S}_{G2}(0)$, $\mathbf{S}_{G3}(0)$, $\mathbf{S}_{G4}(0)$, $\mathbf{S}_{G5}(0)$, and $\mathbf{S}_{Deck}(0)$

$\mathbf{P}_{G1}$, $\mathbf{P}_{G2}$, $\mathbf{P}_{G3}$, $\mathbf{P}_{G4}$, $\mathbf{P}_{G5}$, and $\mathbf{P}_{Deck}$

$P_{(CFi|CSi = j)}(t)$

$P_{(SFi|CFi)}(t)$

192

$t_L = 70$ years

$\overline{C}_{Direct,i}$ and $\overline{C}_{Indirect}$, $r = 0$

So that:

minimize max($L^M_{Total}(t)$)

minimize EMC_{Total}

Subject to:

$\Delta t_{mi} \geq 5$ years

$n_t = 5$

where t_L is the lifespan of the structure and n_t is the total number of maintenance actions on the bridge during its lifetime.

The total number of design variables is 15. These include the time intervals between the maintenance actions for girders (5 design variables), and the maintenance options for interior girders (5 design variables) and exterior girders (5 design variables). The maintenance actions for the exterior and interior girders are considered to be performed at the same time. However, since maintenance options include the "do nothing" option, interior girders may receive no maintenance while exterior girders do. The optimization problem is solved using the genetic algorithm available in Global Optimization Toolbox of MATLAB (Mathworks 2012).

The Pareto optimal solutions for the problem to find the optimum maintenance options and timing for the components of the bridge superstructure considering a lifespan of 70 years is presented in Figure 6.11, in terms of the objectives of the problem. Each point in this figure corresponds to a different combination of maintenance options and timing of these options, resulting in different objective

193

values. *A* is high risk − low maintenance cost solution while *C* is a low risk − high maintenance cost solution. *B* is a more balanced solution compared to the others. For instance, *A* in Figure 6 represents an optimum solution with lifetime maximum total expected loss of $ 1,740,000 and lifetime total expected maintenance cost of $ 12,400. Solution *A* includes the following maintenance actions: (1) restore the condition of the exterior girders to at least condition state 2 at $t = 9$ years, (2) restore the condition of the exterior girders to at least condition state 2 at $t = 14$ years, and (3) restore the condition of the interior girders to at least condition state 3 at $t = 9$ years. In Figure 6.12(a), the time-variant condition state probabilities of exterior girders (1 and 5) including the effects of maintenance actions for solution *A* are presented. At $t = 9$ years and $t = 14$ years, the probabilities of exterior girder condition states 3, 4, and 5 are reduced to zero due to the maintenance action $m^E = 2$ (m^E: maintenance option for exterior girder), while the probability of condition state 1 remains since it is already a better condition state than the maintenance option $m^E = 2$ dictates. In Figure 6.12(b), the time-variant condition state probabilities of interior girders (2, 3, and 4) including the effects of maintenance actions for solution *A* are presented. At $t = 9$ years, similarly, the probability of interior girder condition states 3, 4, and 5 are reduced to zero due to the maintenance action $m^I = 2$ (m^I: maintenance option for interior girder), while the probability of condition states 1 remains same since it is already a better condition state than the maintenance option $m^I = 2$ dictates. The time-variant total expected loss for solution *A* is presented in Figure 6.12(c).

Solution *B* in Figure 6.11 represents an optimum solution with lifetime maximum total expected loss of $ 730,000 and lifetime total expected maintenance

cost of $ 110,000. This solution includes the following maintenance actions: (1), (2), (3), (4), (5) restore the condition of the exterior girders to condition state 1 at $t = 7$ years, $t = 12$ years, $t = 24$ years, $t = 33$ years and $t = 39$ years, respectively, (6) restore the condition of the interior girders to at least condition state 2 at $t = 7$ years, and (7) restore the condition of the interior girders to at least condition state 3 at $t = 12$ years. The time-variant condition state probabilities of exterior girders including the effects of maintenance actions for solution B are presented in Figure 6.13(a). At $t = 7$ years, $t = 12$ years, $t = 24$ years, $t = 33$ years and $t = 39$ years, the probabilities of exterior girder condition states 2, 3, 4, and 5 are reduced to zero due to the maintenance action $m^E = 1$ and the probability of condition state 1 is restored to 1.0. In Figure 6.13(b), the probabilities of interior girder condition states 3, 4, and 5 are reduced to zero due to the maintenance action $m^I = 2$ at $t = 7$ years. At $t = 12$ years, the probability of interior girder condition states 4 and 5 are reduced to zero due to the maintenance action $m^I = 3$. The time-variant total expected loss for solution B is presented in Figure 6.13(c).

Solution C represents an optimum solution with lifetime maximum total expected loss of $ 80,800 and lifetime total expected maintenance cost of $ 340,000. It includes the following maintenance actions: (1), (2), (3), (4), (5) restore the condition of the exterior girders to condition state 1 at $t = 13$ years, $t = 25$ years, $t = 37$ years, $t = 50$ years and $t = 61$ years, respectively, (6) restore the condition of the interior girders to condition state 1 at $t = 13$ years, (7), (8), (9), and (10) restore the condition of the interior girders to at least condition state 2 at $t = 25$ years, $t = 37$ years, $t = 50$ years and $t = 61$ years, respectively. The time-variant condition state probabilities of exterior and interior girders including the effects of maintenance actions for solution C are

195

presented in Figures 6.14(a) and (b). The time-variant total expected loss for solution C is presented in Figure 6.14(c).

The lifetime maximum expected loss depends on the considered lifespan of the bridge. The variation of Pareto front for different values of lifespan $t_L = 30$ years, $t_L = 50$ years, and $t_L = 70$ years is illustrated in Figure 6.15. The lifetime maximum expected loss is reduced significantly with smaller lifespan resulting in a Pareto front with much less expected cost of maintenance for the same value of maximum expected loss. For instance, in Figure 10, both solutions D and E have the same value, $ 420,000, of objective 1. However, the value of objective 2 for the solution E is $ 150,000 while it is much less for solution D which is $ 50,000. The values of objective 1 for Pareto solutions with $t_L = 30$ years are negligible compared to those for $t_L = 50$ years and $t_L = 70$ years.

The effects of the availability of maintenance options in the formulation of the optimization are also investigated. In Figure 6.16, the Pareto fronts for three cases are presented: (a) all maintenance actions ($m = 1, 2, 3, 4$ and 5) are available in the formulation of the problem, (b) maintenance option $m = 1$ is not available ($m = 2, 3, 4$ and 5 are available), and (c) maintenance options $m = 1$ and $m = 2$ are not available. The results indicate that the optimum solutions benefit from the availability of the maintenance options. For instance, in Figure 6.16, the solutions F, G, and H correspond to the same expected maintenance cost $ 170,000, while the lifetime maximum expected loss is highest for solution F with $ 810,000 and is lowest for solution H with $ 250,000.

196

The proposed maintenance optimization methodology is applied in two computational steps: (a) computation of failure probabilities for component and system and (b) Markov chain computations, cost calculations and optimization using GA. The computation time for step (a) depends on the time efficiency of the reliability software used to compute the probability of failure and can take several hours. The computational step (b) is carried out on a Dell Precision R5500 Workstation with dual six core Intel Xeon processor (3.0 GHz) and 24 MB. The Pareto optimal solutions in Figure 6, for instance, are obtained after 60 generations in 247 seconds.

6.7 CONCLUSIONS

A risk-based maintenance optimization methodology for bridges with deteriorating components to find the optimum maintenance options and timing is presented. In this optimization, a risk assessment methodology combining the time-variant probabilities of different condition states regarding the deterioration level of bridge components, time-variant component and system failure probabilities for various scenarios is used. A multi-criteria optimization problem in which the lifetime maximum value of expected losses associated failure and the lifetime total expected maintenance cost are the conflicting objectives is formulated to find the optimum maintenance actions and schedule for different bridge components of bridges. The effects of maintenance actions are included by modifying the time-variant condition state probabilities that are evaluated using Markov chains. The methodology is illustrated on the superstructure of a bridge. The Pareto optimal solutions associated with the

197

maintenance options and timing of maintenance actions are obtained using genetic algorithms. In addition, the effects of assumed lifespan and availability of maintenance options are investigated.

The following conclusions are drawn:

1. The proposed risk-based optimization methodology is applicable to structures where the deterioration of the components can be represented by a set of mutually exclusive and collectively exhaustive condition states.

2. The proposed methodology is computationally efficient due to the fact that the deterioration process and maintenance effects are represented using Markov chains and the reliability analyses are not required to be performed for the candidate solutions of the optimization algorithm.

3. The Pareto optimum solutions range between high risk–low maintenance cost and low risk–high maintenance cost. The decision maker can select an optimum solution depending on the available budget. Each point on the Pareto front corresponds to the optimum solution of a single-objective optimization problem with a fixed budget.

4. The maintenance actions can cause a sudden significant change in condition state probabilities and, consequently, in the expected loss. The lifetime maximum expected loss can be reduced significantly depending on the risk-attitude of the decision maker.

5. The assumed lifespan of the structure has significant impact on the lifetime maximum expected loss and consequently on Pareto optimum solutions.

The Pareto front moves upward, yielding higher expected loss values, as the considered lifespan increases.

6. The availability of maintenance options also affects the Pareto front. If certain maintenance options (e.g., restoring the condition to initial state) are not available, the optimization problem yields solutions with higher risk for the same level of maintenance cost.

The proposed optimization methodology is developed to assist risk-informed decision making regarding the maintenance of deteriorating bridges. The efficiency of the methodology depends on the accuracy of the risk assessment approach. Further research is needed on the risk-based maintenance optimization of deteriorating structures in connection with accurate assessment of condition states and costs associated with maintenance actions.

(a)   No Maintenance (Do Nothing)

(b) Maintenance Strategy 1

(c) Maintenance Strategy 2

(d) Maintenance Strategy 3

(e) Maintenance Strategy 4
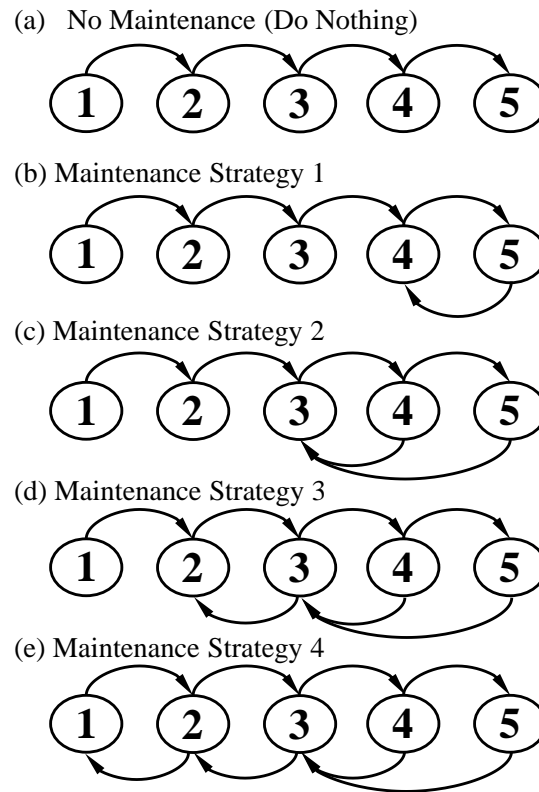
Figure 6.1   Maintenance strategies
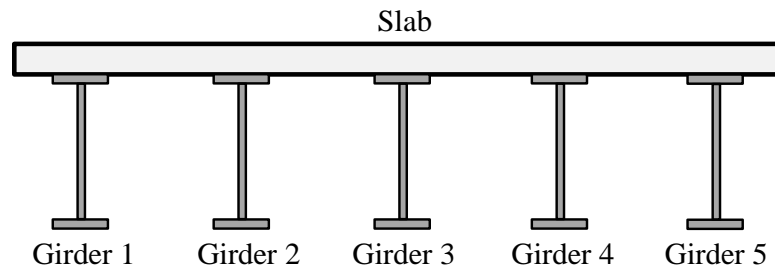
Figure 6.2   The superstructure of the E-16-FK Bridge
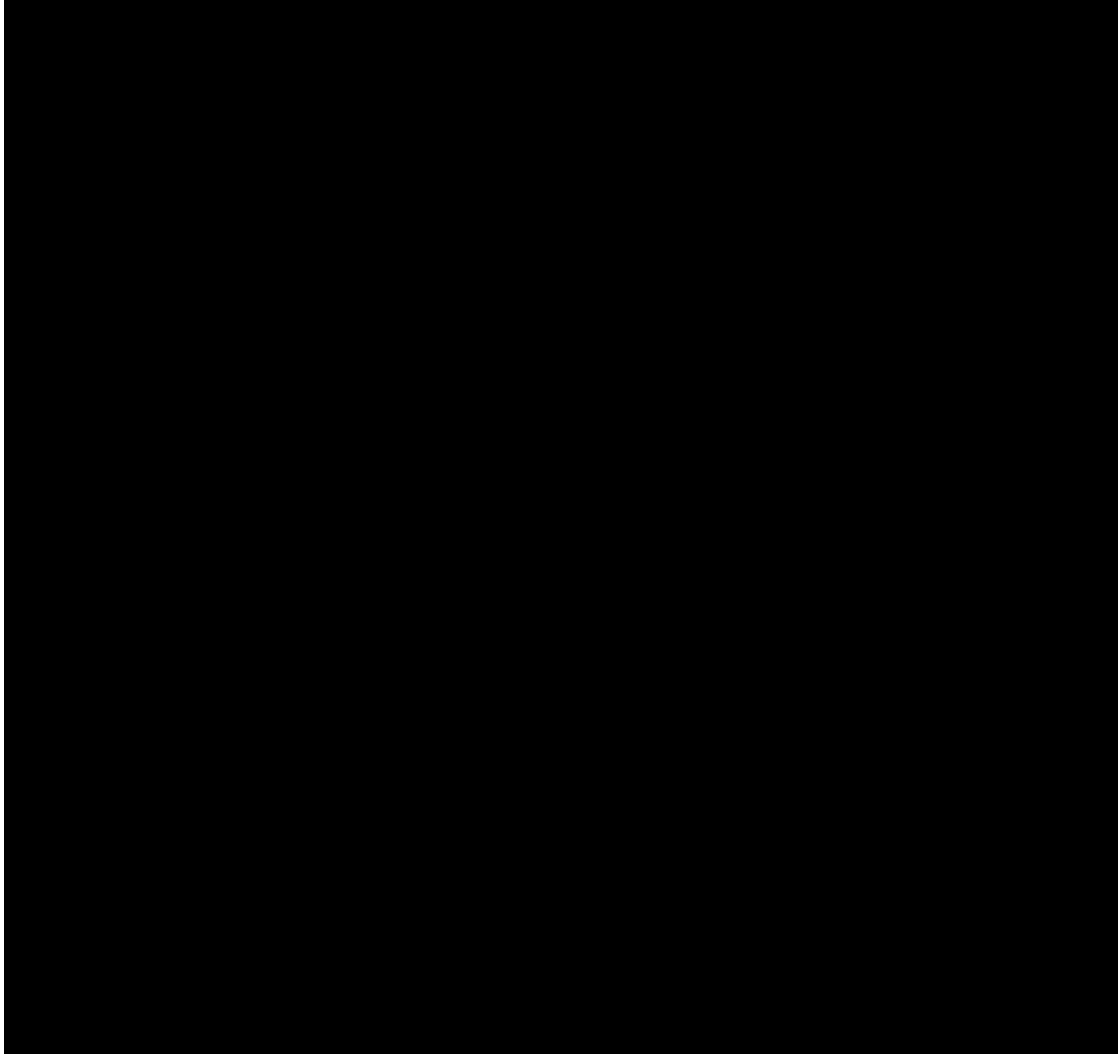
Figure 6.3   Time-dependent condition state probabilities for girder 1 with respect

to various maintenance strategies

Figure 6.4   Component probability of failure in different condition states for girder

1

(a)

(b)

(c)

(d)

S_F : Flexural failure of slab $G3_F$: Flexural failure of girder 3
$G1_F$: Flexural failure of girder 1 $G4_F$: Flexural failure of girder 4
$G2_F$: Flexural failure of girder 2 $G5_F$: Flexural failure of girder 5
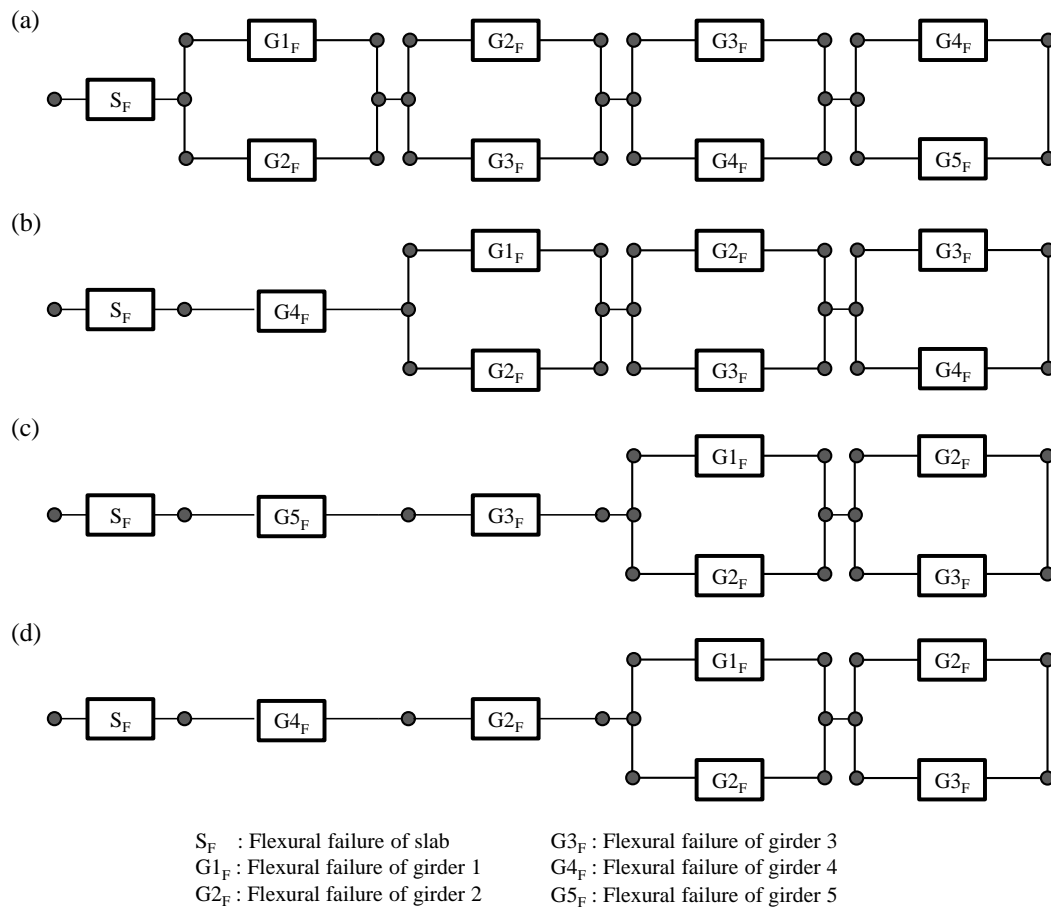
Figure 6.5   System reliability models for (a) intact case, (b) failure of girder 5, (c)

failure of girder 4, and (d) failure of girder 3

204

Figure 6.6   (a) Annual expected loss for different maintenance strategies and (b)
annual expected cost of these maintenance strategies
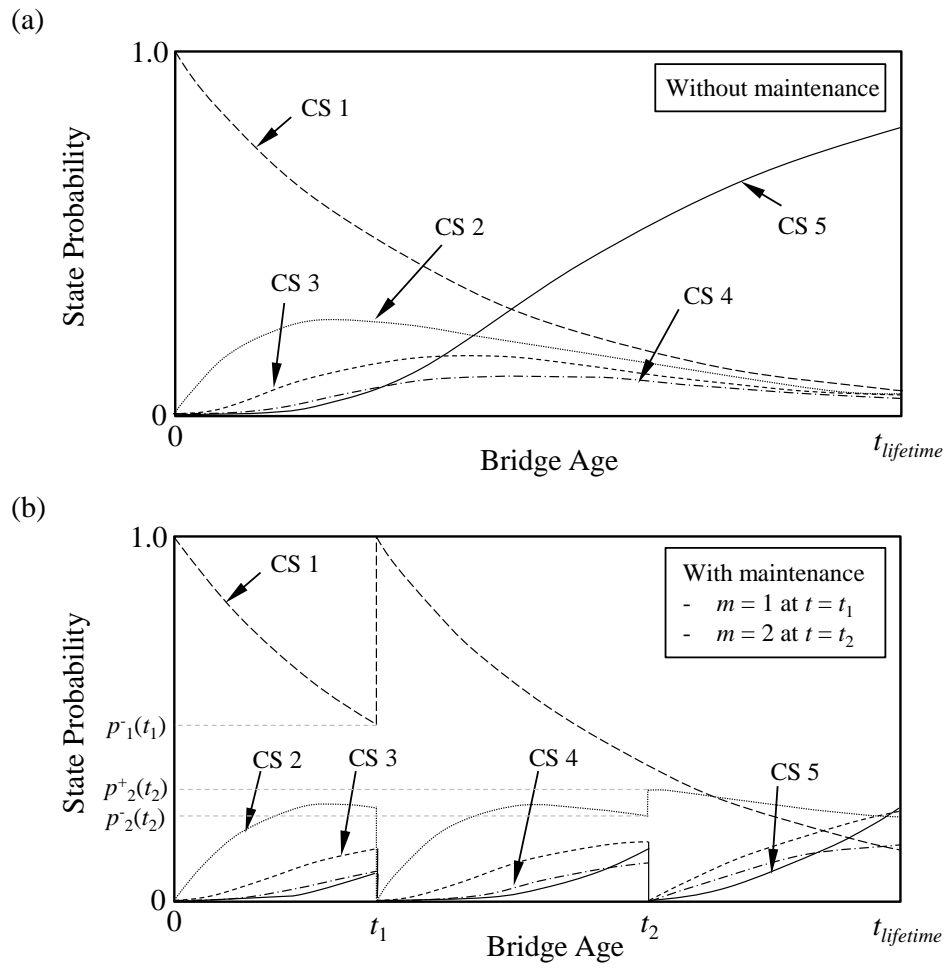
Figure 6.7   Qualitative representation of time-variant condition state probabilities

(a) without maintenance and (b) with maintenance

206
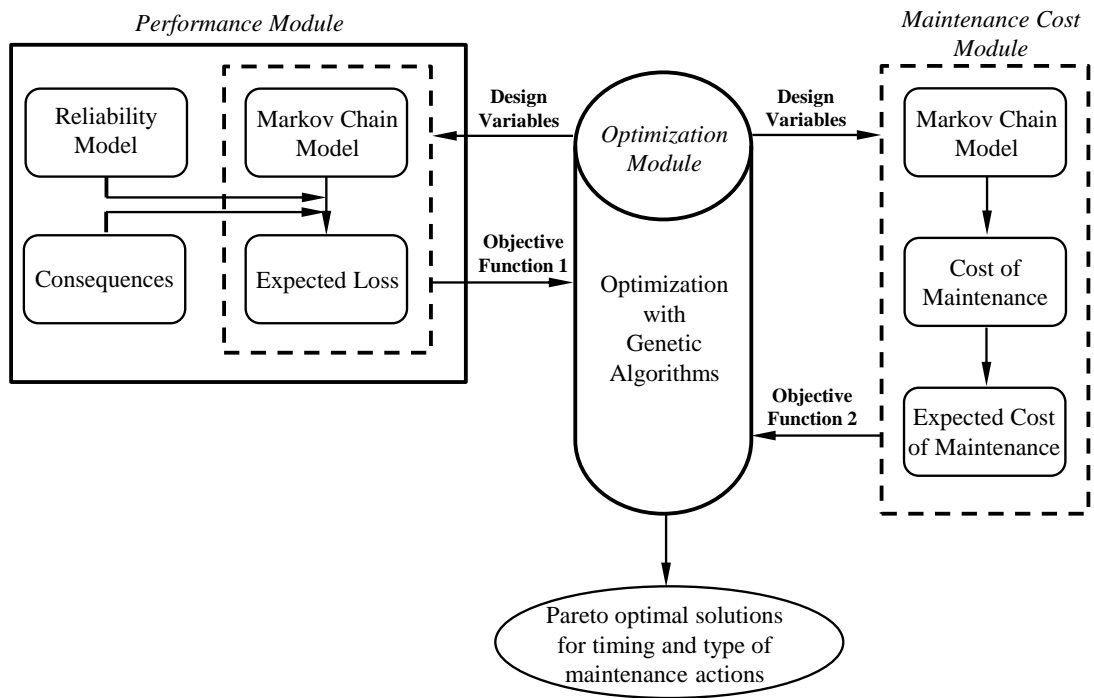
Figure 6.8   The interaction among the modules of the maintenance optimization

methodology
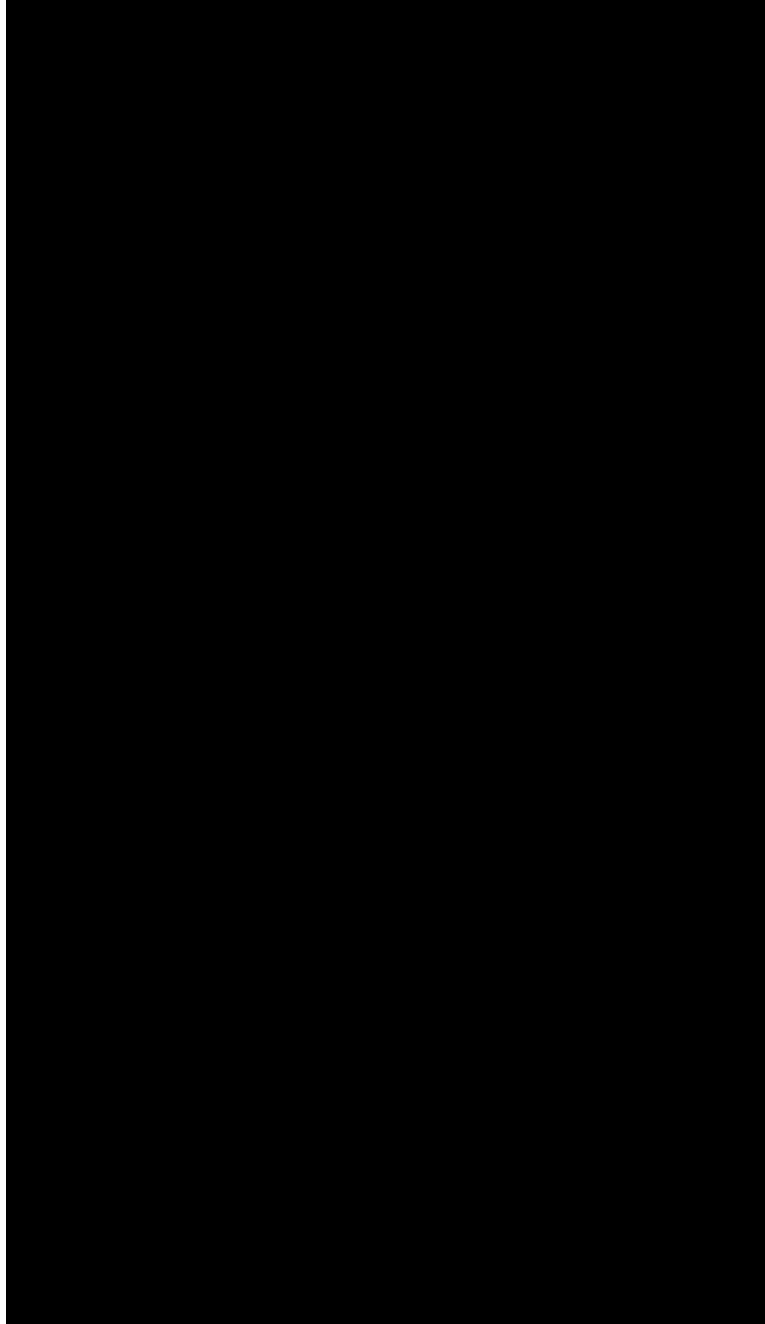
Figure 6.9   Time-variant condition state probabilities without maintenance for (a)
exterior girders, (b) interior girders, and (c) time-variant total expected
loss without maintenance

208
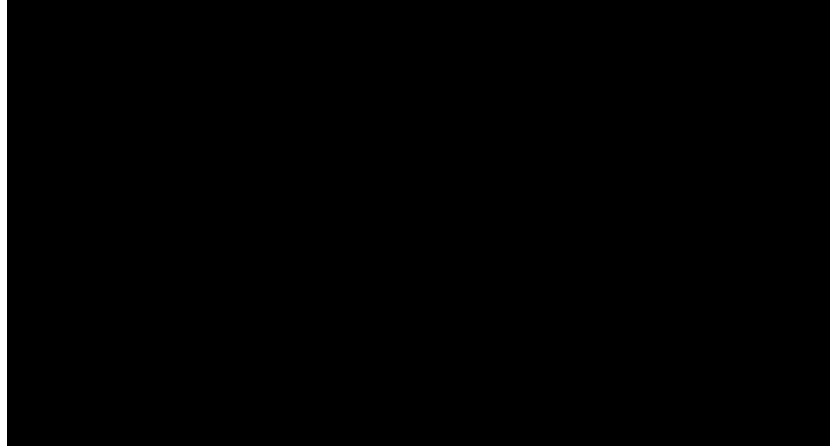
Figure 6.10   Failure probabilities of exterior girders (1 and 5) in different condition
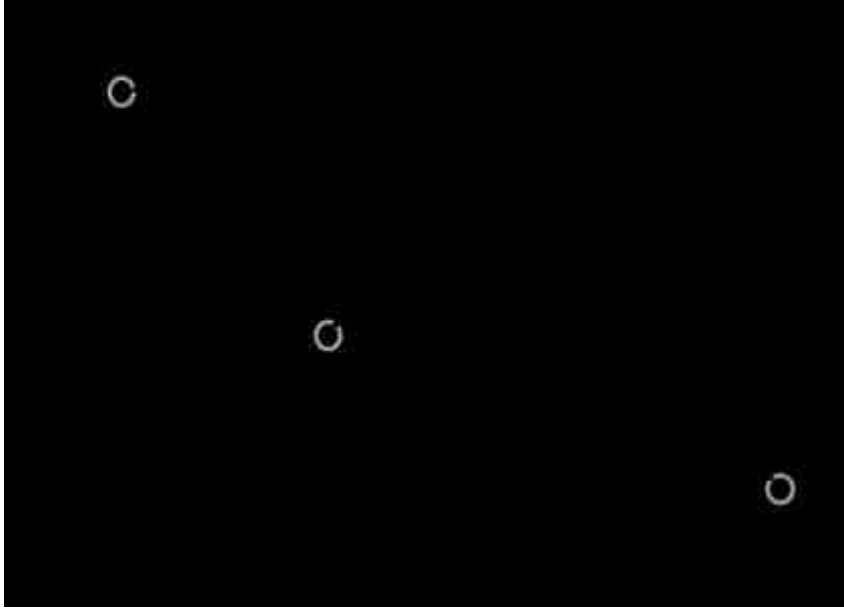
states

Figure 6.11   Pareto optimal solutions considering t_L = 70 years
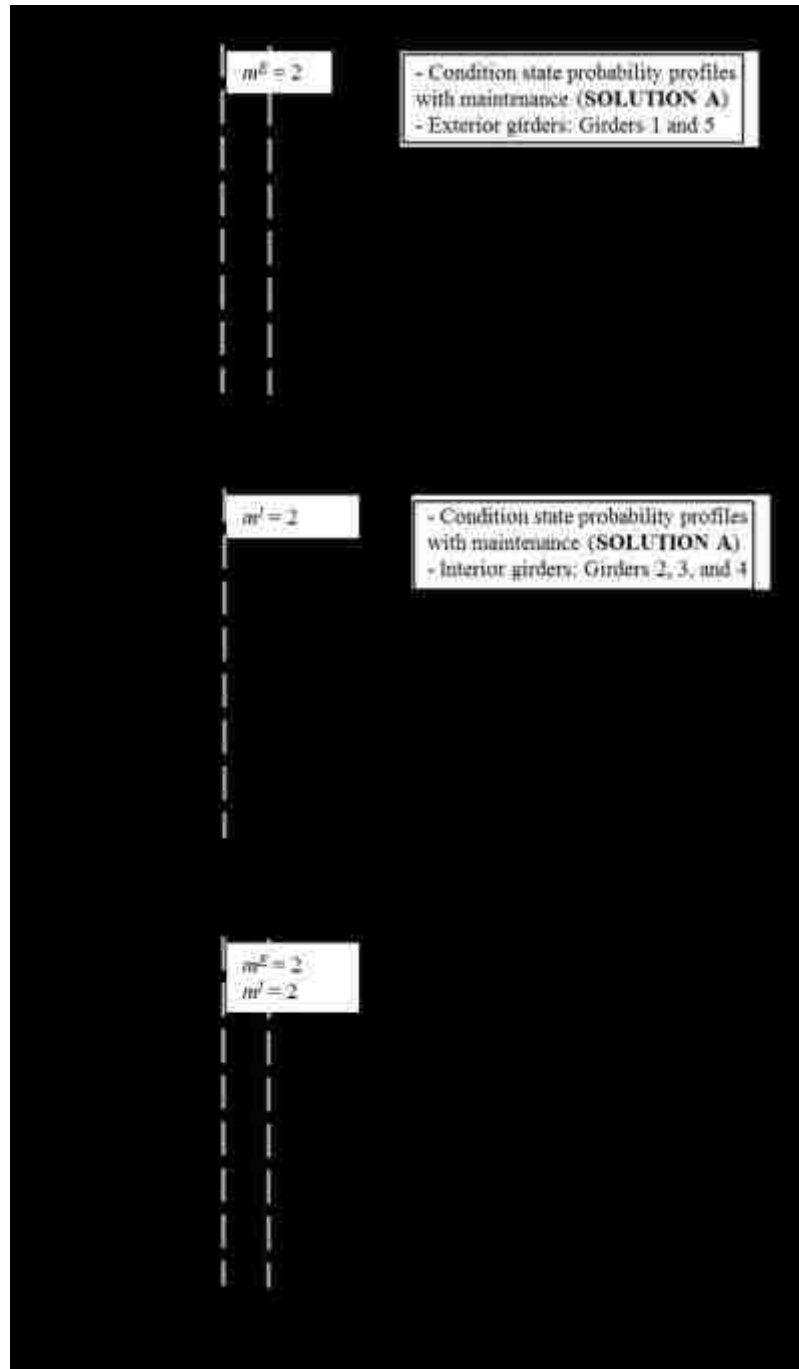
Figure 6.12   Time-variant condition state probabilities with maintenance (Solution

A) for (a) exterior girders, (b) interior girders, and (c) time-variant total

expected loss without maintenance
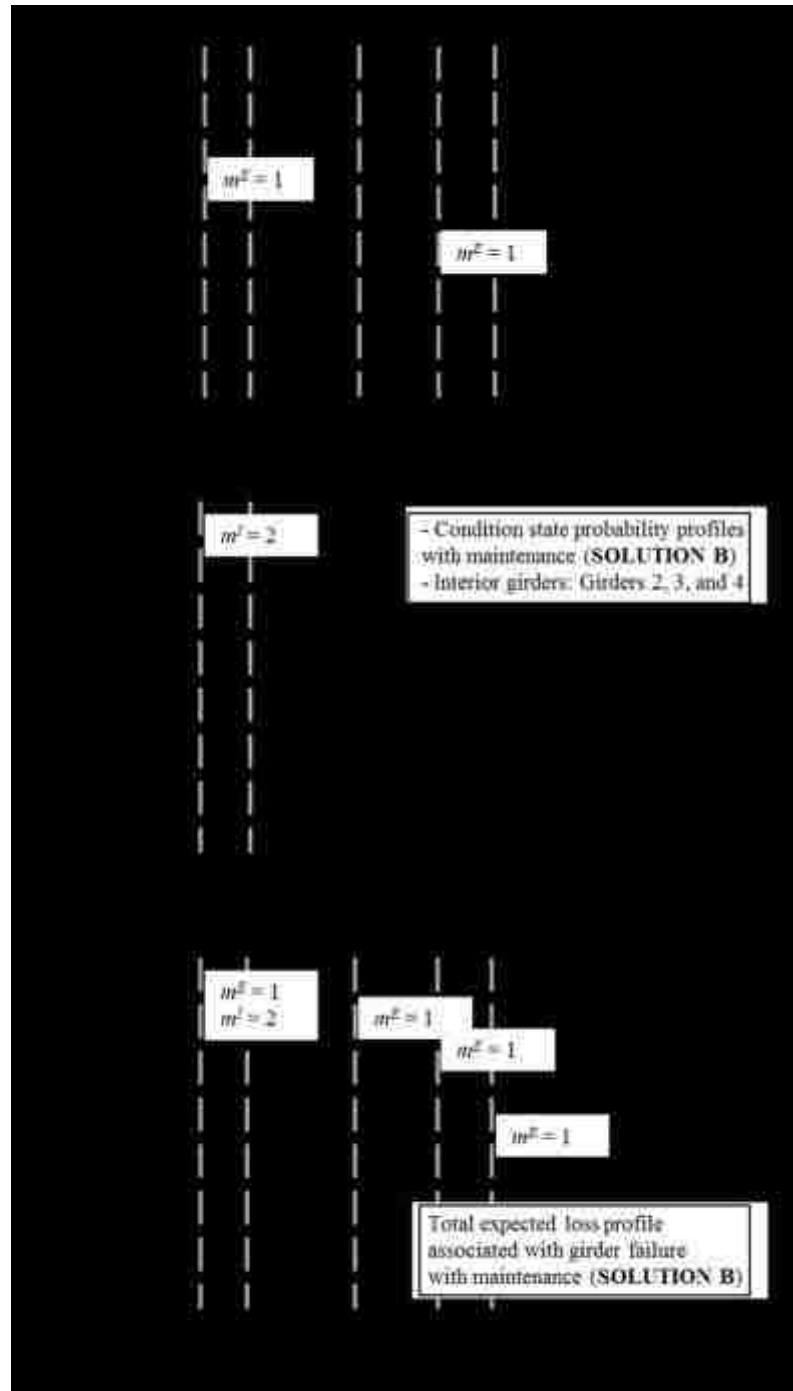
Figure 6.13   Time-variant condition state probabilities with maintenance (Solution

B) for (a) exterior girders, (b) interior girders, and (c) time-variant total

expected loss without maintenance
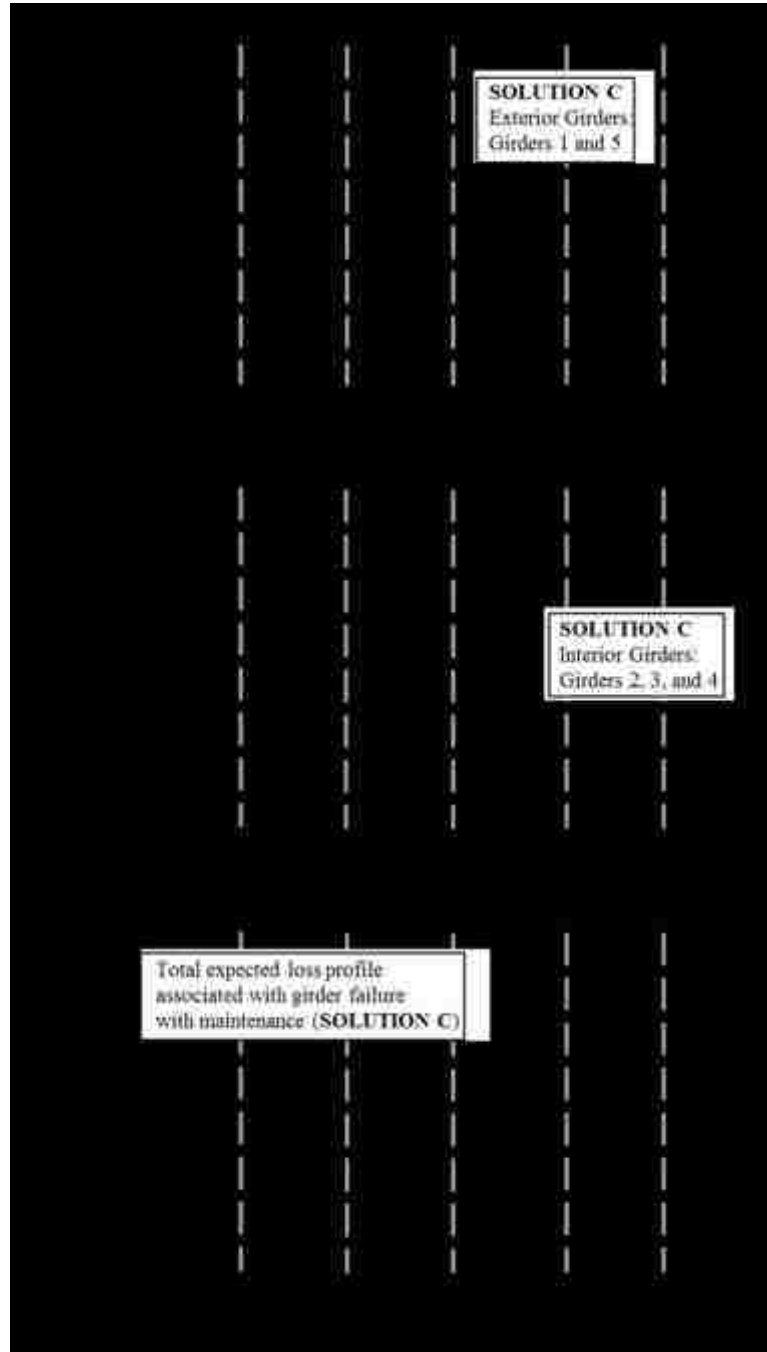
Figure 6.14   Time-variant condition state probabilities with maintenance (Solution

C) for (a) exterior girders, (b) interior girders, and (c) time-variant total

expected loss without maintenance
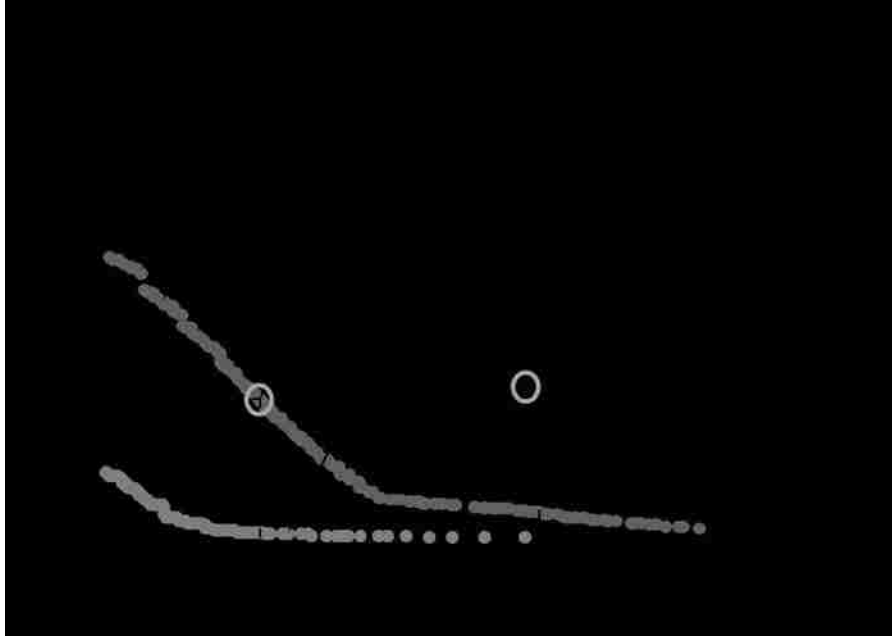
Figure 6.15   Effect of considered lifespan on Pareto optimal solutions
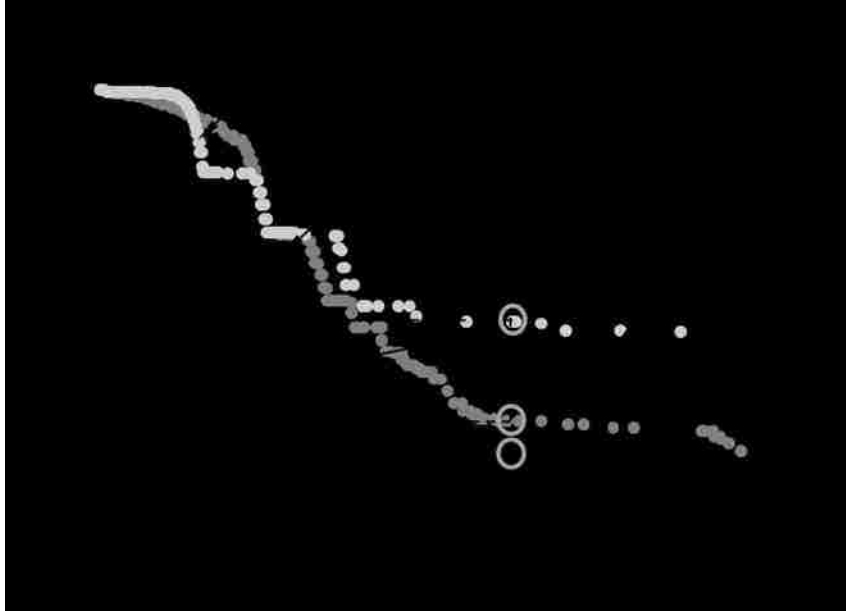
Figure 6.16   Effect of available maintenance options on Pareto optimal solutions

CHAPTER 7

TIME-DEPENDENT RISK AND RISK-BASED ROBUSTNESS ANALYSIS OF HIGHWAY BRIDGE NETWORKS USING A MARKOV MODEL

7.1 INTRODUCTION

In this chapter, a methodology to assess the time-dependent expected losses and risk-based robustness of highway bridge networks consisting of deteriorating bridges is summarized. A detailed description was presented in Saydam, Bocchini, and Frangopol (2013). A Markov model (Bocchini, Saydam, and Frangopol 2013) which can combine the effects of time-dependent deterioration rates and the impacts of rehabilitations/reconstructions is used to predict the time-dependent performance of the individual bridges. The time-dependent direct, indirect and total risk is investigated. Furthermore, the time-dependent risk-based robustness index, which is the ratio of expected value of direct loss to the expected value of total loss, is assessed.

7.2 ESTIMATION OF HIGHWAY BRIDGE PERFORMANCE

The overall methodology for assessing time-dependent risk of bridge networks using a Markov chain model is illustrated in Figure 7.1. The goal of this framework is to compute the direct and indirect losses associated with bridge failure scenarios. In order to compute the expected losses, the probability of occurrence of these scenarios and the consequences associated with these scenarios should be computed.

216

Due to the Markov property, the future states are independent of the past states given the current state and, therefore, the effects of time-dependent deterioration rates and of rehabilitation/reconstruction cannot be combined in a conventional Markov model without some approximations. A Markov model is used to predict the time-dependent performance of bridges within a network (Bocchini, Saydam, and Frangopol 2013). Compared to other approaches in the literature, this model has three advantages. Figure 7.2 represents the five states of the Markov model. In state S (service), the bridge is in normal operational conditions and no failure experienced in the past. In state M (maintenance shutdown), the bridge is out-of-service due to minor preventive maintenance activities. State R (restoration/reconstruction) represents that the bridge had structural failures and is out-of-service due to rehabilitation/reconstruction activities. State S' represents the same operational conditions of state S, in which the bridge is perfectly in service. The difference is that the transition probability from S' to R is time-independent and reflects the effect of a previous rehabilitation/reconstruction activity (i.e., the reliability is high and the transition probability is low). Similarly, M' represents the same bridge operational conditions (i.e., same direct and indirect consequences in case of a risk analysis) of state M. However, the transition probability from M to R increases in time due to deterioration, whereas the transition probability from M' to R is time-independent. The constant value of the transition probability from S' to R and from M' to R means that bridges in states S' and M' are not affected by any type of deterioration.

The state vector for the five-state Markov model, in Figure 7.2, is expressed as

$$\mathbf{S} = \begin{bmatrix} S & M & R & S' & M' \end{bmatrix}^T \tag{7.1}$$

217

where S, M, R, S' and M' are the states defined previously.

In the conventional reliability analysis of bridge structures, it is most common to use the reliability index associated with the conditional failure probability as a measure of performance. This approach may be useful and practical for investigating and managing life-cycle of bridges individually. However, this measure indicates the conditional probability of failure given that the bridge survived until that time. This is acceptable when the focus is on a single bridge (i.e. on its first failure), but it is not appropriate when an entire network is considered and the analysis has to continue even after the failure and rehabilitation of individual bridges. One advantage of using the five-state Markov model in risk assessment is the fact that the state probabilities are unconditional (i.e., independent of the history) and it accounts for the failure and rehabilitation/reconstruction of individual bridges.

7.3 QUANTIFYING CONSEQUENCES AT THE NETWORK LEVEL

The consequences of a component failure within a system are categorized in two groups: direct consequences and indirect consequences. The various costs could be included in either category depending on the purpose of the analysis and the scale at which the analysis is performed (e.g., individual bridge, transportation network). For instance, when assessing the risk of a bridge component, the monetary value of the human health expenses and life loss due to collapse can be included in the indirect consequences since these costs are induced by the failure of the bridge system, not directly by the component failure. However, if the interest is the risk assessment of a bridge failure within a highway bridge network, the entire bridge is the "component"

and these costs can be considered as direct consequences. In other words, direct consequences are the costs incurred instantly, due to the structural failure; indirect consequences are the costs that accumulate in time, due to the improper functionality of the bridge. In the following, the direct and indirect consequences of a bridge failure within a network system are discussed in details.

The direct consequences of bridge failure impact the highway agency that is responsible for the bridge. When a bridge failure occurs, the highway agency performs the rehabilitation or reconstruction activities as soon as possible in order to minimize the impact of failure on traffic. Therefore, the cost of the activities to restore the full functionality or the reconstruction of the bridge is among the direct consequences. HAZUS-MH MR4 (FEMA 2009) is a software for the loss analysis of spatially distributed systems within the United States. It has a vast database of bridges, that includes their reconstruction cost. The cost of restoring the full functionality of a bridge after failure is assumed to be the reconstruction cost (C_R) obtained from this database. In addition, the failure of a bridge may cause severe accidents involving the vehicles on the bridge at the instant of failure. Therefore, the cost of accidents (C_A) and the human health and life costs (C_H) are included in the direct consequences. Also, the costs associated with the environmental damage, C_E, and the cost associated with the impact on general public, C_P, are considered among direct consequences. The total direct consequence of bridge failure is expressed as

$$C_{Dir} = C_R + C_A + C_H + C_E + C_P \tag{7.2}$$

In reality, different highway agencies use different models for these costs and they should be considered random variables. However, the focus of this study is the

219

integration of a broad number of concepts. Therefore, to keep the approach feasible, these consequences are treated as deterministic quantities.

The indirect costs of the bridge failure impact the users of the highway route where the bridge is located and are often called "user costs". Following the failure of a bridge, the users of the highway need to by-pass the bridge with alternative routes. However, the capacity of the alternative routes may be less than that of the original route, causing traffic congestion, and the alternative routes may be longer, which might affect the user preferences on deciding their travel paths. Therefore, computation of the indirect consequences of bridge failure within a network requires a complex traffic assignment analysis accounting for the detour length of the bridge.

The network performance is quantified by updating the highway segment capacities depending on the functionality levels of the bridges. Then, the joint traffic distribution and assignment problem is solved. A gravitational model (Levionson and Kumar 1994) that measures the attraction between two points as inversely proportional to the time required to go from one to the other is used to distribute the travels of the users within the network among the pairs of origin and destination nodes. Although there are more sophisticated methods for the assignment of the travels among the various routes, a procedure based on the user equilibrium (Frank and Wolfe 1956) is used herein for two reasons. First, it allows a "fair" comparison among the performance levels of the network associated with different scenarios. For instance, when a more sophisticated approach that accounts for the adaptation of the traffic Origin-Destination (OD) matrix is used, the traffic delay due to a more severe failure scenario can be smaller than the traffic delay due to a less severe failure scenario. This

220

is due to the fact that the adaptive OD matrices in these two cases are not identical. The second advantage is that the Frank and Wolfe algorithm is computationally very efficient and can be used for a large number of repeated analyses with a short computational time. Two basic performance indicators can be computed by using this procedure. These are the total travel time, *TTT*, and the total travel distance, *TTD*. The difference in *TTT* and *TTD* between the reference and the other scenarios are indicated by ΔTTT and ΔTTD, respectively.

The traffic demand on a highway network varies throughout the day. Therefore, it is convenient to divide the duration of a day into *k* intervals in which the traffic demand (origin-destination data) is assumed constant. In this way, the indirect consequences can be computed in a more realistic manner.

The indirect consequences of bridge failure include basically the additional running cost of the vehicles and the additional time costs for the travelers. The total additional running cost of the vehicles within a network due to the out-of-service state of a set of bridges, for the duration of the time step of the analysis, can be computed as

$$C_{VR} = c_{VR} \cdot t_d \cdot \sum_{i=1}^{k} \Delta TTD_i \cdot \frac{t_i^f}{t_{day}} \tag{7.3}$$

where c_{VR} is the cost of running vehicle per unit length, t_d is the duration of the time step (in which the bridge is out-of-service) used for risk analysis, ΔTTD_i is the additional total travel distance for a certain interval of the day, t_i^f is the duration of this time interval, and t_{day} is the duration of one day. The additional time cost for the passenger cars and trucks, for the time step of the analysis, can be computed as

221

$$C_T = c_T \cdot t_d \cdot \sum_{i=1}^{k} \Delta TTT_i \cdot \frac{t_i^f}{t_{day}} \qquad (7.4)$$

where c_T is the cost of additional time for the travelers per unit time and ΔTTT_i is the additional total travel time associated with interval i of a day. The total indirect consequence of bridge failure is expressed as

$$C_{Ind} = C_{VR} + C_T \qquad (7.5)$$

7.4 QUANTIFYING RISK AND ROBUSTNESS AT THE NETWORK LEVEL

7.4.1 Risk

Risk is the probability distribution of loss. In its general form, risk can be formulated as (CIB, 2001)

$$R = \iint \cdots \int C(x_1, x_2, \cdots, x_m) \cdot f_{\mathbf{X}}(x_1, x_2, \cdots, x_m) dx_1 dx_2 \cdots dx_m \qquad (7.6)$$

where $\mathbf{x} = \{x_1, x_2, \ldots, x_m\}$ is the set of random variables involved in the problem, C represents the consequences and $f_{\mathbf{X}}(\mathbf{x})$ is the joint probability density function of the random variables. Risk assessment is based on the quantification of the expected value of losses. The marginal probabilities of being in each service states can be computed by means of the Markov model presented previously. On the other hand, the consequences associated with various scenarios can be assessed as explained in the previous section. In this section, probabilities and consequences are combined to estimate the time dependent expected loss.

If the time-dependent failure probabilities are computed using the Markov model described previously, a combination of transition and state probabilities offers a rational way to determine the occurrence probabilities of the scenarios. The state

222

transitions of bridges are assumed to be statistically independent (i.e. deterioration and restoration activities on the various bridges are statistically independent). According to this approach, the expected value of direct loss depends on the transition probabilities from an in-service state (*S* and *S′*) to an out-of-service state (*M*, *M′*, and *R′*). On the other hand, when computing the indirect risk, the state probability is under consideration.

In this study, the expected value of indirect loss associated with the out-of-service states of bridges within a network is computed based on scenarios consisting of single or multiple bridge outages. Bridges are assumed to be out-of-service due to either maintenance shutdown or failure. The bridges can be categorized in three groups for quantifying expected value of indirect loss. The first group **S** consists of the bridges which are in state *S* or state *S′* and thus are in service. The second group **M** includes the bridges which are in state *M* or state *M′* and thus are out-of-service. The bridges in the third group **R** are in state *R* and thus are out-of-service. Since each bridge is in only one state at a given time instant, the partition of the entire set of the bridges of the network **B** defines subsets that are mutually exclusive (i.e., $\mathbf{S} \cap \mathbf{M} = \phi$, $\mathbf{S} \cap \mathbf{R} = \phi$, and $\mathbf{M} \cap \mathbf{R} = \phi$, where ϕ is the impossible event) and collectively exhaustive (i.e., $\mathbf{S} \cup \mathbf{M} \cup \mathbf{R} = \mathbf{B}$). Each scenario *sc* is associated with a specific partition ($\mathbf{S}_{sc}$, $\mathbf{M}_{sc}$, and $\mathbf{R}_{sc}$) of the set **B**. The total expected value of indirect loss can be computed based on these three subsets as

$$L_{Ind} = \sum_{sc} \left(\prod_{b \in \mathbf{S}} \left(P^b(S) + P^b(S') \right) \cdot \prod_{b \in \mathbf{M}} \left(P^b(M) + P^b(M') \right) \cdot \prod_{b \in \mathbf{R}} \left(P^b(R) \right) \right) \cdot C_{Ind}^{sc} \qquad (7.7)$$

223

where $P^b(S)$ and $P^b(S')$ are the Markov state probabilities for states S and S', respectively for $b \in \mathbf{S}$, $P^b(M)$ and $P^b(M')$ are the Markov state probabilities for states M and M', respectively for $b \in \mathbf{M}$, $P^b(R)$ is the Markov state probability for states R for $b \in \mathbf{R}$, and C_{Ind}^{sc} represents the indirect consequence of scenario sc. The total expected value of indirect loss is the summation of the expected value of indirect loss associated with the individual scenarios over all considered scenarios. All the variables in this equation are functions of the investigated time step, even if the dependence on time has been omitted from the equation for the sake of clarity.

The total expected value of direct loss is considered as the sum of the expected direct loss due to maintenance shutdown and failure of each bridge within the network. This includes the contributions of bridges transitioning to states M, M' and R. The total expected value of direct loss at a time step can be expressed as

$$L_{Dir} = \sum_{b \in \mathbf{B}} \left[\left(P^b(S) \cdot TP_{SM}^b \right) \cdot C_M^b + \left(P^b(S') \cdot TP_{S'M'}^b \right) \cdot C_M^b + \right.$$
$$\left. + \left(P^b(S) \cdot TP_{SR}^b + P^b(M) \cdot TP_{MR}^b + P^b(S') \cdot TP_{S'R}^b + P^b(M') \cdot TP_{M'R}^b \right) \cdot C_{Dir}^b \right] \tag{7.8}$$

where index b runs over the entire set of bridges $\mathbf{B}$; $P^b(S)$, $P^b(S')$, $P^b(M)$ and $P^b(M')$ are the state probabilities for bridge b; TP_{SM}^b is the transition probability from state S to M; $TP_{S'M'}^b$ is the transition probability from state S' to state M; TP_{SR}^b is the transition probability from state S to R, $TP_{S'R}^b$ is the transition probability from state S' to state R, TP_{MR}^b is the transition probability from state M to R, $TP_{M'R}^b$ is the transition probability from state M' to state R; C_M^b is the cost of the maintenance activity; and C_{Dir}^b represents the direct consequences. All the variables in this equation are

functions of the investigated time step but this notation is avoided for the sake of clarity.

7.4.2 Robustness

The risk-based robustness indicator (Baker, Schubert, and Faber 2008) accounts for both the likelihood of component failure and the consequences of component failure. Furthermore, the risk-based robustness indicator can represent the combined effects of different individual scenarios. The indirect consequences of component failure, as well as the direct consequences, significantly involve the economic aspects regarding a transportation network. It is more appropriate to combine the economic aspects and the theory of structural reliability when prioritizing the components of a transportation network. Therefore, the risk-based robustness indicator is selected for assessing the time-dependent robustness of highway bridge networks.

Baker, Schubert, and Faber (2008) defined a robust system as the one where indirect risks do not contribute significantly to the total system risk. An index of robustness is proposed as the ratio of the direct risk to the total risk (Baker, Schubert, and Faber 2008). In order to be consistent with the rigorous definitions of risk and expected value of loss, the robustness index is formulated as

$$I_{Rob} = \frac{L_{Dir}}{L_{Dir} + L_{Ind}}$$
(7.9)

where L_{Dir} and L_{Ind} are the expected values of direct and indirect losses, respectively. This index varies between 0 and 1 with larger values representing a larger robustness.

7.6 CASE STUDY

The proposed approach is applied to a highway bridge network adapted from an existing network located in the lower Bay Area, California, USA. The detailed case study was presented in Saydam, Bocchini, and Frangopol (2012). A brief review is presented herein. The network studied is simplified by selecting only some of the highway segments of the existing network and only some of the bridges on the selected segments. The network investigated consists of 7 nodes, 11 links, and 16 highway bridges. The layout of the network is presented in Figure 7.3.

The geographical data regarding nodes, links and bridges are obtained from the database of the software HAZUS-MH MR4 (FEMA, 2009). Three different sets of origin-destination data are considered during a day. The first period, which accounts for the peak traffic hours, is assumed to have total duration of 4 hours. The second period, which reflects regular traffic hours, is assumed to last 8 hours. The number of trips originated and attracted by the nodes for the second period is considered half of that associated with the first period. The third period covers the remaining 12 hours and reflects the minimum traffic hours. The hourly number of trips originated and attracted by the nodes during the third period is considered as one fourth of that associated with the first period. The number of trips originated and attracted by the nodes for the different periods of a day is provided in Table 7.1. Although the proposed methodology can be applied to cases with time-variant origin-destination data, in this case study, the trips generated and attracted by the nodes are assumed to remain constant over the years in order to put emphasis on the effects of the time-

226

dependent bridge performance. The characteristics of the links in Figure 3 are presented in Table 7.2.

7.6.1 Time-Dependent Performance of Individual Bridges

A monthly time resolution is selected for the Markov analysis. The reliability values provided by Akgül (2002) were annual. The mean duration of a maintenance shutdown, N_m, is assumed to be 3 months for all the bridges (in general this value can be different for each bridge type). Therefore, the probability of transition from state M to state S is 1/3. The mean duration of rehabilitation/reconstruction activities, N_r, which recovers full functionality of the bridges, is assumed to be 18 months for all the bridges (also this value can be different for each bridge, in general). Then, the probability of transition from state R to state S' is 1/18.

The resulting time-dependent state probabilities are presented in Figure 7.4 (a), (b) and (c) for bridges B1, B10 and B16, respectively. In Figure 7.4 (a), the probability of Bridge B1 being in state S is decreasing very rapidly between the years 20 and 40. On the other hand, the probability of being in state S' is increasing rapidly due to the reconstruction rate. The probability of being in state R and the probability of being in state M have their peak values in the vicinity of the intersection of the profiles associated with states S and S'.

7.6.2 Consequences

The reconstruction cost, C_R, of each bridge is obtained from the database of the software HAZUS-MH MR4 (FEMA, 2009). Ang (2011) expressed the various

227

components of total consequences of bridge failure as percentages of the initial cost of the bridge and stated the health and life safety costs as 500% of the initial cost. In this study, the health and life safety costs are taken as the same percentage, 500%, of the reconstruction cost. Similarly, the cost of accidents, C_A; the costs associated with the environmental damage, C_E; and the impact on the general public, C_P, are assumed to be 80%, 60% and 60% of the reconstruction cost, respectively. The direct consequences of individual bridge failures are presented in Table 7.3.

As already mentioned, the classification of consequences depends on the purpose and the level (e.g., component, structure, and network) of the analysis. In this study, for transportation networks, robustness is considered as the ability of the network to redistribute the traffic with minimum economic losses if one or multiple links of the network are not functioning with the original capacity. With this purpose in mind, the indirect risk is considered to be due to the additional travel distance and travel time caused by the out-of-service state of any bridge within the network. Since the indirect risk is associated with scenarios including multiple bridges out-of-service, the indirect consequences are computed based on 3873 scenarios consisting of different combinations of bridge operational conditions. These scenarios can be classified in the following groups: (a) only one bridge is under maintenance shutdown; (b) two bridges are under maintenance shutdown simultaneously; (c) only one bridge is out-of-service due to failure; (d) one bridge is under maintenance shutdown and one bridge is out-of-service due to failure simultaneously; (e) two bridges are out-of-service due to failure simultaneously; (f) two bridges are under maintenance shutdown and one bridge is out-of-service due to failure simultaneously; and (g) two bridges are

228

out-of-service due to failure and one bridge is under maintenance shutdown simultaneously.

For each scenario, the total travel distance, *TTD*, and the total travel time, *TTT*, are higher than those for the case with all bridges in service. The considered out-of-network detour lengths of the bridges are tabulated in Table 7.3. The duration of a day is divided into three periods, as explained previously, and the additional total travel distance, ΔTTD, and the additional total travel time, ΔTTT, are computed for these three periods by using a computer program (Bocchini and Frangopol 2011b, 2012) capable of solving the traffic distribution and assignment problem. The cost of running vehicle per unit distance, c_{VR}, is assumed as 0.30 \$/km for mixed traffic including both passenger cars and trucks (based on Stein et al., 2006). The cost of additional time for the travelers depends on the average daily traffic. The average daily truck traffic is assumed to be 10 % of the average daily traffic. The unit costs of additional time for trucks and passenger cars are taken as 20 \$/h and 7 \$/h, respectively. The monthly discount rate of money 0.17% is used to compute the variation of the consequences in time.

7.6.3 Time-dependent Risk and Risk-based Robustness

Figure 7.5 (a) presents the time-variation of the expected monthly direct loss associated with failure for bridge B1, expected direct loss associated with failure for bridge B3, expected direct loss associated with maintenance shutdown for bridge B1, and expected direct loss associated with maintenance shutdown for bridge B3. It is clear that the maximum lifetime expected loss associated with failure is much larger

229

than the maximum expected loss due to maintenance shutdown, although the probability of maintenance shutdown is larger than the probability of failure. This is due to the fact that the direct consequences of failure are much larger than the direct consequences of maintenance shutdown. The maximum expected direct losses associated with failure of bridge B1 and bridge B3 occur around t=30 years and t=40 years, respectively.

In Figure 7.5 (b), the time-dependent expected monthly indirect loss of several scenarios is presented. These scenarios include failure of bridge B1, maintenance shutdown of bridge B1, failure of bridge B1, maintenance shutdown of bridge B3, failure of bridges B1 and B3 simultaneously, and maintenance shutdown of bridges B1 and B3 simultaneously. The maximum expected indirect loss of failure of bridge B1 is the largest among those presented in Figure 7.5 (b). This is because, although the indirect consequences of simultaneous bridge failure events are much higher, the probability that two bridges fail simultaneously is very small. Similarly, the maximum expected indirect loss of maintenance shutdown of bridge B1 is the largest among the three scenarios associated with maintenance shutdown. All the expected loss profiles show a pattern that first increases and then decreases due to the variation of the Markov chain state probabilities in time. The expected indirect loss can start increasing again very slowly after the first peak. Depending on a specific scenario (i.e., one bridge is under maintenance shutdown and the others are functional), these probabilities can be obtained from the Markov model. For illustration, let's consider an example scenario in which bridge B1 is under maintenance shutdown, in other words B1 is in subset **M** (in states *M* or *M'*), and all other bridges are functional, in

230

other words all other bridges are in subset **S** (in states *S* or *S'*). The probabilities of a bridge to be in subset **M** (in states *M* or *M'*) and subset **S** (in states *S* or *S'*) are time-dependent and different for each bridge at a time step. The probability of B1 to be in subset **M** (in states *M* or *M'*) and the probabilities of all other bridges to be in subset **S** (in states *S* or *S'*) are multiplied by each other. The product also varies over time. Depending on the probability contribution of each bridge this product can increase or decrease over time even after the main peak caused by the dominant event within the scenario (e.g., maintenance shutdown of bridge B3 in the example scenario).

The scenarios accounted for the computation of direct consequences include the failure of each bridge (16 scenarios) and the maintenance shutdown of each bridge (16 scenarios). A total of 3873 scenarios are considered for the computation of total expected indirect loss. The total expected values of direct and indirect losses are basically the summation of the expected losses associated with the various scenarios. The time-dependent expected monthly total direct, total indirect and total losses are illustrated in Figure 7.6 (a). The expected monthly loss values are converted to expected annual loss values and presented in Figure 7.6 (b). The results indicate that the maximum total expected indirect loss is much higher than the maximum total expected direct loss. Both the total expected direct and indirect losses manifest a peak at the middle of the investigated time period with values $ 6,844,700 and $ 92,851,000, respectively. The overall trend over the investigated time horizon mimics those of the individual scenarios. The ratio of the total expected direct loss to total expected loss (i.e., total expected direct loss + total expected indirect loss) defines the robustness index and its evolution in time is presented in Figure 7.7. The robustness

231

index starts with a value of 0.19 and decreases very rapidly to 0.084 within the first 5 years of the investigated time period due to the high rate of increase of the expected indirect loss over this period. Throughout the investigated time span, the robustness index shows a decreasing trend, in general. However, there are periods when the robustness index increases. The time period between years 45 and 55 is a period where this trend is significant. It can be concluded that the risk-based robustness indicator is a more reliable performance measure for relatively longer periods.

7.7 CONCLUSIONS

This chapter presents a methodology to assess the time-dependent expected losses and risk-based robustness of highway bridge networks accounting for deterioration and restoration. A five-state Markov model is used to predict the time-dependent performance of the individual bridges. The model accounts for the failure and restoration of the bridges in contrast to the conventional approach (condition-based). The direct consequences are identified on the basis of the individual bridge failure or closure for maintenance. The indirect consequences are quantified on the basis of scenarios including single and multiple bridges out-of-service. The traffic assignment problem is solved to quantify the network performance under various failure scenarios. The variation of expected direct, indirect and total losses in time is investigated. Furthermore, the time-dependent risk-based robustness is computed.

The following conclusions are drawn:

232

1. Markov models provide a rational and efficient way to assess the probabilistic time-dependent performance of bridges, especially in large networks. The time-dependent Markov state probabilities show significantly different patterns (e.g., the probability of state R first increases and then decreases in time) for the five-state Markov model than those for conventional model (which make use of conditional failure probabilities) where probability of state R will increase throughout the lifetime.

2. The expected loss profiles show a pattern that first increases and then decreases, depending on the Markov chain state probabilities. This is basically due to the five-state Markov model which accounts for the failure and rehabilitation/reconstruction of each individual bridge.

3. The maximum total expected indirect loss is much higher than the lifetime maximum total expected direct loss for a highway bridge network. The difference between these risks may depend on the investigated time span as well as the size of the network (i.e., number of bridges).

4. The risk-based robustness index may provide a good measure for long investigation periods. However, this indicator may show fluctuations throughout the lifetime and is not a reliable measure for shorter time intervals.

5. The time-dependent expected loss and risk-based robustness index are sensitive to the time-dependent parameters of the Markov model.

The presented methodology relies on the availability of reliability data of each bridge within a network. Techniques for reliability assessment of individual bridge

233

structures are well established. However, predicting lifetime reliability profiles of all bridges within a large network is tedious and, sometimes, impossible. For this reason, methodologies based on statistical data of various types of bridges may offer a more practical way of risk assessment of very large networks. For instance, the condition rating systems based on visual inspection data can be used for predicting the performance of individual bridges. The purpose of obtaining lifetime profiles of expected loss and risk-based robustness is to use them in design and maintenance optimization of structures. Some objectives of such optimization problems can be the minimization of expected losses, the maximization of robustness, and the minimization of total life-cycle cost of a highway bridge network.

Table 7.1   Characteristics of nodes

Node	Longitude (°)	Latitude (°)	Daily Period 1		Daily Period 2		Daily Period 3	
			Trips Generated (cars/h)	Trips Attracted (cars/h)	Trips Generated (cars/h)	Trips Attracted (cars/h)	Trips Generated (cars/h)	Trips Attracted (cars/h)
1	-122.069	37.409	15000	15000	7500	7500	3750	3750
2	-121.927	37.374	8000	8000	4000	4000	2000	2000
3	-122.055	37.333	8000	8000	4000	4000	2000	2000
4	-121.891	37.324	20000	20000	10000	10000	5000	5000
5	-121.851	37.340	8000	8000	4000	4000	2000	2000
6	-121.858	37.256	8000	8000	4000	4000	2000	2000
7	-121.766	37.242	15000	15000	7500	7500	3750	3750

235

Table 7.2   Characteristics of the links in Figure 7.3

First Node	Second Node	Free Flow Time (min)	Practical Capacity (cars/h)
N1	N2	8.2	8000
N2	N1	8.2	8000
N1	N3	5.4	6000
N3	N1	5.4	6000
N2	N4	4.0	6000
N4	N2	4.0	6000
N2	N5	5.0	8000
N5	N2	5.0	8000
N3	N4	9.6	8000
N4	N3	9.6	8000
N3	N6	13.3	6000
N6	N3	13.3	6000
N4	N5	2.5	8000
N5	N4	2.5	8000
N4	N6	4.9	6000
N6	N4	4.9	6000
N5	N7	8.3	8000
N7	N5	8.3	8000
N6	N7	5.1	6000
N7	N6	5.1	6000

Table 7.3   Parameters associated with consequences of bridge failure

Bridge No	Direct Consequences (1000 \$)					Detour Length (km)	T_m (years)
	C_R	C_A	C_H	C_E	C_P		
B1	4703	3762	23516	2822	2822	3.00	73
B2	2714	2171	13569	1628	1628	6.00	84
B3	3814	3051	19070	2288	2288	2.00	75
B4	11974	9579	59871	7185	7185	5.00	90
B5	1927	1542	9634	1156	1156	2.00	79
B6	8842	7074	44211	5305	5305	4.00	81
B7	841	673	4206	505	505	3.00	77
B8	2301	1841	11504	1380	1380	6.00	88
B9	2245	1796	11223	1347	1347	2.00	92
B10	1063	851	5316	638	638	5.00	73
B11	1063	851	5316	638	638	2.00	83
B12	5187	4149	25933	3112	3112	4.00	77
B13	4093	3275	20466	2456	2456	3.00	88
B14	1954	1564	9772	1173	1173	6.00	84
B15	1954	1564	9772	1173	1173	2.00	81
B16	1954	1563	9768	1172	1172	5.00	73

237
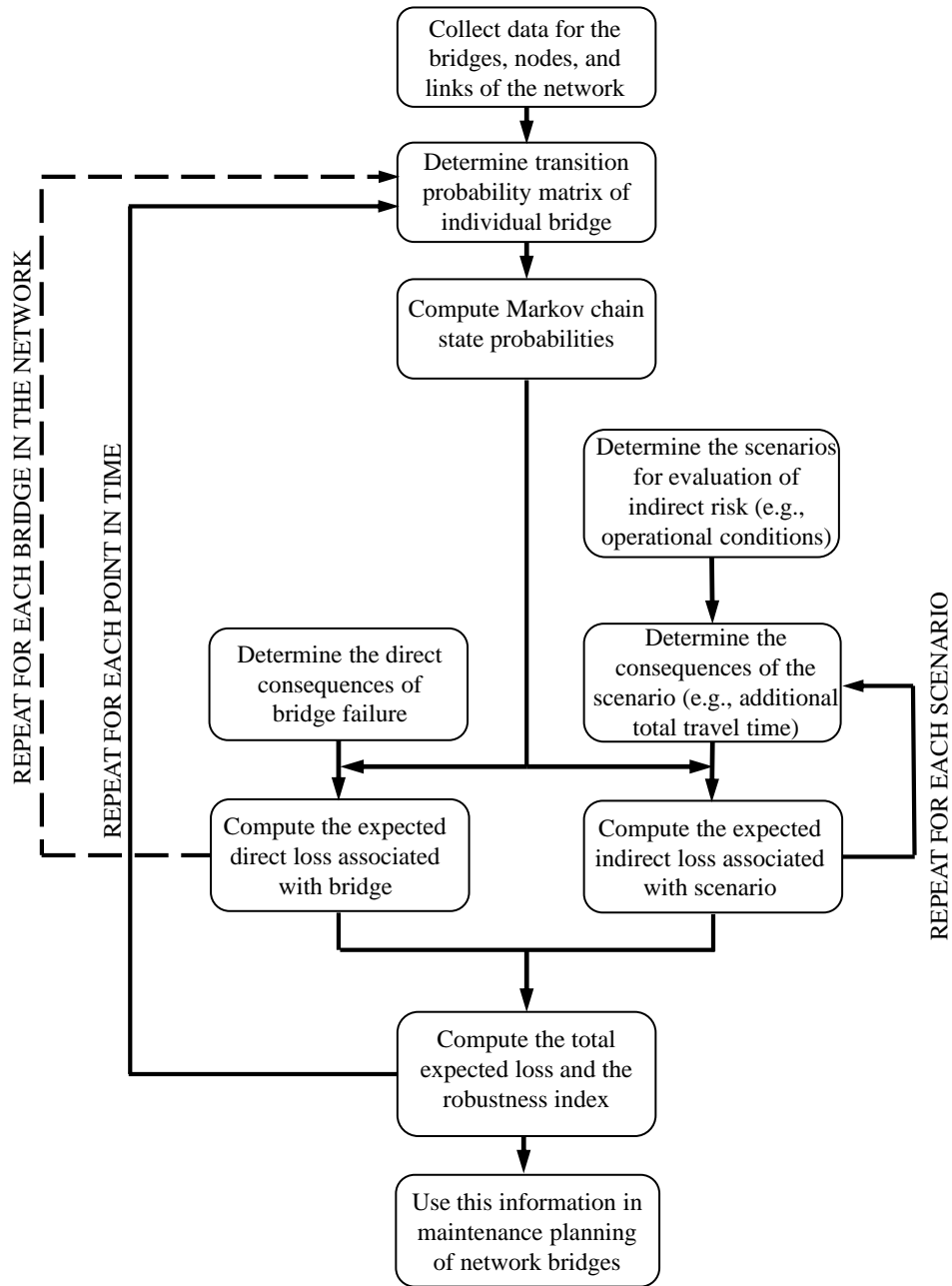
Figure 7.1   The methodology of assessing time-variant risk associated with bridge

networks
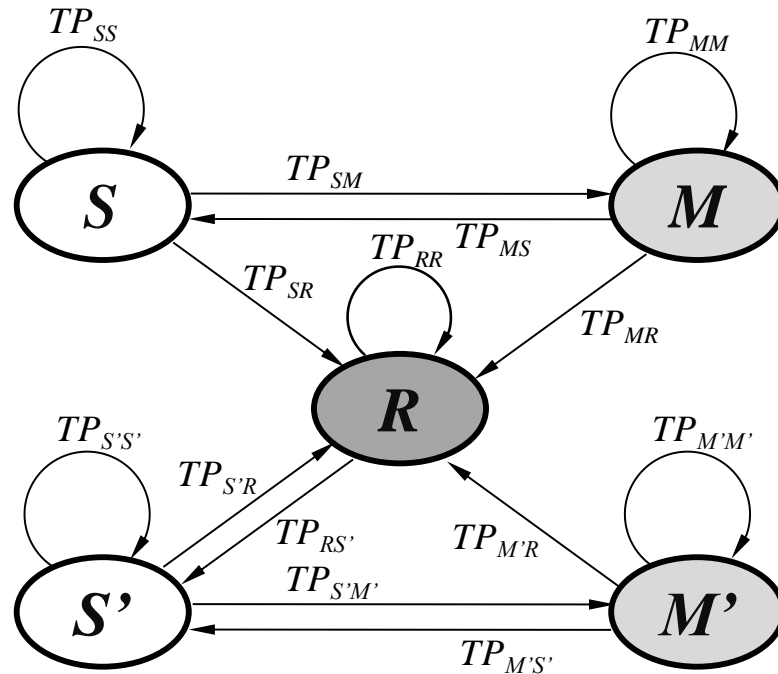
Figure 7.2　　　Five-state Markov chain model
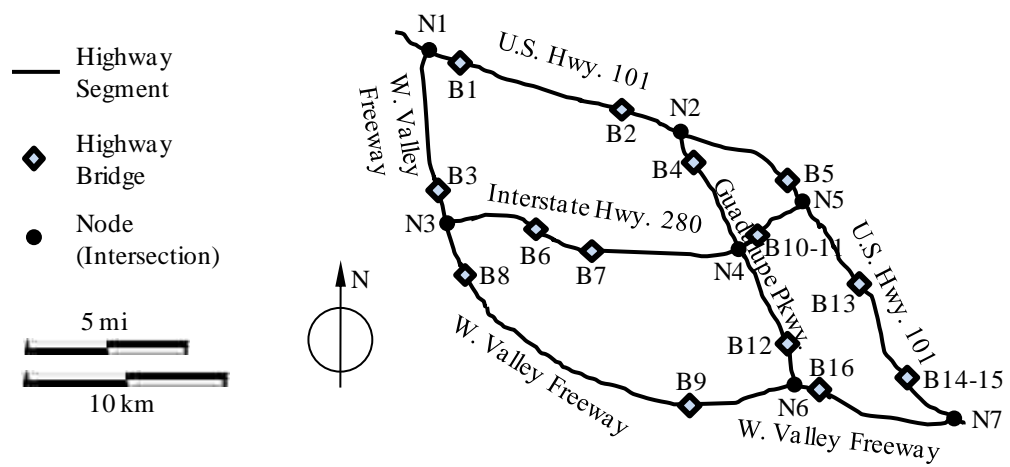
Figure 7.3   Layout of the network
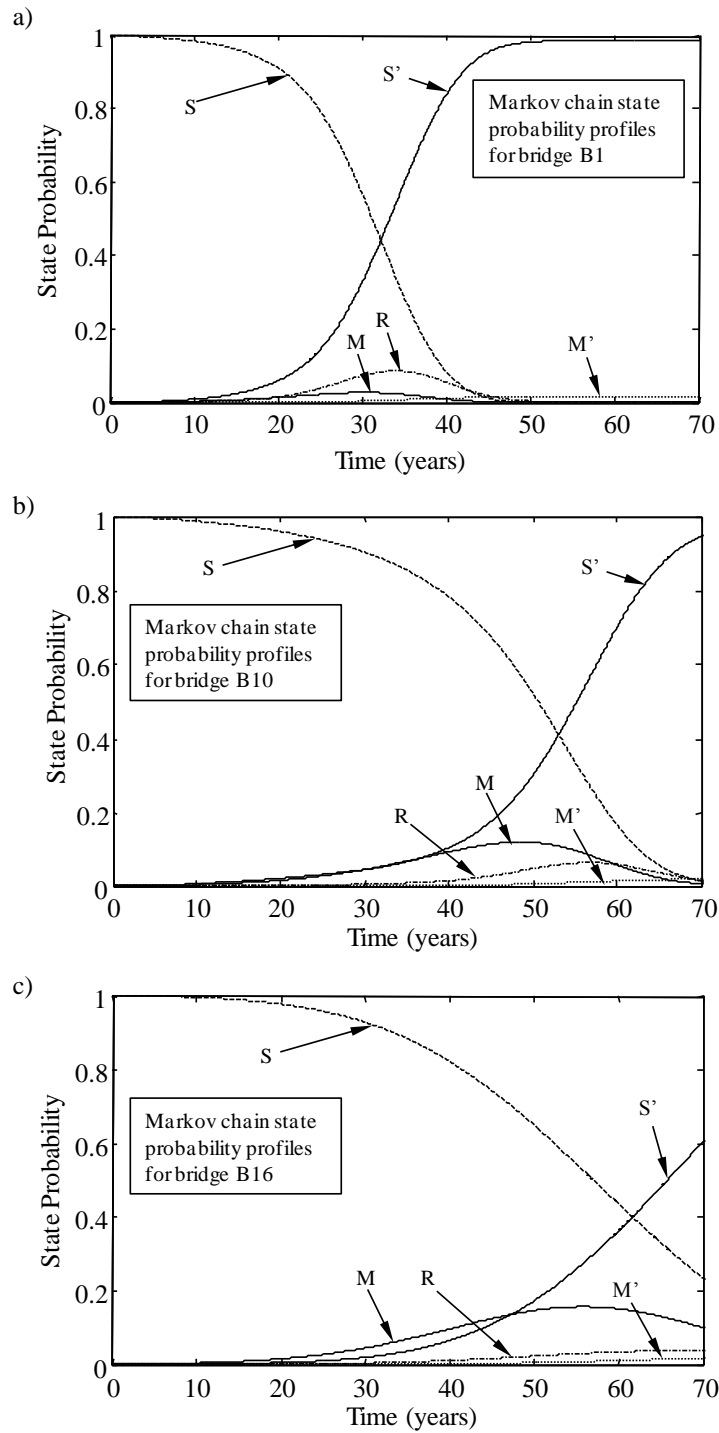
Figure 7.4   Time-dependent Markov Chain state probabilities for (a) bridge B1, (b)

bridge B10, and (c) bridge B16

a)

b)
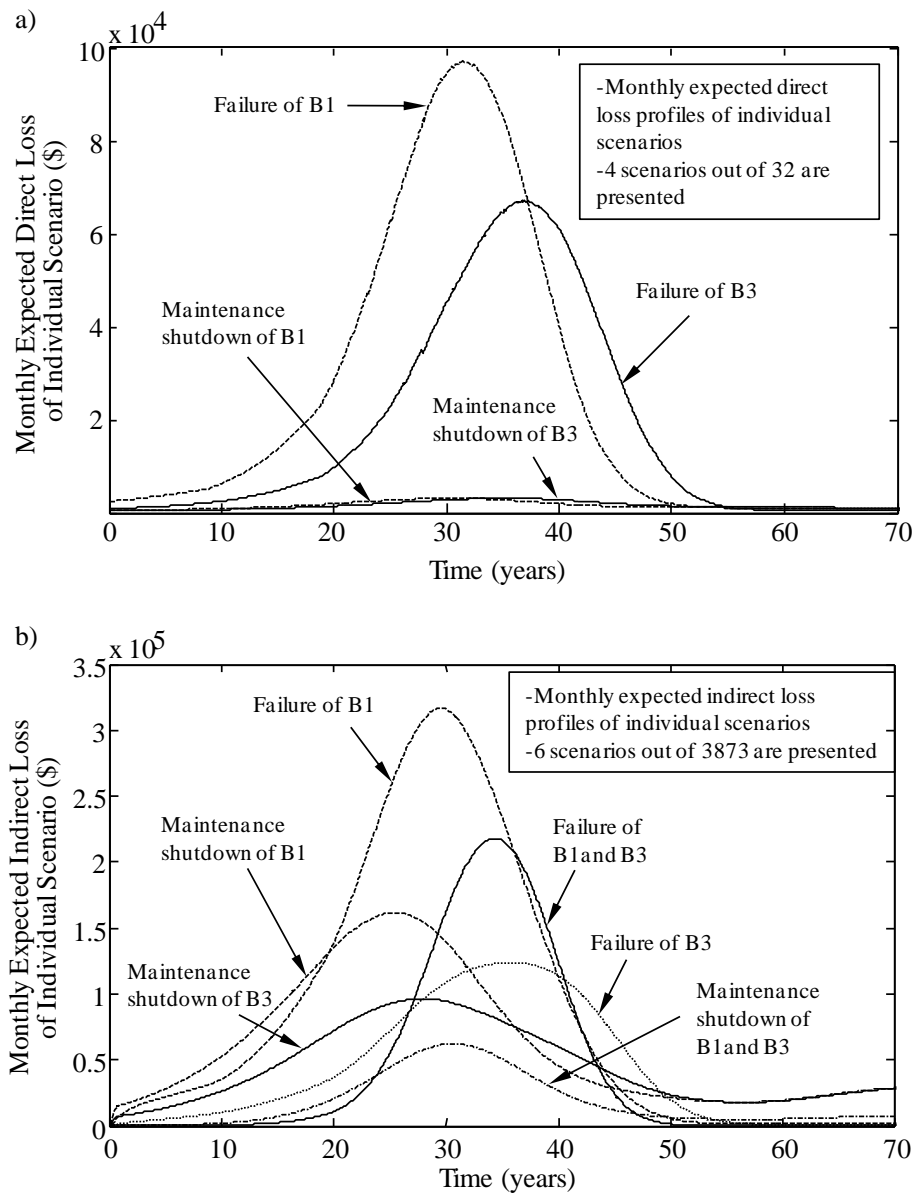
Figure 7.5   (a) Time-dependent monthly expected direct loss for individual scenarios, and (b) time-dependent monthly expected indirect loss for individual scenarios

242
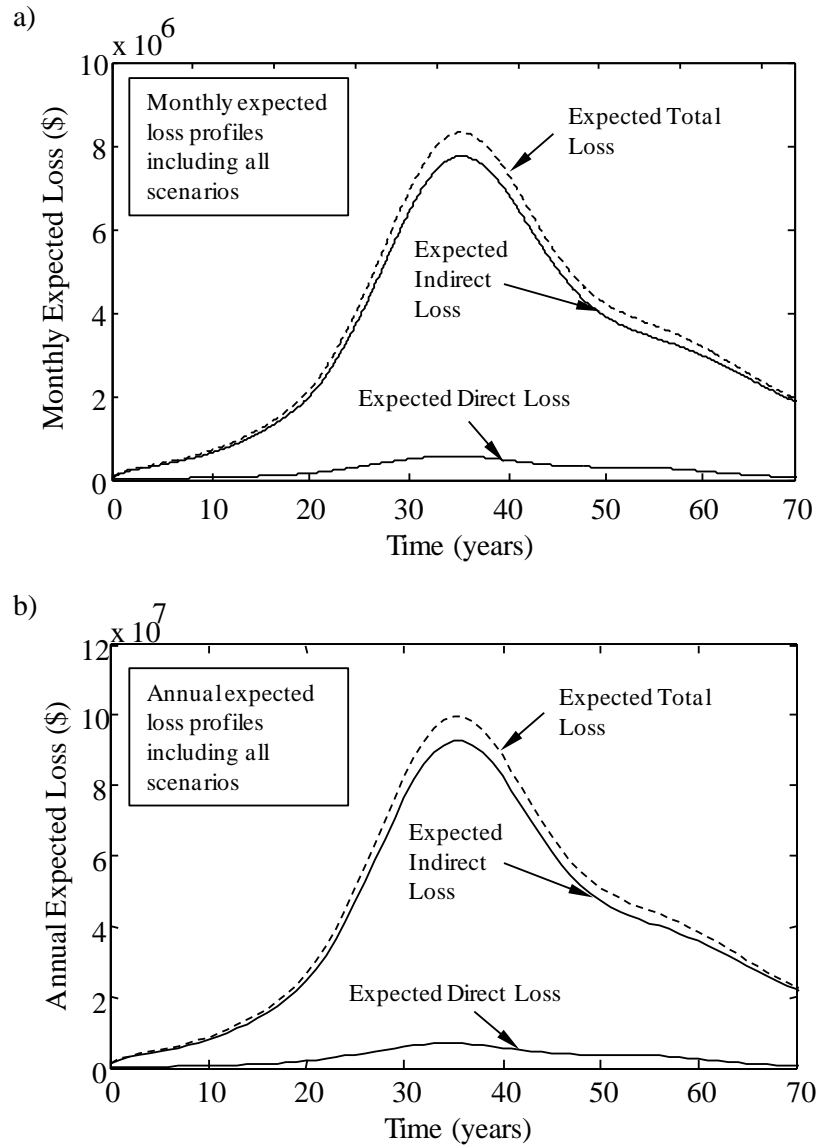
Figure 7.6   (a) Time-dependent monthly expected direct, indirect and total losses,

and (b) time-dependent annual expected direct, indirect and total losses

including all scenarios

243
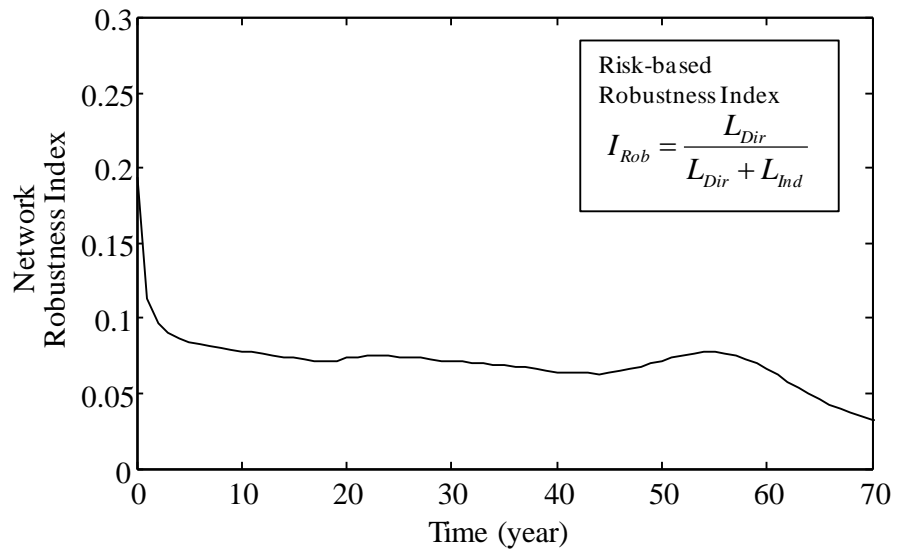
Figure 7.7   Time-dependent risk-based robustness index

The figure shows a plot with "Network Robustness Index" on the y-axis (ranging from 0 to 0.3) and "Time (year)" on the x-axis (ranging from 0 to 70). A box in the upper right contains:

Risk-based Robustness Index

$$I_{Rob} = \frac{L_{Dir}}{L_{Dir} + L_{Ind}}$$

CHAPTER 8

PERFORMANCE ASSESSMENT OF DAMAGED SHIP HULLS

8.1 INTRODUCTION

Safety evaluation of damaged ship hull structures is crucial for informed-decision making after an accident. Grounding and collision are the most common accidents resulting in destruction of ships (Khan and Das, 2008). Evaluation and prediction of ship performance involve uncertainties due to the randomness in the material properties, the deterioration processes under the aggressive environmental conditions, and the imperfections in our engineering models. Nevertheless, these uncertainties should be treated properly in order to assess the performance of damaged ships. Reducing risk associated with loss of ship due to a post-accident collapse or disintegration of the hull during tow or rescue operations is of vital importance.

Research on performance assessment of damaged ships has attracted significant interest in the last two decades. Vertical bending moment capacity at critical sections has been the major performance indicator investigated. Paik et al. (1998) studied the residual strength of hull structures based on section modulus and ultimate bending strength and proposed a method for investigating the hull girder failure following collision and grounding. Wang et al. (2002) provided a review of the state-of-the-art research on ship collision and grounding focusing on the definition of accident scenarios, evaluation approaches and acceptance criteria. Zhu, James, and Zhang (2002) studied the statistics of ship grounding incidents and presented damage extent distributions for certain types of ships. Wang, Spencer, and Chen (2002)

245

proposed an analytical expression for assessing the residual strength of hull girders with damage and provided simple equations correlating residual strength with damage extent. Fang and Das (2005) applied structural reliability concepts to ship structures. They used Monte Carlo Simulation to assess the failure probability of damaged ships for different grounding and collision damage scenarios and external load conditions. Hussein and Guedes Soares (2009) studied the residual strength and reliability of double hull tankers for different damage scenarios. Decò, Frangopol, and Okasha (2011) investigated the time-variant reliability and redundancy of ship structures. Lee at al. (2012) compared the wave-induced loads on intact ship and damaged ship by means of experimental tests and computational analyses. Decò, Frangopol, and Zhu (2012) proposed a framework for the assessment of structural safety of ships under different operational conditions by evaluating performance indicators such as reliability and redundancy.

The availability of information on the residual strength of a damaged hull structure can be very helpful for making decisions on how to proceed with the damaged ships after accidents. Moreover, the decision making process could be enhanced greatly when the information regarding the reliability of damaged ship hulls after grounding and collision is available. It is necessary to establish methods for reliability assessment of damaged ships for different operational conditions. For instance, the reliability information for different ship speeds, heading angles and sea states could provide guidance to avoid the ultimate failure of the damaged hull structures. In addition, the aging effects should be integrated in this approach.

246

In this chapter, a probabilistic framework for performance assessment of ship hulls under sudden damage accounting for different operational conditions is presented (Saydam and Frangopol 2013b). Grounding and collision accidents are considered as sudden damage scenarios. The combined effects of sudden damage and progressive deterioration due to corrosion are investigated. The reliability index and a probabilistic robustness index are selected as the performance indicators to account for the uncertainties. The longitudinal bending moment failure is considered as the limit state. The longitudinal bending moment capacity of the intact and damaged ship hulls is assessed using an optimization-based version of incremental curvature method. In order to investigate the ship performance under different operational conditions, the wave-induced loads for different ship speeds, headings and sea states are identified based on hydrodynamic analysis. The approach is illustrated on an oil tanker. Under different operational condition, the reliability index of intact and damaged ship hulls and the robustness index associated with various damage scenarios are presented in polar plots. In addition, aging effects on ship reliability are investigated.

8.2 GROUNDING AND COLLISION DAMAGE

Performance assessment of damaged ships includes identifying accident scenarios, estimating the probability of occurrence of different accidents, reliability analysis of the structure under the accident scenarios, and evaluating the consequences of structural damage and failure. This chapter primarily focuses on the reliability analysis under various damage scenarios associated with grounding and collision. The extent of the damage on the ship hull after grounding and collision accidents depends on several

247

parameters such as the speed at contact, contact angle, and mechanical properties of the structures in contact, among others. In this study, alternate load path approach is adopted, where several damage scenarios are considered regardless of the cause of the damage. In grounding and collision damage scenarios, it is assumed that the damaged part of the hull is unable to carry longitudinal stresses and is excluded from the ultimate bending moment computations.

Grounding with a forward speed on a rocky sea bed may result in considerable rupture of the bottom of the hull structure. The damage should be assumed to be located unfavorably anywhere on the flat bottom. ABS guidelines (1995) consider the damage to be within the fore part of the hull between 0.5 L and 0.2 L aft from forward perpendicular, where L is the length of the ship. The width of the damage is assumed to be the greater of 4 m or B/6 (i.e., one sixth of breadth B). According to ABS (1995), the damaged members are excluded from the hull girder section modulus calculation.

A collision with another ship on one side may result in extensive rupture of the side of the hull structure. ABS guidelines (1995) assume that the damage is in the most unfavorable location anywhere between 0.15 L aft from the forward perpendicular and 0.2 L forward from the aft perpendicular. The collision damage is assumed to be located at upper part of the side shell, down from the stringer plate of the strength deck. The shell plating for vertical extent of the greater of 4 m or D/4 (i.e., one fourth of the depth D) and the attached girders and side longitudinals are supposed to be excluded from the capacity analysis.

The damage levels indicated in the guidelines are moderate rather than extreme (Paik et al. 1998). The size of the damage considered is at least that defined in ABS

248

(1995). The effects of more severe damage scenarios are investigated. The damage scenarios and the size of the damage are described in the illustrative example.

8.3 METHODOLOGY FOR PERFORMANCE ASSESSMENT OF DAMAGED SHIP HULLS

The methodology for assessing the performance of damaged ship hull considering aging effects is illustrated in Figure 8.1. The first step of the methodology is identifying the failure mode to investigate. In general, longitudinal bending moment failure at the mid-section of the ship hull is considered as the limit state. The next steps can be basically categorized in two parts. These are the computations for resistance and loads. The random variables associated with the resistance must be identified. The hull capacity associated with this failure mode should be computed considering uncertainties for the intact and damaged (sudden damage) hull associated with the selected grounding and collision damage scenarios. One component of the load effects is due to the still water. The load effects produced by the still water can be subjected to change as the effect of sudden damage to the ship increases and the load distribution over the length changes. Still water load effects can be evaluated based on expressions given in codes or hydrostatic analysis. A proper probability distribution type and its parameters should be identified. Another component of the load effects is due to waves. Wave-induced load effects depend on the operational conditions (e.g., ship speed, heading, sea state). In order to compute the loads for different operational conditions, hydrodynamic analyses of the ship should be performed. The performance function including the hull capacity, still water load effects and wave-induced load

249

effects can be established at this stage. Using a software program capable of performing first order reliability method (FORM) or second order reliability method (SORM), the instantaneous reliability index associated with a sudden damage scenario, a operational condition, and at a point in time can be computed. In order to obtain, time-variation of the reliability the procedure should be repeated with time-variant values of hull capacity as it is reducing in time due to the effects of corrosion. The effects of different levels of still water loads on reliability can be investigated by repeating the procedure for different values of still water load effects. Furthermore, the procedure should be repeated for different operational conditions to obtain the reliability index with respect to speed, heading and sea state. The steps of the methodology are explained in details in the following sections.

8.4 RESISTANCE MODEL

A combination of vertical and horizontal bending moments is expected while the ship is in service. However, the horizontal moment is often very small and for practical purposes it may be appropriate to deal only with the vertical bending moment (Guedes Soares and Teixeira 2000). In fact, the maximum value of the vertical bending moment is the most important load effect in the analysis and design of ship structures (Hughes 1983). In this study, since the longitudinal bending failure mode is considered, the hull strength is expressed in terms of the longitudinal bending moment at the mid-section of the hull. The ultimate flexural capacity of the hull can be evaluated based on finite element analysis, incremental curvature method (IACS 2008) and progressive collapse method (Hughes 1983). However, computing hull strength

using these methods in a probabilistic manner can be time-inefficient. Okasha and Frangopol (2010b) proposed an efficient deterministic method for computation of the ship hull strength based on optimization. In this method, the ship hull cross-section is discretized into elements, each composed of a longitudinal stiffener and its attached plate. Stresses in the hull section are determined using the constitutive models of these elements. The constitutive models take into account the various possible failure modes of stiffened panels. Initial imperfections are also taken into account. For a given curvature, the bending moment of the section is determined in a way similar to that of the incremental curvature method. However, instead of finding the ultimate strength by incrementing the curvature, the ultimate strength is found by an optimization search algorithm. The curvature is treated as a design variable and the objective is to find the curvature that maximizes the bending moment. In order to find the moment capacity of the hull in a probabilistic manner, the sample space regarding the random variables should be created using a sampling method. Latin Hypercube Sampling is a technique allowing the reduction of the number of necessary samples to reach a certain level of confidence (McKay, Beckman, and Conover 1979). By combining these two steps, a probability distribution for the maximum moment capacity of the ship hull section can be obtained.

The problem of finding the maximum bending moment of a ship hull cross section is described by an unconstrained single objective nonlinear optimization problem as follows:

Given: Ship section dimensions and material properties

Find: κ

251

To Maximize: $|M(\kappa)|$

Such that: $\kappa > 0$ (for sagging)

$\kappa < 0$ (for hogging)

The curvature κ is the design variable and $M(\kappa)$ is the "implicit" objective function to maximize. The details of this method and its applications to ship structures can be found in Okasha and Frangopol (2010b), Decò, Frangopol, and Okasha (2011), and Decò, Frangopol, and Zhu (2012).

In many studies, incremental curvature method is used to method compute the ultimate strength of the damaged ship (Gordo and Guedes Soares, 1997; Fang and Das, 2004; Jia and Moan 2008; Khan and Das 2007). The damage is modeled by removing the damaged elements from the most critical section section and computing the ultimate strength of the damaged section. Guedes Soares et al. (2008) checked the adequacy of this approach by comparing the estimations in codes with the results of a finite-element analysis of a damaged ship hull.

8.4.1 Effects of Corrosion

The ultimate bending capacity of the ship hull decreases in time as the thickness of the plates and stiffeners reduce in time due to corrosion. The corrosion model used to estimate the time-variant thickness loss of components of the hull is (Paik. et al. 1998, Akpan et al. 2002)

$$r(t) = C_1 (t - t_0)^{C_2} \tag{8.1}$$

252

where $r(t)$ is the thickness loss in mm, t_0 is the corrosion initiation time based on coating life in years, C_1 is the annual corrosion rate in mm/year, C_2 is a coefficient that ranges from 1/3 to 1 in general, and t indicates the time in years. In reality, t_0, C_1, and C_2 are random variables.

8.5 LOAD MODEL

Reliability assessment of ships under different operational conditions requires probabilistic characterization of the loads. The hull is subjected to still water bending moment and wave-induced bending moment.

8.5.1 Still Water Bending Moment

According to IACS common rules (2008), the minimum hull girder bending moment in sagging ($M_{sw,sag}$) and hogging ($M_{sw,hog}$) for seagoing operations in the intact case should be computed as

$$M_{sw,sag} = 0.05185 \cdot C_{wv} \cdot L^2 \cdot B \cdot (C_b + 0.7) \tag{8.2}$$

$$M_{sw,hog} = 0.01 \cdot C_{wv} \cdot L^2 \cdot B \cdot (11.97 - 1.9 \cdot C_b) \tag{8.3}$$

where C_b is the ship block coefficient, L is the ship length (m), B is the ship breadth (m), and C_{wv} is a wave coefficient calculated as (IACS 2008)

$$C_{wv} = \begin{cases} 10.75 - \left(\dfrac{300 - L}{100} \right)^{\frac{3}{2}} & \text{for } 150 \leq L \leq 300 \\ 10.75 & \text{for } 300 < L \leq 350 \\ 10.75 - \left(\dfrac{L - 350}{150} \right)^{\frac{3}{2}} & \text{for } 350 < L \leq 500 \end{cases} \tag{8.4}$$

253

Still water load effects are subjected to change in time due to the variations in the distribution of the cargo on the ship. Guedes Soares and Moan (1988) identified that the vertical still water bending moments at the mid-ship can be described by a normal distribution. According to Hussein and Guedes Soares (2008), the maximum still water bending moment can be taken as 90% of the rule value. Hørte, Wang, and White (2007) and Hussein and Guedes Soares (2009) considered the still water bending moment following normal distribution with mean value of 70% of the rule value (IACS 2008) and standard deviation of 20% of the rule value. In this study, these values are adopted.

8.5.2 Wave-Induced Bending Moment

The internal forces within a hull structure due to sea waves can be evaluated based on linear response theory. In this theory, the wave spectrum for a wide range of wave configurations can be obtained through the linear superposition of single waves. Wave-induced vertical bending moments vary for different ship operation conditions. The operational conditions are represented by a set of parameters including ship speed, heading, and sea state. Detailed information on the general approach to be followed in order to obtain a comprehensive set of structural response based on linear theory can be found in Decò, Frangopol, and Zhu (2012).

The response of ship structures due to natural sea waves depends on hydrodynamics. In general, hydrodynamic analysis is highly complex and time consuming. Hydrodynamic analysis of ship structures can be performed using strip method (Korvin-Kroukowski and Jacobs 1957). Strip method introduces some

254

simplifications such that the ship hull is divided into prismatic segments. The interaction between the adjacent segments is ignored and the hydrodynamic forces due to harmonic waves are evaluated within the individual segments. The hydrodynamic forces within the segments are integrated to obtain the global load effects. More information on strip theory and it its applications can be found in Faltinsen (1990), Hughes (1983), and Decò, Frangopol, and Zhu (2012).

In hydrodynamic analysis of ships, Response Amplitude Operators (RAOs) are very useful for linear systems. In this section, brief information on obtaining a proper probability distribution for vertical bending moment based on RAO is provided. For a linear system, if both the input $X(t)$ and the output $Y(t)$ of the system are expressed by spectral density functions, their relation associated with the transfer function $\Phi(\omega)$ is

$$S_Y(\omega) = |\Phi(\omega)|^2 \cdot S_X(\omega) \tag{8.5}$$

where $S_Y(\omega)$ and $S_X(\omega)$ are the spectral density functions of the output and input, respectively; and ω is the circular frequency (rad/s).

In linear theory, RAOs are defined as the ratio between the amplitude of the harmonic function of the response and the amplitude of the wave elevation. In other words, RAOs are the ship responses obtained by imposing unitary amplitude to the exciting regular waves. A practical way to find the RAOs is the analysis of structural responses due to different waves with unitary amplitude by varying their lengths.

The loads on ship hulls for different operational conditions are computed based on the encounter frequency. This frequency depends on the frequency of the sea waves, the speed of the ship and the heading angle. Consequently, RAOs also depend on these parameters. The encounter frequency $\omega_{e,U,H}$ is expressed as (ABS 2010)

255

www.manaraa.com

$$\omega_{e,U,H} = \left| \omega - U \cdot \frac{\omega^2}{g} \cdot \cos(H) \right| \qquad (8.6)$$

where ω is the circular frequency of the sea waves, g is the gravitational acceleration (m/s^2), U is the forward ship speed (m/s), and H is the heading angle considering 0º, 90º, 180º for following, beam, and head seas, respectively.

The wave-induced load effects exhibit high uncertainty due to the irregularities of the ocean surface. A modified version of the Pierson–Moskowitz sea spectrum is used as the spectrum for fully developed sea. This spectrum is expressed as (Faltinsen 1990)

$$S_{w,SS}(\omega) = \frac{0.11 \cdot H_{1/3}^2 \cdot T_1}{2\pi} \cdot \left(\frac{\omega \cdot T_1}{2\pi} \right)^{-5} \cdot \exp\left[-0.44 \cdot \left(\frac{\omega \cdot T_1}{2\pi} \right)^{-4} \right] \qquad (8.7)$$

where $S_{w,SS}(\omega)$ is the sea spectrum for a given sea state SS, T_1 is the mean period of wave (s), and $H_{1/3}$ is the significant wave height which is the mean of the one third highest waves (m).

RAOs can be obtained by using a software program that performs linear analysis. Among others, PDSTRIP (PDSTRIP 2006) is a freeware that was developed to compute the response of floating bodies according to strip method. The wave-induced vertical bending moment corresponding to different operational conditions can be computed if the RAO curves are obtained. The relation between the response spectrum and the sea spectrum is (Hughes 1983)

$$S_{M,SS,U,H}(\omega) = \left| \Phi(\omega_{e,U,H}) \right|^2 \cdot S_{w,SS}(\omega_{e,U,H}) \qquad (8.8)$$

256

The structural response quantity under interest considering different operational conditions can be represented by Rayleigh distribution with the following probability distribution function (Hughes 1983)

$$f(M_{w,SS,U,H}) = \frac{M_{w,SS,U,H}}{m_{0,SS,U,H}} \cdot \exp\left[-\frac{\left(M_{w,SS,U,H}\right)^2}{2m_{0,SS,U,H}}\right] \tag{8.9}$$

where $M_{w,SS,U,H}$ is wave-induced vertical bending moment and $m_{0,SS,U,H}$ is the zero-th moment of the wave spectrum. The parameter α of the distribution is

$$\alpha(M_{w,SS,U,H}) = \sqrt{m_{0,SS,U,H}} \tag{8.10}$$

The mean value $\mu(M_{w,SS,U,H})$ and the standard deviation $\sigma(M_{w,SS,U,H})$ are

$$\mu(M_{w,SS,U,H}) = \sqrt{\frac{\pi}{2}} \cdot \alpha(M_{w,SS,U,H}) \tag{8.11}$$

$$\sigma(M_{w,SS,U,H}) = \sqrt{\frac{4-\pi}{2}} \cdot \alpha(M_{w,SS,U,H}) \tag{8.12}$$

The parameters used in Equations 8.7 to 8.12 vary for different cross-sections of a ship structure. Since the response quantity under interest is the vertical bending moment amidship, these parameters are considered for the mid-section of the ship through the entire chapter.

8.6 LIMIT STATES AND RELIABILITY ANALYSIS

In this study, the safety evaluation of intact and damaged hull structures is based on reliability theory. The limit state under concern is associated with the flexural failure of the hull girder at mid-section, where the overall vertical bending moment is expected to be maximum over the length. In this illustrative example, the most critical

257

load effect is the vertical bending moment. However, it should be noted that horizontal bending moment can be more critical in some cases where the reduction in the horizontal hull strength is very significant. The limit state equations are time-variant since the resistance is affected by the corrosion in time. The time-variant limit state equations associated with the flexural failure of amidship for different operational conditions in sagging and hogging, respectively, are expressed as

$$g_{sag,SS,U,H}(t) = x_R \cdot MC_{sag}(t) - x_{sw} \cdot M_{sw,sag} - x_w \cdot M_{w,SS,U,H} = 0 \qquad (8.13)$$

$$g_{hog,SS,U,H}(t) = x_R \cdot MC_{hog}(t) - x_{sw} \cdot M_{sw,hog} - x_w \cdot M_{w,SS,U,H} = 0 \qquad (8.14)$$

where $MC_{sag}(t)$ and $MC_{hog}(t)$ are the random variables associated with the time-variant vertical bending moment capacity of the mid-section of the ship in sagging and hogging, respectively; $M_{sw,sag}$ and $M_{sw,hog}$ are the random variables associated with the still water bending moments amidship in sagging and hogging, respectively; $M_{w,SS,U,H}$ is the random variable associated with wave-induced bending moment amidship reflecting the effects of different operational conditions; x_R, x_{sw}, and x_w are the random model uncertainties associated with the resistance, still water bending moment, and wave-induced bending moment, respectively. In fact, $MC_{sag}(t)$ and $MC_{hog}(t)$ depend on other random variables associated with resistance (e.g., yield stress of steel, corrosion parameters). Appropriate probability distributions for $MC_{sag}(t)$ and $MC_{hog}(t)$ can be obtained combining hull strength formulations and sampling techniques. The elastic modulus E, the deck and keel yielding stress σ_{Yp}, and the side panels yielding stress σ_{Ys} are considered as random variables associated with hull load carrying capacity. Latin-Hypercube Technique is used to generate the samples of these random variables. Obtaining probability distribution parameters for $M_{sw,sag}$, $M_{sw,hog}$, and $M_{w,SS,U,H}$ is

258

explained in the previous section. Once the random variables and their probability distribution parameters are identified, the probability of hull failure and the associated reliability index can be computed based on the limit states in Equations 8.13 and 8.14 using FORM, SORM or simulation methods (e.g., Monte Carlo Simulation). The same limit state equation is used for both intact and damaged cases in this study. The effects of the damage are reflected by the resistance terms ($MC_{sag}(t)$ and $MC_{hog}(t)$) in the limit state equations (Equations 8.13 and 8.14). The random model uncertainties (x_R, x_{sw}, and x_w) can be updated so that the additional uncertainties due to the damage are also considred.

8.7 OTHER PERFORMANCE INDICATORS INVESTIGATED

In addition to the reliability index, several performance indicators are investigated. The residual strength factor provides a measure for the strength of the system in a damaged condition compared to the intact system. It is defined as the ratio of the capacity of the damaged structure or element to the capacity of the intact structure (Frangopol and Curley, 1987). The residual strength factor for each damage scenario i is formulated as

$$RSF_i = \frac{\mathrm{E}(MC_i)}{\mathrm{E}(MC_0)} \tag{8.15}$$

where $\mathrm{E}(MC_i)$ and $\mathrm{E}(MC_0)$ are the mean values of the vertical bending moment capacity of the damaged and intact hull, respectively. Residual strength factor takes values between 0, when damaged structure has zero capacity, and 1.0, when damaged structure does not have any reduction in load-carrying capacity.

259

Another performance indicator investigated is used to quantify the robustness of the ship hull in a probabilistic manner. A measure of robustness is formulated as

$$RI_i = \frac{\beta_i}{\beta_0} \tag{8.16}$$

where RI_i is the robustness index for associated with damage scenario i, and β_i and β_0 are the reliability indices associated with the damaged and intact hull, respectively.

8.8 ILLUSTRATIVE EXAMPLE 1

The proposed methodology is illustrated on a hull structure which was analyzed by Akpan et al. (2002). The length of the ship L is 220 m, breadth B is 38.1 m, height H is 17.4 m, block coefficient C_b is 0.75, the elastic modulus E is 208 MPa, the deck and keel yielding stress σ_{Yp} is 315 MPa, and the side panels yielding stress σ_{Ys} is 281 MPa. The cross-section of the mid-ship and its six type of stiffeners denoted as 1, 2, 3, 4, 5, and 6 are shown in Figure 8.2. The stiffener dimensions are presented in Table 8.1.

8.8.1 Sudden Damage Scenarios

In order to investigate the residual strength and performance of the damaged hull, six sudden damaged scenarios are considered. The first three are grounding damage scenarios. In these scenarios, a part of the bottom of the hull is assumed to be damaged with an extent proportional to the ship breadth B. The considered damage extents are $B/6$, $B/3$, and $B/2$, the smallest one being the damage extent suggested by ABS (1995). The center of the damaged part is assumed to coincide with the symmetry line of the hull section. The three grounding damage scenarios are illustrated in Figure 8.3(a), (b),

and (c). The remaining three are collision damage scenarios (Figure 8.3(d), (e), and (f)). In these scenarios, a part of the side hull is assumed to be damaged with an extent proportional to the depth of the ship (*D*). The considered damage extents are *D*/4, *D*/3, and *D*/2, the smallest one being the damage extend suggested by ABS (1995). The damage is assumed to start from the top of the side hull and extent downwards.

8.8.2 Resistance

The hull flexural strength is evaluated based on the method by Okasha and Frangopol (2010b) described previously. In order to account for the uncertainty, the elastic modulus *E*, the deck and keel yielding stress σ_{Yp}, and the side panels yielding stress σ_{Ys} are considered to follow lognormal distribution with mean values 208 MPa, 315MPa, and 281 Mpa, respectively. The coefficients of variation of these random variables are assumed 0.03, 0.1, and 0.1, respectively (Paik and Frieze 2001). Latin-Hypercube Technique with 5000 samples is used to compute the moment capacity of the mid-section of the ship in a probabilistic manner. The generated samples of flexural capacities are fitted to a log-normal distribution, which is found to be the best fit according to the results of goodness of fit test, in order to obtain the appropriate probability parameters of the hull strength. This procedure is repeated for all sudden damage scenarios and all points in time as the hull strength deteriorates. The investigated time span of the ship service life is 30 years. The flexural hull strength for the damaged hull is computed by completely removing the damaged part of the ship from the resistance model. The variation of the hull strength in time is evaluated based on Equation 8.1. Corrosion initiation time t_0 is assumed to have log-normal

261

distribution with mean of 5 years and coefficient of variation of 0.40. The coefficient C_2 is taken as a constant equal to unity. The probability distribution of annual corrosion rate C_1 for different locations on the hull (Akpan et al. 2002) is considered as lognormal distribution with mean value 0.03 and coefficient of variation 0.1 for side shell plating and side stiffener web; mean value 0.065 and coefficient of variation 0.5 for deck plating, deck stiffener web, and bottom stiffener web; and mean value 0.17 and coefficient of variation 0.5 for bottom shell plating. The mean vertical bending moment capacity of the hull with respect to ship age for different sudden damage scenarios and the hull with no sudden damage is presented in Figure 8.4(a) and (b) for sagging and hogging, respectively. The strength of the hull in hogging is slightly higher than that in sagging. Among the damaged scenarios, the last two grounding damage scenarios DS 2 and DS 3 result in the largest reduction in the ship hull. The first collision damage scenario DS 4 has almost no effect on the vertical bending moment capacity of the structure. In Figure 8.4(a), Curve A represents the mean vertical bending moment capacity profile for sagging if sudden damage scenario DS 3 occurs at $t = 10$ years and no repair action is taken afterwards. The sudden drop at $t = 10$ years is the result of the sudden damage and the progressive reduction is due to corrosion. Similarly, Curve B represents the mean vertical bending moment capacity profile for sagging if sudden damage scenario DS 6 occurs at $t = 15$ years. In Figure 8.4(b), Curve C represents the mean vertical bending moment capacity profile for hogging if sudden damage scenario DS 2 occurs at $t = 25$ years.

8.8.3 Residual Strength Factor

www.manaraa.com

Residual strength factors for the sudden damage scenarios are computed based on Equation 8.15. These factors indicate the remaining percentage of the bending moment capacity. The time-variation of residual strength factors for different sudden damage scenarios is presented in Figure 8.5(a) and (b) for sagging and hogging, respectively. DS 4 and DS 1 yield the highest residual strength factors in sagging while DS 4 and DS 5 yield the highest residual strength factors in hogging. The lowest residual strength factors belong to DS 3 and DS 2 both in sagging and hogging. These factors are decreasing in time due to the effects of corrosion. For instance, the initial residual strength factor for DS 3 in hogging is 0.75. At the end of 30 years of service, it is reduced to 0.68. This indicates that if DS 3 occurs when ship is 30 years old, additional 0.07 decrease in the bending moment capacity due to effects of deterioration has to be considered.

8.8.4 Load Effects

The loads due to still water can vary for missions. The loading manual of the investigated ship is not available to the authors. Therefore, the vertical bending moment induced by still water is evaluated based on Equations 8.2 to 8.4 (IACS 2008). As described previously, the still water bending moment is considered to follow normal distribution with mean value of 70% of the rule value and standard deviation of 20% of the rule value (Hussein and Guedes Soares 2009).

The hydrodynamic analyses are performed using the software PDSTRIP (PDSTRIP 2006) that adopts strip theory for computation of hydrodynamic forces under different operational conditions. The 3-D geometrical model of the ship,

263

illustrated in Figure 8.6, is obtained by the program FREE!ship (FREE!ship 2001). RAOs for different values of ship speed and heading angles are obtained through the software PDSTRIP (PDSTRIP 2006). The effects of damage on RAOs are ignored in this illustrative example. Then, the probability distribution (Rayleigh distribution) parameters associated with the wave-induced bending moment for a certain operational condition including different ship speeds, heading angles, and sea states are evaluated based on Equations 8.5 to 8.12. The reliability of the hull associated with these cases will be discussed in the following section.

8.8.5 Reliability

The reliability of the intact and damaged ship hull is evaluated in time for various operational conditions. The following ship speeds are considered: 0 knots, 10 knots, and 20 knots. Ship structural performance is evaluated for different ship headings. Angles between 0° (following sea) and 180° (head sea) by increments of 15° are considered. Wind sea accounting for sea states 5, 6, and 7 (SS 5, SS 6, and SS 7) described by statistical properties according to Table 8.2 is included in the analysis. An effective way of representing performance of ships for different operational conditions is using polar plots. A polar plot has an angular coordinate axis representing the variation of heading angle, and the radial coordinate axis representing the performance indicator. In this chapter, the variation of reliability and robustness indices for different operational conditions are presented in polar plots with one half of the plot is associated with performance in sagging and the other half is associated with

264

performance in hogging. Qualitative representation of ship performance in both hogging and sagging is illustrated in Figure 8.7.

The reliability analyses are conducted based on FORM and the limit states defined in Equations 8.13 and 8.14 using reliability software RELSYS (Estes and Frangopol 1998). In Figure 8.8(a), the variation of the reliability index β with respect to heading angle for sudden damage scenarios DS 1, DS 2, and DS 3 with constant sea state 5, ship speed $U = 10$ knots, and time $t = 0$ is presented. At $t = 0$, the structure is intact of corrosion (there is no section loss in structural members), however, the effects of accidental scenarios are illustrated for this initial time instant. The lowest reliability index with respect to heading angle is obtained at 180° and the highest one is obtained at 90°. The reliability indices in hogging are less than those in sagging. DS 1 causes a very slight reduction in reliability index while DS 2 and DS 3 reduce the reliability index, by around 0.5 and 0.6, respectively.

In Figure 8.8(b), the variation of the reliability index with respect to heading angle for sudden damage scenarios DS 4, DS 5, and DS 6 with constant sea state 5, ship speed $U = 10$ knots, and time $t = 0$ is presented. The lowest reliability index with respect to heading angle is obtained at 180° and the highest at 90°. The reliability indices in hogging are less than those in sagging. DS 4 does not cause a reduction in reliability index at all; however, DS 5 and DS 6 reduce the reliability index by around 0.2 and 0.4, respectively. These results indicate that the contribution of the bottom shell to the bending reliability is very significant.

The effect of sea state on reliability index is also investigated. In Figures 9(a) and (b), the variation of the reliability index with respect to heading angle and sea

265

state for DS 1 and DS 6, respectively, with constant ship speed $U = 10$ knots and time $t = 0$ is presented. The reliability indices for all three sea states are almost identical at 90° where the reliability is maximum. In these figures, the difference between the reliability indices associated with SS 5 and SS 6 is not significant between the angles 0° and 105° in general. However, as the heading angle approaches 180°, the reliability decreases very significantly for SS 6 and SS 7. The lightest grounding damage scenario considered (DS 1) yields very slightly higher reliability index compared to the most severe collusion scenario (DS 6). Similar to the previous results, hogging is associated with lower reliability than sagging.

The effect of ship speed on reliability is also investigated. In Figures 10(a) and (b), the variation of the reliability index with respect to heading angle and ship speed for DS 3 and DS 5, respectively, with constant sea state 5, and time $t = 0$ is presented. These figures indicate that the reliability index reduces significantly as the ship moves with higher speed at 180°. Ship speed is one main condition that is manageable for the transportation of damaged ships to avoid ultimate breakdown.

The results explained above do not consider the effects of flooding after sudden damage. Hussein and Goades Soares (2009) showed that the still water bending moment is increased with flooding. The effect of flooding is investigated by increasing the still water bending moment by 25% and 50%. In Figure 8.11(a), the variation of the reliability index with respect to the heading angle and still water bending moment for DS 2 under constant sea state 5, ship speed $U = 0$ knots, and time $t = 0$ is presented. Increase in still water bending moment reduces the reliability significantly. At 0° heading angle, 25% increase in still water bending moment

266

reduces the reliability index by 0.9 while 50% increase in still water bending moment reduces the reliability index by 1.5. In Figure 8.11(b), the variation of the reliability index with respect to the heading angle and time for DS 4 with constant sea state 5 and ship speed $U = 0$ knots is presented. The results indicate that the corrosion causes significant reduction in safety in long term if proper maintenance actions are not taken.

8.8.6 Robustness Index

The robustness for the sudden damage scenarios is evaluated based on Equation 8.16. In the cases mentioned below, β_0 is taken as the highest reliability index of the hull with no sudden damage with respect to heading angle. In Figure 8.12(a), the variation of the robustness index with respect to heading angle for sudden damage scenarios DS 1, DS 2, and DS 3 with constant sea state 5, ship speed $U = 10$ knots, and time $t = 0$ is presented. The lowest robustness index with respect to heading angle is obtained at 180° and the highest one is obtained at 90°. The robustness indices in hogging are less than those in sagging. DS 3 yields the lowest robustness index, which means that is it is the most severe scenario. In Figure 8.12(b), the variation of the robustness index with respect to the heading angle and time for DS 4 with constant sea state 5 and ship speed $U = 0$ knots is presented.

In Figure 8.13(a), the variation of the reliability index with respect to heading angle for sudden damage scenarios DS 1, DS 2, and DS 3 with constant sea state 6, ship speed $U = 10$ knots, time $t = 0$ is presented. In Figure 8.13(b), the variation of the reliability index with respect to the heading angle and time for DS 4 with constant sea

267

state 7 and ship speed $U = 0$ knots is presented. Finally, Figure 8.13(c) uses Cartesian plots to present the variation of the robustness index with respect to the heading angle and time for DS 4 with constant sea state 5 and ship speed $U = 0$ knots. It is important to note that the results obtained in this example have value only for this specific ship under the considered operational conditions.

8.9 ILLUSTRATIVE EXAMPLE 2

The aim of this example is to investigate the time-variation of several deterministic and probabilistic performance indicators using the same ship in Illustrative Example 1. In this example, wave-induced bending moment is based on the method used by Akpan et al. (2002). This method benefits the seakeeping tables pre-computed based on parametric ship motion studies considering the variation in ship size, operating speed, significant wave height, and block coefficient.

The deterministic performance indicators evaluated include reserve strength factor and residual strength factor, which are based on mean vertical bending moment capacity of the midsection. The mean vertical bending moment capacity of the hull with respect to ship age for different sudden damage scenarios and the hull with no sudden damage is presented in Figure 8.14(a) and (b) for sagging and hogging, respectively. The strength of the hull in hogging is slightly higher than that in sagging. The grounding damage scenarios S 2 and S 3 result in the largest reduction in the ship hull. The damage scenario S 4 has almost no effect on the vertical bending moment capacity of the structure. The variation of reserve strength ratio with respect to ship age for different sudden damage scenarios is presented in Figure 8.14(c) and (d) for

268

sagging and hogging, respectively. In the computation of these curves, the applied load is assumed to be the sum of the mean values of still water bending moment and wave induced bending moment. In Figure 8.14(e) and (f), the variation of residual strength ratio with respect to ship age for different sudden damage scenarios is presented for sagging and hogging, respectively. Both reserve strength factor and residual strength factor decrease in time significantly due to the effects of corrosion for each damage scenario. S 4 and S 1 result in the highest residual strength factors in sagging while S 4 and S 5 yield the highest residual strength factors in hogging.

The probabilistic performance indicators evaluated include probability of failure, vulnerability, and redundancy index. The variation of probability of failure with respect to ship age for different sudden damage scenarios is presented in Figure 8.15(a) and (b) for sagging and hogging, respectively. The probability of failure of the midsection for each damage scenario is increasing significantly in time due to deterioration. The vulnerability with respect to ship age for different sudden damage scenarios is presented in Figure 8.15(c) and (d) for sagging and hogging, respectively. The vulnerability of the midsection for each damage scenario is also increasing significantly in time due to deterioration. The redundancy index with respect to ship age for different sudden damage scenarios is presented in Figure 8.15(e) and (f) for sagging and hogging, respectively. The redundancy index of the midsection for each damage scenario is decreasing significantly in time due to deterioration.

8.10 CONCLUSIONS

269

In this chapter, a framework for performance assessment of damaged ship hulls under different operational conditions considering grounding and collision accidents as sudden damage is proposed. The combined effects of sudden damage and aging on ship performance are investigated. The performance of ship hull is quantified in terms of several performance indicators. The longitudinal bending moment failure is considered as the limit state. The longitudinal bending moment capacities of the intact and damaged ship hulls are assessed based on an optimization-based version of incremental curvature method. The wave-induced loads for different ship speeds, headings and sea states are identified based on hydrodynamic analysis and the performance under different operational conditions is investigated. The approach is illustrated on an oil tanker.

The following conclusions can be drawn.

1. After accidents, ultimate failure of ships may occur depending on the extent of the damage. The outlined methodology can be very helpful in decision making on how to deal with damaged ship by providing information on the reliability of the damaged ship under different operational conditions. The methodology can be used to investigate the effects of ship damage scenarios occurring at different points in the service life.

2. Residual strength factor can be used time effectively to quantify the loss of hull strength under different scenarios and comparison. The results show that corrosion can have significant impact on the residual strength of ships. Time effects should be included in the reliability, redundancy, and robustness of aging ships.

270

3. The performance of damaged ships can be evaluated in a probabilistic manner. The results indicate that operational conditions have very significant effects on reliability. Reliability for different operational conditions has to be evaluated for damage scenarios. Reliability of a ship highly depends on speed, heading angle, sea state, age of the ship and damage condition. Corrosion may cause significant reduction in reliability. The reliability information of a damaged ship under different operational conditions considering time effects is very important, during tow or rescue operations. For instance, the ship speed could be adjusted so that the reliability of the damaged ship remains above a predefined threshold.

4. The robustness index is useful for comparison of the severity of sudden damage scenarios. Compared to the residual strength factor, it contains additional information as it is based on reliability index rather than the mean hull strength.

5. Some operational conditions result in significant reduction in the performance. In general, the worst performance is obtained under head sea. The effect of the sea state becomes more dominant when ship speed is increasing.

6. The proposed methodology can be effectively used when combined with the real time structural health monitoring tools. The information obtained from different critical locations of the ship in real time will give the possibility to adjust the operational condition to keep the integrity of a damaged ship.

The proposed framework is aimed to be used in optimization of the design and maintenance of ships and actions after ship accidents. The effects of different sudden

damage scenarios are investigated separately. Further research on this topic should include a methodology for combining the effects of different scenarios in one performance indicator. This is very useful for direct comparison of alternatives in decision making.

272

Table 8.1   Stiffener dimension of the investigated ship hull (adopted from Akpan et al. 2002). The stiffeners 1, 2, 3, 4, 5, and 6 are indicated in Figure 2.

Stiffener	Web (mm)	Flange (mm)
1	450x36	None
2	1000x16	400x16
3	465x18	190.5x25.5
4	1220x16	350x25.5
5	370x16	100x16
6	297x11.5	100x16

273

Table 8.2   Statistical properties of sea states (Resolute Weather 2011)

Sea State	Significant Wave Height (m)	Average Wave Period (s)	Average Wave Length (m)
5	2.44	5.5	32
6	4.27	7.5	56.09
7	7.62	10	100.13

274
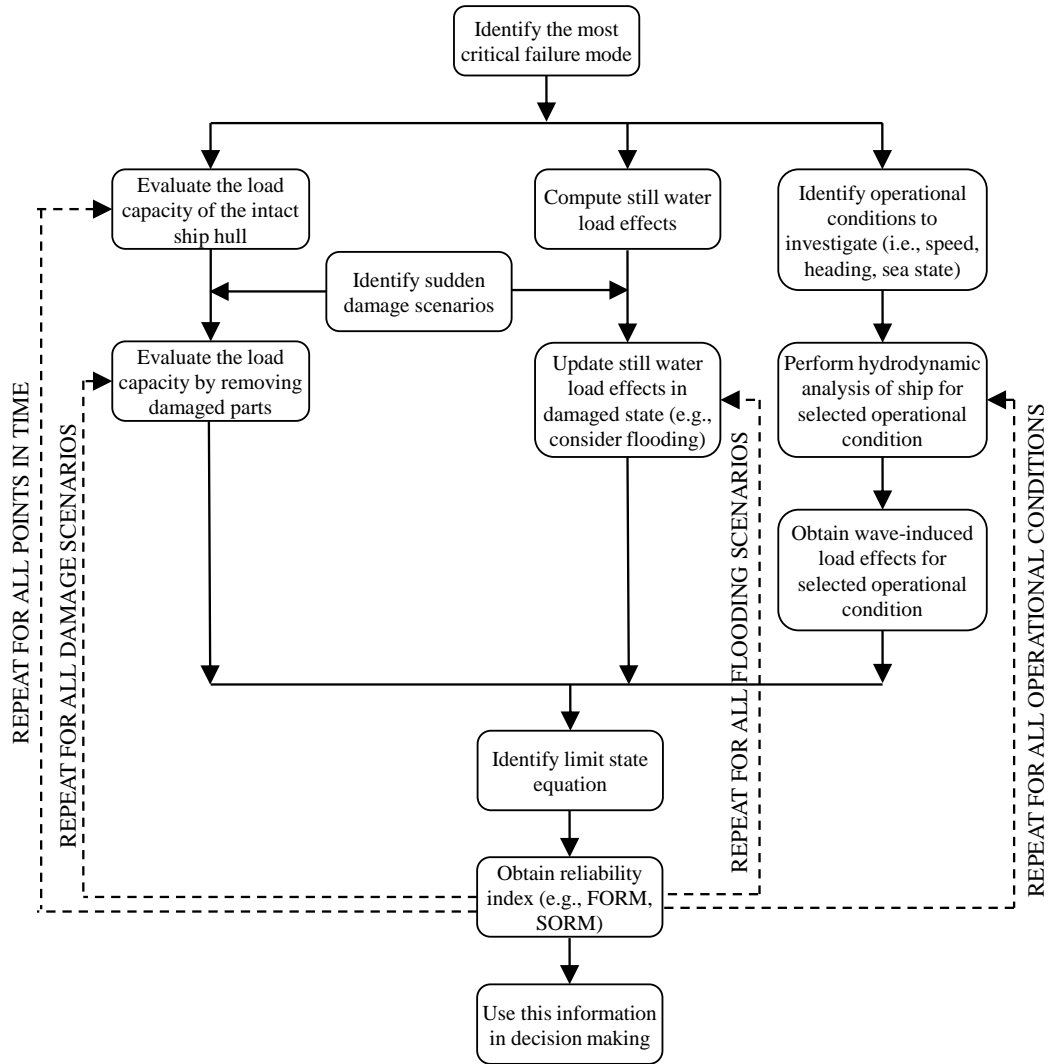
Figure 8.1   Methodology of assessing time-variant performance of damaged ship hulls

Figure 8.2   Mid-section dimensions of the investigated ship and its six type of

stiffeners (adapted from Akpan et al. 2002)
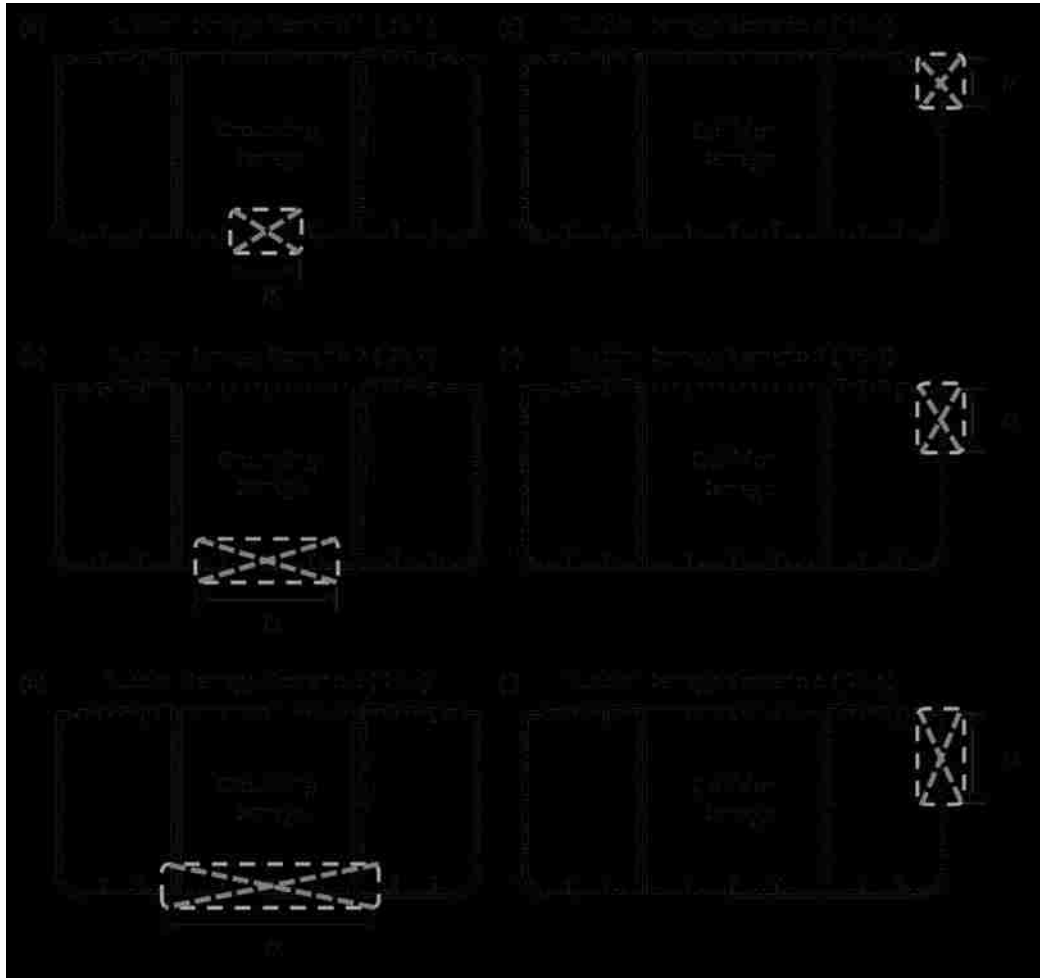
Figure 8.3   Sudden damage scenarios investigated

SAGGING

Figure 8.4   Variation of mean bending capacity of mid-ship for the six different sudden damage scenarios shown in Figure 8.3, (a) sagging and (b) hogging

278
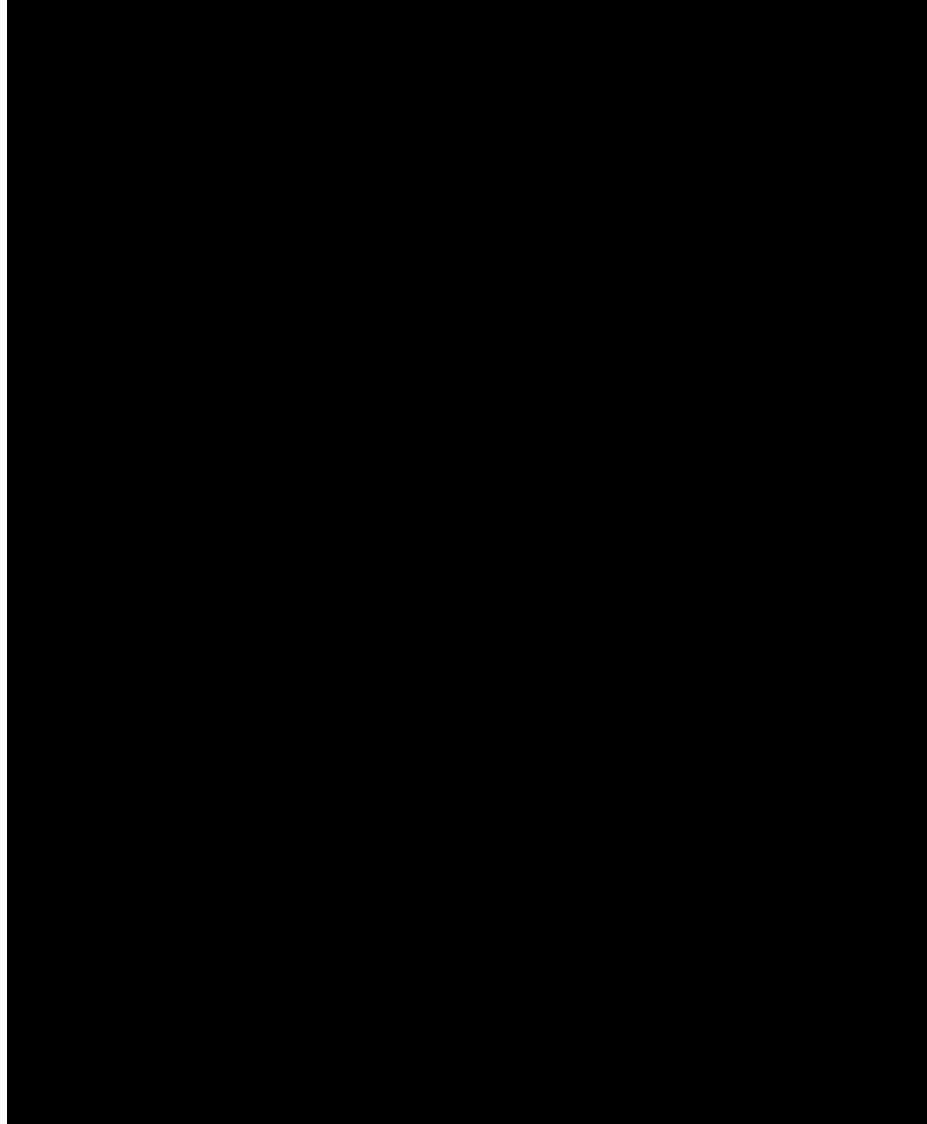
Figure 8.5   Variation of residual strength for the six different sudden damage scenarios shown in Figure 8.3, (a) sagging and (b) hogging

Model obtained using
FREE!ship (FREE!ship 2006)

B = 38.1 m
D = 17.4 m
L = 220 m
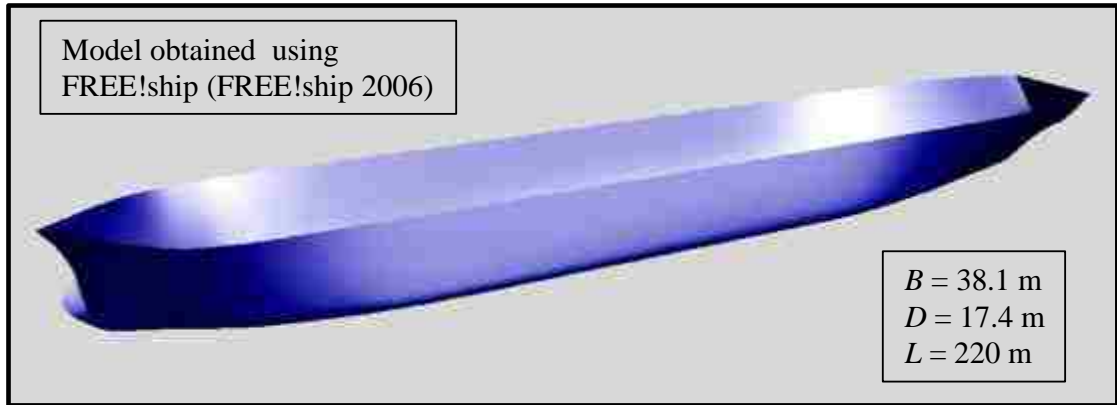
Figure 8.6   Model of the ship body used in hydrodynamic analysis
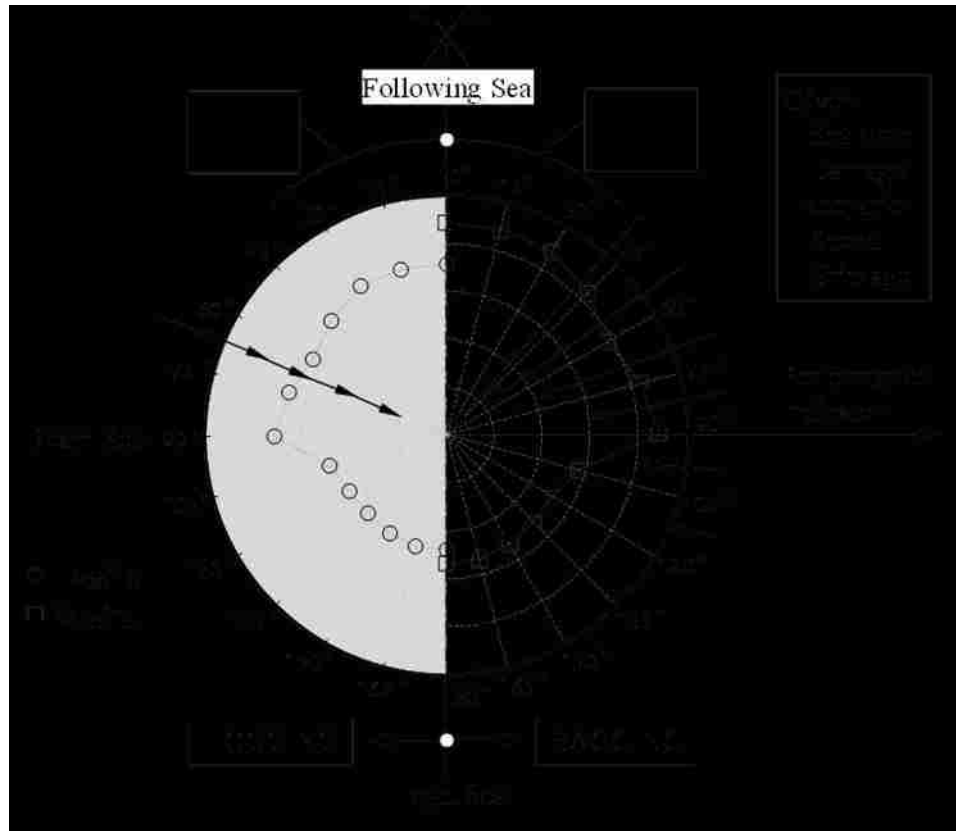
Figure 8.7   Qualitative representation of ship performance for both hogging and sagging in a polar plot
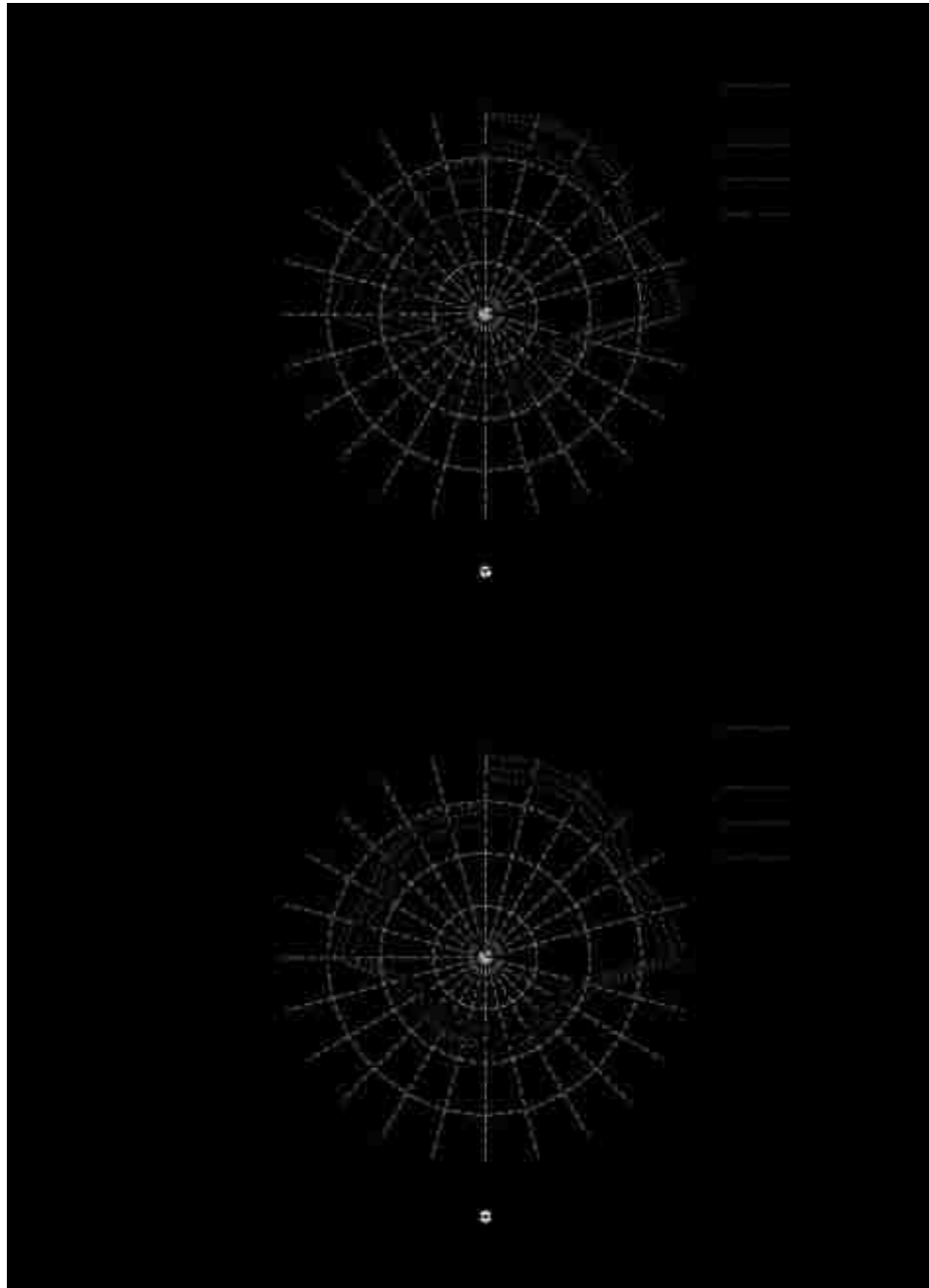
Figure 8.8   Variation of reliability index with respect to heading angle for sea state

5, ship speed $U = 10$ knots, time $t = 0$, (a) sudden damage scenarios 1,

2, and 3 and (b) sudden damage scenarios 4, 5, and 6

282
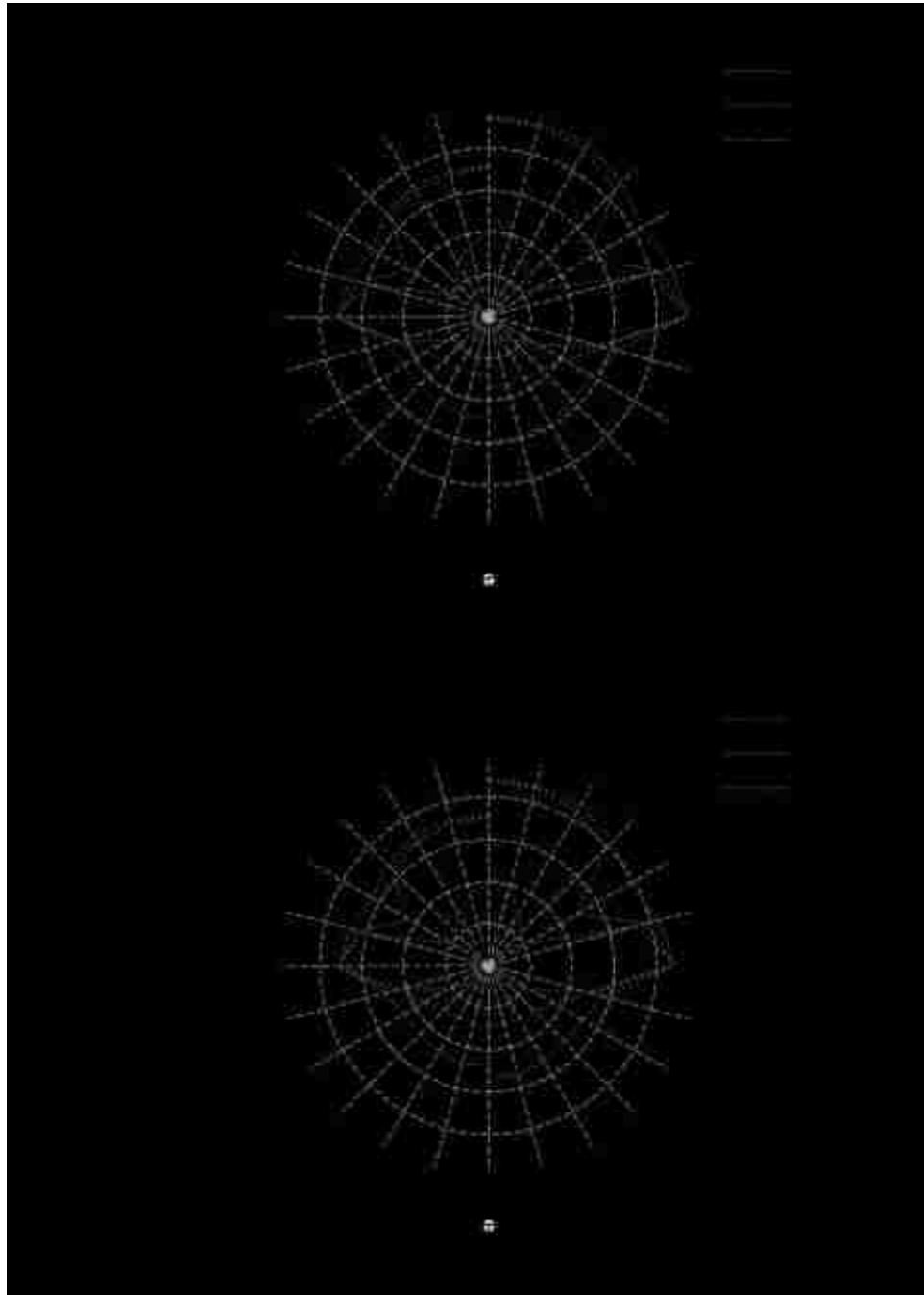
Figure 8.9   Variation of reliability index with respect to heading angle and sea state

for ship speed $U = 10$ knots, time $t = 0$, (a) damage scenario 1 (b)

sudden damage scenario 6
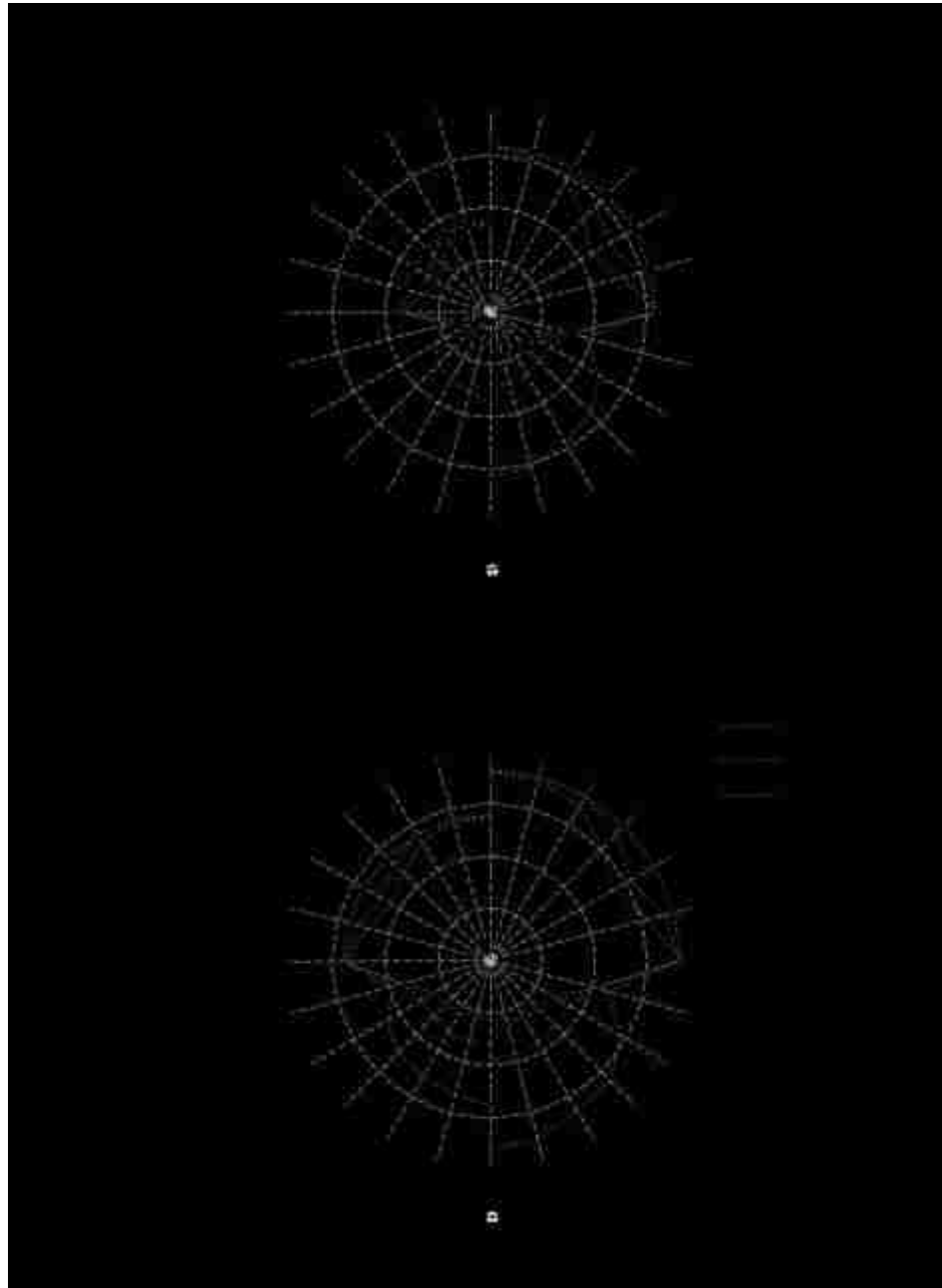
Figure 8.10   Variation of reliability index with respect to heading angle and ship speed for sea state 5, time $t = 0$, (a) damage scenario 3 (b) sudden damage scenario 5

284
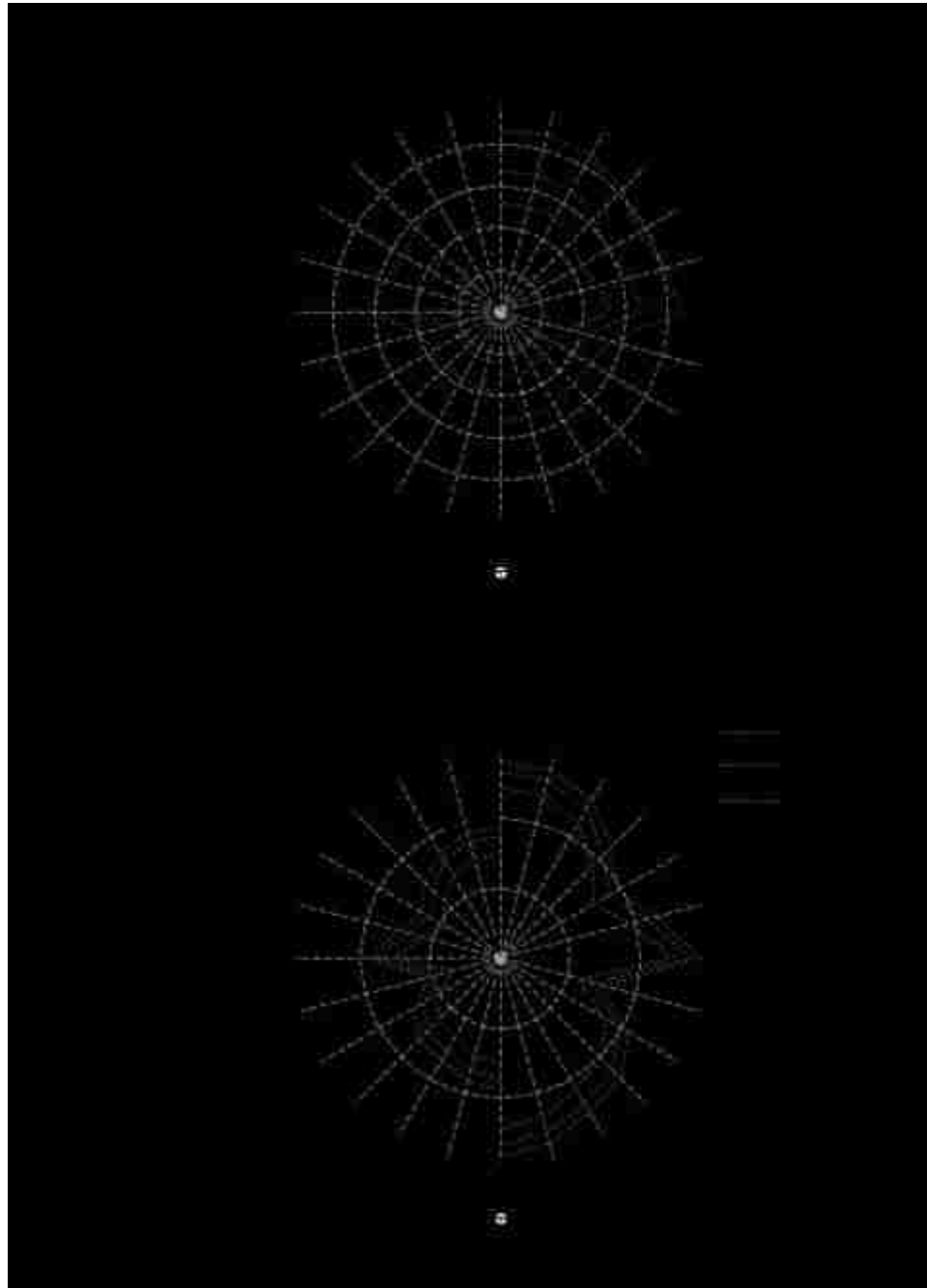
Figure 8.11   Variation of reliability index with respect to heading angle for (a) different values of still water bending moment and (b) different points in time

285
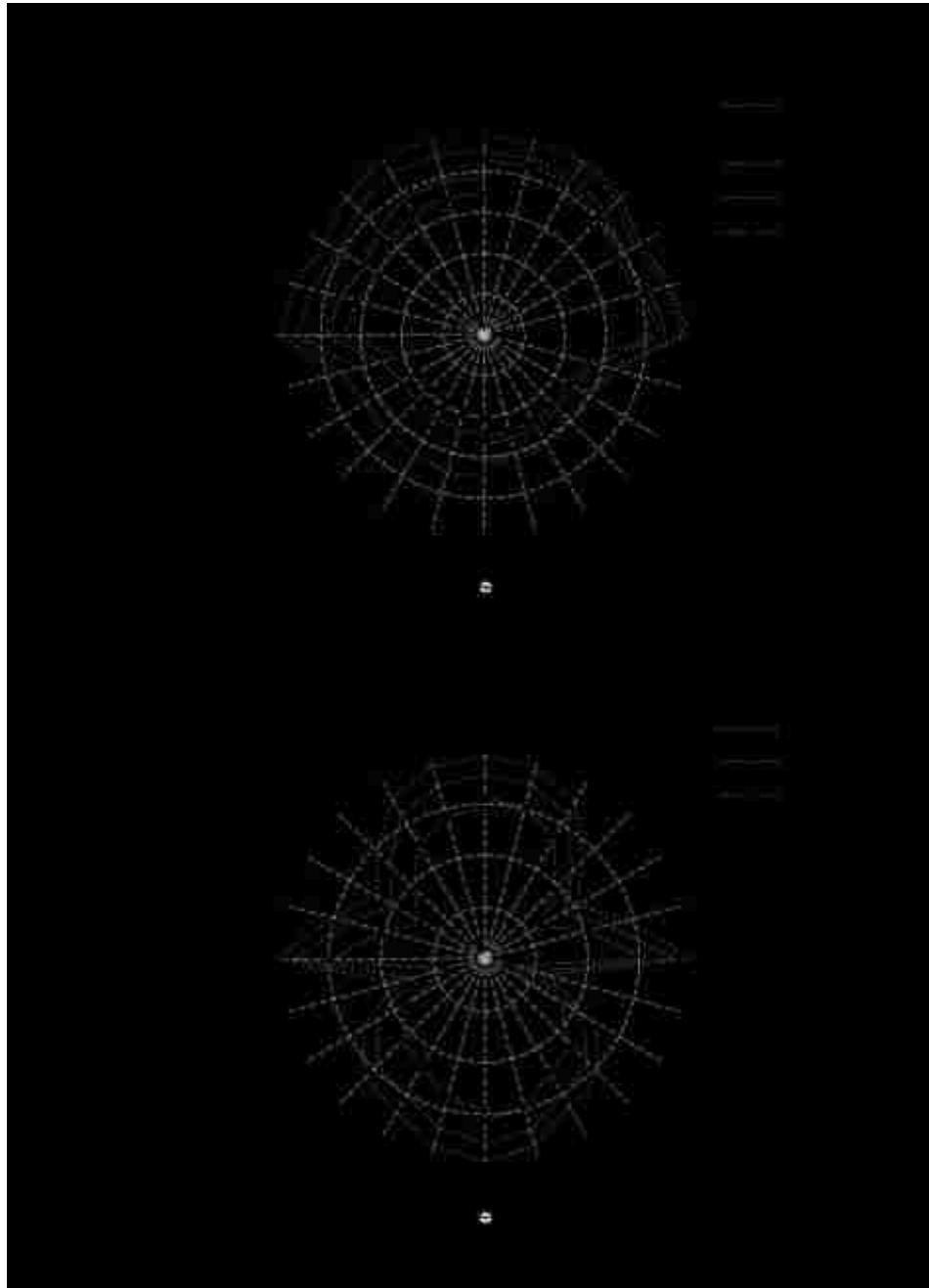
Figure 8.12   Variation of robustness index with respect to heading angle for (a) different sudden damage scenarios, and (b) different points in time
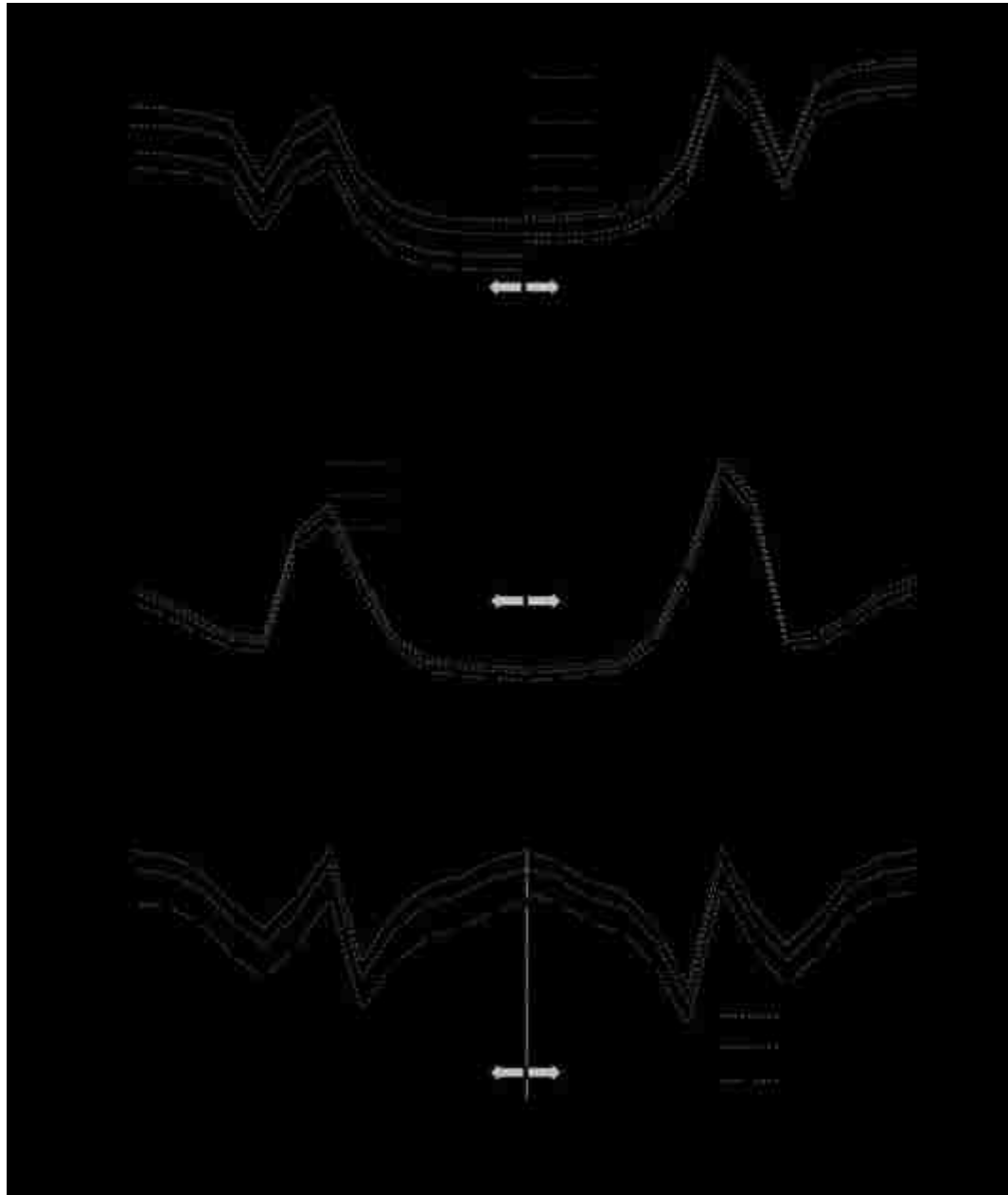
Figure 8.13   Variation of reliability index with respect to heading angle for (a) different sudden damage scenarios and (b) different points in time, and (c) variation of robustness index with respect to heading angle for different points in time. FS: following sea, HS: head sea
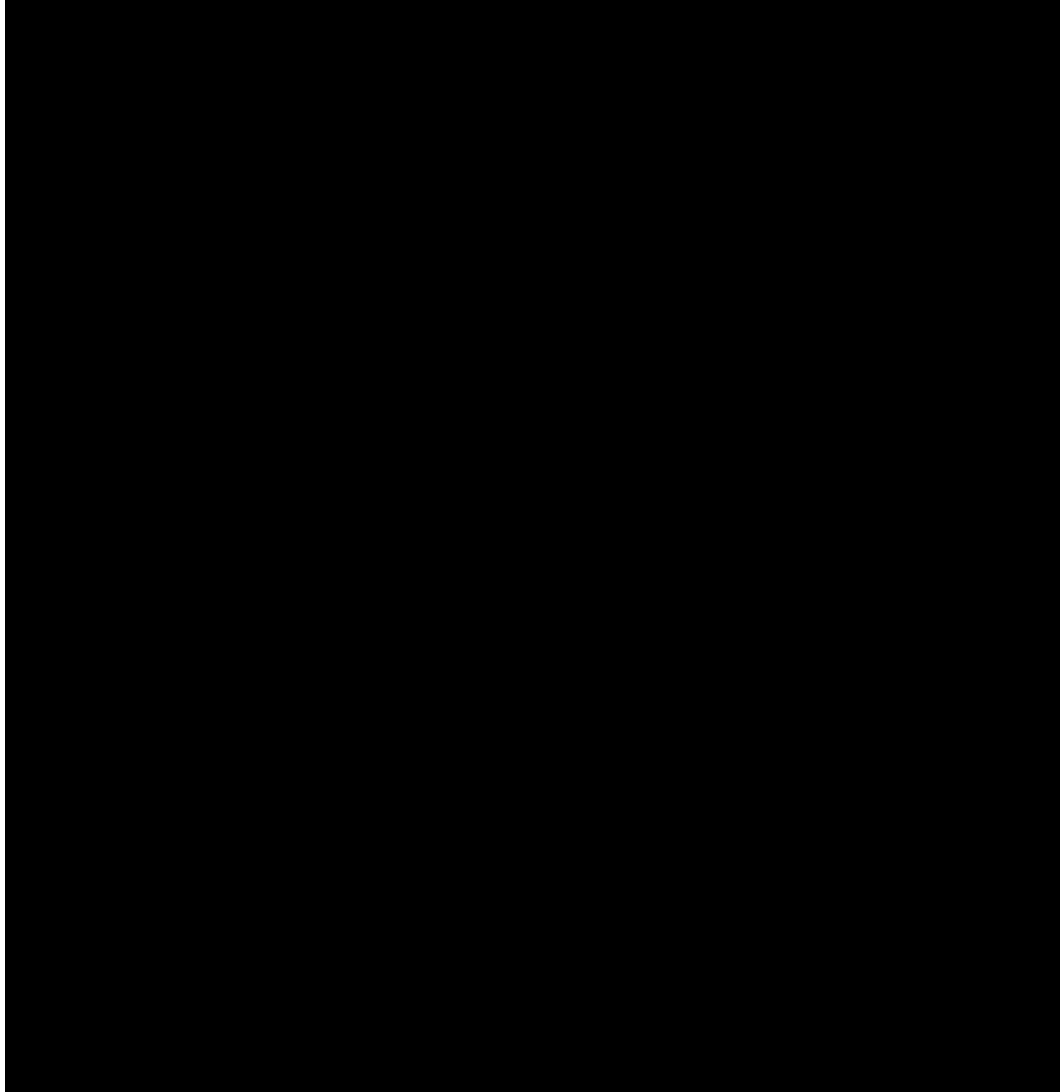
Figure 8.14   Variation of (a), (b) mean vertical bending moment capacity, (c), (d) reserve strength factor, and (e), (f) residual strength factor, in sagging and hogging, respectively.

288
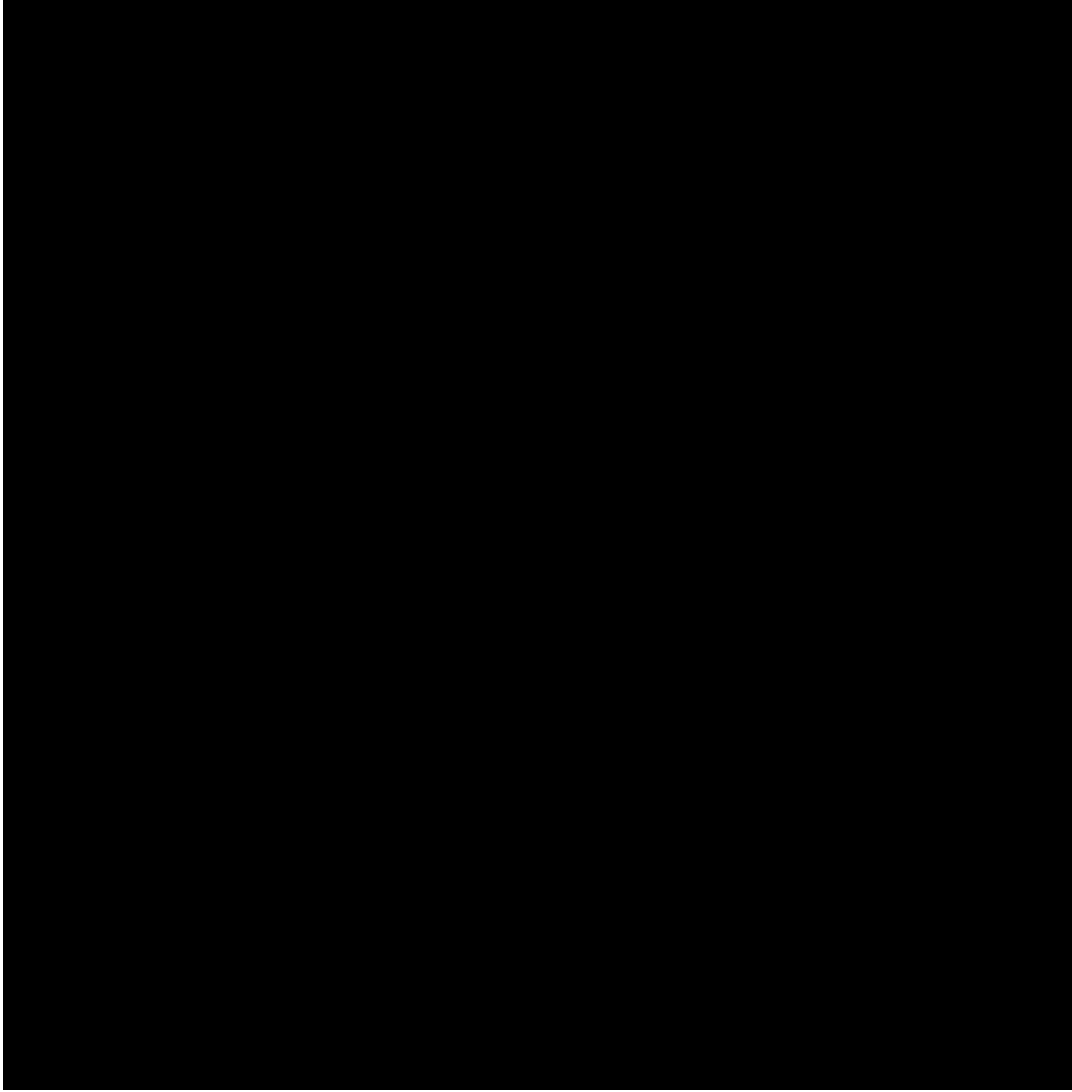
Figure 8.15   Variation of (a), (b) probability of failure, (c), (d) vulnerability, and (e),

(f) redundancy index, in sagging and hogging, respectively.

CHAPTER 9

SUMMARY, CONCLUSIONS, AND SUGGESTIONS FOR FUTURE WORK

9.1 SUMMARY

This study developed methodologies for integrating the reliability-based and risk-based performance indicators in a life-cycle management framework for structures undergoing progressive and sudden damage. These methodologies are aimed to be effective tools for establishing rational support for decision making on life-cycle management of civil and marine structures and infrastructures.

Structural performance assessment and prediction, optimization of inspection and monitoring activities, updating the performance with information from inspection and monitoring, optimization of maintenance and repair activities and decision making are the main tasks of a comprehensive life-cycle management framework. This study focused on the tasks "Structural Performance Assessment and Prediction" and "Optimization of Maintenance and Repair Activities".

The objectives of this study include developing a methodology for quantifying time-variant reliability, redundancy, vulnerability, and robustness of structural systems and integrating these performance indicators into a comprehensive life-cycle management framework; developing an approach for quantifying lifetime risk associated with the component failure and risk-based robustness of bridge superstructures, accounting for the possibility of different corrosion levels; developing a novel risk-based maintenance optimization methodology for deteriorating bridges based on most common condition rating system and Markov Chains to minimize both

290

risk and maintenance costs; developing a methodology to assess the lifetime risk and risk-based robustness of highway bridge networks based on a recent Markov Chain model; developing a probabilistic framework for performance assessment of ship hulls under sudden damage accounting for different operational conditions; and providing the applicable range of simple expressions based on FOSM for bridge system reliability assessment by investigating the amount of error associated with these simple expressions.

A methodology for estimation of time-dependent performance indicators of civil structures and infrastructures including vulnerability, redundancy and robustness was developed. This methodology is based on probabilistic performance assessment supported by finite element analysis. Nonlinear incremental static analyses were performed to find the load carrying capacity of the bridge superstructure in probabilistic manner. Several local damage scenarios were considered by removal of structural members. The time-dependent effects of corrosion on structural reliability, vulnerability, redundancy and robustness were investigated.

A methodology for quantifying lifetime risk associated with the component failure and risk based robustness of bridge superstructures was proposed. The risk was quantified in terms of the expected losses. The probabilities of different deterioration levels at a point in time were considered by means of a set of mutually exclusive and collectively exhaustive condition states. The proposed methodology of loss estimation was designed to account for the failure probability of different levels of component deterioration weighted by the occurrence probabilities of these levels. Pontis element condition rating system was integrated in a scenario-based approach to identify

291

expected losses. The deterioration process of bridge components regarding the transition between the condition states was modeled as a Markov process. The variation of expected losses and risk-based robustness index in time was investigated.

A risk-based maintenance optimization methodology for bridges with deteriorating components was proposed to find the optimum maintenance options and timing. The risk assessment methodology combining the time-variant probabilities of different condition states regarding the deterioration level of bridge components, time-variant component and system failure probabilities for various scenarios was integrated in a maintenance optimization approach. A multi-criteria optimization problem in which the lifetime maximum value of expected losses associated failure and the lifetime total expected maintenance cost are the conflicting objectives was formulated to find the optimum maintenance actions and schedule for different bridge components.

A methodology to assess the time-dependent expected losses and risk-based robustness of highway bridge networks accounting for deterioration and restoration was developed. A recent Markov Chain model was used to predict the time-dependent performance of the individual bridges. The direct consequences were identified on the basis of the individual bridge failure or closure for maintenance. The indirect consequences were quantified on the basis of scenarios including single and multiple bridges out-of-service. The traffic assignment problem was integrated in a scenario-based risk assessment approach to quantify the network performance under various failure scenarios. The variation of expected direct, indirect and total losses for a bridge network in time was investigated.

An approach for performance assessment of damaged ship hulls under different operational conditions considering grounding and collision accidents as sudden damage in a probabilistic manner was proposed. The combined effects of sudden damage and aging on ship performance were investigated. The performance of ship hull was quantified in terms of several performance indicators including residual strength factor, reliability index, and robustness index. The longitudinal bending moment capacities of the intact and damaged ship hulls were assessed based on an optimization-based version of incremental curvature method. The wave-induced loads for different ship speeds, headings and sea states were identified based on hydrodynamic analysis and the performance under different operational conditions was investigated.

Assuming that the system performance of a bridge structure can be represented by a single limit state function based on probabilistic finite element analysis, the amount of error introduced by using simple expressions to compute bridge system reliability index was investigated. A comparison of expressions used for exact and approximate results was provided. The amount of error introduced by using the expression which provides approximate results instead of the expression which provides exact results was presented in function of central safety factor for various coefficients of variation of system resistance and load effect.

9.2 CONCLUSIONS

The following conclusions can be drawn from the performance assessment and maintenance optimization of single bridges and bridge networks:

293

- It is shown that the time-variant performance of deteriorating structures under uncertainty can be predicted in a probabilistic manner using advanced tools such as finite element modeling, response surface approximation, and Latin Hypercube Sampling. In this way, the system performance of a structure can be evaluated accurately. The effects of sudden damage to components can be accounted based on scenarios efficiently.

- Performance measures for bridges associated with reliability, vulnerability, redundancy and robustness deteriorate in time due to various causes such as corrosion and live load increase. The dominant cause of performance reduction may change throughout the lifespan. In general, at the early stages of lifetime, the live load increase is dominant; however, the effect of corrosion gets significant at later stages. This may not always be the case depending on the environmental conditions and the traffic that the bridge is subjected to. For a predefined sudden damage scenario, the vulnerability may increase while the redundancy and robustness may decrease rapidly in time due to the corrosion and the live load increase.

- It is not always recommended to use simple expressions for computing the system reliability of bridges. On the other hand, the expression which gives approximate results for the case with lognormal system resistance and lognormal load effect can provide acceptable approximations even for the case with lognormal system resistance and extreme value type I largest load effect especially on the conservative side. The amount of error introduced by using simple expressions in system reliability analysis depends not only on the

294

coefficient of variation of the resistance and load effect but also the ratio between the mean values of resistance and load effect.

- It is shown that lifetime total risk of bridge structures can be quantified based on the risks associated with single component using scenario-based approach. The probabilities of different deterioration levels at a point in time can be considered by means of a commonly used bridge component condition rating system using a Markov Chain model to effectively predict time-variant performance of components.

- In a risk analysis, the contribution of the considered damage scenarios to the total expected loss can be very different. In fact, a relatively small number of scenarios can yield a significant contribution to the total expected loss.

- The detour duration due to the reconstruction of a bridge has an impact on the expected losses. The impact of this parameter on the overall trend of expected loss and risk-based robustness index is increasing in time significantly. The average daily traffic diverted due to lane closure of a bridge also has an impact on the expected loss. This impact fades over time.

- It is shown that risk-based maintenance optimization of structures can be performed efficiently when the deterioration of the components can be represented by a set of mutually exclusive and collectively exhaustive condition states. This optimization methodology is computationally efficient due to the fact that the deterioration process and maintenance effects are represented using Markov chains and the reliability analyses are not required to be performed for the candidate solutions of the optimization algorithm.

295

- The Pareto optimum solutions range between high risk–low maintenance cost and low risk–high maintenance cost. The decision maker can select an optimum solution depending on the available budget. Each point on the Pareto front corresponds to the optimum solution of a single-objective optimization problem with a fixed budget. The maintenance actions can cause a sudden significant change in condition state probabilities and, consequently, in the expected loss. The lifetime maximum expected loss can be reduced significantly depending on the risk-attitude of the decision maker.

- The maximum total expected indirect loss is much higher than the lifetime maximum total expected direct loss for a highway bridge network. The difference between these risks may depend on the investigated time span as well as the size of the network (i.e., number of bridges). The risk-based robustness index may provide a good measure of bridge networks for long investigation periods. However, this indicator may show fluctuations throughout the lifetime and is not a reliable measure for shorter time intervals. The time-dependent expected loss and risk-based robustness index are sensitive to the time-dependent parameters of the Markov Chain model.

The following conclusions can be drawn from the performance assessment of ships:

- After accidents, ultimate failure of ships may occur depending on the extent of the damage. The methodology presented in Chapter 8 can be very helpful in decision making on how to deal with damaged ship by providing information on the reliability of the damaged ship under different operational conditions.

The methodology presented in Chapter 8 can be used to investigate the effects of ship damage scenarios occurring at different points in the service life.

- The performance of damaged ships can be evaluated in a probabilistic manner. Operational conditions have very significant effects on reliability. Reliability for different operational conditions has to be evaluated for damage scenarios. Reliability of a ship highly depends on speed, heading angle, sea state, age of the ship and damage condition. Corrosion may cause significant reduction in reliability. The reliability information of a damaged ship under different operational conditions considering time effects is very important, during tow or rescue operations. For instance, the ship speed could be adjusted so that the reliability of the damaged ship remains above a predefined threshold.

- Residual strength factor can be used time effectively to quantify the loss of hull strength under different scenarios and comparison. Corrosion can have significant impact on the residual strength of ships. Time effects should be included in the reliability, redundancy, and robustness of aging ships. The robustness index is useful for comparison of the severity of sudden damage scenarios. Compared to the residual strength factor, it contains additional information as it is based on reliability index rather than the mean hull strength.

- Some operational conditions can result in significant reduction in the performance. In general, the worst performance is obtained under head sea. The effect of the sea state becomes more dominant when ship speed is increasing. The methodology presented in Chapter 8 can be effectively used

297

when combined with the real time structural health monitoring tools. The information obtained from different critical locations of the ship in real time will give the possibility to adjust the operational condition to keep the integrity of a damaged ship.

9.3 SUGGESTIONS FOR FUTURE WORK

- The availability of reliable data regarding the transition probabilities between condition states of bridge components is essential for the risk assessment methodology used in this study. Further investigations are needed to obtain transition probabilities of components of different types of bridges located in regions with different environmental characteristics.

- Reliable relationships should be established between the visual inspection-based condition states and the respective corrosion penetration in order to improve the accuracy of the risk assessment for individual bridges.

- The efficiency of risk-based maintenance optimization methodology depends on the accuracy of the risk assessment approach. Further research is needed on the risk-based maintenance optimization of deteriorating structures in connection with accurate assessment of condition states and costs associated with maintenance actions.

- The purpose of obtaining lifetime risk profiles for bridge networks is to use them in maintenance optimization. Some objectives of such optimization problems can be the minimization of expected losses, the maximization of robustness, and the minimization of total life-cycle cost of a highway bridge

298

network. The risk assessment methodology should be integrated with a maintenance optimization approach.

- In the performance assessment of ships, the effects of different sudden damage scenarios were investigated separately. Further research on this topic should include a methodology for combining the effects of different scenarios in one performance indicator. This is very useful for direct comparison of alternatives in decision making.

- The performance assessment methodologies presented in this study should be integrated with the other tasks of the comprehensive life-cycle management framework such as optimization of inspection and monitoring activities and updating the performance with information from inspection and monitoring.

REFERENCES

AASHTO (2007). LRFD bridge design specifications, 4th Ed., American Association of State Highway and Transportation Officials, Washington, D.C.

AASHTO (2010). LRFD bridge design specifications, 5th Ed., American Association of State Highway and Transportation Officials, Washington, D.C.

ABAQUS (2009). ABAQUS/Standard sersion 6.9 user's manuals. Hibbit, Karlsson, and Soreson, Inc., Pawtucket, Rhode Island.

ABS (1995). Guide for assessing hull-girder residual strength for tankers. American Bureau of Shipping.

ABS (2010). Guidance notes on springing assessment for container carriers. American Bureau of Shipping (ABS), Houston, TX.

Adey, B., Hajdin, R. and Brühwiler, E. (2003). Supply and demand system approach to development of bridge management strategies. *Journal of Infrastructure Systems*, 9(3), 117.

Akgül, F. (2002). Lifetime system reliability prediction of multiple structure types in a bridge network. Ph.D. Thesis, University of Colorado at Boulder, Boulder, Colorado, USA.

Akgül, F. and Frangopol, D. M. (2003). Rating and reliability of existing bridges in a network. *Journal of Bridge Engineering*, 8 (6), 383-393.

Akgül, F. and Frangopol, D. M. (2004a). Computational platform for predicting lifetime system reliability profiles for different structure types in a network. Journal of Computing in Civil Engineering, ASCE, 18 (2), 92-104.

300

Akgül, F. and Frangopol, D.M. (2004b). Bridge rating and reliability correlation: Comprehensive study for different bridge types. Journal of Structural Engineering, ASCE, 130 (7), 1063-1074.

Akgül, F. and Frangopol, D. M. (2004c). Computational platform for predicting lifetime system reliability profiles for different structure types in a network. *Journal of Computing in Civil Engineering*, 18 (2), 92–104.

Akpan, U. O., Koko, T. S., Ayyub, B. and Dunbar, T. E. (2002). Risk assessment of aging ship hull structures in the Presence of Corrosion and Fatigue. *Marine Structures*, Elsevier, 15(3), 211-231.

Al-Wazeer, A.A.R. (2007). Risk-based bridge management strategies. University of Maryland, College Park, Ph.D. dissertation.

Ang, A. H.-S. (2011). Life-cycle considerations in risk-informed decisions for design of civil infrastructures. *Structure and Infrastructure Engineering*, 7(1), 3-9.

Ang, A. H.-S. and De Leon, D. (1997). Target reliability for structural design based on minimum expected life-cycle cost. Reliability and optimization of structural systems, D. M. Frangopol, R. B. Corotis, and R. Rackwitz, eds., Pergamon, New York, 71–83.

Ang, A. H.-S. and Tang, W. H. (1984). Probability concepts in engineering planning and design Volume II – decision, risk and reliability. *John Wiley & Sons, Inc.,* New York.

Ang, A. H.-S., Lee, J-C. and Pires, J.A. (1998). Cost-effectiveness evaluation of design criteria. Optimal performance of civil infrastructure systems, D.M. Frangopol, ed., ASCE, Reston, Va., 1–16.

301

Ang, A. H.-S. and Tang, W.H. (2007). Probability Concepts in Engineering: Emphasis on Applications to Civil and Environmental Engineering, second ed., John Wiley & Sons, New Jersey, USA.

Augenbroe, G. & Park, C-S. (2002). Towards a maintenance performance toolkit for GSA. Georgia institute of Technology, Atlanta, August 27, 2002.

Augusti, G., Ciampoli, M., Frangopol, D.M., (1998). Optimal planning of retrofitting interventions on bridges in a highway network. Engineering Structures, 20(11), 933-939.

Baker, J. W., Schubert, M., Faber, M. H. (2008). On the assessment of robustness. *Structural Safety*, Elsevier, 30, 253-267.

Barker, R. M. and Puckett, J. A. 2007. Design of highway bridges: An LRFD approach. Second Edition, John Wiley & Sons, Inc., Hoboken, NJ.

Biondini, F. and Frangopol, D.M. (2010). Structural robustness and redundancy of deteriorating concrete bridges. Bridge Maintenance, Safety, Management, Health Monitoring and Optimization, D.M. Frangopol, R. Sause, and C.S. Kusko, eds., CRC Press/Balkema, Taylor & Francis Group plc, London, full paper on CD-ROM, Taylor & Francis Group plc, London, 2473-2480.

Biondini, F., Frangopol, D.M. and Restelli, S. (2008). On structural robustness, redundancy and static indeterminacy. Proceedings of the ASCE Structures Congress, Vancouver, Canada, April 24-26, 2008; in Structures 2008: Crossing Borders, ASCE, 2008, 10 pages on CD-ROM.

Blockley, D. I., Agarwal, J., Pinto, J. T., Woodman, N. J., (2002). Structural vulnerability, reliability and risk. *Progress in Structural Engineering and Materials*, Wiley Interscience, 4(2), 203-212.

302

Bocchini, P. and Frangopol, D.M. (2011a). Generalized bridge network performance analysis with correlation and time-variant reliability. *Structural Safety*, 33(2), 155-164.

Bocchini, P. and Frangopol, D.M. (2011b). A stochastic computational framework for the joint transportation network fragility analysis and traffic flow distribution under extreme events. *Probabilistic Engineering Mechanics*, 26 (2), 182–193.

Bocchini, P. and Frangopol, D.M. (2012). Optimal resilience- and cost-based post-disaster intervention prioritization for bridges along a highway segment. *Journal of Bridge Engineering*, 17 (1), 1–13.

Bocchini, P., Saydam, D., and Frangopol, D.M. (2013). Efficient, accurate, and simple Markov chain model for the life-cycle analysis of bridge groups. Structural Safety, Elsevier, 40, 51-64.

Box, G. E. P. and Wilson, K. B., (1951). On the experimental attainment of optimum conditions (with discussion)", *Journal of the Royal Statistical Society* Series B 13(1), 1–45.

Bruneau, M., Chang, S.E., Eguchi, R.T., Lee, G.C., O'Rourke, T.D., Reinhorn, A.M., Shinozuka, M., Tierney, K., Wallace, W. and Winterfelt, D.V. (2003). A framework to quantitatively assess and enhance the seismic resilience of communities. Earthquake Spectra, EERI, 19(4), 733-752.

Bucher, C.G. and Bourgund, U. (1990). A fast and efficient response surface approach for structural reliability problems. Structural Safety, 7, 57-66.

Cambridge Systematics, Inc. (2009). Pontis Release 4.5 User Manual, AASHTO, Washington, D.C.

303

Chang, S.E. and Shinozuka, M. (1996). Life-cycle cost analysis with natural hazard risk. Journal of Infrastructure Systems, 2(3), 118–126.

CIB (2001). Risk assessment and risk communication in civil engineering. TG 32 Report 259, Rotterdam: Council for Research and Innovation in Building and Construction.

Colorado Department of Transportation (CDOT) (1998). Pontis bridge inspection coding guide, Denver, Colorado.

Corley, W. G. (2002). Applicability of seismic design in mitigating progressive collapse. Proceedings of Workshop on Prevention of Progressive Collapse, National Institute of Building Sciences, Washington, D.C.

Cornell, C.A. (1969). Probability-based structural code. ACI Journal, 66, 974-985.

Decò, A. and Frangopol, D. M. (2011). Risk assessment of highway bridges under multiple hazards. *Journal of Risk Research*, Taylor & Francis, 14(9), 1057-1089.

Decò, A., Frangopol, D. M. and Okasha, N. M. (2011). Time-variant redundancy of ship structures. *Journal of Ship Research*, SNAME, 55(3), 208-219.

Decò, A., Frangopol, D. M. and Zhu, B. (2012). Reliability and redundancy assessment of ships under different operational conditions, *Engineering Structures*, Elsevier, 42, 457-471.

Der Kiureghian, A. and Taylor, R.L. (1983). Numerical methods in structural reliability, Proceedings of the Fourth International Conference on Applications of Statistics and Probability in Soil and Structural Engineering, ICASP-4, Florence, Italy, June, 1983, Pitagora Editrice.

Ditlevsen. O and Bjerager. P. (1986), Methods of structural systems reliability. *Structural Safety*, Elsevier, 3 (3-4), 195-229.

Dong, Y., Frangopol, D.M., Saydam, D. (2013). Time-variant sustainability assessment of seismically vulnerable bridges subjected to multiple hazards. *Earthquake Engineering & Structural Dynamics*, John Wiley & Sons, (in press, available online) doi: 10.1002/eqe.

Dueñas-Osorio, L., and Vemuru, S. M. (2009). Cascading failures in complex infrastructure systems. *Structural Safety*, 31 (2), 157-167.

Ellingwood, B. (1996). Reliability-based condition assessment and LRFD for existing structures. Structural Safety, 18(2+3), 67-80.

Ellingwood, B. R. (2006). Mitigating Risk from Abnormal Loads and Progressive Collapse. *Journal of Performance of Constructed Facilities,* ASCE, 20(4), 315-323.

Ellingwood, B. R. and Dusenberry, O. D. (2005). Building Design for Abnormal Loads and Progressive Collapse. *Computer-Aided Civil and Infrastructure Engineering,* 20, 194-205.

Ellingwood, B., Galambos, T.V., MacGregor, J.G. and Cornell, C.A. (1980). Development of a probability-based load criterion for American National Standard A58. NBS Special Publication 577, U.S. Department of Commerce, Washington, D.C.

Enright, M. P. and Frangopol, D. M. (1999a). Reliability-based condition assessment of deteriorating concrete bridges considering load redistribution. Structural Safety, Elsevier, 21, 159-195.

Enright, M.P. and Frangopol, D.M. (1999b). Condition prediction of deteriorating concrete bridges. Journal of Structural Engineering, ASCE, 125 (10), 1118-1125.

Estes, A.C. (1997). A system reliability approach to the lifetime optimization of inspection and repair of highway bridges. PhD Thesis, Department of Civil, Environmental, and Architectural Engineering, University of Colorado at Boulder.

Estes, A. C. and Frangopol D. M. (1998). RELSYS: A computer program for structural system reliability analysis. *Structure Engineering and Mechanics*, Techno Press, 6(8), 901-19.

Estes, A. C. and Frangopol, D.M. (2001). Bridge lifetime system reliability under multiple limit states. *Journal of Bridge Engineering*, ASCE, 6(6), 523-528.

Estes, A.C. (1997). A system reliability approach to the lifetime optimization of inspection and repair of highway bridges. PhD Thesis, Department of Civil, Environmental, and Architectural Engineering, University of Colorado at Boulder.

Estes, A.C. and Frangopol, D.M. (1998). RELSYS: A computer program for structural system reliability analysis. Structural Engineering and Mechanics, Techno Press, 6(8), 901-919.

Estes, A.C. and Frangopol, D.M. (1999). Repair optimization of highway bridges using system reliability approach. Journal of Structural Engineering, ASCE, 125(7), 766-775.

Estes, A.C. and Frangopol, D.M. (2001). Bridge lifetime system reliability under multiple limit states. Journal of Bridge Engineering, ASCE, 6 (6), 523-528.

306

Estes, A.C. and Frangopol, D.M. (2003). Updating bridge reliability based on bridge management systems visual inspection results. Journal of Bridge Engineering, ASCE, 8(6), 374-382.

Faber, M.H., Maes, M.A., Straub, D., and Baker, J. (2006). On the quantification of robustness of structures. Proceedings OMAE2006, 25th Offshore Mechanics and Arctic Engineering Conference, Hamburg, Germany, June 4-9, 2006, (OMAE2006-92095).

Faltinsen, O. M. (1990). Sea loads on ships and offshore structures. Cambridge University Press, Cambridge, UK, 328p.

Fang, C. L., and Das, P.K., 2005. Survivability and reliability of damaged ships after collision and grounding. *Ocean Engineering*, 32, 293–307.

Fang, C., and Das, P.K., 2004. Hull girder ultimate strength of damaged ships. In: Proceedings of the Ninth Symposium on Practical Design of Ships and Other Floating Structures. Luebeck-Travemuende, Germany, 309–316.

Federal Highway Administration (FHWA) (1995). Recording and coding guide for structure inventory and appraisal of the nation's bridge, Report No. FHWA-PD 96-001, U.S. Department of Transportation, Washington, D.C.

FEMA, (2009). HAZUS-MH MR4 earthquake model user manual. Department of Homeland Security. Federal Emergency Management Agency, Whashington, D.C.

Fiessler, B., Neumann, H-J. and Rackwitz, R. (1979). Quadratic limit states in structural reliability. Journal of Engineering Mechanics, ASCE, 105, 661-676.

Frangopol, D. M. (2011). Life-Cycle performance, management, and optimization of structural systems under uncertainty: Accomplishments and challenges. *Structure and Infrastructure Engineering*, Taylor & Francis, 7(6), 389-413.

Frangopol, D.M. and Klisinski, M. (1989). Material behavior and optimum design of structural systems. *Journal of Structural Engineering*, ASCE, 115(5), 1054-1075.

Frangopol, D.M., Klisinski, M., Iizuka M. (1991). Optimization of damage-tolerant structural systems. *Computers and Structures*, Pergamon Press, 40(5), 1085-1095.

Frangopol, D.M. (2011). Life-cycle performance, management, and optimization of structural systems under uncertainty: accomplishments and challenges. *Structure and Infrastructure Engineering*, Taylor & Francis, 7(6), 389-413, DOI: 10.1080/15732471003594427.

Frangopol, D.M. and Bocchini, P. (2012). Bridge network performance, maintenance and optimization under uncertainty: accomplishments and challenges. *Structure and Infrastructure Engineering*, 8(4), 341-356.

Frangopol, D.M. and Curley, J.P. (1987). Effects of damage and redundancy on structural reliability. Journal of Structural Engineering, ASCE, 113(7), 1533-1549.

Frangopol, D.M. and Liu, M. (2007a). Maintenance and management of civil infrastructure based on condition, safety, optimisation, and life-cycle cost. Structure and Infrastructure Engineering, 3(1), 29-41.

Frangopol, D.M. and Liu, M. (2007b). Bridge network maintenance optimization using stochastic dynamic programming. Journal of Structural Engineering, 133(12), 1772-1782.

308

Frangopol, D.M. and Nakib, R. (1991). Redundancy in highway bridges. Engineering Journal, American Institute of Steel Construction, Chicago, IL, 28(1), 45-50.

Frangopol, D.M., Bocchini, P., Decò, A., Kim, S., Kwon, K., Okasha, N.M., and Saydam, D. (2012). Integrated life-cycle framework for maintenance, monitoring, and reliability of naval ship structures. *Naval Engineers Journal*, Wiley, 124(1), 59-69.

Frangopol, D.M., Kong, J.S., and Gharaibeh, E.S. (2001). Reliability-based life-cycle management of highway bridges. *Journal of Computing in Civil Engineering*, ASCE, 15(1), 27-34.

Frangopol, D.M., Lin, K-Y. and Estes, A.C. (1997). Life-cycle cost design of deteriorating structures. Journal of Structural Engineering, ASCE, 123(10), 1390–1401.

Frangopol, D.M., Saydam, D., and Kim, S. (2012). Maintenance, management, life-cycle design and performance of structures and infrastructures: A brief review. Structure and Infrastructure Engineering, Taylor & Francis, 8(1), 1-25.

Frank, M. and Wolfe, P. (1956). An algorithm for quadratic programming. *Naval Research Logistics Quarterly*, 3 (1– 2), 95–110.

FREE!ship (2006). FREE!ship manual - Version 2.6. Website: www.freeship.org.

Fu, G. and Devaraj, D. (2008). Methodology of homogeneous and non-homogeneous Markov chains for modeling bridge element deterioration. Michigan Department of Transportation, Michigan.

Fu, G. and Frangopol D.M. (1990). Balancing weight, system reliability and redundancy in a multiobjective optimization framework. *Structural Safety*, 7(2–4), 165–175.

309

Ghosn, M. and Frangopol, D.M. (2007). Structural redundancy and robustness measures and their use in assessment and design. Applications of Statistics and Probability in Civil Engineering, Kanda, J., Takada, T., and Furuta, H., eds., Taylor & Francis Group plc., London, 2007, 181-182, and full 7 page paper on CD-ROM.

Ghosn, M. and Moses, F. (1998). Redundancy in highway bridge superstructures. NCHRP Report 406, Transportation Research Board, Washington DC.

Ghosn, M., Moses, F., and Frangopol, D.M. (2010). Redundancy and robustness of highway bridge superstructures and substructures. *Structure and Infranstructure Engineering*, Taylor & Fancis, 6(1-2), 257-278.

Golabi, K., Kulkarni, R., and Way, G. (1982). A Statewide pavement management system. *Interfaces*, 12(6), 5-21.

Goldberg, D.E. (1989). Genetic algorithms in search, optimization, and machine learning. Addison-Wesley Publishing, New York.

Gopal, S. and Majidzadeh, K. (1991). Application of markov decision process to level-of-servicebased maintenance systems. Highway maintenance operations and research, Transportation Research Board, 12–18.

Gordo, J.M., and Guedes Soares, C., (1997). Interaction equation for the collapse of tankers and container ships under combined bending moments. *Journal of Ship Research*, 41(3), 230–340.

Guedes Soares, C., and Teixeira A.P. (2000). Structural reliability of two bulk carrier designs, marine structures, 13(2), 107–28.

Guedes Soares, C., and Moan, T. (1988). Statistical analysis of still water load effects in ship structures. *Transactions of the Society of Naval Architects and Marine Engineers*, SNAME, 96, l29-156.

Guedes Soares, C., Luís, R.M., Nikolov, P.I., Modiga, M., Quesnel, T., Dowes, J., Toderan, C., Taczala, M., (2008). Benchmark study on the use of simplified structural codes to predict the ultimate strength of a damaged ship hull, International Shipbuilding Progress, 55, 87–107.

Hasofer, A.M. and Lind, N.C. (1974). An exact and invariant first order reliability format. Journal of Engineering Mechanics Division, ASCE 100, 111-121.

Hendawi. S., and Frangopol, D. M. (1994), "System reliability and redundancy in structural design and evaluation." *Structural Safety*, Elsevier, 16 (1-2), 47-71.

Hohenbichler, M. and Rackwitz, R. (1981). Non-normal dependent vectors in structural safety. Journal of Engineering Mechanics Division, ASCE, 107, 1227-1237.

Hohenbichler, M., Gollwitzer, S., W. Kruse and Rackwitz, R. (1987). New light on first- and second-order reliability methods, Structural Safety, 4, 267-284.

Holland, J. (1972). Genetic Algorithms. Scientific American, July, 1972.

Hørte, T., Wang, and G.,White, N. (2007). Calibration of the hull girder ultimate capacity criterion for double hull tankers. In: Proceedings of the Conference on Practical Design of Ships and Offshore Structures, Houston, USA, October, 2007.

Hughes, O. F. (1983). Ship Structural Design: A Rationally-Based, Computer-Aided, Optimization Approach. Wiley and Sons, New York.

311

Hussein, A. W., and Guedes Soares, C. (2009). Reliability and residual strength of double hull tankers designed according to the new IACS common structural rules. *Ocean Engineering*, Elsevier, 36(17-18), 1446-1459.

Hussein, A.W., and Guedes Soares, C. (2008). Partial safety factors assessment for double hull tankers following the new common structural rules. In: Proceedings of the 27th International Conference on Offshore Mechanics and Arctic Engineering (OMAE2008), paper OMAE2008-57949.

IACS (2008). Common structural rules for double hull oil tankers. International Association of Classification Societies (IACS), London, UK. Website: http://www.iacs.org.uk.

Jia, H., and Moan, T., (2008). Reliability analysis of oil tankers with collision damage. In: Proceedings of the 27th International Conference on Offshore Mechanics and Arctic Engineering (OMAE2008), Estoril, Portugal, June 15–20, 2008, paper no. OMAE2008-57102.

Jiang, Y., Saito, M., and Sinha, K.C. (1988). Bridge performance prediction model using the markov chain. *Bridge Design and Testing*, Transportation Research Board, 1180, 25–32.

Khan, I.A., and Das, P.K., 2007. Structural safety assessment of damaged ships. In: Proceedings of 26th International Conference on Offshore Mechanics and Arctic Engineering, San Diego, USA, June 10–15, 2007, paper no. OMAE2007- 29121.

312

Khan, I.A., and Das, P.K., 2008. Reliability analysis of intact and damaged ships considering combined vertical and horizontal bending moments. *Ships and Offshore Structures*, 8(3), 371–384.

Kiremidjian, A., Moore, J. E., Fan, Y. Y., Yazlali, O., Basoz, N., Williams, M. (2008). Seismic risk assessment of transportation network systems. *Journal of Earthquake Engineering*, 11 (3), 371-382.

Korvin-Kroukowski, B. V. and Jacobs, W. R. (1957). Pitching and heaving motions of a ship in regular waves. Transactions, SNAME, 65, 590-632.

Kuhn, K.D., and Madanat, S.M. (2005). Model uncertainty and the management of a system of infrastructure facilities. Transportation Research Part C: Emerging Technologies, 13(5-6):391-404.

Lee, Y., Chan, H.-S., Pu, Y., Incecik, A, Dow R.S. (2012). Global wave loads on a damaged ship. *Ships and Offshore Structures*, Taylor & Francis, 7(3), 237-268.

Levinson, D. & Kumar, A. (1995). A multi-modal trip distribution model. *Transportation Research Record* 1466, 124-131.

Lind, N.C. (1995). A measure of vulnerability and damage tolerance. Reliability Engineering and System Safety, Elsevier, 43(1), 1-6.

Liu, D., Ghosn, M., Moses, F. (2000). Redundancy in highway bridge substructures. NCHRP Report 458, Transportation Research Board, Washington D.C.

Liu, M. and Frangopol, D. M. (2006). Probability-based bridge network performance evaluation. *Journal of Bridge Engineering*, 11 (5), 633-641.

313

Liu, M. and Frangopol, D.M. (2005a). Bridge annual maintenance prioritization under uncertainty by multiobjective combinatorial optimization. Computer-Aided Civil and Infrastructure Engineering, 20(5), 343-353.

Liu, M. and Frangopol, D.M. (2005b). Multiobjective maintenance planning optimization for deteriorating bridges considering condition, safety, and life-cycle cost. Journal of Structural Engineering, 131(5), 833-842.

Liu, P.L., Lin, H. Z., Der Kiureghian, A. (1989). CALREL user manual. Report No. UCB/SEMM-89/18, Department of Civil Engineering, University of California, Berkeley, CA.

Liu, Y.W. and Moses, F. (1994). A sequential response surface method and its application in the reliability analysis of aircraft structural systems. Structural. Safety, 16(1+2), 39-46.

Lounis, Z. (2004). Risk-based maintenance optimization of bridge structures. http://irc.nrc-cnrc.gc.ca/fulltext/nrcc47063/nrcc47063.pdf (Dec. 2004).

Lounis, Z. (2006). Risk-based maintenance optimization of aging highway bridge decks. Advances in Engineering Structures, Mechanics & Construction Solid Mechanics and Its Applications, 140, 723-734.

Luís, R. M., Teixeira, A. P. and Guedes Soares, C. (2009). Longitudinal strength reliability of a tanker hull Accidentally Grounded. *Structural Safety*, Elsevier, 31(3), 224-233.

Madanat, S. (1993). Optimal infrastructure management decisions under uncertainty. Transportation Research Part C, 1, 77-88.

314

Maes, M.A., Fritzson, K.E. and Glowienka, S. (2006). Structural robustness in the light of risk and consequence analysis. Structural Engineering International, IABSE, 16(2), 101-107.

Mahmoud, H.N., Connor, R.J., Bowman, C.A. (2005). Results of the fatigue evaluation and field monitoring of the I-39 Northbound Bridge over the Wisconsin River. ATLSS Report 05-04. Lehigh University, Bethlehem, PA, USA.

Marjanishvili, S. M. (2004). Progressive analysis procedure for progressive collapse. *Journal of Performance of Constructed Facilities*, ASCE, 18(2), 79-85.

Marsh, P.S. and Frangopol, D.M. (2008). Reinforced concrete bridge deck reliability model incorporating temporal and spatial variations of probabilistic corrosion rate sensor data. Reliability Engineering and System Safety, 93(3), 394-409.

Mathworks (2012). MATLAB User's Guide. The Mathwork Inc.

McKay, M. D., Beckman, R. J., and Conover, W. J. (1979). A comparison of three methods for selecting values of input variables in the analysis of output from a computer code. *Technometrics*, American Statistical Association, 21(2), 239–245.

Melchers, R.E. (1999). Structural reliability analysis and prediction, second ed., John Wiley & Sons, West Sussex, England.

Moses, F. (1982). System reliability development in structural engineering. Structural Safety, 1(1), 3-13.

315

Neves, L.C., Frangopol, D.M. and Cruz, P.J. (2006a). Probabilistic lifetime-oriented multi-objective optimization of bridge maintenance: Single maintenance type. Journal of Structural Engineering, 132(6), 991-1005.

Neves, L.C., Frangopol, D.M. and Petcherdchoo, A. (2006b). Probabilistic lifetime-oriented multi-objective optimization of bridge maintenance: Combination of maintenance types", Journal of Structural Engineering, 132(11), 1821-1834.

Okasha, N.M. and Frangopol, D.M. (2009). Lifetime-oriented multi-objective optimization of structural maintenance considering system reliability, redundancy and life-cycle cost using GA. Structural Safety, Elsevier, 31(6), 460-474.

Okasha, N. M. and Frangopol, D. M. (2010a). Time-variant redundancy of structural systems. *Structure and Infrastructure Engineering*, Taylor & Francis, 6(1-2), 279-301. DOI: 10.1080/15732470802664514.

Okasha, N. M. and Frangopol, D. M. (2010b). Efficient method based on optimization and simulation for the probabilistic strength computation of the ship hull. *Journal of Ship Research*, SNAME, 54(4), 1-13.

Okasha, N. M. and Frangopol, D. M. (2010c). Advanced modeling for efficient computation of life-cycle performance prediction and service-life estimation of bridges. *Journal of Computing in Civil Engineering*, ASCE, 24(6), 548-556.

Okasha, N.M., Frangopol, D.M., Saydam, D., and Salvino, L.W. (2011). Reliability analysis and damage detection in high speed naval crafts based on structural

health monitoring data. Structural Health Monitoring, Sage Publication, 10(4), 361-379.

Orcesi, A.D. and Frangopol, D.M. (2011). Use of lifetime functions in the optimization of nondestructive inspection strategies for bridges. Journal of Structural Engineering, ASCE, 137(4), 531-539.

Padgett, J.E., Desroches, R., and Nilsson, E. (2010). Regional seismic risk assessment of bridge network in Charleston , South Carolina. *Journal of Earthquake Engineering*, Taylor & Francis, 14(6), 918-933.

Paik, J. K. and Frieze, P. A. (2001). Ship structural safety and reliability. *Progress in Structural Engineering and Materials*, Wiley and Sons, 3(2), 198-210.

Paik, J. K., Thayamballi, A. K., Kim, S. K. and Yang, S. H. (1998). Ship hull ultimate strength reliability considering corrosion. *Journal of Ship Research*, SNAME, 42(2), 154-165.

Park, C. H. and Nowak, A.S. (1997). Lifetime reliability model for steel girder bridges. In Safety of Bridges, ed. P.C. Das, Thomas Telford Publishing, London.

PDSTRIP (2006). Program PDSTRIP: Public domain strip method - User manual. Website: http://sourceforge.net/projects/pdstrip.

Ramakumar, R. (1993). Engineering reliability: Fundamentals and applications. Prentice Hall, New Jersey.

Rausand, M. and Høyland, A. (2004). System reliability theory: Models. Statistical Methods and Applications, Wiley, New Jersey.

Resolute Weather (2011). Pierson-Moskowitz sea spectrum, http://www.eustis.army.mil/weather, [accessed August 2012].

317

Robelin C.-A. and Madanat, S.A. (2007). History-dependent bridge deck maintenance and replacement optimization with Markov decision processes. Journal of Infrastructure Systems, ASCE, 13(3), 195–201.

Saydam, D. and Frangopol, D. M. (2010). Performance assessment of bridges under progressive damage and abnormal actions. Proceedings of Fifth International Conference on Bridge Maintenance, Safety and Management, IABMAS 2010, D.M. Frangopol, R. Sause, and C.S. Kusko, eds., CRC Press/Balkema, Taylor & Francis Group plc, London, CD-ROM, 3523-3530.

Saydam, D. and Frangopol, D.M. (2011a). Performance indicators for structures and infrastructures. Structures Congress 2011, ASCE, Las Vegas, Nevada.

Saydam, D. and Frangopol, D.M. (2011b). Time-dependent performance indicators of damaged bridge superstructures. Engineering Structures, Elsevier, 33(9), 2458-2471.

Saydam, D. and Frangopol, D.M. (2013a). Applicability of simple expressions for bridge system reliability assessment. Computers & Structures, Elsevier, 114-115, 59-71.

Saydam, D. and Frangopol, D.M. (2013b). Performance assessment of damaged ship hulls. Ocean Engineering, Elsevier, 68, (65-76).

Saydam, D., Bocchini, P., and Frangopol, D.M. (2013). Time-dependent risk associated with deterioration of highway bridge networks. Engineering Structures, Elsevier, 54, 221-233.

Saydam, D., Frangopol, D.M., and Dong, Y. (2013). Assessment of risk using bridge element condition ratings. Journal of Infrastructure Systems, ASCE, 9(3), doi: 10.1061/(ASCE)IS.1943-555X.0000131.

318

Schubert, M. (2006). Probabilistic assessment of the robustness of structural systems. Proceedings of the 6th International PhD Symposium in Civil Engineering Zurich, August 23-26, 2006.

Scott, D., Novak, D., Aultmanhall, L, and Guo, F (2006). Network robustness index: a new method for identifying critical links and evaluating the performance of transportation networks. *Journal of Transport Geography*, 14(3), 215-227.

Shinozuka, M., Zhou, Y., Banerjee, S., and Murachi, Y. (2006). Cost-effectiveness of seismic bridge retrofit. In: Cruz, Frangopol & Neves (eds.), in Bridge Maintenance, Safety, Management, Life-Cycle Performance and Cost, Taylor and Francis, CRC press.

Smilowitz, K. and Madanat, S. (2000). Optimal inspection and maintenance policies for Infrastructure Networks. Computer-Aided Civil and Infrastructure Engineering, 15(1), 5-13.

Stein, S. M., Young, G.K., Trent, R.E., and Pearson, D.R. (1999). Prioritizing scour vulnerable bridges using risk. Journal of Infrastructure Systems, ASCE, 5(3), 95-101.

Thoft-Christensen, P. (2011). Corrosion crack based assessment of the life-cycle reliability of concrete structures. In Proc., Eighth International Conference on Structural Safety and Reliability June 17-22, R. B. Corotis, G. I. Schueller, and M. Shinozuka, eds., A. A. Balkema Publishers, Newport Beach, California, 2001.

319

Thompson, P. D., Small, E. P., Johnson, M., Marshall, A. R. (1998). The Pontis bridge management system. *Structural Engineering International*, IABSE, 8(4), 303-308.

van Noortwijk, J. M. and Klatter, H. E. (2004). The use of lifetime distributions in bridge maintenance and replacement modelling. Computers & Structures, Elsevier, 82(13–14), 1091–1099.

Vanderplaats (2010a). VisualDOC, Design optimization software version 6.2.2, Theoretical manual. Vanderplaats R&D, Colorado Springs, CO.

Vanderplaats (2010b). VisualDOC, Design optimization software version 6.2.2, User's manual. Vanderplaats R&D, Colorado Springs, CO.

Wang, G., Chen, Y., Zhang, H., and Peng, H. (2002a). Longitudinal strength of ships with accidental damages. Marine Structures, 15, 119–138.

Wang, G., Spencer, J., Chen,Y.J. (2002b). Assessment of ship's performance in accidents. Marine Structures, 15, 313–333.

Wang, N., Ellingwood, B. and Zureick, A. (2011). Bridge rating using system reliability assessment II: Improvements to bridge rating practices. Journal of Bridge Engineering., ASCE, 16(6), 863-871.

Yang, S-I., Frangopol, D. M., Neves, L. C. (2004). Service life prediction of structural systems using lifetime functions with emphasis on bridges. Reliability Engineering & System Safety, Elsevier, 86(1), 39-51.

Zhang, Y. & Vidakovic, B. (2005). Uncertainty analysis in using Markov chain model to predict roof life cycle performance. Proceedings of the 10DBMC

International Conférence On Durability of Building Materials and Components, Lyon, France, April 17-20, 2005.

Zhu, B. and Frangopol, D.M. (2012). Reliability, redundancy and risk as performance indicators of structural systems during their life-cycle. Engineering Structures, 41, 34-49.

Zhu, B. and Frangopol, D.M. (2013). Risk-based approach for optimum maintenance of bridges under traffic and earthquake loads. Journal of Structural Engineering, ASCE, 139(3), 422-434.

Zhu, L., James, P., Zhang, S. (2002). Statistics and damage assessment of ship grounding. Marine Structures, 15, 515-530.

321

APPENDIX A

COMPUTATIONAL PLATFORM

The Life-Cycle Structural Engineering Computer Laboratory at ATLSS Engineering Research Center, Lehigh University, is equipped with the proper hardware and software to perform lifetime performance analyses of structural components and systems with a probabilistic approach. The unique feature of this laboratory is the comprehensive array of commercial programs and scientific codes specifically selected and interfaced to provide an efficient and robust computational infrastructure. The effective and automated interaction among the various software packages provides a computational framework for life-cycle analysis that has already been successfully adapted and applied to multiple engineering systems, such as bridges, ships, and distributed infrastructure lifelines.

The facilities of the laboratory include a 12-core and two 8-core servers, and six workstations loaded with a complete software library, specifically conceived for life-cycle engineering. Moreover, ten personal workstations are assigned to the researchers in the Life-Cycle Structural Engineering Group in their offices. Researchers can use their workstations to take advantage of all the hardware and software facilities of the lab through a high-speed local network. In addition, researchers have also access to the general purposes high-performance computing (HPC) resources of Lehigh University. These resources include the local servers

322

LEAF, ALTAIR and HPC-Cluster and access to the facilities of Pittsburg Supercomputing Center.

The most important software packages available on the computers of Life-Cycle Engineering Laboratory include:

• RELSYS: reliability software (first order reliability method)

• CALREL: reliability software (first and second order reliability method)

• MONTE: software for Monte Carlo Simulation

• RELTSYS: time-dependent reliability software

• VISUALDOC: optimization software

• HAZUS-MH MR5: software for distributed system probabilistic analysis

• REDARS2: software for distributed system performance analysis

• ABAQUS: finite element software

• OPENSEES: finite element software

• DRAIN-2DX: finite element software

• SAP2000: finite element software

• MATLAB: general purpose numerical programming environment

• MATHEMATICA: general purpose symbolic programming environment

• Specific libraries developed by the group for integrating and connecting the other software packages and for accomplishing other specific tasks

Several disciplines are involved in the probabilistic life-cycle analysis of structural systems, such as structural analysis, reliability analysis, risk analysis, structural optimization, and deterioration modeling (Figure A.1). Therefore, establishing effective interactions between software packages that perform tasks associated with all

323

these disciplines is necessary. The connections among the various software packages are provided by specific computational libraries developed by the Life-Cycle Engineering group members over the years. In this way, for instance, an optimization algorithm can provide the input for reliability software and use it to evaluate the objective functions. Some of the interactions among the software packages are schematically illustrated in Figure A.2.
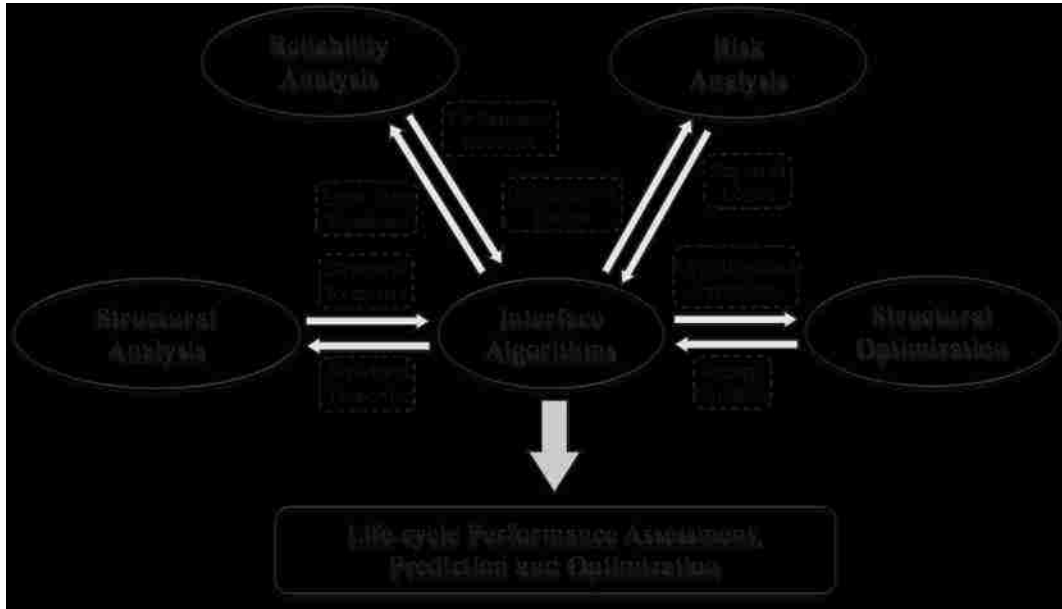
Figure A.1   Interaction among computational tasks of life-cycle analysis
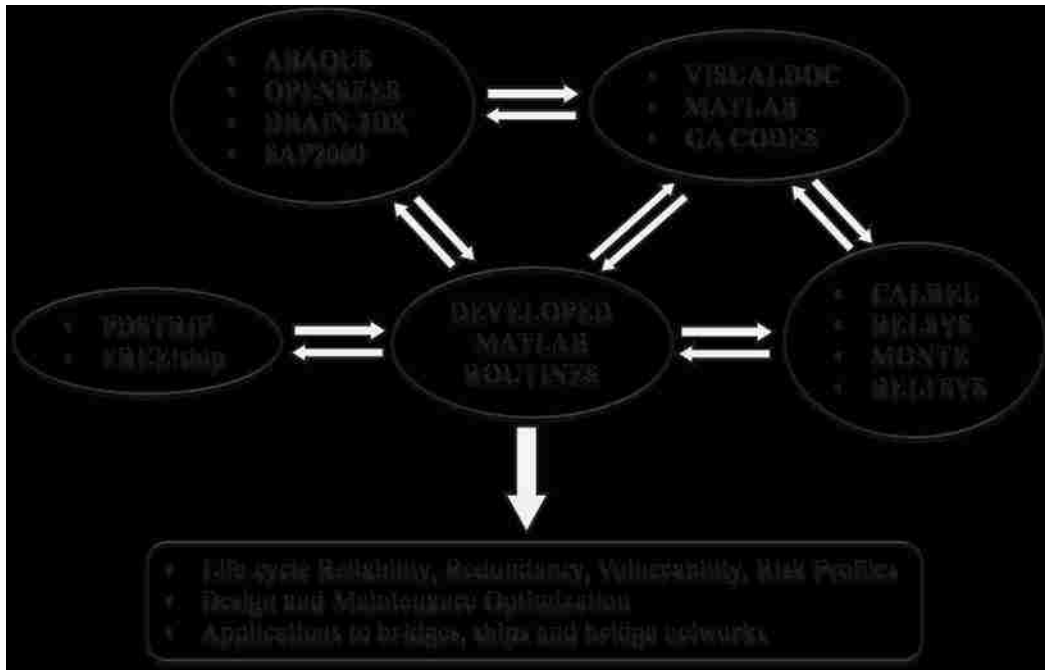
Figure A.2   Interaction among computer programs for lifecycle analysis

APPENDIX B

OTHER ACCOMPLISHED WORK

In this appendix, some of the other accomplished work by the author is mentioned. Several journal papers co-authored are briefly summarized.

B.1 Reliability Analysis and Damage Detection in High-Speed Naval Craft Based on Structural Health Monitoring Data

Okasha, Frangopol, Saydam, and Liming (2010) presented an approach for using the data obtained from structural health monitoring (SHM) in the reliability analysis and damage detection in high speed naval craft (HSNC) structures under uncertainty. The statistical damage detection technique used benefits from vector autoregressive (ARV) modeling for detection and localization of damage in the HSNC structure. The methodology is illustrated on an HSNC, HSV-2 which is a 98-m long, high speed, all aluminum, wave-piercing catamaran and uses data obtained from previous seakeeping trials.

B.2 Efficient, Accurate, and Simple Markov Chain Model for the Life-Cycle Analysis of Bridge Groups

Bocchini, Saydam, and Frangopol (2013) presented a time-efficient and accurate Markov chain model for the life-cycle analysis of individual bridges and bridge groups, which includes the effect of deterioration, maintenance actions, failures, and rehabilitations. This model is very briefly described in Chapter 7. Bocchini, Saydam,

327

and Frangopol (2013) investigated the accuracy of this model by comparing it to the exact Monte Carlo Simulation and showed that the proposed model yields results very close to those from Monte Carlo Simulation while providing high computational efficiency.

B.3 Time-Variant Sustainability Assessment of Seismically Vulnerable Bridges Subjected to Multiple Hazards

Dong, Frangopol, and Saydam (2013) presented a methodology for assessing the time-variant sustainability of bridges under seismic hazard, considering the effects of deterioration, which accounts for the effects of flood-induced scour on seismic fragility. Sustainability was quantified in terms of its social, environmental, and economic metrics. These include the expected downtime and number of fatalities, expected energy waste and carbon dioxide emissions, and the expected loss. The seismic fragility curves were obtained using nonlinear finite element analysis. The costs and losses associated with seismic hazard were evaluated based on a set of damage states, which are mutually exclusive and collectively exhaustive. The time-variation of the metrics of sustainability was investigated. The effects of flood-induced scour on both seismic fragility and sustainability were considered.

B.4 Maintenance, Management, Life-Cycle Design and Performance of Structures and Infrastructures: A Brief Review

Frangopol, Saydam, and Kim (2012) provided a brief review of the recent research accomplishments in the field of design, maintenance, life-cycle management, and

328

optimization of structures and infrastructures reported in papers published in Structure

and Infrastructure Engineering during the period 2005–2011.

329

C.1 CHAPTER 2

C_{Dir} : cost of the direct consequences

C_{ET} : total expected cost

C_F : expected failure cost

C_{Ind} : cost of the indirect consequences

C_{INS} : expected cost of inspections

C_{PM} : expected cost of routine maintenance cost

C_{REP} : expected cost of repair

C_T : initial cost

$E(.)$: mean value

$F(t)$: cumulative distribution function of time to failure T

$f(t)$: probability density function of time to failure, T

FD : failure domain

f_Q : probability density function of Q

F_R : cumulative distribution function of R

FS : factor of safety

g : performance function

$h(t)$: failure (hazard) rate function

k : normalizing constant

L : load effect

330

LF : load factor

LL : live load effect

M_{DLC} : moment due to composite dead load

M_{DLNC} : moment due to non-composite dead load

M_{LL+I} : moment due to live load including impact

M_u : ultimate moment capacity

N_0 : initial number of items

$N_S(t)$: number of surviving items at time t

ϕ : resistance factor

P_f : probability of failure

P_{f_i} : system failure probability assuming one impaired member i

P_{f_0} : system failure probability of the undamaged system

$P_{f(dmg)}$: probability of damage occurrence to the system

$P_{f(sys)}$: probability of system failure

Q_i : load effect in mode i

R : resistance

r_0 : pristine system state

r_d : damaged system state

R_{dir} : direct risk

RI : redundancy index

R_{ind} : indirect risk

R_n : member nominal resistance

331

ROI : robustness index

S(*t*) : survivor function

t : time

T : time to failure

V : vulnerability

X : vector of random variables

X_i : random variable

β : reliability index

$\beta_{damaged}$: reliability index of the damaged system

β_{intact} : reliability index of the intact system

γ_i : load factor

η_i : load modifier

$\sigma(.)$: standard deviation

$\Phi(.)$: standard normal distribution function

C.2 CHAPTER 3

a_0 : constant associated with response approximation

a_i : coefficient associated with the random variable x_i

e : approximation error

$LF(t)$: time-dependent load factor

$LL(t)$: time-dependent live load effect

$P_f(t)$: time-dependent probability of failure

P_{s0} : system failure probability of the undamaged system

P_{si} : system failure probability assuming one impaired member i

$Q(t)$: time-variant prospective loading

R : approximated response

R : robustness index

r_0 : pristine system state

r_d : damaged system state

$RI(t)$: time-variant redundancy index

$V(t)$: time-variant vulnerability

x_i : random variable i in response approximation

$\beta(t)$: time-dependent reliability index

$\beta_{damaged}(t)$: time-variant reliability index of the damaged system

β_{intact} : reliability index of the intact system

333

C.3 CHAPTER 4

$E(.)$: mean value

e_A : error type A

e_B : error type B

e_C : error type C

f_X : probability density function of random variable X

LF : load factor

LL : live load effect

P_f : failure probability

$P_{HS\text{-}20}$: weight of AASHTO HS-20 vehicle

u_n : most probable value of random variable Y_n

$Var(.)$: variation

X : random variable

Y_n : random variable from type I largest extreme value distribution

α_n : an inverse measure of the dispersion of values of random variable Y_n

β_1 : reliability index for case 1

β_2 : reliability index for case 2

$\delta(.)$: coefficient of variation

θ_0 : central safety factor

ζ : dispersion parameter of lognormal distribution

λ : central value parameter of lognormal distribution

$\Phi^{-1}(.)$: inverse of cumulative distribution function of standard normal variate

334

C.4 CHAPTER 5

$A(t)$: average daily traffic (ADT) at year t

c : distance from the concrete surface to the steel reinforcement

c_{ATC} : average wage per hour for trucks

c_{AW} : average wage per hour for cars

$C_{Direct}(t)$: direct consequence of the failure of component

c_g : price of the girder for unit weight in unit length

c_{good} : time value of the goods transported in a cargo

$C_{Indirect}(t)$: indirect consequence of the failure of component

c_{Reb} : rebuilding cost per unit area of the bridge

$C_{Reb}(t)$: rebuilding of the bridge

$C_{Run}(t)$: running cost of detouring vehicles

$c_{Run,car}$: running cost for cars

$c_{Run,truck}$: running cost for trucks

$C_{Tl}(t)$: cost of time loss

d : duration of detour

D : original bar diameter

d_{bf} : width of the bottom flange

D_l : the detour length

d_{tf} : width of the top flange

d_w : height of the web

$FV(t)$: value of an expenditure made after t years

G_g : weight of the girder in unit length

335

I_{Rob} : robustness index

L : length of bridge

$L_{Direct}(t)$: expected direct loss

L_g : length of the girder

$L_{Indirect}(t)$: expected indirect loss

m : number of condition states for a component

n : number of components included in the risk analysis

O_{car} : occupancy rate for cars

O_{truck} : occupancy rate for trucks

$P_{(CFi|CSi = Si)}(t)$: conditional failure probability of component i given the component is in

condition state j at time t

$P_{(CFij)}(t)$: component failure probability

$P_{(CSi=Sj)}(t)$: is the probability of component i being in condition state j at time t

$P_{(SFij)}(t)$: system failure probability

p_{ij} : transition probability from state i to state j

PV : present value of the expenditure

r : annual discount rate

S : average detour speed

$\mathbf{S}(t)$: time-variant state probability vector

T : average daily truck traffic

t_{bf} : thickness of the bottom flange

$\mathbf{TP}$: transition probability matrix

t_{tf} : thickness of the top flange

336

t_w : thickness of the web

W : width of the bridge

α_d : ratio of density of the corrosion rust product to the density of the reinforcing

steel

δ : corrosion penetration on the surface

Δ : percentage of section loss

C.5 CHAPTER 6

a : total number of vulnerable components included in the risk analysis

b : total number of condition states for a component

$C'_{Direct,i}$: direct consequence of component failure in terms of monetary value

$C_{Direct,i}(t)$: direct consequence of the failure of component i including the discount rate

CF_i : failure of component i

$C'_{Indirect}$: indirect consequence of component failure in terms of monetary value

$C_{Indirect}(t)$: indirect consequence of system failure including the discount rate

CS_i : condition state of component i

$EMC_i(t)$: expected cost of i-th maintenance action

$EMC^i_{Lifetime}$: lifetime expected maintenance cost of component i

EMC_{Total} : total expected maintenance cost for the entire structure

$L_{Direct}(t)$: expected direct loss

$L_{Indirect}(t)$: expected indirect loss

m : maintenance option

MC : maintenance cost matrix

mc_{ij} : cost of the maintenance action which refers to restoring condition state i if the structure was in condition state j

m^E : maintenance option for exterior girder

m^I : maintenance option for interior girder

$P_{(CFi|CSi=j)}(t)$: conditional failure probability of component i given the component is in condition state j

$P_{(CSi=j)}(t)$: probability of component i being in condition state j

338

$P_{(SFi|CFi)}(t)$: conditional probability of system failure given that component i has already failed

$p^{+}_{i}(t)$: probability of the component being in condition state i after the maintenance action

$p^{-}_{i}(t)$: probability of the component being in condition state i before the maintenance action

p_{ij} : probability of transition from state i to state j

r : discount rate of money

$\mathbf{S}(t)$: state vector

$\mathbf{S}^{+}(t)$: state vector including the effects of maintenance at time instant t (approaching t from right side)

SF_i : system failure induced by failure of component i

t : time

t_m : time of maintenance activity

$\mathbf{TP}$: transition probability matrix

z : number of the maintenance actions within the lifetime

Δt_m : time span between successive maintenance actions

C.6 CHAPTER 7

B   : entire set of bridges within the network

C_A : cost of accidents

C^b_M : cost of maintenance activity for bridge b

C_{Dir} : direct consequence

C_E : costs associated with the environmental damage

C_H : human health and life costs

C_{Ind} : indirect consequence

C_P : cost associated with the impact on general public

C_R : reconstruction cost

I_{Rob} : robustness index

M   : bridge group consists of the bridges which are in state M or state M'

M : state M

M' : state M'

$P^b(i)$: probability of state i for bridge b

R   : bridge group consists of the bridges which are in state R

R : state R

S   : bridge group consists of the bridges which are in state S or state S'

S : state S

S   : state vector

S' : state S'

TP^b_{ij} : transition probability from state i to state j for bridge b

TTD : total travel distance

TTT　: total travel time

ΔTTD　: extra travel distance associated with damage scenarios

ΔTTT　: extra travel time associated with damage scenarios

ϕ　　: impossible event

341

C.7 CHAPTER 8

B : ship breadth

C_1 : annual corrosion rate

C_2 : coefficient

C_b : ship block coefficient

C_{wv} : wave coefficient

D : depth of the ship

E : elastic modulus

$E(MC_0)$: mean vertical bending moment capacity of the intact hull

$E(MC_i)$: mean vertical bending moment capacity of the damaged

g : gravitational acceleration

$g_{hog,SS,U,H}$: performance function associated with the flexural failure in hogging

$g_{sag,SS,U,H}$: performance function associated with the flexural failure in sagging

H : heading angle

$H_{1/3}$: significant wave height which is the mean of the one third highest waves

L : ship length

$M(\kappa)$: bending moment

$m_{0,SS,U,H}$: zero-th moment of the wave spectrum

$MC_{hog}(t)$: time-variant vertical bending moment capacity in hogging

$MC_{sag}(t)$: time-variant vertical bending moment capacity in sagging

$M_{sw,hog}$: still water bending moment in hogging

$M_{sw,sag}$: still water bending moment in sagging

$M_{w,SS,U,H}$: wave-induced vertical bending moment

342

$r(t)$: thickness loss

RI_i : robustness index for associated with damage scenario i

$RSFi$: residual strength factor for damage scenario i

$S_{M,SS,U,H}(\omega)$: response spectrum

$S_{w,SS}(\omega)$: sea spectrum for a given sea state SS

$S_X(\omega)$: spectral density functions of the input

$S_Y(\omega)$: spectral density functions of the output

t_0 : corrosion initiation time

T_1 : mean period of wave

U : forward ship speed

x_R : random model uncertainty associated with the resistance

x_{sw} : random model uncertainty associated with the still water bending moment

x_w : random model uncertainty associated with the wav-induced bending moment

β_0 : reliability index associated with the intact hull

β_i : reliability index associated with the damaged hull

κ : curvature

σ_{Yp} : keel yielding stress

σ_{Ys} : side panels yielding stress

$\Phi(\omega)$: transfer function

ω : circular frequency

$\omega_{e,U,H}$: encounter frequency

343

VITA

Duygu Saydam was born on June 3, 1982 in Izmir, Turkey to Şevki Saydam and his wife, Ruhan Saydam. He graduated from Ankara Science High School in 2000. He received his Bachelor of Science Degree in Civil Engineering from Istanbul Technical University, Istanbul, Turkey in 2004. Duygu received his Master of Science Degree in Civil Engineering from Boğaziçi University, Istanbul, Turkey in 2006. He attended the Ph.D. Program in Structural Engineering at Lehigh University, Bethlehem, PA in 2007.